Alterations of synaptic plasticity and network functions in APP and APLP-deficient mice

Von der Fakultät für Lebenswissenschaften

der Technischen Universität Carolo-Wilhelmina zu Braunschweig

zur Erlangung des Grades einer

Doktorin der Naturwissenschaften

(Dr. rer. nat.)

genehmigte

D i s s e r t a t i o n

von Ulrike Herrmann
aus Magdeburg

1. Referent:	Professor Dr. Martin Korte
2. Referent:	Professor Dr. Reinhard Köster
eingereicht am:	09.03.2015
mündliche Prüfung (Disputation) am:	08.05.2015
Druckjahr:	2015

“Wir sind, was wir denken.

Alles, was wir sind, entsteht aus unseren Gedanken.

Mit unseren Gedanken formen wir die Welt.

We are what we think.

All that we are arises with our thoughts.

With our thoughts, we make the world.”

-Buddha-

Diese Arbeit widme ich meinen wunderbaren Großeltern Eleonore und Günter Rottländer sowie meinen großartigen Eltern Claudia und Rainer Herrmann.

Vorveröffentlichungen der Dissertation

Teilergebnisse aus dieser Arbeit wurden mit Genehmigung der Fakultät für Lebenswissenschaften, vertreten durch den Mentor der Arbeit, in folgenden Beiträgen vorab veröffentlicht:

Publikationen

Korte M, **Herrmann U**, Zhang X, Draguhn A. *The role of APP and APLP for synaptic transmission, plasticity, and network function: lessons from genetic mouse models.* Exp Brain Res. 2012 Apr; 217(3-4):435-40.

Zhang X, **Herrmann U**, Weyer SW, Both M, Müller UC, Korte M, Draguhn A. *Hippocampal network oscillations in APP/APLP2-deficient mice*. PLoS One. 2013 Apr 9; 8(4):e61198.

Weyer SW, Zagrebelsky M, **Herrmann U**, Hick M, Ganss L, Gobbert J, Gruber M, Altmann C, Korte M, Deller T, Müller UC. *Comparative analysis of single and combined APP/APLP knockouts reveals reduced spine density in APP-KO mice that is prevented by APPsα expression.* Acta Neuropathol Commun. 2014 Mar 31; 2:36. doi: 10.1186/2051-5960-2-36.

Hick M*, **Herrmann U***, Weyer SW, Mallm J, Tschäpe J, Borgers M, Mercken M, Roth FC, Draguhn A, Slomianka L, Wolfer DP, Korte M, Müller UC. *Acute function of secreted amyloid precursor protein fragment APPsα in synaptic plasticity.* Acta Neuropathol. 2015 Jan; 129(1):21-37.
(***equal contribution**)

Klevanski M, **Herrmann U**, Weyer SW, Voikar V, Wolfer DP, Caldwell JH, Korte M, Müller UC. *The APP intracellular domain is required for normal synaptic morphology, synaptic plasticity and hippocampus dependent behavior.* **In preparation**.

Tagungsbeiträge

Herrmann U, Delekate A, Zhang A, Weyer S, Hick M, Draguhn A, Müller U, Korte M. *Alterations of synaptic functions in APP and APLP2 deficient mice.* (Poster) The 8th FENS forum of European Neuroscience, Barcelona, Spain, July 14 - 18, 2012.

Herrmann U, Hick M, Müller U, Korte M. *Analysis of conditional APP/APLP2 double knock-out mice reveals a strong hippocampal CA3-CA1 LTP defect.* (Poster) The 10th Göttingen Meeting of the German Neuroscience Society, Germany, March 13 - 16, 2013.

Herrmann U, Hick M, Müller U, Korte M. *Conditional APP/APLP2 double knockout mice reveal pronounced deficits in synaptic transmission and plasticity of CA1-CA3 pathway.* (Poster) The 2nd RMN2 Biennial Meeting, Oberwesel, Germany, 2014, June 25 - 27, 2014.

Table of Contents

Abstract

Dementia currently is and will be in the future a worldwide spread disease which predominantly affects elderly people. Alzheimer's disease (AD) is the most common form of dementia. It is characterized by an aggregation of hyperphosphorylated tau protein tangles and Aβ plaques which derives from the amyloidogenic processing pathway of the Amyloid Precursor Protein (APP). To understand the pathology of AD it is essential to assess the proteins relevance in the intact brain. So far the physiological functions of APP, its homologues APLP1/2 and their cleavage fragments in the healthy organism are poorly understood. Using gene targeted mice I investigated the role of the APP protein-family for synaptic transmission and activity-dependent synaptic plasticity in the hippocampus as a cellular correlate for learning and memory. My studies uncovered a synergistic and age-related compensatory function of APP and APLP2 in LTP induction and maintenance. Moreover, I could distinguish a role of both proteins for brain development and an acute function at active synapses in the adult brain. An involvement during development was indicated by abnormal brain morphology as well as an impaired neuromuscular junction in triple ($APP^{-/-}APLP2^{-/-}APLP1^{-/-}$) and most of double KO ($APP^{-/-}APLP2^{-/-}$) mice which caused lethality. My observations in organotypic hippocampal slice cultures point towards an important function of APPsα during synaptogenesis indicated by an impaired activity-dependent synaptic plasticity and recently reported reduced spine number. I also showed a LTP defect in a viable conditional double KO mouse strain in which the APP gene is targeted at E11 only in the CNS on an APLP2 deficient background. This might suggest a role of these proteins for an intact neuronal network formation. Additionally, the observed LTP defect might be reasoned by an altered excitation-inhibition balance. However, the time point of the APP excision on an APLP2 deficient background seems to be important since a postnatally induced double KO revealed only a subtle LTP impairment. Furthermore, an acute function of APP processing products was confirmed by mice in which APP lacks 15 amino acids C-terminally on an APLP2 deficient background leading to an impaired synaptic plasticity. Consistently, I identified another APP full length cleavage product APPsα as a crucial peptide for LTP induction and maintenance since it was capable to restore the impaired synaptic plasticity in a gain and rescue of function experiment by recombinant APPsα application. Since Ca^{2+} is a key molecule for changes in the activity-dependent synaptic plasticity I investigated whether the Ca^{2+} dynamic is affected and thus might contribute to the functional LTP defect. Indeed, I showed reduced Ca^{2+} dynamics before and upon chemically induced LTP which were, however, not significantly altered when the relative increase of Ca^{2+} was quantified upon cLTP induction. An inhibition of the SERCA, which reloads Ca^{2+} into the ER, revealed an impaired Ca^{2+} response upon cLTP induction. This suggests that APP might contribute to proper Ca^{2+} dynamics in the intact brain through APP dependent mechanisms in the ER. Consistent with the functional LTP defect an expression of APPsα rescued the defect in Ca^{2+} dynamics. Furthermore, this peptide even enhanced LTP induction in acute slices from control mice. These observations suggest that APPsα might be a potential preventive and therapeutic target for Alzheimer's disease.

Zusammenfassung

Demenz ist derzeit und wird auch in Zukunft eine weltweit stark verbreitete Erkrankung sein, die vornehmlich ältere Menschen betrifft. Die Alzheimersche Erkrankung ist dabei die häufigste Demenzform. Sie ist durch die Ablagerung von hyperphosphoryliertem Tau Protein als *tangles* und Aβ Plaques, welche durch die amyloidogene Spaltung des *Amyloid Precursor Proteins* (APP) entsteht, charakterisiert. Zum Verständnis der Pathologie der Alzheimerschen Erkrankung ist es essentiell, die Relevanz des Proteins im intakten Organismus zu verstehen. Die physiologischen Funktionen von APP, seinen Homologen APLP1/2 und deren Spaltprodukte im gesunden Organismus sind jedoch weitgehend unbekannt. Die Verwendung transgener Mäuse ermöglichte mir die Rolle der APP-Familie hinsichtlich der synaptischen Transmission und Plastizität im Hippokampus zu untersuchen, welches ein zelluläres Korrelat für Lernen und Gedächtnis darstellt. Meine Studien zeigen eine synergistische und altersabhängige kompensatorische Funktion von APP und APLP2 für die LTP Induktion und Stabilität. Des Weiteren konnte ich eine Rolle beider Proteine für die Gehirnentwicklung sowie eine akute Funktion an aktiven Synapsen belegen. Eine Beteiligung in der Entwicklung wurde durch eine veränderte Hirnmorphologie in letalen dreifach- ($APP^{-/-}APLP2^{-/-}APLP1^{-/-}$) sowie doppel-KO ($APP^{-/-}APLP2^{-/-}$) Mäusen impliziert. Meine Beobachtungen in organotypischen hippokampalen Schnittkulturen implizieren eine wichtige Funktion von APPsα während der Synaptogenese. Dies äußerte sich durch eine veränderte aktivitätsabhängige synaptische Plastizität und eine kürzlich gezeigte reduzierte *spine* Anzahl. Weiterhin konnte ich einen LTP Defekt in einem lebensfähigen konditionalen APP-KO zeigen, welcher bei E11 auf einem $APLP2^{-/-}$ Hintergrund aktiviert wird. Dies könnte bedeuten, dass diese Proteine an der Bildung intakter neuronaler Netzwerke beteiligt sind. Zusätzlich könnte der LTP Defekt durch eine gestörte Erregungs-Inhibitionsbalance bedingt sein. Allerdings scheint der Zeitpunkt der APP Entfernung auf einem $APLP2^{-/-}$ Hintergrund entscheidend zu sein, da ein postnatal induzierter doppel-KO nur einen geringfügigen LTP Defekt zur Folge hatte. Außerdem bestätigte sich eine akute Funktion der APP Spaltprodukte dadurch, dass der Verlust von 15 C-terminalen Aminosäuren im APP bei einem $APLP2^{-/-}$ Hintergrund eine beeinträchtigte synaptische Plastizität zur Folge hatte. Übereinstimmend identifizierte ich APPsα als unabdingbar für die LTP Induktion und Stabilität, da es den Defekt der synaptischen Plastizität in einem Rettungsexperiment durch Applikation des rekombinanten Peptides wiederherstellte. Da Ca^{2+} ein zentrales Molekül während aktivitätsabhängiger synaptischer Plastizität ist, untersuchte ich eine potenzielle Beeinträchtigung der Ca^{2+} Dynamik, die möglicherweise zum funktionellen LTP Defekt beträgt. Ich konnte eine reduzierte Ca^{2+} Dynamik vor und nach chemisch induziertem LTP belegen. Wurde jedoch der relative Ca^{2+} Anstieg nach cLTP Induktion quantifiziert, war kein signifikanter Unterschied messbar. Eine Inhibition der SERCA, welche das ER mit Ca^{2+} belädt, zeigte eine beeinträchtigte Ca^{2+} Antwort nach cLTP Induktion. Dies lässt vermuten, dass APP möglicherweise durch Interaktionen im ER zu einer intakten Ca^{2+} Dynamik im gesunden Gehirn beiträgt. Konsistent stellte eine APPsα Expression eine veränderte Ca^{2+} Dynamik vor und nach cLTP wieder her. Außerdem verstärkte das Peptid die LTP Induktion in Akutschnitten der Kontrollgruppe. Diese Beobachtungen bestätigen APPsα als potenziell präventives und therapeutisches Ziel in der Alzheimerschen Erkrankung.

1 Introduction

The mechanisms how thinking, memory formation and behavior adaptations are realized in the brain fascinate people since centuries. Experiences, positive as well as negative, thereby shape ones individual facets and provide the opportunity to acquire new ideas and adjust behavior. Memory storage upon learning involves changes in the brain which can make it persistent throughout life time on the one hand but permits on the other hand forgetting as well.

How memory is established has been extensively studied in the past paralleled by resolving technical limitations of tissue fixation as well as visualization by histological protocols and microscopic techniques. To understand how learning and memory work in detail it is essential to investigate the processes at the cellular level. The brain is characterized by a high variety of different cell types. Thereby, the key players are neurons with a quantity of ~100 billion. To pass information from one to the other neuron they build on average synaptic contacts to 5000 - 10000 adjacent neurons finally forming a widespread network for communication. Overall, ~15 trillion synapses make the human brain the most complex vertebrate organ. Synapses are dynamic structures being characterized by their ability to adapt their function and structure in response to changed activity levels. This feature is termed synaptic plasticity and is regarded as a correlate for learning and memory at the cellular level. Still, the question remains which brain structures are primarily involved in converting short-term memory into a long-term persisting memory. Lesion studies identified the hippocampus to be directly involved in the formation of complex memories. Therefore, it is an appropriate structure to investigate learning and memory processes on the cellular and molecular base during health as well as disease. Specific disorders affect the ability to learn and store new memory. Some of those like fragile X mental retardation or Down syndrome are genetically linked and occur already from childhood on whereas others like dementia progress with age. Currently ~35 million elderly people worldwide suffer from Alzheimer's Disease, a subtype of dementia. This disease is mainly characterized by the formation of aggregates of intracellular tau and extracellular Aβ protein. The latter is a cleavage product of the Amyloid Precursor Protein (APP) which is implicated to be involved not only in the disease status but also to be important for learning and memory. This study focusses on the physiological functions of APP and its various processing products as well as its homologue Amyloid Precursor-Like Protein 2 (APLP2) in synaptic plasticity.

1.1 Synaptic Plasticity

The fundamental principle how an information flow between neurons is carried out relays on the concept of translating an electrical code into a chemical one that in turn is encoded again as an electrical signal. Briefly, the incoming action potential along the axon alters the ion distribution at the membrane thereby changing its electrical potential. The resulting Ca^{2+} influx triggers the release of a chemical transmitter from the presynapse into the synaptic cleft. Opposing to the presynapse the postsynapse is localized. Its membrane contains specific ionotropic receptors which open upon neurotransmitter binding causing again a change of membrane polarity termed depolarization for excitatory and hyperpolarization for inhibitory neurons. Importantly, the chemical excitatory glutamatergic synapse is not a static element to transmit information throughout the network. In fact it is a highly dynamic structure reacting with an increase or decrease of efficacy called synaptic plasticity. Both components of the synapse are adaptable. While presynaptically the neurotransmitter release is modifiable the postsynapse can adapt with changing the structural and functional plasticity in response to defined stimuli described in detail in 1.1.2 (Yang and Calakos, 2013; Bellot et al., 2014).

In particular Donald O. Hebb significantly contributed to the nowadays understanding of mechanisms that underlie activity-dependent synaptic plasticity. In his famous postulate he proposed that the information is spread through the neuronal network with the synapses to be the site for modulation, leaving an imprint of memory:

"When an axon of cell A … [excites] cell B and repeatedly or persistently takes part in firing it, some growth process or metabolic change takes place in one or both cells so that A's efficiency as one of the cells firing B is increased." (Hebb, 1949)

The general concept is based on the fact that synapses of two neurons that fire simultaneously both enhance their strength paralleled to pre- and postsynaptic activity. On the molecular base this is accompanied by biochemical and structural modifications resulting in an enhanced communication efficacy between previously active neurons. These alterations represent the basis for processes of learning and memory. An intensely studied structure shown to be crucial for the formation of long-term memory is the hippocampus.

1.1.1 The Hippocampus

Anatomically the hippocampus belongs to an evolutionary old part of the cortex, the limbic system. It is localized bilaterally in both cerebral hemispheres displaying a characteristic curved shape. The Hippocampus is indispensable for memory consolidation. This process is the transfer of short- into long-term memory which is stored by distinct cortical regions receiving hippocampal projections. The knowledge that the declarative memory formation (facts, events) is essentially based on the hippocampus was initially proven half a century ago in studies of the amnesic patient "H.M.". After removal of both hippocampi in an epilepsy surgery, he could no longer form new declarative memories. His short-term and working memory functions were still intact as well as the acquisition of new non-declarative memories (Scoville and Milner, 1957).

In addition, the hippocampus is essential for the cognitive map formation about the environment. Evidence was gained by investigating rodents with a hippocampal lesion which precludes spatial memory formation in the Morris water maze (Mumby et al., 1999). This feature makes the hippocampus suitable for investigating Alzheimer's disease (AD) since spatial navigation as well as short-and long-term memory is severely affected. It is also the first brain region affected in AD exhibiting an extensive neuronal loss accompanied by volume reduction.

The hippocampus is part of the hippocampal formation which is a complex structure consisting of fornix, fimbria, subiculum, dentate gyrus (DG) and the *cornu ammonis* (CA). A further subdivision distinguishes 4 subfields CA1, CA2, CA3 and CA4 with a characteristic pyramidal neuron distribution whereby traditionally only CA3 and CA1 are illustrated (Figure 1.1 A and B).

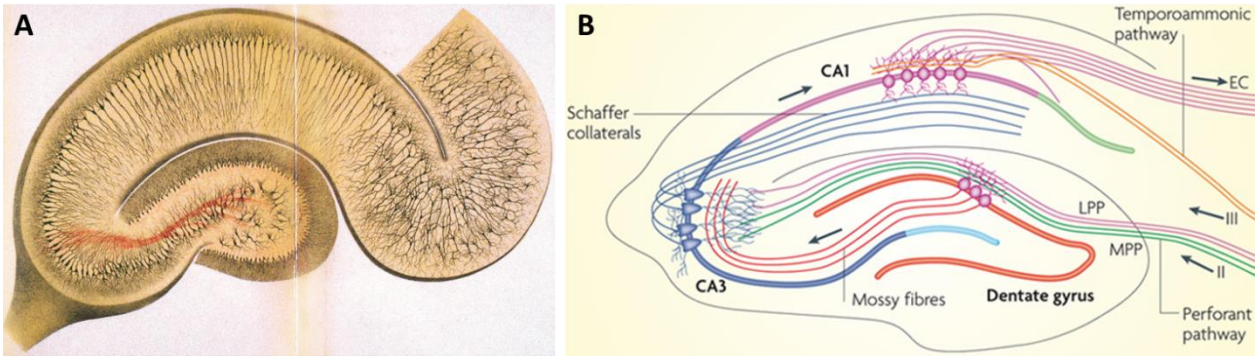

Figure 1.1 The neuronal circuitry in the rodent hippocampus.
(A) *Drawing of the hippocampus and the prevalent neuronal cell types from Camillo Golgi (Golgi et al., 2001). Red fibers are blood vessels.* ***(B)*** *Scheme of a transversal slice from the hippocampus depicting the major input and output fibers as well as projections from the intrinsic trisynaptic circuitry (Deng et al., 2010). CA = cornu ammonis, EC = entorhinal cortex, LPP = lateral performant pathway, MPP = medial performant pathway.*

DG, CA3 and CA1 are three clearly differentiated structures along the longitudinal axis. This enables to analyze specific synaptic contacts in between these subregions since the distribution of somata and the axonal projections are highly organized following the intrinsic trisynaptic circuitry (Figure 1.1 B). Histologically the hippocampus displays 3 characteristic layers (Figure 1.2). In CA1 and CA3 the *stratum pyramidale* comprises the somata of pyramidal neurons already illustrated by Camillo Golgi (Figure 1.1 A and Figure 1.2). Their basal dendrites are located in the *stratum oriens* while the apical dendrites form the *stratum moleculare* which is subdivided into the *stratum radiatum* and *lacunosum-moleculare* (Figure 1.2). Importantly, the inner layer *stratum lacunosum-moleculare* of the CA1 and CA3 region receives direct or indirect input from the entorhinal cortex (EC) which itself is connected to various cortical areas (Figure 1.1 B). The DG comprises the granular cell layer and receives the major input via the perforant pathway from the adjacent EC layer II. The axons of the granular cells pass on their information via mossy fibers onto the dendritic compartment of CA3 pyramidal neurons. Those send their bundled axonal projections as Schaffer collaterals onto the dendrites of CA1 pyramidal neurons (Figure 1.1 B). The main source of hippocampal output via the subiculum targets again the EC but also the amygdala. As a unique feature of the hippocampal formation each field is linked and thus permits an unidirectional information flow. The majority of neurons is excitatory (~95 %) using glutamate as neurotransmitter. However, a projection from the *medial septum* provides excitatory input by cholinergic and inhibitory input by GABAergic fibers to all hippocampal subregions acting as rhythm generator (Buzsaki, 2002; Drever et al., 2011). The interneurons have locally restricted target regions in the hippocampus itself and characteristically bear few or no spines at all (Freund and Buzsaki, 1996). In the DG those inhibitory neurons are represented by basket cells from which axons project directly onto the somata of granule cells. Moreover, axo-axonic neurons target the initial segments of excitatory pyramidal neurons and thus influence action potential initiation. Finally, bistratified cells project onto apical and basal dendrites of pyramidal neurons. All interneurons are inter-connected to ensure synchronization.

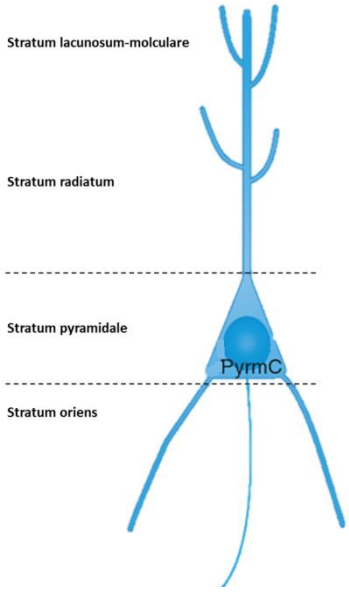

Figure 1.2 Hippocampal layers in the CA3 and CA1 region. PyrmC: pyramidal neuron.

Thereby they display oscillations with variable frequencies like theta (5 Hz) and gamma (40 Hz) (Buzsaki, 2002; Colgin and Moser, 2010). Destruction of the septal area abolishes the hippocampal theta rhythm and impairs spatial memory (Winson, 1978). Additionally, these interneurons send their dendrites to the *stratum radiatum* and *stratum oriens* receiving input from surrounding excitatory neurons to modulate the network activity by feed-forward and -backward inhibition.

The highly organized hippocampal structure is well suited to study the mechanisms of Hebbian plasticity in various transgenic mouse models. For the purpose of this dissertation the electrophysiological investigations focused on the CA3 to CA1 Schaffer collateral pathway whereto the stimulation as well as recording electrodes are positioned in the *stratum radiatum* of the respective hippocampal subregions (see 2.4.3 and Figure 2.2).

1.1.2 Bidirectional Plasticity: Long-term Potentiation and Long-term Depression

At the end of the 19th century Ramon y Cajal postulated that processes of learning and memory are fulfilled by neurons and their specific connections. Moreover, he hypothesized that new neuronal pathways are formed upon learning (Cajal, 1907). These suggestions were supported by Donald O. Hebb (Hebb, 1949). He intended to understand how perceptual memory works from the systemic down to the cellular/molecular level. He combined prevailing data of behavior, like the acquisition of conditioned reflexes shown by Pavlov, to the neurons as sites of changes during memory acquisition. The Hebbian postulate states that interconnected and simultaneous active neurons permanently enhance their effectiveness. This process is required for strengthening and stabilization of synaptic connection in neuronal networks and the formation of associative memories. However, Hebb himself didn't mention the nowadays well established importance of the hippocampus for learning and memory. It was first implicated in 1973 when Bliss and colleagues discovered the Long-Term Potentiation (LTP) and proposed this process as a cellular correlate for activity-dependent modulation of synaptic efficacy. They reported a long lasting, hours or even days, increase of synaptic transmission in neurons of the dentate gyrus after *in vivo* tetanic stimulation of the perforant path (Bliss and Gardner-Medwin, 1973; Bliss and Lomo, 1973; Bliss and Collingridge, 1993). To date this concept of LTP is widely

used to assess memory related processes at the cellular and molecular level (Pastalkova et al., 2006; Whitlock et al., 2006; Kenney and Manahan-Vaughan, 2013).

Since several observations could not be explained by LTP alone, it was presumed that excitatory synapses also undergo an activity-dependent reduction in efficacy, termed Long-Term Depression (LTD) (Dudek and Bear, 1992). This discovery indicates that long-term plasticity is bi-directionally modifiable (Dudek and Bear, 1993; Heynen et al., 1996; Malenka and Bear, 2004). Those studies focused on CA3-CA1 Schaffer collateral pathway and identified the N-methyl-D-aspartate receptor (NMDAR) as a major component for LTP and LTD, respectively (Collingridge et al., 1983; Collingridge et al., 1988). The NMDAR is an ionotropic receptor for its ligand glutamate and the co-agonist glycine or D-serine (Henneberger et al., 2013). Through its pore extracellular Na^+ and Ca^{2+} enter the postsynapse. Although synaptic plasticity clearly depends on the activation of NMDARs, as pharmacological blocking studies showed (Morris, 1989), it doesn't contribute to the basal synaptic transmission (Figure 1.3). This is predominately mediated by the α-amino-3-hydroxy-5-methyl-4-isoxazole propionic acid receptor (AMPAR) which becomes permeable for monovalent cations Na^+ and K^+ when glutamate is bound. Meanwhile, the NMDARs are inactive as the ion channel pore is occluded by Mg^{2+} (Mayer et al., 1984; Nowak et al., 1984). The influx of Na^+ through AMPARs induces an Excitatory Postsynaptic Potential (EPSP). Upon stimulation the membrane depolarizes thereby expelling the Mg^{2+} block from the NMDAR channel. If simultaneously glutamate is bound, the NMDARs become permeable for Na^+ and Ca^{2+}. This characterizes the receptor as a coincidence detector being only conductive when pre- and post-synapse are co-active. These findings furthermore define the first of three key features of LTP (Nicoll et al., 1988). The associativity means that in a pairing protocol a weak and a strong synaptic input induce LTP at both synapses (Wigstrom et al., 1986). Another characteristic is input specificity whereby merely synaptic contacts of neurons are modified which participate in network activity. The postsynaptic compartment is formed as dendritic spine, a bottleneck like shaped protrusion, being separated from the less electrically active dendrite. However, when the postsynaptic membrane is depolarized this is conducted through the spine to the dendrite. This feature is termed cooperativity showing that LTP can only be induced by the coincident activation of a critical number of synapses by repetitive stimulation.

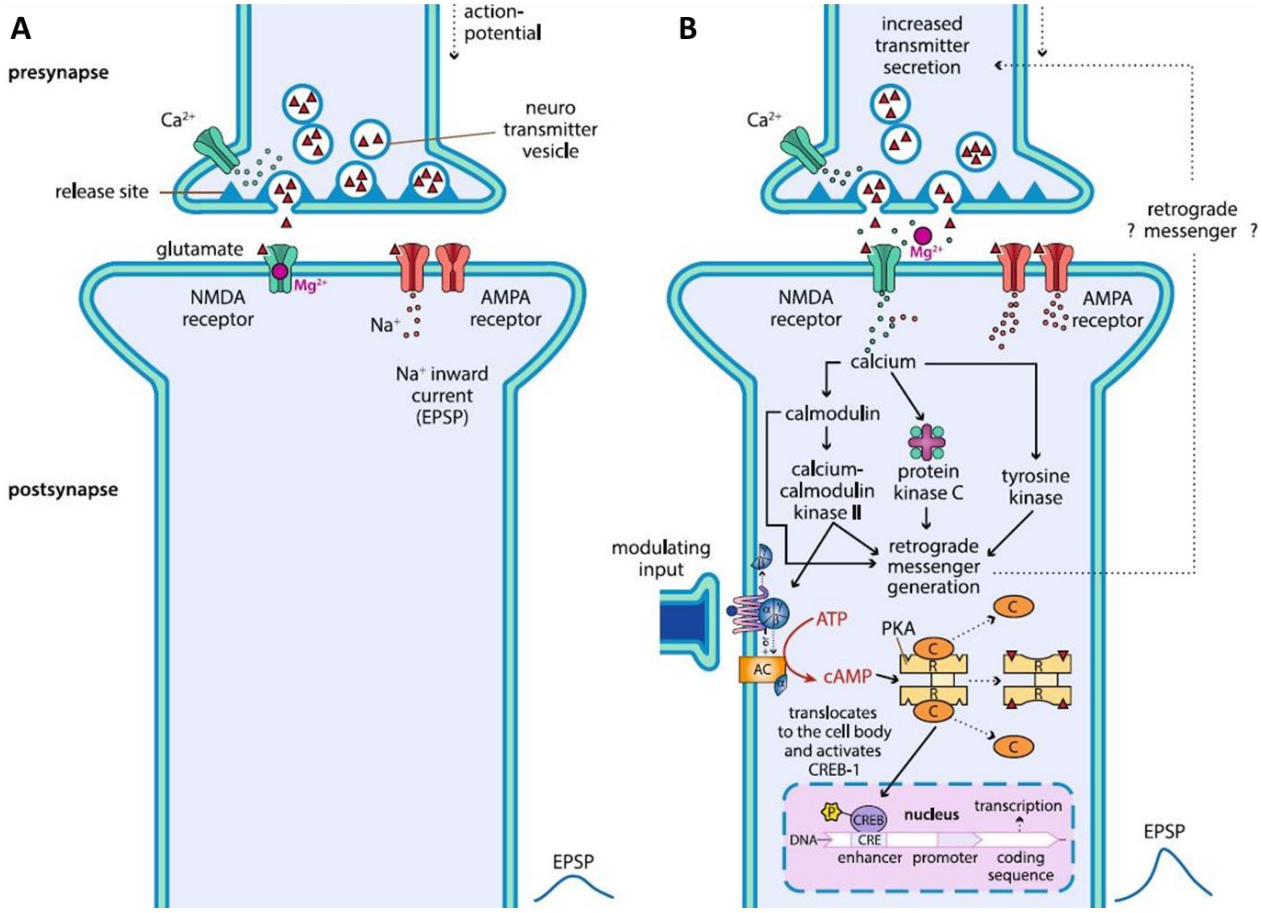

Figure 1.3 Mechanism of LTP induction.
(A) *During basal synaptic transmission only a low amount of glutamate is released from the presynapse binding to NMDA and AMPA receptors respectively. Since the NMDAR is blocked by Mg^{2+}, only AMPAR promote the influx of monovalent kations generating an excitatory postsynaptic potential (EPSP) in the postsynaptic compartment.* ***(B)*** *In case of postsynaptic membrane depolarization the Mg^{2+} is removed from the ion channel of the NMDAR. Thus, in addition more kations enter the postsynape. One of these is Ca^{2+} which functions as a potent second messenger triggering various biochemical cascades to promote Long-Term Potentiation (LTP) and strengthening of the synaptic transmission. In case of LTP the massive and rapid influx of Ca^{2+} predominately activates kinases and modulates gene expression to maintain the potentiation for long lasting changes. The figure is reproduced from (Galizia and Lledo, 2013). However synaptic plasticity is bidirectional therefore a decrease in synaptic transmission is observed when Long-Term Depression (LTD) is induced. The inflow of Ca^{2+} through NMDAR is thereby slow and prolonged activating predominately phosphatases (not shown in the scheme).*

At hippocampal Schaffer collateral synapses LTP and LTD primarily depend on Ca^{2+} influx being a potent second messenger. It initiates a series of intracellular biochemical signaling cascades that promote the strengthening or weakening of synapses (Figure 1.3). Supportive studies implicated that postsynaptically chelated Ca^{2+} abolishes LTP and LTD respectively (Lynch et al., 1983; Cummings et al., 1996a).

In terms of LTP upon a high frequency stimulation a robust but relatively short Ca^{2+} influx through NMDARs activates mainly effector kinases which display a low affinity to Ca^{2+} (Bliss and Lomo, 1973). The most prominent is the calcium / calmodulin-dependent kinase II (CaMKII) confirmed by studies with inhibitors and gene-targeted mice for this kinase, which all lead to an impairment in LTP (Malenka et al., 1989; Malinow et al., 1989; Silva et al., 1992). The NMDAR driven rise of intracellular Ca^{2+} permits CaMKII activation by autophosphorylation. Amongst numerous substrates it phosphorylates membrane associated AMPARs to further increase their conductance (Derkach et al., 1999; Lee et al., 2003; Whitlock et al., 2006; Kristensen et al., 2011). Recent studies show an enhanced accumulation of AMPARs at the PSD when CaMKII phosphorylates the scaffolding protein stargazin (Opazo et al., 2010). Interestingly, the number of AMPARs defines the strengths of synaptic transmission in response to stimulation. This is executed via two individual mechanisms. First, AMPARs can reach the PSD from the periphery by lateral diffusion (Takahashi et al., 2003). Second, receptor containing vesicles are inserted extra-synaptically via exocytosis (Patterson et al., 2010). Thus a relatively fast increase in synaptic strength is gained (Opazo and Choquet, 2011; Huganir and Nicoll, 2013). However, while this early phase of LTP is not protein synthesis dependent the maintenance of a long lasting (hours-days) increase in synaptic efficacy requires the expression of plasticity-related proteins (Krug et al., 1984; Frey et al., 1988; Otani and Abraham, 1989; Abraham and Williams, 2008; Rosenberg et al., 2014). In addition to CaMKII, one key molecule in this process is the atypical protein kinase C (aPKC) isoform PKMζ. During LTP it is synthesized *de novo* as a constitutively active kinase (Ling et al., 2002). Interestingly, its inhibition abolishes already established LTP, supporting its essential role in long-term plasticity (Sajikumar et al., 2005; Serrano et al., 2005; Pastalkova et al., 2006). However, its role is debated since PKMζ-KO mice lacked any defect in activity- dependent synaptic plasticity and memory formation (Lee et al., 2013; Volk et al., 2013). In later stages of LTP the link to gene expression is provided by the activity of adenylyl cyclase (AC) which itself is stimulated by CaMKII. AC mediated cAMP generation triggers protein kinase A (PKA) which directly or indirectly through ERK activates the cAMP response element-binding protein (CREB). As a transcription factor CREB initiates the expression of plasticity-related genes. Amongst those, immediate early genes like c-Fos and the

neurotrophin BDNF are shown to be crucial (Korte et al., 1995; Tao et al., 1998; Strekalova et al., 2003).

As the complementary bidirectional part to LTP the LTD is induced by a low frequency stimulation protocol initiating a moderate and prolonged Ca^{2+} influx through NMDARs (Lisman, 1989; Dudek and Bear, 1992; Cummings et al., 1996b). This in turn predominantly activates phosphatases which display a high affinity to Ca^{2+} (Mulkey et al., 1993). Main effects are thereby mediated through the complex of Ca^{2+} / calmodulin dependent phosphatase calcineurin, AKAP and PSD95 which internalizes AMPARs via endocytosis from the PSD (Lee et al., 1998; Beattie et al., 2000; Shepherd and Huganir, 2007; Jurado et al., 2010). Comparably to late phases of LTP, maintained LTD requires *de novo* protein synthesis likewise (Manahan-Vaughan et al., 2000; Sajikumar and Frey, 2003).

Beside NMDAR-dependent forms further mechanisms exist to enhance or decrease synaptic efficacy. Throughout the hippocampus metabotropic glutamate receptor (mGluR) mediated LTP and LTD are common (Mukherjee and Manahan-Vaughan, 2013). Furthermore, long lasting changes can also be conveyed exclusively or in addition to NMDARs by voltage gated calcium channels (VGCCs) promoting the influx of Ca^{2+} (Morgan and Teyler, 1999; Moosmang et al., 2005). Interestingly, DG-CA3 mossy fiber LTP and LTD are mediated through presynaptic mechanisms representing a non-Hebbian form of activity-dependent synaptic plasticity (Manabe, 1997; Lopez-Garcia, 1998). In that case the modulation of synaptic strength does not require a simultaneous pre- and postsynaptic depolarization for its induction.

The increase of cytosolic Ca^{2+} through NMDAR and/or VGCC activation stimulates supplementary Ca^{2+} release from internal stores of the endoplasmatic reticulum (ER) through ryanodine and inositol-1, 4, 5-tris-phosphate receptors. This causes the spread of LTP or LTD to neighboring, co-active synapses (Nishiyama et al., 2000; Maggio and Vlachos, 2014; Segal and Korkotian, 2014). The clearance of Ca^{2+} and restoration of basal Ca^{2+} concentrations is executed by the sarco / endoplasmatic reticulum Ca^{2+} ATPase (SERCA) pump. Another major player for the regulation of Ca^{2+} signals are mitochondria.

The functional increase or decrease of synaptic strength is accompanied by rapid equivalent structural changes of enlargement and shrinkage as well gain and loss of the dendritic spines (Ultanir et al., 2007; Bosch and Hayashi, 2012; Bellot et al., 2014). Modifications of the actin

cytoskeleton including enhanced polymerization for LTP and increased depolymerization for LTD are essential (Matsuzaki et al., 2004; Okamoto et al., 2004; Honkura et al., 2008).

Although LTP primarily considers a postsynaptic phenomenon, presynaptic mechanisms are likely to contribute to the observed alterations in synaptic efficacy (Figure 1.3). Through retrograde signaling the neurotransmitter release is increased further promoting the postsynaptic strengthening. Retrograde messengers like nitric oxide (NO) and the brain-derived-neurotrophic factor (BDNF) play a crucial role (Korte et al., 1995; Park and Poo, 2013).

1.1.3 Short-term and Long-term Synaptic Plasticity

The before described changes at the synapse in response to an alteration of activity reflect its ability to undergo synaptic plasticity. Briefly, two forms are distinguished regarding persistence. Long lasting changes which include four major processes: regulation of AMPA receptors, local protein synthesis, modulation of actin dynamics and gene expression in the nucleus (see 1.1.2). However, this is preceded by short-term plasticity which modulates synaptic strength for seconds up to minutes and mechanistically is thought to underlie information processing.

An action potential, generated near the cell body, propagates along the axon directed to the presynapse where it opens voltage-gated Ca^{2+} channels. A transient elevation of presynaptic Ca^{2+} through short bursts of activity is crucial to enhance the fusion probability of neurotransmitter bearing vesicles at the active zone and induces short-lived synaptic modulations (Katz and Miledi, 1968). Therefore, the analysis of short-term plasticity predicts presynaptic functionality. A simple protocol to test presynaptic properties is to apply two single stimuli spaced by a defined time interval. Depending on the length of the Inter Stimulus Interval (ISI) and type of stimulus used the second signal is facilitated (Paired Pulse Facilitation, PPF) or depressed (Paired Pulse Depression, PPD). At shorter ISIs of <20 ms PPD is observed whereas larger ISIs >20 ms lead to PPF. Several factors contribute to PPD (Figure 1.4 a). Importantly the Readily Releasable Pool (RRP) is depleted. More vesicles fuse to the membrane in response to the initial stimulus thus fewer vesicles are available for the second stimulus. The lack of vesicles in the RRP is refilled within seconds by the recycling pool (Zucker and Regehr, 2002). Furthermore, voltage gated Ca^{2+} channels are inhibited (Catterall and Few, 2008).

PPF is characterized by the residual Ca^{2+} hypothesis (Figure 1.4 b). In response to an arising action potential from the first stimulus the presynaptic Ca^{2+} level is elevated inducing the neurotransmitter release. The remaining / residual Ca^{2+} drives an increased release upon the second stimulus leading to a facilitated second signal (Zucker and Regehr, 2002; Regehr, 2012) (see Figure 2.3 D). Still additional mechanisms are proposed. Complementary to PPD voltage gated Ca^{2+} channel conductance is enhanced (Catterall and Few, 2008; Mochida et al., 2008). Likewise, the facilitation is additionally regulated by presynaptic Ca^{2+} sensor kinases with different Ca^{2+} affinities and saturation of Ca^{2+} buffering proteins leading to more unbound Ca^{2+} increasing the neurotransmitter release upon the second stimulus (Zucker and Regehr, 2002; Matveev et al., 2004; Mochida et al., 2008; Regehr, 2012).

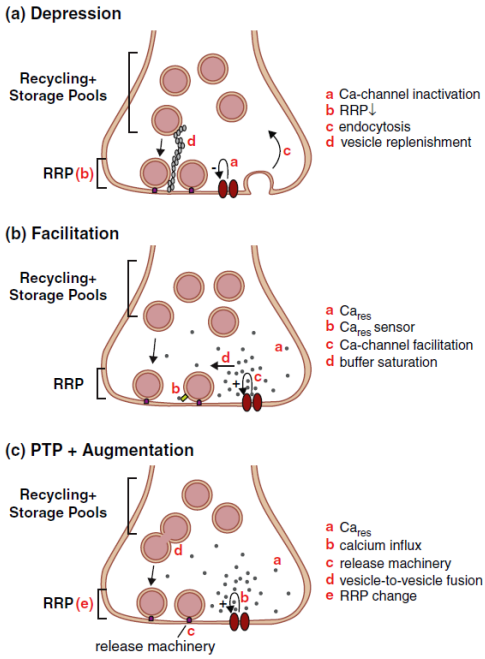

Figure 1.4 Presynaptic mechanisms of short-term plasticity.
Schematic drawing depicts proposed mechanism for ***(a)*** *depression,* ***(b)*** *facilitation,* ***(c)*** *post-tetanic potentiation (PTP) and augmentation. Readily releasable pool (RRP); residual calcium (Ca_{res}). The figure is reproduced from (Fioravante and Regehr, 2011).*

Upon high frequent tetanic stimulation longer persistent forms of short-term plasticity occur termed augmentation, lasting five to ten seconds, and Post-Tetanic Potentiation (PTP), lasting tens of seconds to minutes (Figure 1.4 c). However, a distinction between both phenomena is not always clear. Mechanistically an increased transmitter release is proposed resulting either from an elevated presynaptic Ca^{2+} influx or a modification of the release machinery (Zucker and Regehr, 2002; Regehr, 2012). Additionally, Ca^{2+} independent mechanisms such as PKC activity increase release probabilities by decreasing the Ca^{2+} cooperativity thus more free Ca^{2+} is available (Korogod et al., 2007; Lou et al., 2008). Moreover, tetanic stimulation causes fusion of neurotransmitter vesicles (Figure 1.4 c) before they fuse to the membrane thus increasing the miniature synaptic current (He et al., 2009). Short- and long-term synaptic plasticity is a feature of neurons that is preserved throughout lifetime in an intact brain. However, these processes are tightly regulated and an imbalance contributes to the establishment of neurodegenerative diseases. For the current understanding thereby the synapse is the first location affected.

1.2 Alzheimer's Disease

In 1901 the psychiatrist Alois Alzheimer examined a patient named Auguste Deter who suffered from disorientation, progressive memory loss, depression and finally died at an age of 55. Alzheimer described his observations from brain autopsy as an *"unusual disease of the cerebral cortex"* which was accompanied by a "*paucity of cells in the cerebral cortex and clumps of filaments between nerve cells"* later on named Alzheimer's Disease (AD) (Alzheimer, 1907). In today's widely used terminology he already found the two major pathological processes of tau (neurofibrillary tangles, NFT) and amyloid beta deposition (Aβ or senile plaques). With ~50-60 % of cases AD is the most common form of dementia from which currently ~35 million people suffer. The risk to develop this disease increases dramatically with age and life standard. Therefore, it is predicted that every 20 years the incidence of AD will almost double (Wimo et al., 2013). Since its discovery many scientific breakthroughs led to more insights of this disease. However, besides the knowledge that NFT and Aβ plaques are major hallmarks additionally molecular, genetic, epidemiological as well as immunological hypothesis have been proposed to contribute to AD (Heneka and O'Banion, 2007; Povova et al., 2012; Heneka et al., 2014). To date the cause of AD remains unidentified. Recent studies suggest that the onset already starts 10-20 years before clinical symptoms occur (Perrin et al., 2009). The early stage of mild AD is characterized by difficulties in short-term memory and decline of cognitive abilities while the more proceeded and severe stage includes loss of long-term memory and inability of handling daily life (Holtzman et al., 2011). At the microscopic level this is accompanied by a high density NFT and Aβ plaques as well as extensive neuronal loss. NFT are intracellular agglomerations of the microtubule-associated, stabilizing protein tau which is hyperphosphorylated and bears oxidative modifications (Goedert et al., 1988; Goedert and Spillantini, 2006). Tau detaches from the microtubules and accumulates in the somato-dendritic compartment thereby disturbing cellular transport mechanisms (Spillantini and Goedert, 2013). First, entorhinal cortex layer II neurons are affected by NFT formation (Hyman et al., 1987). Progressive spreading and additional tau propagation throughout the neurons of the hippocampal formation have been shown (Braak and Braak, 1991; de Calignon et al., 2012). However, it was proposed that NFT alone contribute less to neuronal death in AD than Aβ plaques (Gomez-Isla et al., 1997). After Aβ was proven to be the major component of plaques a lot of effort has been made to

understand its origin, function and pathology (Masters and Selkoe, 2012; Spires-Jones and Hyman, 2014). Plaque deposition occurs early in AD and progresses with time (Beyreuther and Masters, 1991). However, recent studies showed that soluble Aβ oligomers are the toxic species rather than dense plaques of aggregated Aβ causing synaptic dysfunction and less connectivity finally leading to neuronal loss (Schaeffer et al., 2011). Aβ oligomers are supposed to disrupt mechanisms involved in synaptic plasticity most likely by influencing the NMDAR dependent regulation of the spine cytoskeleton (Hsieh et al., 2006a; Selkoe, 2008). Furthermore Aβ was shown to reduce surface expression of both AMPAR and NMDAR (Almeida et al., 2005; Snyder et al., 2005; Hsieh et al., 2006b). This is in line with the observation that Aβ can disrupt LTP at nanomolar concentrations (Selkoe, 2008; Shankar et al., 2008). However, it was also shown that a concentration of picomolar Aβ acts contrariwise by positively modulating synaptic plasticity in the healthy brain (Puzzo et al., 2008; Puzzo et al., 2011).

Processes of activity-dependent synaptic plasticity are tightly linked to an intact Ca^{2+} homeostasis. In AD it is proposed that calcium dynamics is perturbed probably by downstream cascades of the NMDAR and thus contributes to the functional impairment. Aβ was shown to directly bind to NMDAR thereby causing hyperexcitability accompanied by increased intracellular Ca^{2+} levels (LaFerla, 2002; Popugaeva and Bezprozvanny, 2013). Indeed, it is still an intriguing question how other APP cleavage products like non-Aβ polypeptides additionally contribute to AD pathology by their reduced generation itself or modulating gene expression (Nhan et al., 2014). Nevertheless, independent of the role of APP and its proteolytic cleavage products in the disease status, their physiological functions in the healthy brain are still poorly understood.

1.3 Amyloid Precursor Protein Family Members

The Amyloid Precursor Protein (APP) gene is localized at the chromosome 21. Its expression results in a ~87 kDa protein which is found in three major isoforms (APP_{695}, APP_{751}, APP_{770}) generated by alternative splicing and posttranslational modifications. Depending on isoforms electrophoretic separation gives rise to bands of 110-140 kDa. APP_{695} is the predominant isoform in neurons (Robakis et al., 1987; Yoshikai et al., 1990). APP is synthesized in the ER

where it is shown to form stable dimers which are in turn transported through the secretory pathway via the Golgi apparatus to the cell surface (Isbert et al., 2012; Tan and Evin, 2012). Furthermore, APP is classified as a type I transmembrane glycoprotein revealing one membrane spanning domain, a large extracellular N-terminus and a small intracellular C-terminus illustrated in Figure 1.5 (Dyrks et al., 1988).

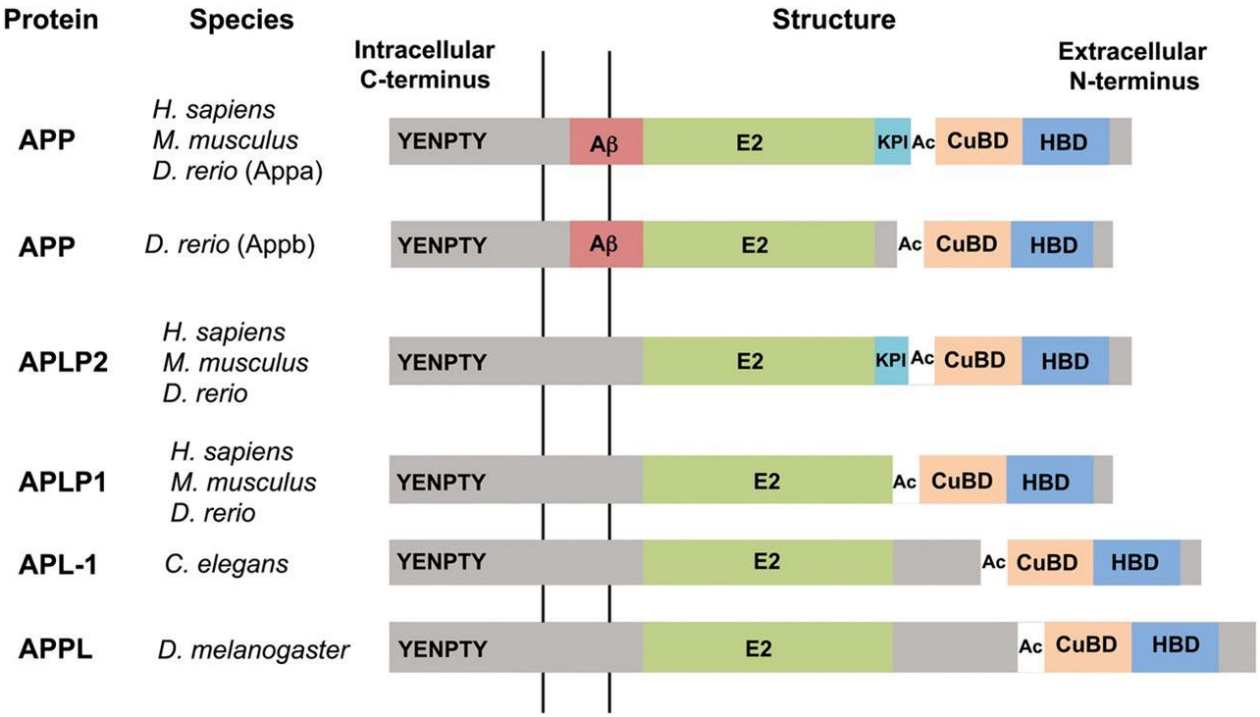

Figure 1.5 The domain structure of APP family members.
The domain structure of APP and its homologs is displayed for human (H. sapiens), mouse (M. musculus), zebrafish (D. rerio), worm (C. elegans) and fruit fly (D. melanogaster). All members share a high degree of homology regarding the large extracellular N-terminus always composed of the heparin-binding domain (HBD), copper-binding domain (CuBD), acidic (Ac) domain, E2 domain and the short intracellular C-terminus which includes the YENPTY motif. Across the different species the Aß sequence is exclusively present in APP. The Kunitz protease inhibitor (KPI) domain is also found in APP and APLP2. The figure is reproduced from (Nicolas and Hassan, 2014).

Its structure is widely conserved though species with APL-1 in *C. elegans*, APPL in *Drosophila* as well as APPa and b in zebrafish *D. rerio* (Nicolas and Hassan, 2014). The mammal APP is part of a larger gene family including the paralogues Amyloid Precursor-Like Proteins 1 and 2 (APLP1 and APLP2) which are prevalently expressed throughout the body (Wasco et al., 1993; Aydin et al., 2012). APP and APLP2 are widespread found in the brain with a particular high expression and largely overlapping pattern in pyramidal neurons of cortex and hippocampus (Bendotti et al., 1988; Lorent et al., 1995). The APP family members differ only slightly in their peptide domain

structure and are therefore highly homological displaying a similar proteolytic processing (Figure 1.5 and see 1.3.1). The intracellular part consists of a small C-terminus termed APP intracellular domain (AICD) which contains the YENPTY motif. This is shown to promote various functions like clathrin mediated endocytosis, modulation of Aβ generation, interference with Ca^{2+} homeostasis, interaction with multiple kinases and adapter proteins (Perez et al., 1999; Leissring et al., 2002; Hamid et al., 2007; Ring et al., 2007; Jacobsen and Iverfeldt, 2009). The extracellular part of APP is composed of the large E2 and E1 domains. The latter is further subdivided into Kunitz protease inhibitor domain (KPI), acidic domain (Ac), copper-binding domain (CuBD) and heparin-binding domain (HBD). All of them are interaction sites for multiple binding partners like F-spondin, LRP1, Nogo-66 receptor, Notch 2, Netrin, Alcadein, sorL1/LR11 and extracellular matrix components (Muller and Zheng, 2012). Additionally, the E1 domain was shown to be crucial for the homo- and heterodimerization of APP family members (Soba et al., 2005). Interestingly, the Aβ motive is unique for APP only, conserved in mammals and zebrafish while the APLPs lack this sequence.

Although the structure of both APP and APLPs are well known the precise function remains mostly elusive. Extensive posttranslational modifications and the various cleavage products of APP and APLP processing (see 1.3.1) hampered investigations. Nevertheless, several studies assessed putative functions and evidenced a crucial role in the developing as well as the mature nervous system (Jacobsen and Iverfeldt, 2009) (see 1.3.2). Interestingly, constitutive APP-KO mice showed no overt LTP defect at 3-4 months but surprisingly at 12-13 months of age hinting towards an APP involvement in age-related processes (Dawson et al., 1999; Seabrook et al., 1999; Ring et al., 2007). This was rescued by the constitutive expression of the neurotrophic APPsα fragment (Ring et al., 2007). However, to date the mechanism, for instance a putative receptor for this peptide which mediates that effect, remains unknown. Transgenic mouse models of either APP, APLP1 or APLP2 single knock-out show only subtle abnormalities (Muller et al., 1994; Magara et al., 1999; Ring et al., 2007), whereas combined APP/APLP2 double knockout (DKO) and APLP1/APLP2 DKO mice die perinatally (von Koch et al., 1997; Heber et al., 2000). In contrast, APP/APLP1 DKO are viable suggesting an essential function of APLP2 in the absence of either APP or APLP1 (Heber et al., 2000). The triple KO displayed cortical dysplasia caused by defective neuronal migration and died with a penetrance of 100 % (Herms et al.,

2004). However, these studies were hampered by partially redundant functions within the gene family. Intensive studies revealed that the lethality of DKO mice most likely based on important functions of APP and APLP2 at the neuromuscular junction. Double KO mice expressing solely APPsα rescued the mortality of APP/APLP2 DKO. Still, those mice displayed a muscular weakness probably caused by an abnormal neuromuscular junction morphology and a defect in transmitter release (Weyer et al., 2011). To bypass lethality but providing also the possibility to investigate a full DKO of both proteins, mice with a conditional APP/APLP2 DKO were generated and further analyzed regarding activity-dependent synaptic transmission in this study.

1.3.1 Processing Pathways

All members of the APP protein family undergo a comparable way of sequential cleavage by specific secretases since they display a high degree of homology (Figure 1.5) (Walsh et al., 2007; Jacobsen and Iverfeldt, 2009). Thus, only the proteolytic processing of APP will be described in detail. For APP two different catabolic pathways including three distinct cleavage events are known (Figure 1.6).

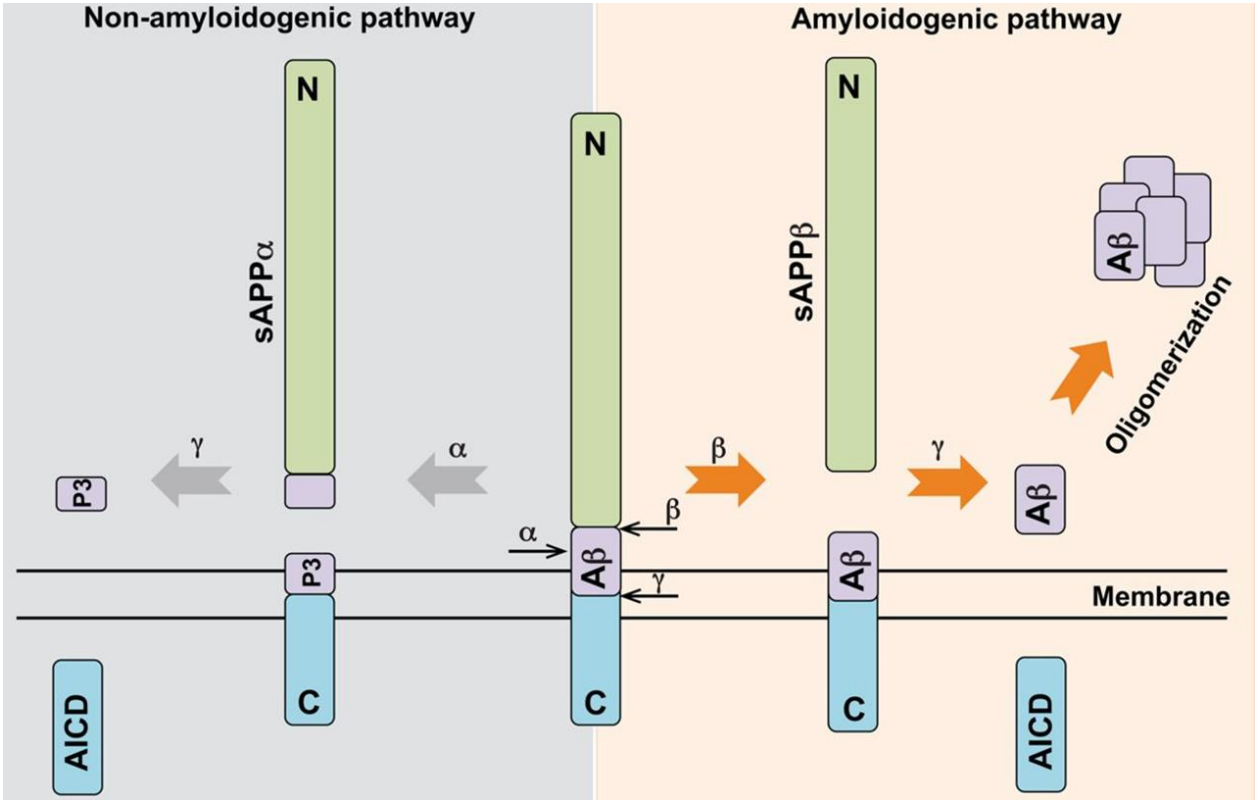

Figure 1.6 The proteolytic processing of APP (previous page).
Full-length APP can be processed by α-, β- and γ-secretases respectively. Thereby, two general pathways are distinguished. The left panel depicts the non-amyloidogenic pathway in which APP is cleaved by the α-secretase precluding Aβ formation since this protease cuts within the Aβ sequence. This processing liberates the soluble APPα (sAPPα or APPsα) fragment at the extracellular side. The remaining membrane bound fragment is then cleaved by the γ-secretase giving rise to the small P3 fragment extracellular and the AICD domain intracellular. The right panel illustrates the amyloidogenic pathway of APP shedding. First β-secretase action results in the secretion of sAPPβ (APPsβ). Subsequent γ-secretase shedding of the membrane tethered fragment gives rise to the extracellular released Aβ and again the intracellular AICD fragment. The figure is reproduced from (Nicolas and Hassan, 2014).

In a healthy organism the full length APP is predominantly (>90 %) cleaved via the non-amyloidogenic pathway in which first the α-secretase cuts within the Aβ domain liberating the large APPsα ectodomain. Thus, Aβ generation is precluded. Subsequently, the membrane-associated C83 fragment is truncated by the γ-secretase resulting in the intracellular released AICD peptide and extracellular secreted p3. Alternatively, a minor amount of full length APP (<10 %) is processed in the amyloidogenic pathway which involves a sequential cleavage by the β-secretase giving rise to the extracellular secreted APPsβ domain. Afterwards, the γ-secretase activity initiates an internal release of the AICD peptide and extracellular secretion of Aβ by shedding of the remaining membrane bound C99 (Jacobsen and Iverfeldt, 2009; Octave et al., 2013). Originally, the non-amyloidogenic processing pathway was thought to be the physiological one since pathological Aβ generation was prevented. However, this was not supported experimentally since during steady state only a small fraction of full length APP (~10 %) was membrane embedded whereas the majority was present in the golgi apparatus and the trans-golgi-network (TGN) (Thinakaran and Koo, 2008). Additionally cell-surface expressed APP reveals a relatively short half-life time of ~10 min and also β- and γ-secretase APP cleavage occurs under physiological conditions (Haass et al., 1992; Koo et al., 1996).

The α-secretases ADAM10, ADAM17/TACE, ADAM9, ADAM19, being all members of a disintegrin and metalloproteinase (ADAM) family, were indicated in APP cleavage at the cell surface (Howard et al., 1996; Buxbaum et al., 1998; Koike et al., 1999; Lammich et al., 1999; Allinson et al., 2003). ADAMs consist of a constitutive and a regulatory component which can be activated by synaptic activity or protein kinase C, triggering APPsα liberation (Nitsch et al., 1992; Buxbaum et al., 1993; LeBlanc et al., 1998; Hoey et al., 2009; Malinverno et al., 2010). It is still debated whether all or only one ADAM family member mediates the α-cleavage. However,

several publications point towards ADAM10 to be the principal constitutive APP α-secretase. This was shown by an overexpression model of ADAM10 in various cell lines leading to a several fold APPsα increase and decreased Aβ secretion, respectively (Kojro et al., 2001; Postina et al., 2004). Moreover, neurons of conditional ADAM10 KO mice or cells with a knock down of ADAM10 show an almost abolished APPsα generation (Jorissen et al., 2010; Kuhn et al., 2010). Consistently, cells or mice being deficient of ADAM17 or 9 failed to show a defect for APPsα production. Nevertheless, an overexpression led to an increase of APPsα under defined conditions suggesting an involvement of ADAM17 and 9 in a more regulated APP cleavage (Weskamp et al., 2002; Kuhn et al., 2010).

The initial and rate-limiting cleavage step in the amyloidogenic pathway is executed by β-secretase BACE1 (β-site APP cleaving enzyme) belonging to the class of aspartyl proteinases (Vassar, 2004). It is likely that APP is internalized and processed via the amyloidogenic pathway since BACE1 was shown to predominantly localize in the golgi apparatus, TGN, secretory vesicles and endosomes (Koo and Squazzo, 1994; Perez et al., 1999; Vassar et al., 1999). Moreover, an abolished Aβ generation in BACE1 KO mice suggests that a sequential cleavage of APP is necessary and that BACE1 is the only β-secretase (Cai et al., 2001).

A widely accepted model is the competition between α- and β-secretase mediated APP processing (Lichtenthaler et al., 2011). In both APP processing pathways the membrane bound fragment is subsequently cleaved by the intramembrane localized γ-secretase. Distinct to α- and β-secretases the γ-secretase is a large complex composed of four major protein subunits including presenilin 1 or 2 (PSEN1 or PSEN2) forming the catalytic core, presenilin enhancer (PEN-2), anterior pharynx-defective 1 (APH-1) and nicastrin (Vetrivel et al., 2006). Mice overexpressing presenilins with familiar AD mutations reveal an elevated amount of Aβ suggesting that this highly contributes to AD in forcing plaque formation (Duff et al., 1996). Remarkably, APP itself was shown to modulate the cell surface delivery of Presenilin 1 (Uemura et al., 2011). Note that all secretases involved in APP processing additionally have various other substrates which should be taken into account under the aspect of being therapeutic targets in AD (Lee et al., 2002; Edwards et al., 2008; De Strooper et al., 2010; Lichtenthaler, 2012).

1.3.2 Physiological Functions of APP and its Cleavage Products

The physiological role of the APP family members and their cleavage products has been intensively studied during the last two and a half decades. Numerous studies point towards an outstanding role of the ectodomain APPsα, liberated by α-secretase shedding, which is primarily associated with trophic properties. *In vitro* this fragment was shown to alter the growth of various cell lines and neurons (Pietrzik et al., 1998; Young-Pearse et al., 2008). Infusion of APPsα after traumatic brain injury enhanced survival of neurons as well as recovery processes (Thornton et al., 2006). Furthermore, a knock-in of APPsα circumvented lethality of APP/APLP2 DKO mice (Weyer et al., 2011). Comparable observations were made for *C. elegans* where the expression of the extracellular fragment rescued the lethal phenotype of APL-1 KO (Hornsten et al., 2007).

APP processing is highly comparable to that of Notch, a regulator of neuronal stem cell differentiation (Ables et al., 2011). Therefore, a similar function for APP is suggested (Kimberly et al., 2001). Several publications implicated APP in stimulating the proliferation of neuronal stem cells whereby it is still debated which cleavage product promotes this process. APPsα is a potential candidate exhibiting again rescue characteristics when the proliferation was reduced by an application of an α-secretase inhibitor (Demars et al., 2011; Baratchi et al., 2012). Moreover, APP overexpression or addition of APPsα enhances neuronal differentiation (Freude et al., 2011). On the contrary Hu and colleagues found an APP induced increase in proliferation that was not due to APPsα secretion but cystatin C release (Hu et al., 2013). These observations indicate that several mechanisms are involved which still need to be clarified. *In vitro* experiments suggested a role of APP and APPsα in neurite outgrowth which might mechanistically be promoted by cell-substrate as well as cell-cell adhesion (Gakhar-Koppole et al., 2008). Thereby, APP binds laminin, collagen and heparin but also forms homo- and heterodimers with APLP1 and APLP2 in cis- and trans-interaction (Kibbey et al., 1993; Beher et al., 1996; Clarris et al., 1997; Soba et al., 2005). In particular trans-dimerization of APP is proposed to stabilize synapses (Wang et al., 2009).

Analysis of aged constitutive APP-KO mice revealed abnormalities in behavior, synaptic plasticity and neuronal morphology suggesting a key role of APP and / or its processing products for both synaptic morphology and functional plasticity (Zheng et al., 1995; Ring et al., 2007; Weyer et al.,

2014). An altered synaptic function perhaps reasoned by an impaired excitation-inhibition balance was indicated by a paired pulse depression of GABA mediated inhibitory postsynaptic currents and a high susceptibility for kainite-induced seizures (Steinbach et al., 1998; Seabrook et al., 1999; Fitzjohn et al., 2000). Interestingly, APP-KO mice also display an age-related defect in learning behavior and LTP, represented in aged but not adult individuals (Dawson et al., 1999; Phinney et al., 1999; Seabrook et al., 1999; Ring et al., 2007). Thereby, APLP2 is suggested to overtake redundant functions in adult but not aged APP-KO mice (Weyer et al., 2011). A disturbed neuromuscular function is observed in lethal APP/APLP2 DKOs underlining the crucial function of APLP2 while APPsα-DM ($APPs\alpha^{+/+}APP^{-/-}APLP2^{-/-}$) are viable supporting the rescue ability of APPsα (Wang et al., 2005; Weyer et al., 2011). APP-family members are also implicated in regulating activity-dependent synaptic plasticity during learning and memory. These processes are tightly linked to NMDA receptors regulating the Ca^{2+} influx upon membrane depolarization. Several publications proposed that APP might affect intracellular Ca^{2+} by regulating the cell-surface expression of NMDAR as well as its subunit composition (Cousins et al., 2009; Hoe et al., 2009; Lee et al., 2010). Moreover, APP-KO mice displayed increased L-type Ca^{2+} channel levels which in turn impacts GABAergic short-term plasticity (Yang et al., 2009). LTP induction furthermore stimulated the APP processing which leads to APPsα secretion (Fazeli et al., 1994; Hoey et al., 2009). This suggests that APP and its processing under physiological conditions might be mandatory for the enhancement of synaptic transmission (Ishida et al., 1997; Seabrook et al., 1999; Taylor et al., 2008).

Since APP and Notch share comparable ways of processing, both interact with each other through their transmembrane domain and Notch has been shown to act as a receptor, APP might be a putative receptor as well (Selkoe and Kopan, 2003). Analog to Notch the γ-secretase processing of APP leads to an AICD fragment which was shown to translocate into the nucleus and modulate the gene expression in a co-complex with Fe65 (Gao and Pimplikar, 2001; Kimberly et al., 2001; Walsh et al., 2003).

Proposed physiological ligands which interact with the APP ectodomain are F-spondin, Dab1, Nogo66 receptor, LRP and SORL1 impacting Aβ generation (Wolfe and Guenette, 2007). Nevertheless, a definitive ligand that activates APP as a putative receptor so far remains elusive.

A recent study suggests an existence of a high-affinity receptor binding those fragments by interaction with the E1 domain (Reinhard et al., 2013). Amongst others p75 neurotrophin receptor and APP itself have been proposed to function as a receptor for APPsα (Bai et al., 2008; Gralle et al., 2009). However, the identification to date is still lacking. Potentially the main physiological contribution of APP is exerted via the ectodomains APPsα or APPsβ.

1.4 Scope of the Study

AD is accompanied by a progressive dysfunction of synaptic contacts between neurons, finally leading to a loss of first the synapse itself, followed by cell death. The hippocampus is the first regions affected by this process. A shift from the non amyloidogenic towards more amyloidogenic processing of the APP liberates additional Aβ which amongst other factors is the candidate to form toxic oligomers and plaques thereby initiating synaptic dysfunction. However, numerous studies implicate that not only Aβ accumulation but also the reduction of other potentially neurotrophic APP processing products might contribute to AD. Thus, it is in addition important to understand the physiological role of APP and its homologues APLP1 and APLP2 in the intact CNS. To assess the specific role of the APP protein family in processes of learning and memory I used different mouse models generated by gene targeted deletion of APP and / or APLP2 or their various cleavage products. Since APP and APLP2 display a high degree of homology a functional redundancy was shown. Recent studies suggest that a potential compensatory effect is only found in adult but not in aged transgenic mice, implicating an age related effect which is further assed in this study. The lethality of constitutive double knock-out mice (DKO) was circumvented by crossing $APP^{floxed/floxed}APLP2^{-/-}$ mice to specific Cre-deleter lines to apply the conditional approach. This provided the opportunity to distinguish between a potential developmental or acute function of the APP protein family members. Furthermore, I assessed whether the α-secretase cleavage product APPsα might be capable to restore memory impairment in DKOs. I intensely studied the excitatory system since these neurons held the majority in the hippocampus. Nevertheless, inhibitory neurons contain APP and APLP2 as well and are essential to regulate network activity. Thus, I as well investigated mice with a conditional DKO restricted to GABAergic interneurons.

Given that the mammalian hippocampus is significantly involved in memory formation and the first region affected in the AD I focused my research on synaptic plasticity of the CA3-CA1 Schaffer collateral pathway. Complementary, I investigated whether deficits in Ca^{2+} dynamic mechanisms might be causative for this altered functional synaptic plasticity and if the defect might be rescued upon expression of solely APPsα in cultures from DKO mice representing a potential target for therapeutic means in AD.

2 Materials and Methods

2.1 Mice Strains

In this study a large variety of transgenic mice were investigated in order to elucidate the role of APP and its homologues in processes of synaptic plasticity. All of them were housed, genotyped and kindly provided by Prof. Dr. Ulrike Müller from the Rubrecht-Karls-University of Heidelberg. Table 2.1 gives an overview about the different genotypes. Thereby, two groups were categorized. On the one hand a constitutive APP / APLP2 knock-out strategy was applied. On the other hand an additional conditional knock-out strategy via Cre / loxP system was used to circumvent early postnatal lethality of double mutants (DM).

Table 2.1 Genotypes of APP and APLP2 transgenic mice.

Name	Genotype
Constitutive knock-out	
APLP2-KO	$APLP2^{-/-}$
APPΔCT15-DM	$APP\Delta CT15^{+/+}$ $APLP2^{-/-}$
APPsα-DM	$APPs\alpha^{+/+}$ $APLP2^{-/-}$
Conditional knock-out	
CaMKIIαCre cDKO	$CaMKII\alpha CreER^{T2\,+/T}$ $APP^{flox/flox}$ $APLP2^{-/-}$
NexCre cDKO	$NexCre^{+/T}$ $APP^{flox/flox}$ $APLP2^{-/-}$
GADCre cDKO	$GAD67Cre^{+/T}$ $APP^{flox/flox}$ $APLP2^{-/-}$
DlxCre cKO	$DlxCre^{+/T}$ $APP^{flox/flox}$
DlxCre cDKO	$DlxCre^{+/T}$ $APP^{flox/flox}$ $APLP2^{-/-}$
littermate control	$APP^{flox/flox}$ $APLP2^{-/-}$

2.1.1 Constitutive Knock-out of APP and APLP2

The basic principle for the generation of constitutive knock-out mice used in this study was the construction of gene targeting vectors containing the new coding sequence. In case of the desired $APLP2^{-/-}$ the gene was inactivated by deleting the promoter and the first exon of the APLP2 gene (von Koch et al., 1997). In case of $APP\Delta CT15^{+/+}$ knock-in the targeting vector contained the coding sequence of APP exon 16 to APP_{695}-cDNA up to amino acid 680 and a stop codon (APP lacked last 15 AS at the C-terminus) thus enabling to selectively replace the endogenous APP gene while the following expression is still realized via the endogenous promoter (Ring et al., 2007). Then the respective vector was inserted into murine embryonic

stem cells by electroporation. Positive clones which underwent homologous recombination were detected and transplanted into C57BL/6 blastocystes obtaining heterozygous chimeric mice. These mice were further intercrossed to generate homozygous individuals (APLP2$^{-/-}$ or APPΔCT15$^{+/+}$). APPΔCT15$^{+/+}$APLP2$^{-/-}$ double mutant mice (APPΔCT15-DM) were obtained by three consecutive intercrosses of APPΔCT15$^{+/+}$ and APLP2$^{-/-}$ mice (similar to APPsα-DM in (Weyer et al., 2011).

2.1.2 Conditional Knock-out of APP and APLP2 in Excitatory Forebrain Neurons

In order to bypass postnatal lethality of constitutive APP / APLP2 double knock-out individuals a conditional knock-out strategy solved that issue (Heber et al., 2000; Wang et al., 2005). Therefore, mice were generated in which the promoter as well as exon 1 of the APP or APLP2 gene was flanked by LoxP-sites (APP$^{flox/flox}$, APLP2$^{flox/flox}$) trough homologous recombination (Mallm et al., 2010). Mice carrying the APP$^{flox/flox}$ were bred with APLP2$^{-/-}$ mice to obtain individuals with conditional APP alleles on an APLP2 deficient background (APP$^{flox/flox}$APLP2$^{-/-}$). These mice built the foundation of further investigations as they could be crossed to various Cre-transgenic deleter strains which enable to selectively knock-out APP at defined time points and in a tissue specific manner. Note that the preference was given to APP$^{flox/flox}$APLP2$^{-/-}$ and not to APP$^{flox/flox}$APLP2$^{flox/flox}$ since APLP2$^{-/-}$ alone revealed no phenotype and the recombination of two different floxed alleles has a high chance to be incomplete.

In a first approach APP$^{flox/flox}$APLP2$^{-/-}$ were crossbred with a CaMKIIαCreER^{T2} strain resulting in a genotype of CaMKIIαCreER^{T2}APP$^{flox/flox}$APLP2$^{-/-}$ (Erdmann et al., 2007). This was characterized by a specific Cre-ER^{T2} expression in excitatory forebrain neurons. Cre-ER^{T2} is an inducible fusion protein composed of Cre recombinase and a mutated part of the human estrogen receptor (ER). As a synthetic ligand tamoxifen bound ER and thereby induced the translocation of the fusion protein from the cytoplasm into the nucleus, where APP excision was preceded. CaMKIIαCreER^{T2}APP$^{flox/flox}$APLP2$^{-/-}$ were mated with APP$^{flox/flox}$APLP2$^{-/-}$ obtaining 50 % CaMKIIαCreER^{T2}APP$^{flox/flox}$APLP2$^{-/-}$ (CaMKIIαCre cDKO) and APP$^{flox/flox}$APLP2$^{-/-}$ (littermate control). In order to induce the APP ablation two strategies were followed. First, I wanted to investigate whether APP is required in an adult brain. Therefore, mice were i.p. injected with 1 mg of tamoxifen twice a day for 5 consecutive days. Second I addressed the question whether APP is

required during synaptogenesis. Hence, lactating mothers were treated with tamoxifen at P5 of the litter. Pubs ingested the drug via mother's milk. Grown up pups were additionally i.p. injected with tamoxifen at adult stages.

Since the CaMKIIα promoter was only active from P1 onwards the gene could not be targeted prenatally. Therefore, mice from the NexCre$^{+/T}$ strain (Goebbels et al., 2006) were crossed to APP$^{flox/flox}$APLP2$^{-/-}$ to receive NexCre$^{+/T}$APP$^{flox/flox}$APLP2$^{-/-}$ individuals which again were crossbred with APP$^{flox/flox}$APLP2$^{-/-}$ obtaining 50 % NexCre$^{+/T}$APP$^{flox/flox}$APLP2$^{-/-}$ (NexCre cDKO) and 50 % APP$^{flox/flox}$APLP2$^{-/-}$ (littermate control). Nex (neuronal helix-loop-helix protein 1) is a transcription factor shown to be involved in neuronal differentiation. From E11.5 onwards it is expressed in excitatory pyramidal forebrain neurons triggering the Cre-mediated APP removal. Thus, the Cre expression was induced much earlier covering also prenatal brain development processes compared to CaMKIIαCre cDKO mice. But here the knock-out was not time-controllable via tamoxifen application since the Nex promoter was constitutively active.

2.1.3 Conditional Knock-out of APP and APLP2 in Inhibitory Interneurons

As the hippocampus comprised only 5 % inhibitory interneurons and APP was implicated as a regulator of GABAergic short-term plasticity in dissociated hippocampal and striatal neurons (Yang et al., 2009), I also investigated if this cell-subtype contributes to functional synaptic plasticity in cDKOs. Thus I followed a complementary approach to excitatory pyramidal neurons. First the GAD67Cre$^{+/T}$ strain (Prof. Dr. Hannah Monyer, DKFZ, Heidelberg (Magno et al., 2011) was bred with APP$^{flox/flox}$APLP2$^{-/-}$ mice to obtain GAD67Cre$^{+/T}$APP$^{flox/flox}$APLP2$^{-/-}$ mice which were crossed to APP$^{flox/flox}$APLP2$^{-/-}$ receiving 50 % GAD67Cre$^{+/T}$APP$^{flox/flox}$APLP2$^{-/-}$ (GADCre cDKO) and 50 % APP$^{flox/flox}$APLP2$^{-/-}$ (littermate control). As an enzyme GAD67 (glutamate decarboxylase) promotes 90 % of GABA synthesis. The promoter is expressed constitutively from E10.5 on.

In order to obtain an APP knock-out in inhibitory neurons comparable to the NexCre cDKOs in excitatory neurons we crossed Dlx5/6Cre$^{+/T}$ mice to APP$^{flox/flox}$APLP2$^{-/-}$ resulting in a genotype of Dlx5/6Cre$^{+/T}$APP$^{flox/flox}$APLP2$^{-/-}$ (Stuhmer et al., 2002). These mice were then again mated with APP$^{flox/flox}$APLP2$^{-/-}$ obtaining 50 % Dlx5/6Cre$^{+/T}$APP$^{flox/flox}$APLP2$^{-/-}$ (DlxCre cDKO) and 50 % APP$^{flox/flox}$APLP2$^{-/-}$ (littermate control). Dlx5/6 is a transcription factor, linked to the hox gene cluster and is expressed from E12.5 on. It promotes the migration of interneurons by repressing

proteins that are normally expressed in almost differentiated neurons. In a second approach we crossed Dlx5/6Cre$^{+/T}$ mice to only APP$^{flox/flox}$ in order to obtain mice bearing APP$^{-/-}$ but still expressing APLP2. Here I wanted to investigate whether the potential compensatory function of APLP2 is also preserved in GABAergic neurons.

2.2 Acute Hippocampal Slices

2.2.1 ACSF

Artificial cerebral spinal fluid (ACSF) consisted of various compounds providing suitable amounts of ions and glucose to ensure optimal conditions for preparation, storage and electrophysiological recording from the hippocampal acute slices and organotypic hippocampal cultures (OHCs). Concentrations were kept at ideal levels to ensure a proper function of neurons. The composition of the ACSF is shown in Table 2.2. In order to reach a physiological pH of 7.3 and to supply the tissue with a sufficient amount of oxygen the ACSF was constantly carbogenated (95% O_2, 5% CO_2). In this study for preparation and electrophysiological recordings an ACSF containing a high Mg^{2+} concentration of 2 mM was used. This prevented the Mg^{2+} block release from the NMDA-receptor which would result in a pre-potentiation in the acute slices due to stress events from the preparation process. Moreover, it was shown in previous studies that APP / APLP2 transgenic mice tend to lower excitability threshold meaning that LTP could be induced very easy if a low Mg^{2+} concentration (1 mM) was used for recordings which then masked potential defects among genotypes.

Table 2.2 Composition of the high Mg^{2+} ACSF. *All chemicals were obtained from Applichem.*

Substance	Molarity [mM]	g/1l bidest H_2O
NaCl	125	7.305
KCl	2.5	0.186
NaH_2PO_4*H2O	1.25	0.172
$MgCl_2$*6 H_2O	2	0.406
NaHCO3	26	2.184
D(+)-Glucose	25	4.504
$CaCl_2$*H_2O	2	0.294

2.2.2 Preparation of Acute Hippocampal Slices

Mice were briefly anesthetized with Isofluran and rapidly decapitated. After opening the skull the brain was quickly removed. In order to reduce neuronal damage this procedure should not take longer than 1.5 min. For keeping the oxidative stress to a minimum the brain was directly transferred to 4 °C cold, carbogenated ACSF for 3 min. Therefore, in the following preparation steps always ice-cold ACSF was used as well.

Figure 2.1 A illustrates the localization of both hippocampi in a rodent brain. For preparation the prefrontal cortex and the cerebellum were removed by a razor blade followed by the separation of both hemispheres. The hippocampi were dissected from the surrounding striatal tissue at the medial side by using two rounded spatula. One spatula was placed underneath the fimbria hippocampi whereas the second spatula loosened the connection to the subiculum. Then the hippocampus could gently be folded out of the cortical tissue with the second spatula. In all preparation steps stretching and direct touching of the hippocampus should be avoided.

The hippocampus was cut along its longitudinal axis by a vibrating microtome (VT 1200S; Leica, Nussloch, Germany) into 400 µm thick transversal slices. Therefore, both hippocampi were fixed with glue onto the specimen plate while leaning in an upright position on an agar block. Thereby, the dentate gyrus faced the agar block (Figure 2.1 B). The specimen plate was rapidly transferred into the buffer-tray containing ice-cold and carbogenated ACSF.

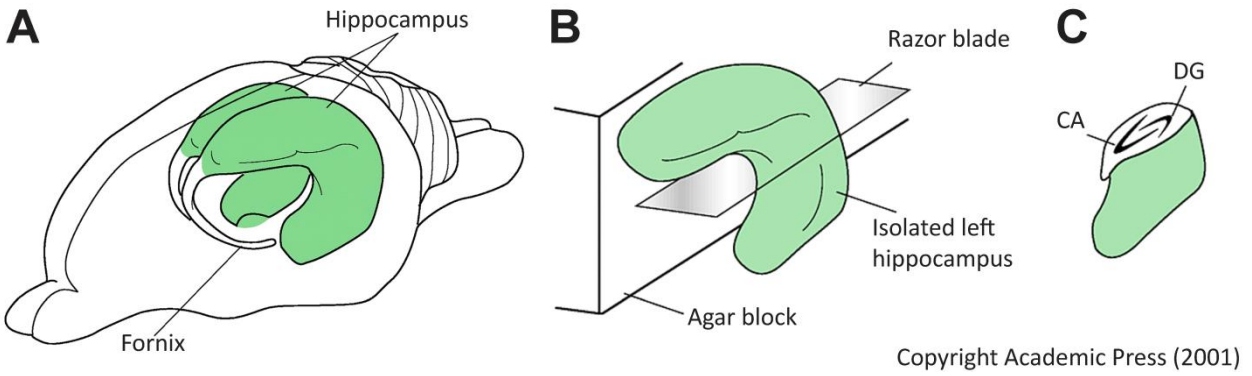

Figure 2.1 Localization in the rodent brain and preparation of hippocampi.
(A) *Scheme illustrates the localization of hippocampi in the rat brain. Murine hippocampi tend to be slightly larger compared to brain volume, but nevertheless in comparable position.* ***(B)*** *Dissected hippocampi were attached to the specimen plate while leaning at the agar block and cut into 400 µm transversal slice by a vibrating razor blade.* ***(C)*** *Plan view on cut hippocampus. Transversal slicing keeps intra-hippocampal projections between areas intact. CA = Cornu ammonis, DG = dentate gyrus. Adapted from (Hammond, 2001).*

After setting the cutting borders the vibrating razor blade gently cut slice by slice in a slow (0.1 mm/s) and tissue protecting manner. Although this way of cutting was relatively time consuming compared to techniques like the tissue shopper or egg slicer the neuronal damage and thus stress for neurons next to the slice surface was reduced to a minimum. For storage the slices were transferred into a custom-made submerged chamber directly after they were cut. There the slices were maintained and allowed to rest in carbogenated ACSF for at least 2 h at room temperature (RT).

2.3 Organotypic Hippocampal Cultures

Organotypic hippocampal cultures (OHCs) are a suitable tool to investigate neurons in their typical network and surrounding. Although the hippocampus was cut into transversal slices projections to the sub-regions stayed intact therefore providing the possibility to investigate structure and function of neurons in these networks. Furthermore, it was feasible to treat the cultures with drugs over a longer time range of several days by adding drugs to the medium as acute hippocampal slices are short-lived (Gähwiler et al., 1997). In this study the OHCs of C57Bl/6, APLP2-KO and APPΔCT15-DM were treated either with DMSO (Dimethyl sulfoxide, Roth) as control or a specific inhibitor of the α-secretase ADAM10 (GI254023X, 10 µM) (Andrews et al., 2000; Ludwig et al., 2005) for five consecutive days starting at DIV 14-19. Subsequently, synaptic plasticity was investigated at the Schaffer collateral pathway.

2.3.1 Media and Solutions

Gey's Balanced Salt Solution pH 7.4 (GBSS)

KCl	0.37 g
KH_2PO_4	0.03 g
$MgCl_2 * 6H_2O$	0.21 g
$MgSO_4 * H_2O$	0.07 g
NaCl	8 g
$NaHCO_3$	0.227 g

NaH_2PO_4	0.12 g
D-Glucose	1g
$CaCl_2 * {}_2H_2O$	0.22 g
MilliQ water	fill up to 1000 ml

Kynurenic acid

Dissolve 0.946 g Kynurenic acid (Sigma) in exactly 5 ml 1 M NaOH, vortex mix, add 45 ml MilliQ water, filter sterile, store in 1 ml fractions at -20 °C.

Preparation solution pH 7.2

GBSS	98 ml
Glucose (50 %)	1 ml
Kynurenic acid	1 ml

Medium for OHCs

BME Medium	100 ml
HBSS	50 ml
Equine donor serum	50 ml
L-Glutamine (200 mM)	1 ml
Glucose (50 %)	2 ml

Antimitotic drug

Uridin (Sigma)	2.422 mg in 10 ml dH_2O (1 M)
Cytosin-β-D-Arabino-furanosid*Hydrochlorid	2.797 mg in 10 ml dH_2O (1 M)
5-Fluoro-2´-Deoxyuridin	2.462 mg in 10 ml H_2O (1 M)

Stock solution is prepared 1:1, filtered sterile and stored at -20 °C.

Fungizone

Stock solution 250 µg Fungizone / ml

Dilution is 1:200 = 1.25 µg Fungizone / ml medium.

Penicillin/Streptomycin

Stock solution 10000 U Penicillin / 10000 µg streptomycin per ml

Dilution is 1:100 = 100 U Penicillin / 100 µg streptomycin per ml medium.

2.3.2 Preparation of Organotypic Hippocampal Cultures

Organotypic hippocampal slice cultures were prepared as described by Stoppini and colleagues (Stoppini et al., 1991). Directly after birth at P0 mice were decapitated, the skull was opened and removed. By using a round, sharpened spatula the dorsal part of the brain was dissected from the skull. All preparation steps were performed in a petri dish filled with preparation solution while placed on a cooling pack. Remaining cerebellum was removed and both hemispheres were separated. Hippocampi were then dissected from the surrounding tissue with the spatula and transferred with two larger spatulas onto a Teflon plate being part of the tissue shopper (McIllwain). Here, 400 µm thick transversal slices were cut by a razor blade and afterwards washed with cold preparation solution from the Teflon plate back into the petri dish, where they were separated and afterwards kept for 15 – 30 min at 4 °C. Meanwhile 1.1 ml of pre-warmed medium was filled in each of a 6 well plate. Additionally, in every well a cell culture inserts (Millicell®) was placed. Three slices were positioned onto one insert. The plates were kept at 36.5 °C, 5 % CO_2 and a high humidity of 99 % in the incubator. Three days after preparation 15.4 µl of antimitotic drug was added to the medium in each well. 24 h later the medium was exchanged completely. Consecutively, 500 µl of the medium was replaced by fresh one once a week. From DIV 7 on the medium was supplemented with Fungizone, Penicillin and Streptomycin to prevent contamination.

2.4 Electrophysiology

Due to its lamella structure the main projections are still well preserved in transversal acute hippocampal slices, therefore providing a useful model for studies of activity-dependent synaptic and functional plasticity. This process reflects the ability of synapses to change their strength and their structure upon changes in neuronal activity (see 1.1.2).

2.4.1 Technical Equipment

All electrophysiological recordings have been performed at two setups composed of almost identical technical equipment, partially obtained from different manufactures. To yield comparable results from both setups, variables like filter settings, liquid levels, flow rates, etc. were kept adjustable. Recordings from both setups have been compared on a regular base and found to be indistinguishable ensuring a legitimation to pool the data.

For recording acute hippocampal slices or OHCs were placed in the submerged-type recording chamber (RC-22, Warner instruments, USA) constantly perfused with carbogenated ACSF at a flow rate of 1.5 ml/min adjusted with a peristaltic pump (Ismatech, Switzerland or Abimed, Germany). A proper flow of ACSF was ensured with PVC tubings (TYGONE, Ismatec) for standard recording procedures whereas silicon tubings (PharMed® Ismaprene, Ismatec) have been proven to be necessary if inhibitors or peptides were applied in order to prevent sticking to the tubing walls. The recording chamber was fixed onto vibration damped platform (Spindler & Hoyer, Germany and TMC, Massachusetts, USA). Additionally, a constant temperature was essential for stable extracellular recordings. Therefore, the chambers were mounted onto an aluminum heating base (PH-1, Warner Instruments) which was connected to a thermistor measuring the current temperature. Upstream an additional preheating element (in-line solution heater SC-20, Warner Instruments) was positioned. Both, chamber and in-line solution heater, were connected to an adjustable Dual Channel Heater Controller (TC-334B, Warner Instruments). In the chamber a constant temperature of 22 – 24 °C (RT) for fiber volley experiments and 32 ± 0.2 °C for all following recordings was adjusted. A relieved steel cannula connected to tubings with a larger diameter for suction than input as well as an optimally adjusted pump prevented pulsing of the ACSF flow and therefore supported signal stability.

After the acute hippocampal slice or OHC was transferred into the recording chamber the electrodes were positioned by visual control using a stereo microscope (SMZ 654, Nikon, Japan or Heerbrugg at Leica Microsystems). For placing the stimulation electrode it was fixed to a mechanical micromanipulator (Leitz, Germany). For positioning the recording electrode an electrical micromanipulator (SM-5, Luigs and Neumann or Nano-Stepper, WSE Electronics), moved by a motor driven remote control, was used.

2.4.2 Stimulation Protocols and Extracellular Recordings

Since presynaptically released neurotransmitters bind to postsynaptic ligand-gated ion channels which in turn immediately open and therefore evoke a synaptic currents, changes of these currents can be recorded by microelectrodes. Those processes can be monitored in single cells by patch clamp technique or in a cell population by field Excitatory Postsynaptic Potentials (fEPSPs) recordings. The latter provides advantages as cell membranes are not damaged and the summated response to stimuli reflects the physiological state.

For stimulation of the Schaffer collaterals a lacquer coated, monopolar tungsten electrode (WPI, USA) with a resistance of 0.1 MΩ was used. The tip was freed from lacquer by a chemical procedure therefore allowing a highly precise current application. The electrode was fixed onto the mechanical micromanipulator enabling exact placing in the slice. Additionally the negative electrode pole was connected to a stimulus isolator (A360 or A365, WPI, USA) generating and applying a pattern of stimuli preprogrammed in the master pulse generator Master 8 (A.M.P.I., Israel). The positive pole was connected to an indifferent electrode consisting of an Ag/AgCl pellet (E201, WPI, USA) being in contact with the liquid in the chamber and connected to the amplifier's headstage. Stimuli consisted of monophasic square pulses of 0.2 ms duration and ranging from 4 – 65 µA in size for baseline stimulation depending on mice strain, age, preparation quality, recording system (acute slice or OHC) and treatment.

For monitoring evoked potentials the recording electrodes from borosilicate glass capillaries (0.58 x 1.00 x 100 mm, Biomedical Instruments, Germany) were pulled by a horizontal pipette puller (program 33, P-97, Sutter Instruments, USA) and afterwards filled air bubble free with 3 M NaCl solution. Pulling settings were adjusted to yield a resistance of 2 – 10 MΩ. Following the recording electrode was inserted into an electrode holder (WPI, USA) which in turn was

mounted either on the amplifier's headstage (Axoclamp-2B, Axon Instruments at Molecular Devices, USA) directly or indirectly by a cable.

Placing the stimulation electrode in the *stratum radiatum* of CA3, thereby stimulating the Schaffer collateral pathway, evoked fEPSPs recorded in the *stratum radiatum* of hippocampal CA1 region by a recording electrode at a depth of 150 – 200 µM (Figure 2.2). For investigations in OHCs the recording electrode was placed 100 – 150 µM directly in the cell body layer of CA1. To ensure exact positioning the slice surface, as zero-point, had to be determined by monitoring changes in electrode resistance. Signals were visualized and followed on an oscilloscope (HM507, HAMEG, Germany) and digitalized with a National Instruments LabView based software (see 2.4.3). In all recordings the initial negative slope of the fEPSP was measured (Figure 2.3 A).

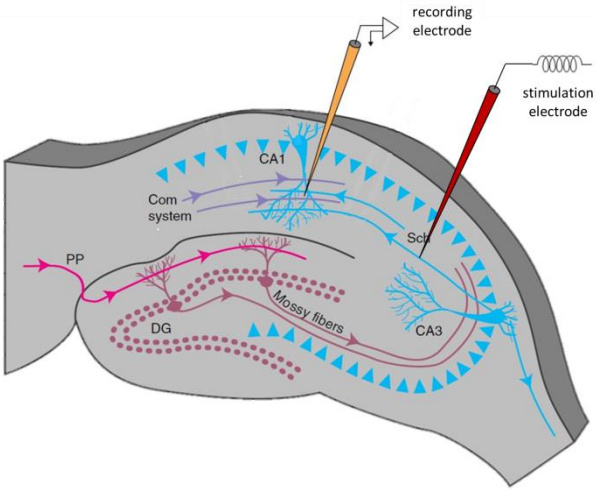

Figure 2.2 Positioning of electrodes in the transversal acute hippocampal slice.
The stimulation electrode was placed in the CA3 region to stimulate the Schaffer collateral pathway. The recording electrode was positioned in the stratum radiatum of the CA1 region. Adapted from (Byrne and Roberts, 2009).

After slices adapted to 32 °C chamber temperature and confirmed to be healthy by a stabile basal synaptic response and hence an equal fEPSP slope size, recordings began. To keep settings reliable and uniform for each experiment, baseline activity of LTP recordings were always performed at stimulus strengths resulting in a fEPSP slope size of 40 % of the maximal slope, which was defined as that slope not increasing further and barely not revealing a population spike (Figure 2.3 B).

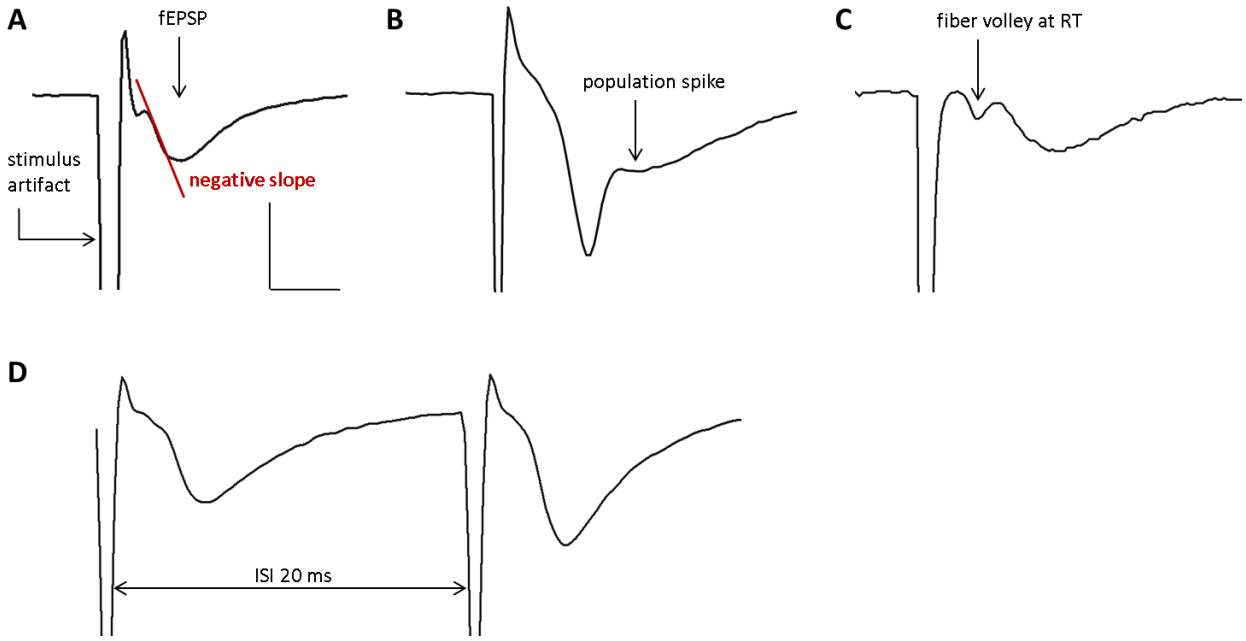

Figure 2.3 Overview about fEPSP, population spike, fiber volley and PPF
(A) *Excitatory Postsynaptic field Potential (fEPSP) including stimulus artifact and the negative slope which was measured before and after LTP induction.* ***(B)*** *fEPSP contaminated by the population spike.* ***(C)*** *fEPSP and fiber volley signal are clearly separated at room temperature.* ***(D)*** *Example for Paired Pulse Facilitation (PPF) at an inter-stimulus interval (ISI) of 20 ms. Second signal is larger than the first depending on size of ISIs. Vertical scale bar = 0.5 mV, horizontal scale bar = 5 ms.*

Stimulation protocols for assessment of basal synaptic transmission as wells as LTP induction were preassigned in the Master-8, triggering the stimulus isolator. These protocols included a defined frequency and voltage with which the stimulus was applied.

Investigation of the basal synaptic transmission was performed by input-output-(IO) measurements. Therefore, the fEPSP slope size was correlated to given sizes of the fiber volley amplitude (0.1 stepwise from 0.1 – 0.8). The fiber volley represents the presynaptic part of the fEPSP more precisely the summated action potentials of a population of axons (Figure 2.3 C). The fiber volley amplitude is proportional to the number of firing axons and thus allows evaluation of the input strength. These recordings were performed at 22 – 24 °C to prevent overlapping of fiber volley and fEPSP signal. In a second approach basal synaptic transmission was judged by correlating the fEPSP slope size to defined stimulus intensities (stepwise 25 µA from 25 µA to 250 µA) at 32 °C.

Presynaptic function and thus short-term plasticity was assessed by the Paired Pulse Facilitation (PPF) paradigm. PPF is believed to induce short-term plasticity due to presynaptic

neurotransmitter release. When two single pulses with defined inter-stimulus intervals (ISIs) ranging from 10, 20, 40, 80 to 160ms were applied, the second fEPSP slope is larger than the first (Figure 2.3 D). These recordings were done at 32 °C chamber temperature.

Next, long-lasting effects of changes in activity-dependent synaptic plasticity upon stimulation were investigated by inducing Long-Term Potentiation (LTP) in acute hippocampal slices or OHCs. Therefore, 20 min (in case of OHCs 10 min) of stable baseline recordings at 0.1 Hz were followed by the LTP induction protocol and subsequent monitoring of increase in synaptic efficacy over 60 min for LTP, 180 min for protein synthesis dependent Late – LTP (L-LTP) and 30 min in OHCs. LTP induction was carried out by the Theta Burst Stimulation (TBS) whereby a train of stimuli activated the densely packed afferent axons of the Schaffer collaterals briefly at high frequencies (3 trains/repetitions at 10 s intervals, each train consisting of 10 stimuli delivered at 5 Hz, each burst composed of 4 pulses at 100 Hz, Figure 2.4). This protocol based on naturally occurring firing patterns *in vivo* and thus reflected physiological changes (Larson and Lynch, 1986). Freely exploring rats and mice were shown to exhibit bursts of 5 Hz in hippocampal pyramidal neurons. These patterns were described as “theta” rhythm (Bland, 1986; Sainsbury et al., 1987). Until today a wide range of different LTP induction protocols ranging from weak over mild to strong stimulation have been established and discussed whether reflecting physiological events during processes of learning and memory (Albensi et al., 2007; Kumar, 2011).

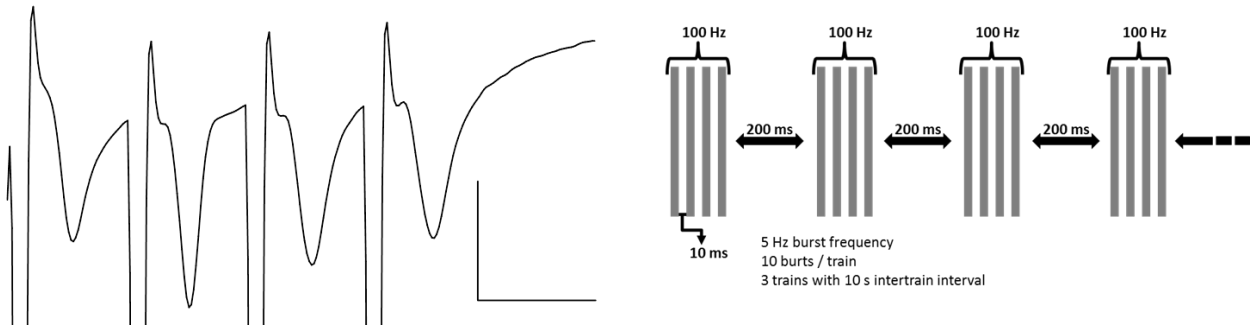

Figure 2.4 Theta Burst Stimulation
Theta Burst stimulation (TBS) consists of 3 trains/repetitions at 10 s intervals, each train consisting of 10 stimuli delivered at 5 Hz, each burst composed of 4 pulses at 100 Hz. This high frequency protocol was used for LTP induction and reflects physiological firing patterns in vivo.

2.4.3 Data Acquisition

fEPSP signals were recorded in the bridge mode by the Axoclamp2B differential amplifier (Axon Instruments Molecular Devices, USA) and thereby 200x amplified. Additionally, the signal was band-pass filtered with borders set at 1 – 1700 Hz (LHBF – 48x – 4HL, NPI, Germany). A 50 – 60 Hz filter eliminated noise contaminating the results (Hum Bug, Quest Scientific, UK). This way processed signals were collected at 5 kHz and sent to a computer via multi – IO card (National Instruments, USA). For online illustration and signal acquisition a program written by M. Korte and V. Staiger (DAP Version 4.751) basing on the National Lab View Software (National Instruments, USA) was used. Basically, the negative slope of the elicited fEPSP signal was measured in a defined, manually set window. Furthermore, a trend display window depicted resulting curve of recordings over time.

2.4.4 Data Analysis

For analysis of the raw data gained from recordings again custom made programs (by M. Korte, V. Staiger) based on National Lab View Software were consulted.

In order to precisely analyze data obtained from fiber volley, EPSP and LTP recordings ANA_DAB (version 4.755) program was used to measure the negative fEPSP slope in a defined, manually placed window.

Data obtained from PPF recordings were analyzed by the program ANA_PPF (version 4.2). Here, the ratios of two stimuli, separated by varying ISIs, were calculated as follows:

$$\left(\frac{slope\ fEPSP_2}{slope\ fEPSP_1}\right) * 100$$

Both programs generated a Microsoft Excel file (Microsoft, USA) containing all single values of each fEPSP slope measurement per 10 s. For experiments about basal synaptic transmission (FV, EPSP, PPF) three values for each condition were averaged and plotted. In case of LTP recording data six values were averaged representing the mean for each minute plotted in the graph. Since the LTP data were depicted as an increase compared to basal synaptic activity all fEPSP slope sizes for the 20 min baseline were averaged and set to 100 %.

All values obtained after TBS application, were normalized to the baseline by the equation:

$$\left(\frac{slope\ EPSP_{minute}}{slope\ EPSP_{baseline}}\right) * 100$$

Parameters leading to an exclusion of single experiments were an unstable baseline (variability more than $\pm$ 10 %) or a large population spike after TBS resulting in an abnormal large and thus not physiological LTP.

2.4.5 Pharmaca and Peptides

In this study additional electrophysiological recordings were performed upon pre-treatment with a specific α – secretase inhibitor or recombinant secreted α or β peptide (recAPPsα, recAPPsβ) of full length APP. As all substances were diluted in ACSF for administration to the chamber, the volume used had to be restricted to a minimum. Previous investigations showed that a volume of 30 ml of ACSF is sufficient for experiments in a closed loop configuration where the fluid circulated during the entire experiment. In order to circumvent sticking of peptides to the surface silicon tubings (PharMed® Ismaprene, Ismatec) were used. Changes in the osmolarity, due to evaporation of liquid, was a highly critical factor influencing the recordings. Therefore, a custom-made system moisturized the Carbogen before it was introduced into the Falcon-tube containing 30 ml ACSF plus the respective substance (Table 2.3). Additionally, the Falcon-tube was covered with Parafilm® (Bemis, USA).

To investigate the role of APPsα for synaptic transmission and plasticity no acute hippocampal slices were used since they cannot be kept alive longer than 22 h. Moreover, the acute treatment revealed no effect on LTP after 6 h of incubation. OHCs provided the opportunity to prolong the incubation time. Cultures of C57BL/6, APLP2-KO and APPΔCT15-DM pubs were treated with a specific ADAM10 α – secretase inhibitor GI254023X (Andrews et al., 2000; Hoettecke et al., 2010; Weyer et al., 2011) for five consecutive days by adding the substance to the media in which they were cultivated. The inhibitors stock solution concentration was 20 mM diluted in DMSO (Roth, Germany), final concentration for OHCs treatment and during recording was 10 µM (Table 2.3). DMSO treatment at same concentrations served as control.

The recombinant peptides used in this study were kindly provided by Prof. Dr. Ulrike Müller from the Rubrecht-Karls-University of Heidelberg and derived from HEK cells which were stably transfected with pIRES3Hyg-His-Xa-APPsα or pIRES3Hyg-His-Xa-APPsβ (Hick et al., 2015). Next, the question was addressed whether recombinant APPsα (10 nM in DMSO) or APPsβ (50 nM in DMSO) could restore the LTP defect observed in NexCre cDKOs (Table 2.3). Heat inactivated (20 min at 95 °C) peptides served as control. Acute hippocampal slices of APLP2-KO (littermate control) and NexCre cDKO were pre-incubated in 30 ml gently carbogenated ACSF containing the respective peptide in a custom made incubation chamber for 1 h at RT. Afterwards, slices were transferred into the recording chamber where again 30 ml of ACSF with the respective peptide were circulating in a closed loop during the entire experiment. Recordings were performed as described before.

Table 2.3 Inhibitor and recombinant peptides used in this study.

Substance	Target	Concentration	Reference
GI254023X (inhibitor)	α-secretase	10 µM	(Andrews et al., 2000; Hoettecke et al., 2010; Weyer et al., 2011)
recAPPsα	unknown	10 nM	(Hick et al., 2015)
recAPPsβ	unknown	50 nM	(Hick et al., 2015)

2.5 Primary Hippocampal Dissociated Neuronal Cultures

2.5.1 Media and solutions

Borate buffer pH 8.5

Dissolve 0.31 g boric acid and 0.475 g borax in 100 ml sterile MilliQ water, adjust pH to 8.5.

Poly-L-Lysine stock solution

10 mg / ml in MilliQ water

Gey's balanced salt solution (GBSS)

See 2.3.1

Serum medium

FCS	200 µl
DMEM (2 %)	10 ml

Medium for dissociated hippocampal cultures

Neurobasal	50 ml
B27	1 ml
L-Glutamin (200 mM)	125 µl
N2 (10x)	5 ml

2.5.2 Preparation of Primary Embryonic Hippocampal Cultures

Primary embryonic cultures of hippocampal neurons were prepared at embryonic day (E) 18.5. Therefore, the pregnant mouse was sacrificed by cervical dislocation. Under sterile conditions all embryos were taken from the uterus and rapidly decapitated. The upper half of the brain containing cortex and hippocampus was dissected from the skull and kept in ice-cold GBSS / Glucose solution. Remaining tissue from the midbrain and brainstem was removed under visual control using a dissecting microscope (Stemi 2000, Zeiss). Hippocampi were dissected from the cortical tissue and digested in 1 ml Trypsin / EDTA (Sigma) for 30 min at 36.5 °C. The digestion was stopped by removing the Trypsin / EDTA solution and subsequent adding of 1 ml serum medium followed by three washing steps. The cells were dissociated further by mechanical separation via a Pasteur pipette. The suspension was centrifuged 5 min at 1500 rpm, the supernatant was removed and cells were re-suspended in 1 ml medium. Afterwards the cells were counted, plated at a density of 7 x 10^4 cells / well on poly-L-Lysine coated coverslips and kept in medium at 36.5 °C, 5 % CO_2 and 99 % humidity. Medium was exchanged at DIV9. Cultures were used for experiments at DIV 12-16.

For coating glass coverslips (Ø 13 mm, 1 mm thick, VWR) with poly-L-Lysine they were first incubated in 10 M NaOH for 3-5 h at 100 °C and washed 5x with MilliQ water. Next, the coverslips were sterilized at 225 °C for 6 h and coated with 0.5 mg / ml poly-L-Lysine (P2636,

Sigma) in boric acid buffer at 36.5 °C for 2-3 h. Finally, they were washed 5x with sterile water, dried and stored at 4 °C.

2.6 Ratiometric Calcium Imaging

2.6.1 Media and solutions

Fura-2 Calcium Calibration Kit

zero to 10 mM CaEGTA, 50 µM fura-2 (11 x 1 ml) (Invitrogen)

1x Hank's Balanced Salt Solution (HBSS) for live imaging

HBSS 10x stock solution	50 ml
$CaCl_2 * 2H_2O$	175 mg
$NaHCO_3$	147 mg
D-Glucose	1351 mg
MilliQ water	fill up to 500 ml

Fura-2 AM stock solution

Add 50 µl DMSO to the vial delivered with 50 µg Fura-2 AM (Invitrogen) to receive a stock solution of 1 mM.

20 % Pluronic Acid

Pluronic Acid	1 g
DMSO	5 ml

Glycine stimulation medium (1 mM)

Glycine (1 M in D-PBS)	40 µl
Strychnine (1 mM in $H_2O_{dest.}$)	40 µl
1x HBSS	40 ml

APV medium (50 µM)

APV (10 mM in $H_2O_{dest.}$)	200 µl
Glycine (1 M in D-PBS)	40 µl
Strychnine (1 mM in $H_2O_{dest.}$)	40 µl
1x HBSS	40 ml

CPA medium (10 µM)

CPA (10 mM in DMSO)	40 µl
Glycine (1 M in D-PBS)	40 µl
Strychnine (1 mM in $H_2O_{dest.}$)	40 µl
1x HBSS	40 ml

Nifedipine medium (10 µM)

Nifedipine (10 mM in DMSO)	40 µl
Glycine (1 M in D-PBS)	40 µl
Strychnine (1 mM in $H_2O_{dest.}$)	40 µl
1x HBSS	40 ml

2.6.2 Pharmaca and Viruses

Table 2.4 Chemicals used for calcium imaging.

Substance	Concentration	Reference
DL-2-Amino-5-phosphonopentanoic acid (APV)	50 µM	abcam
Cyclopiazonic acid (CPA)	10 µM	Tocris
Nifedipine	10 µM	Tocris
Strychnine hydrochloride	1 µM	Sigma-Aldrich

Table 2.5 Adeno-associated viruses (AAV) used for calcium imaging.

Substance	Stock titer	Dilution	Reference
AAV9-ss-Syn-Venus-f	$1.4*10^{10}$ U/µl	1 : 25	Tobias Abel (PEI, Langen)
AAV9-ss-Syn-lck-Venus-HA-msAPPsα	$5.63*10^{9}$ U/µl	1 : 5	Tobias Abel (PEI, Langen)

2.6.3 Data Acquisition

2.6.3.1 Ratiometric Calcium Imaging in NexCre cDKO

Ratiometric Ca^{2+} imaging is a feasible method to assess qualitative as well as quantitative values for changes in the intracellular Ca^{2+} concentration. Here, the fluorescent Ca^{2+} indicator dye Fura-2AM is used bearing the cell-permeant acetoxymethyl ester (AM) enabling the dye to passively enter the neuron. After penetration intracellular esterases cleave the AM group and therefore trap the dye inside the cell. Fura-2 is excited with UV light at wavelengths of 340 nm and 380 nm. The excitation peak shifts from 340 nm to 380 nm when Ca^{2+} binds Fura-2. The detection wavelength is 510 nm. The ratio of the emissions at those wavelengths was directly correlated to the amount of intracellular Ca^{2+}. Ratiometric Ca^{2+} imaging was performed at DIV 12-16 of hippocampal dissociated neuronal cultures prepared from APLP2-KO (littermate control) and NexCre cDKO. For dye-load 2 ml of pre-warmed 1x HBSS containing 4 mM Fura-2AM and 2.5 % Pluronic acid were prepared in advance. The coverslip was transferred into this loading solution in a petridish and kept at 37 °C for 60 min in the incubator. After 2 washing steps with pre-warmed 1x HBSS, the coverslip was transferred into the imaging chamber which was constantly perfused (0.5 ml / min) with 1x HBSS at RT. The neurons were allowed to adapt to the new conditions

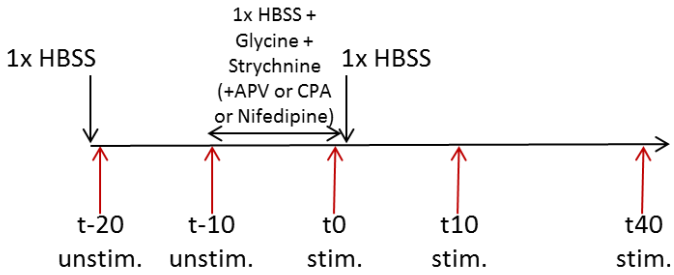

Figure 2.5 Imaging protocol for quantitative Calcium imaging

The scheme illustrates 5 imaging time points and the drug application phase of 10 min. t-20 and t-10 reflect the untreated status of the neurons in 1xHBSS and therefore reflect resting Ca^{2+} concentrations. Directly after imaging t-10 1xHBSS containing 1 mM glycine and 1 µM strychnine (and additionally 50 µM APV, 10 µM cyclopiazoic acid or 10 µM nifedipine) was washed into the chamber for 10 min. t0 depicts the imaging time point directly after stimulation. Solution was switched again to 1xHBSS. Further imaging took place 10 min (t10) and 40 min (t40) after stimulation.

for 20 min. Figure 2.5 illustrates the imaging protocol including time points of drug application. Imaging was performed by using a fluorescence microscope (Olympus, BX61WI) with a LUMPlanFl 40x / 0.80 W JAPAN objective, including a CCD camera (Hamamatsu) with a binning of 4 x 4. For signal detection and image acquisition the 340 nm Fura and 380 nm Fura channels were chosen. Intensity was set to 70,9 % and the exposure time was constantly held at 130 ms for time lapse imaging taking 500 images in a cycle time of 326 ms and 200 cycles repetition. Keeping intervals relatively short ensured as less dye bleaching as possible.

After 20 min of adaption to the chamber conditions, 2 images of spontaneous activity without stimulation were taken at an interval of 10 min (t-20, t-10, Figure 2.5). For stimulation and chemically induced LTP 1x HBSS containing Glycine (1 mM) and Strychnine (1 µM), blocking specifically glycine receptors, were washed into the chamber for 10 min. Afterwards 1x HBSS was perfused and 3 additional time points (t0, t10, t40, Figure 2.5) were imaged. In order to investigate how Ca^{2+} signals change upon treatment either 2-amino-5-phosphonopentanoic acid (APV, 50 µM), Nifedipine (10 µM), or Cyclopiazoic acid (CPA, 10 µM**)** were applied during glycine stimulation to inhibit selectively NDMA receptors, L-type voltage gated Ca^{2+} channels or the reuptake of Ca^{2+} into the endoplasmatic reticulum (ER) respectively (Table 2.4).

2.6.3.2 Ratiometric Calcium Imaging with APPsα Expression via AAV

Since results from ratiometric Ca^{2+} imaging indicated a defect in Ca^{2+} dynamics before and upon glycine stimulation in NexCre cDKO I assessed if this could be restored when APPsα peptide is again expressed. Thus, I used an adeno-associated virus (AAV) expressing a construct with the sequences of the APPsα peptide plus venus fluorescence protein (Figure 2.6 A) or only venus as control (Figure 2.6 B) under the synapsin promoter ensuring exclusive expression in neurons.

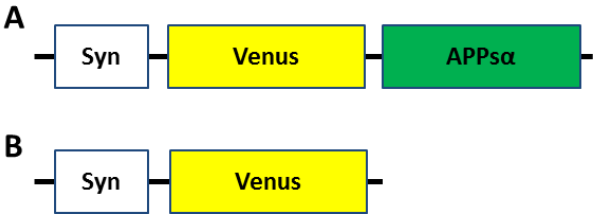

Figure 2.6 AAV constructs
(A) schematic AAV-syn-APPsα-venus vector, neurons expressing this construct under control of synapsin promoter reveal venus fluorescence and therefore also express APPsα. (B) schematic AAV-syn-venus vector, neurons expressing this construct under control of synapsin promoter reveal venus fluorescence but no APPsα.

Table 2.5 gives an overview about vectors, titers and concentrations which were applied. Previous investigations by Dr. Tobias Abel revealed a multiplicity of infection (MOI) for both AAVs of $2*10^4$. As neurons were plated at a density of 7 x 10^4 cells / coverslip, $1.4*10^9$ viruses had to be used. Hence, the AAV stock should be diluted 1 : 10 and 1 : 50 (control). But preliminary experiments revealed concentrations of 1 : 5 and 1 : 25 (control) resulted in higher transduction efficiencies. AAV stocks were stored as 5 µl aliquots at -80 °C and thawed for each experiment to keep virus quality equal. Dilutions were prepared with medium from each dissociated culture and were added back to wells for transduction. Cells were cultured without medium change until imaging for 7 consecutive days.

2.6.4 Data Analysis

2.6.4.1 Calibration Curve of Fura-2

The Ca^{2+} Calibration buffer Kit (Invitrogen) provided a suitable tool to determine the dissociation constant (K_d) for the Fura-2AM fluorescent Ca^{2+} indicator dye which was needed to calculate *in vitro* Ca^{2+} concentrations. It contained 11 Ca^{2+} standard buffers with increasing [CaEGTA] concentrations from 0 to 39 µM premixed with 50 µM Fura-2 and a control buffer without Fura-2. For facilitating coverslip spacing and microscope focusing each buffer contained 15 µm polystyrene microspheres. This kit based on a method described by Tsien and colleagues (Grynkiewicz et al., 1985; Tsien and Pozzan, 1989) where the $[Ca^{2+}]_{free}$ is a function of the K_d of CaEGTA. When the $[Ca^{2+}]$ and [EGTA] were almost similar, the only free Ca^{2+} available is that which was in equilibrium with EGTA. Thus, the K_d of indicator EGTA was defined as the concentration at which it reaches the half saturated point (Figure 2.7).

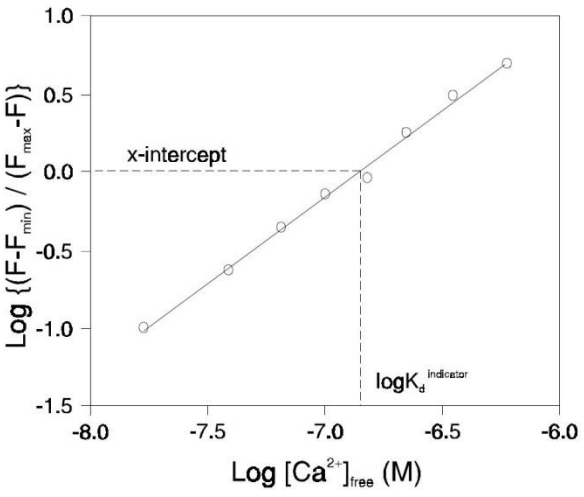

Figure 2.7 Calibration curve of Fura-2
$[Ca^{2+}]_{free}$ is a function of the K_d of CaEGTA. When the $[Ca^{2+}]$ and [EGTA] were almost similar, the only free Ca^{2+} available is that which was in equilibrium with EGTA. Therefore the K_d of EGTA (indicator) was defined as the concentration at which it reaches the half saturated point shown in the double log plot. (Grynkiewicz et al., 1985; Tsien and Pozzan, 1989).

2.6.4.2 Quantification of Calcium Signals

Ca^{2+} release events took place in a neuron during spontaneous activity without or upon stimulation appearing as peaks, which reflect bursting activity, during imaging. Those peaks reflect the fact that if Ca^{2+} entered the cell via receptors and was released from internal stores it immediately bound to Fura-2 which then in turn switched its excitation peak from 340 nm to 380 nm (Figure 2.8).

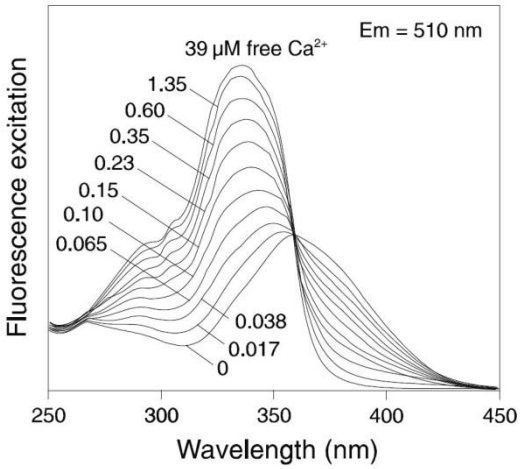

Figure 2.8 Shift of excitation peak from 340-380nm upon calcium binding to Fura-2.

Images obtained from the imaging process of dissociated hippocampal cultures from C57BL/6, APLP2-KO (littermate control) and NexCre cDKO were analyzed by measuring fluorescence intensity changes for both wavelengths expressed as ratio (R).

$$R = \frac{F_{380nm}}{F_{340nm}}$$

Therefore, ratio images were separated to their wavelengths (380 nm and 340 nm) and opened with the imageJ software. Here, somata of 5 neurons were marked by ROIs (Region Of Interest) and grey values were calculated. An additional ROI was drawn to correct for background fluorescence. The following criteria had to be fulfilled for cells included in the analysis: (1) participation of the neuron analyzed in network-activity and thus showing Ca^{2+} signals obvious in ratio images, and (2) in case AAV constructs were expressed in the neurons they additionally had to be positive for venus fluorescence.

The derived fluorescence ratios were plotted against calibrated values for known Ca^{2+} levels obtained from the Calcium Calibration buffer Kit (R_{min}, $R_{max,}$ K_d, $F^{380}{}_{max}$, $F^{380}{}_{min}$) to determine *in vitro* Ca^{2+} concentrations. The relationship of the amount of free Ca^{2+} and the fluorescence emission intensity ratio was calculated as shown by (Grynkiewicz et al., 1985):

$$[Ca^{2+}]_{free} = K_d^{EGTA} * \left(\frac{R - R_{min}}{R_{max} - R}\right) * \left(\frac{F_{max}^{380nm}}{F_{min}^{380nm}}\right)$$

The amplitude and frequency values of Ca^{2+} peaks were analyzed and plotted to assess differences in Ca^{2+} dynamics upon neuronal activity between genotypes and treatments.

2.6.5 Statistical Analysis

The statistical analysis was performed by using Microsoft Excel and GraphPad Prism (GraphPad software, USA). Comparing two groups or experimental conditions a two-tailed student's t-test (type 2) was applied. If data from more than two groups were statistically analyzed a one-way variance ANOVA followed by a post-hoc Bonferroni multiple comparison test was used. Values of $p < 0.05$ were considered as significant while values with $p < 0.01$ and $p < 0.001$ were stated as highly significant. Significances were plotted as $*p < 0.05$, $**p < 0.01$ and $***p < 0.001$. All data shown were generated with GraphPad Prism with mean values ± standard error of the mean (SEM).

3 Results

3.1 The Role of the APP Protein Family for Synaptic Plasticity in Excitatory Neurons

APP and APLP2 are widely expressed throughout the brain, with a particular high expression in excitatory pyramidal cells of the cortex and hippocampus. As the latter is composed of ~95 % excitatory neurons I investigated whether the deletion of defined parts of APP or the entire protein on an APLP2 deficient background impacts basal synaptic properties. This analysis included the input-output strength measured by fiber volley and EPSP size or presynaptic functionality assed by PPF. Furthermore, I investigated whether the induction and maintenance of TBS-induced Long-Term Potentiation (LTP) was impaired. For a detailed analysis the final 5 min of slope recordings were averaged and depicted as bar graphs for each genotype. A complementary approach was established by quantitative Ca^{2+} imaging. This method enabled me to estimate the amount intracellular Ca^{2+} at before and upon glycine stimulation solely or additional drug administration. Notably, chemically induced LTP was shown to mimic LTP induction comparable to TBS (Shahi et al., 1993).

3.1.1 Blocking of APPsα Generation by Inhibiting the α-secretase ADAM10

To elucidate the role of different cleavage products of APP and its homologue APLP2 for activity-dependent synaptic plasticity two constitutive double mutants (DM) were generated. APPsα or APPΔCT15 knock-in (KI) mice used by Ring and colleagues were crossed to APLP2-KO individuals (von Koch et al., 1997; Ring et al., 2007). By this means lethality of APP / APLP2 double knock-out mice was circumvented. Previous investigations revealed that transgenic mice only expressing the soluble membrane-unbound APPsα fragment on an APLP2-KO background (APPsα-DM, $APPs\alpha^{+/+}APP^{-/-}APLP2^{-/-}$) show an impaired LTP but normal basal synaptic transmission (Weyer et al., 2011). In APP-KO mice an age-related LTP defect was observed in aged but not adult animals. It was shown that APPsα-DM revealed the LTP defect in both adult (3-4 months) and aged (12-13 months) animals. Indicating on the one hand a redundant function of APLP2 and on the other hand suggesting that expression of APPsα alone is not sufficient to promote potentiation to littermate control levels.

First, I investigated the role for APPsα in processes of LTP. Therefore, the cleavage of APP as well as APLP2 by the metalloproteinase ADAM10, and thus APPsα and APLP2sα generation, was prevented by application of the specific ADAM10 α-secretase inhibitor GI254023X (Andrews et al., 2000; Hoettecke et al., 2010). The 6 h lasting long-term incubation of acute hippocampal slices revealed an unchanged LTP and was limited by a short tissue survival time (Gähwiler et al., 1997). Hence, organotypic hippocampal cultures (OHC) of C57Bl/6 wildtype (wt), APLP2-KO and APPΔCT15-DM were prepared at P0 and treated either with DMSO as vehicle control or ADAM10 inhibitor for five consecutive days from DIV 14 onwards (see 2.4.5). Since OHCs are less mature compared to acute slices, they displayed a high variability and less stable potentiation levels. Therefore, the baseline recording was reduced to 10 min, followed by Theta Burst Stimulation (TBS) and subsequent recording for 30 min.

LTP induced in wt OHCs resulted in a stable potentiation with statistically indistinguishable levels from t35-40 min of 136 ± 11.9 % for DMSO treatment (n = 12 / 7) and 123 ± 4.0 % (n = 18 / 11) for ADAM10 inhibitor treatment (p = 0.271, t-test, Figure 3.1 A and B). Short-term plasticity assed by the Paired Pulse Facilitation (PPF) paradigm did not differ as well (Figure 3.1 C). Furthermore, postsynaptic functionality was not investigated due to high susceptibility of OHCs to increasing currents and undistinguishable fiber volley from fEPSP signal. First, OHCs from APLP2-KO mice were studied. After 10 min of baseline recording, LTP induction elicited a stable LTP of 145 ± 8.3 % (n = 11 / 9) for vehicle treated group, which was highly significant altered compared to APLP2-KO treated with ADAM10 inhibitor 112 ± 3.3 % (n = 10 / 7, p = 0.002, t-test, Figure 3.1 D and E). Thus long-term treatment with GI254023X, inhibiting APPsα generation, prevented a sufficient LTP induction and maintenance, whereas in controls cleavage products of APP alone were enough to promote LTP. Again, presynaptic functionality was not affected (Figure 3.1 F). To complete the study and compare to results from Weyer and colleagues, where besides others OHCs from APPsα-DM were investigated, OHCs of APPΔCT15-DM ($APP\Delta CT15^{+/+}APP^{-/-}APLP2^{-/-}$) were analyzed as well (Weyer et al., 2011). LTP recordings revealed a significant difference between APPΔCT15-DM DMSO-treated OHCs with potentiation values of 153 ± 14.7 % (n = 7 / 5) and APPΔCT15-DM ADAM10 inhibitor-treated with 107 ± 6.5 % (n = 8 / 7, p = 0.017, t-test, Figure 3.1 G and H). Here, LTP was induced, although to a lesser extend as in controls, but again the maintenance was affected by ADAM10 inhibitor treatment

since fEPSP slope returned almost to baseline level. Notably, the vehicle control group showed LTP which was not seen in APPsα-DM treated with DMSO. In these mutants the concentration of APPsα, which was not membrane anchored, could have been unsufficient to promote LTP due to low concentration or abnormal timed release at activated synapses (Weyer et al., 2011). Short-term plasticity was unaltered as well (Figure 3.1 I). These results suggest that α-secretase ADAM10 dependent APPsα or APLP2sα production is required for LTP induction and maintenance. In wt probably endogenous levels of α-secretase cleavage products APPsα and APLP2sα are still sufficient to promote LTP comparable to controls, since APP and APLP2 shedding might be inadequately suppressed by GI254023X.

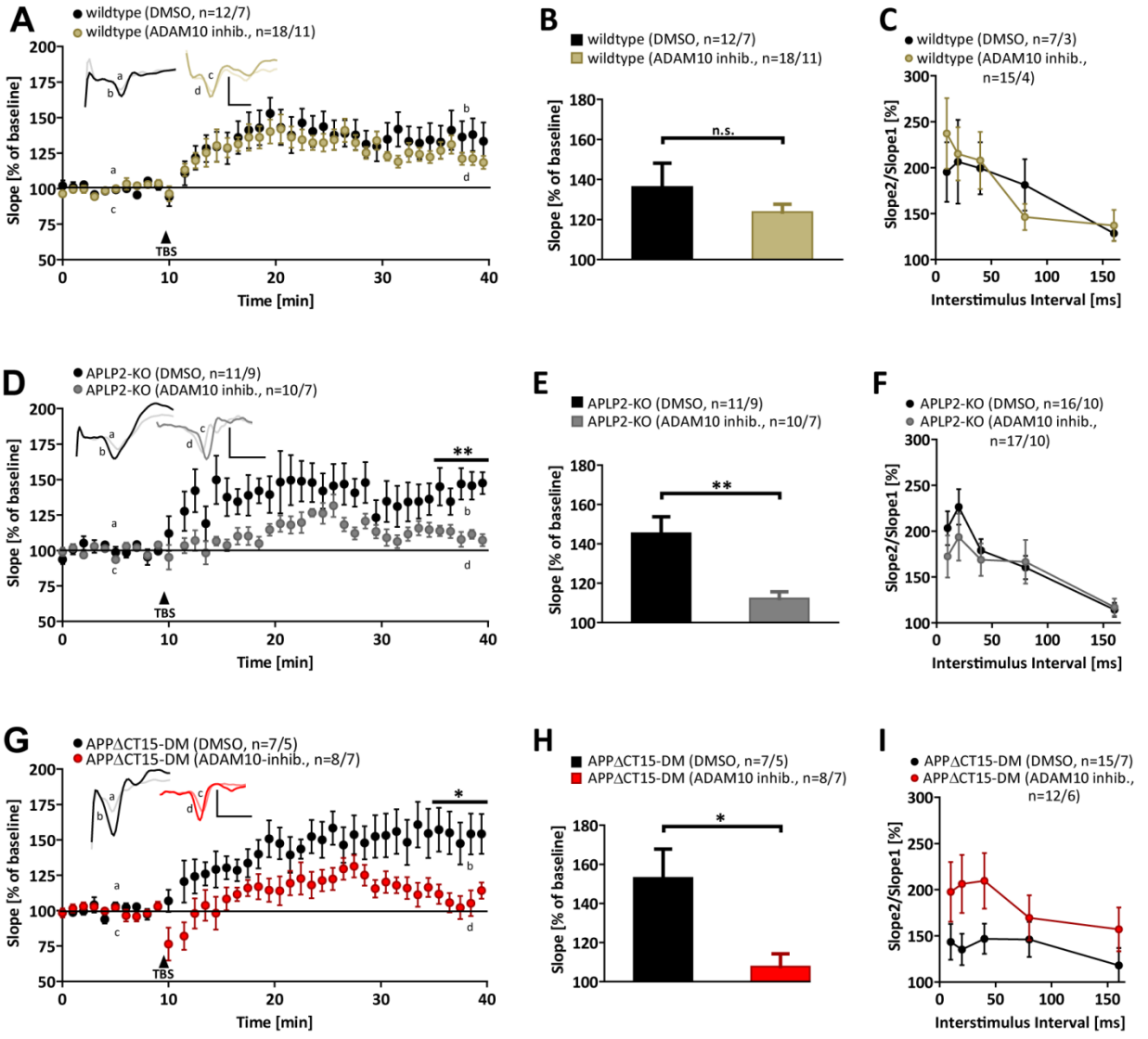

Figure 3.1 LTP experiments in organotypic hippocampal slice cultures prepared at P0 (previous page).
(A+B) *OHCs of wildtype mice were either treated for 5 consecutive days with DMSO as vehicle control (black circles) or ADAM10 inhibitor GI254023X (light green circles). After 10 min of baseline recording LTP was induced by TBS (arrow). In both conditions stable potentiation levels of 136 ± 11.9 % vs. 123 ± 4.0 % for t35-40 min were statistically indistinguishable (p = 0.27, t-test).* ***(C)*** *Short-term plasticity was unaffected.* ***(D+E)*** *OHCs of APLP2-KO individuals revealed a highly significant defect in DMSO treated controls (145 ± 8.3 %, black circles) compared to those treated with ADAM10 inhibitor, where no pronounced LTP was observed (112 ± 3.3 %, grey circles, p = 0.002, t-test).* ***(F)*** *Presynaptic function was found to be unchanged.* ***(G+H)*** *A comparable observation was made for OHCs from APPΔCT15-DM (red circles). Here after TBS application fEPSP slope did not increase initially afterwards but several minutes later compared to vehicle control (black circles) and reached just a short phase of potentiation, which returned to baseline levels during final 5 min of recording (107 ± 6.5 % vs. 153 ± 14.7 %, p = 0.017, t-test).* ***(I)*** *PPF paradigm failed to unravel any significant defects in short-term plasticity. Insets show original traces of representative individual experiments. Vertical scale bar = 0.5 mV, horizontal scale bar = 5 ms. Error bars indicate ± SEM. n.s. = not significant. n = number no of OHCs / number of mice used.*

3.1.2 APPΔCT15-Double Mutant

Since APPsα is not membrane bound in APPsα-DM and lateral diffusion might be accountable for unsufficient concentrations at active synapses I analyzed APPΔCT15-DM mice ($APP\Delta CT15^{+/+}APP^{-/-}APLP2^{-/-}$). Here, a fragment of APP was expressed which lacks the last 15 amino acids at the intracellular C-terminus. The APP intracellular domain (AICD) was shown to modulate gene expression in the nucleus thereby regulating phosphoinositide-mediated Ca^{2+} signaling (Leissring et al., 2002). In all following results presented APLP2-KO mice served as littermate control as they were shown in previous studies to be indistinguishable to wildtype mice in electrophysiological and morphological characteristics (Weyer et al., 2011; Zhang et al., 2013; Weyer et al., 2014).

LTP induction by TBS led to an overall increase in synaptic strength in both APPΔCT15-DM and littermate control (Figure 3.2 A). Whereby, APPΔCT15-DM already revealed a significantly decreased induction phase of post tetanic potentiation (PTP) compared to control. This defect proceeded in the maintenance phase of the LTP showing a significant reduction of average potentiation levels for the final 5 min of 60 min after TBS of 129 ± 6.0 % (n = 15 / 4) for APPΔCT15-DM compared to 160 ± 9.7 % (n = 16 / 5) for littermate control (Figure 3.2 A and B, p = 0.015, t-test). To assess whether this defect persists also during protein synthesis dependent part of Late-LTP (L-LTP), 3 h after TBS were recorded and the mean of the last 5 min was analyzed. Indeed, the same trend became obvious for APPΔCT15-DM with 121 ± 13.0 % (n = 4 / 3) and littermate control 151 ± 11.9 % of potentiation (n = 3 / 3), although it was not significant

between genotypes (Figure 3.2 C and D, p = 0.215, t-test). To test whether the defect is accompanied by an altered basal synaptic transmission first the input-output strength was measured. The correlation of the fEPSP slope to defined stimulus intensities (Figure 3.2 E) revealed a larger fEPSP slope in the double mutants than in the controls which was significant at currents ranging from 100 µA (p = 0.046), 125 µA (p = 0.042) to 150 µA (p = 0.048, t-test). Comparable results were obtained by measuring the slope size at given fiber volley amplitudes (Figure 3.2 F). Again, the slope size was increased in relation to values from littermate controls over the complete measurement while this difference became only significant for a fiber volley amplitude of 0.2 mV (p = 0.007. t-test). As a second approach the presynaptic functionality and short-term plasticity were checked by the PPF. To this end two pulses with defined interstimulus intervals (ISI) were applied and the sizes of slope 2 / 1 were calculated revealing no significant difference (Figure 3.2). Overall this hints to a postsynaptic, but not presynaptic defect which might affect in turn the LTP.

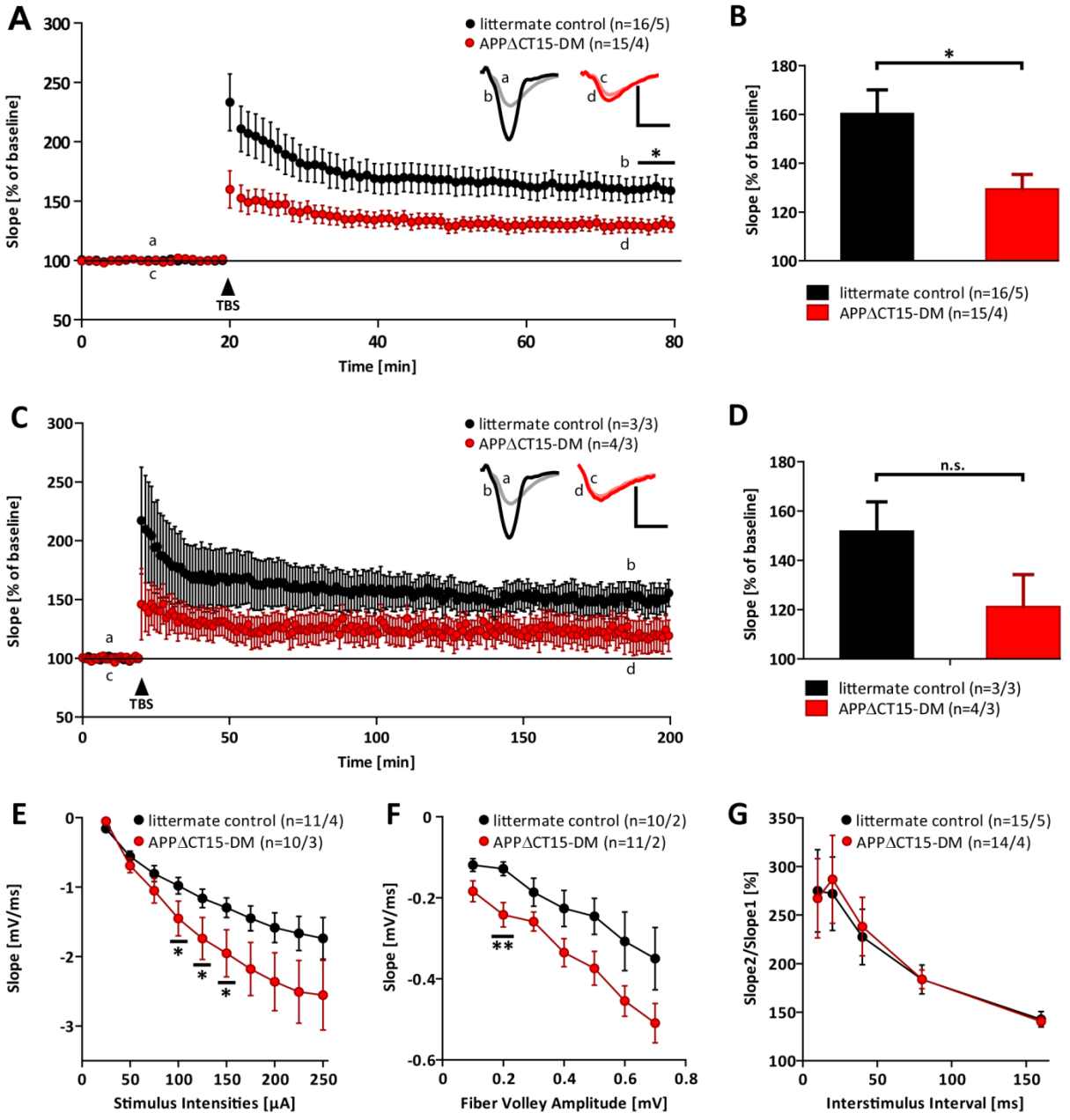

Figure 3.2 LTP and L-LTP experiments of adult APPΔCT15-DM mice.

(A) *After 20 min of baseline recording, LTP was successfully induced by TBS (arrow). APPΔCT15-DM (red circles) revealed significantly lower posttetanic potentiation (PTP) as well as overall potentiation levels compared to littermate control (black circles).* ***(B)*** *Average of fEPSP values for the final 5 min of 60 min LTP recording were depicted as bar graph showing a significant difference in potentiation levels for littermate control 160 ± 9.7 % and APPΔCT15-DM 129 ± 6.0 % (p = 0.015, t-test).* ***(C)*** *Recording time was prolonged to 3 h after LTP induction to investigate protein synthesis dependent L-LTP. Progression of L-LTP exhibited a comparable trend as LTP recordings, whereas the difference between both genotypes was not significant for the mean of the final 5 min with p = 0.215, t-test* ***(D)****.* ***(E)*** *Input-output strength was significantly impaired at defined stimulus intensities of 100 µA (p = 0.046), 125 µA (p = 0.042), 150 µA (p = 0.048, t-test) and* ***(F)*** *at given fiber volley amplitudes of 0.2 mV (p = 0.007, t-test).* ***(G)*** *Presynaptic functions are unchanged among genotypes. Insets show original traces of representative individual experiments. Vertical scale bar = 1 mV, horizontal scale bar = 5 ms. Error bars indicate ± SEM. n.s. = not significant. n = number no of slices / number of mice used.*

3.1.3 Conditional APP Knock-out on APLP2 Deficient Background

The conditional knock-out strategy enables to create time and tissue specific ablation of targeted genes. Here I made use of this technique to tackle the question whether a knock-out of both APP and APLP2 affects activity-dependent synaptic plasticity. This was so far impossible as a constitutive double knock-out (DKO) was lethal due to neuro-muscular weakness (Heber et al., 2000; Ring et al., 2007). Thus $APP^{flox/flox}APLP2^{-/-}$, when crossed to various Cre-deleter mouse lines, resulted in viable DKOs for both proteins. As expression levels are particularly high in pyramidal cells of neocortex and hippocampus we initially focused on the excitatory system.

3.1.3.1 CaMKIIαCre Conditional Double Knock-out

In the next experimental series $APP^{flox/flox}APLP2^{-/-}$ mice were crossed to an inducible CaMKIIαCre line providing a tool for flexible timing of APP deletion in excitatory forebrain neurons by tamoxifen application. I wanted to investigate the requirement of APP and APLP2 in the adult CNS at active synapses in processes of activity-dependent synaptic plasticity. First, adult CaMKIIαCre cDKO and the respective littermate controls were treated with tamoxifen to induce APP excision. Those animals were investigated regarding synaptic plasticity 4 weeks (1x tamoxifen, adult, 3 – 4 months of age) or several months (1x tamoxifen, aged, 12 – 13 months of age) after injection. This should uncover possible age-related and redundant effects of APP and APLP2 DKO. Second, a comparable approach was applied, but now P5 pubs of CaMKIIαCre cDKO and littermate controls received tamoxifen additionally via lactating mothers to receive a maximal Cre activation (for details see 2.1.2). Again, adult (2x tamoxifen, 3 – 4 months of age) and aged (2x tamoxifen, 12 – 13 months of age) mice were analyzed.

In a first recording session 1x tamoxifen treated adult CaMKIIαCre cDKO and littermate controls were assessed by a former PhD student (see dissertation of Andrea Delekate, 2011, Figure 3.16). Results revealed a significant defect in average potentiation of final 5 min in LTP ($p = 0.045$, t-test) and L-LTP ($p = 0.041$) between genotypes. Short-term plasticity was unaltered as well as basal synaptic transmission at given stimulus intensities. However, fEPSP slope sizes of CaMKIIαCre cDKO were significantly increased at defined fiber volley amplitudes ($p \leq 0.05$, t-test).

In order to investigate age-dependent effects next 1x tamoxifen treated aged CaMKIIαCre cDKO and respective littermate controls were examined. In contrast to adult individuals, older mice didn't reveal any significant deficits between genotypes neither in LTP (Figure 3.3 A and B, p = 0.099, t-test) nor in L-LTP (Figure 3.3 C and D, p = 0.499, t-test). The averaged values of potentiation 60 min after TBS were 133 ± 2.7 % for CaMKIIαCre cDKO (n = 22 / 5) and 143 ± 5.4 % for littermate control (n = 23 / 5). The final 5 min of L-LTP recording led to 131 ± 4.5 % for CaMKIIαCre cDKO (n = 7 / 4) and 125 ± 6.0 % for littermate control (n = 9 / 3). Basal synaptic transmission was unaltered as well, since correlation of defined currents and set fiber volley amplitudes were statistically indistinguishable (Figure 3.3 E and F). Furthermore, the ratio of two closely applied stimuli pointed towards normal presynaptic functionality (Figure 3.3 G).

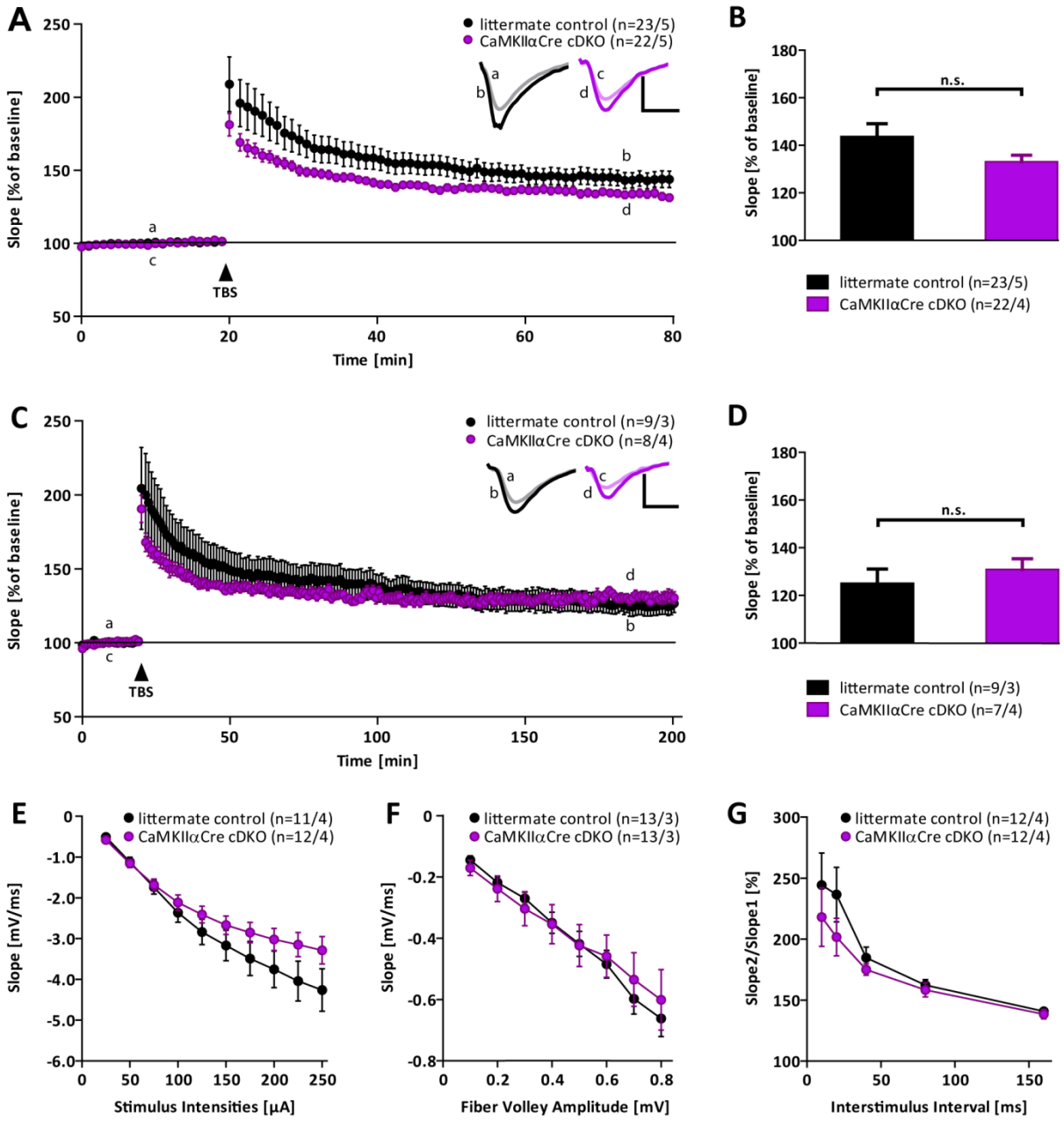

Figure 3.3 LTP experiments in aged 1x tamoxifen treated CaMKIIαCre cDKO mice.
(A+B) *Stable baseline recording of 20 min was followed by LTP induction via TBS (arrow) resulting in a robust and maintained, but not significantly altered LTP in both CaMKIIαCre cDKO (133 ± 2.7 %, purple circles) and littermate control mice (143 ± 5.4 %, p = 0.099, t-test, black circles).* ***(C+D)*** *L-LTP exhibited similar values after TBS for CaMKIIαCre cDKO (125 ± 6.0 %) and littermate control individuals (125 ± 6.0 125 ± 6.0 %, p = 0.499, t-test).* ***(E+F)*** *Postsynaptic functions were unchanged at given stimulus intensities and fiber volley amplitudes among genotypes.* ***(G)*** *Presynaptic functionality was unaltered as well. Insets show original traces of representative individual experiments. Vertical scale bar = 1 mV, horizontal scale bar = 5 ms. Error bars indicate ± SEM. n.s. = not significant. n = number no of slices / number of mice used.*

To reach as much neurons as possible for the Cre activation, CaMKIIαCre cDKO and their littermate controls were treated twice with tamoxifen. Once at P5 via mothers milk and a second time with an age of 6-8 weeks. Since the CaMKIIα promoter is expressed directly after birth this procedure should lead to the maximal APP ablation possible. Figure 3.4 depicts results from recordings of adult mice. After 20 min of stable baseline recording, an induction by TBS resulted in a robust PTP and maintained LTP in both CaMKIIαCre cDKO as well as littermate controls which were statistically indistinguishable at any time point recorded (Figure 3.4 A). A stable potentiation finally led to average levels for t75-80 min of 170 ± 6.9 % for littermate controls (n = 19 / 6) and 165 ± 8.9 % for CaMKIIαCre cDKO (n = 20 / 7, p = 0.659, t-test, Figure 3.4 B). These findings contrasted to results obtained from basal synaptic transmission and long-term recordings. L-LTP measurement of 3 h revealed again a strong induction and stability but now a significant difference in the protein synthesis dependent phase became obvious between genotypes (Figure 3.4 C). 5 min before recordings ended an average potentiation of 160 ± 11.0 % was calculated for littermate controls (n = 5 / 4) and 132 ± 4.5 % for CaMKIIαCre cDKO (n = 6 / 4, p = 0.048, t-test, Figure 3.4 D). While the correlation of fEPSP slope sizes to given stimulus intensities did not differ significantly (Figure 3.4 E), the correlation to defined fiber volley amplitudes uncovered an increased response (Figure 3.4 F). This alteration became significant for amplitudes of 0.1 mV (p = 0.033) and 0.3 mV (p = 0.044, t-test). Additionally, short-term plasticity was affected as indicated by a significant difference for ISI 160 ms in the PPF paradigm (p = 0.034, t-test, Figure 3.4 G). All together these findings suggest an acute role of both APP and APLP2 at active synapses as well as potentially in processes of synaptogenesis.

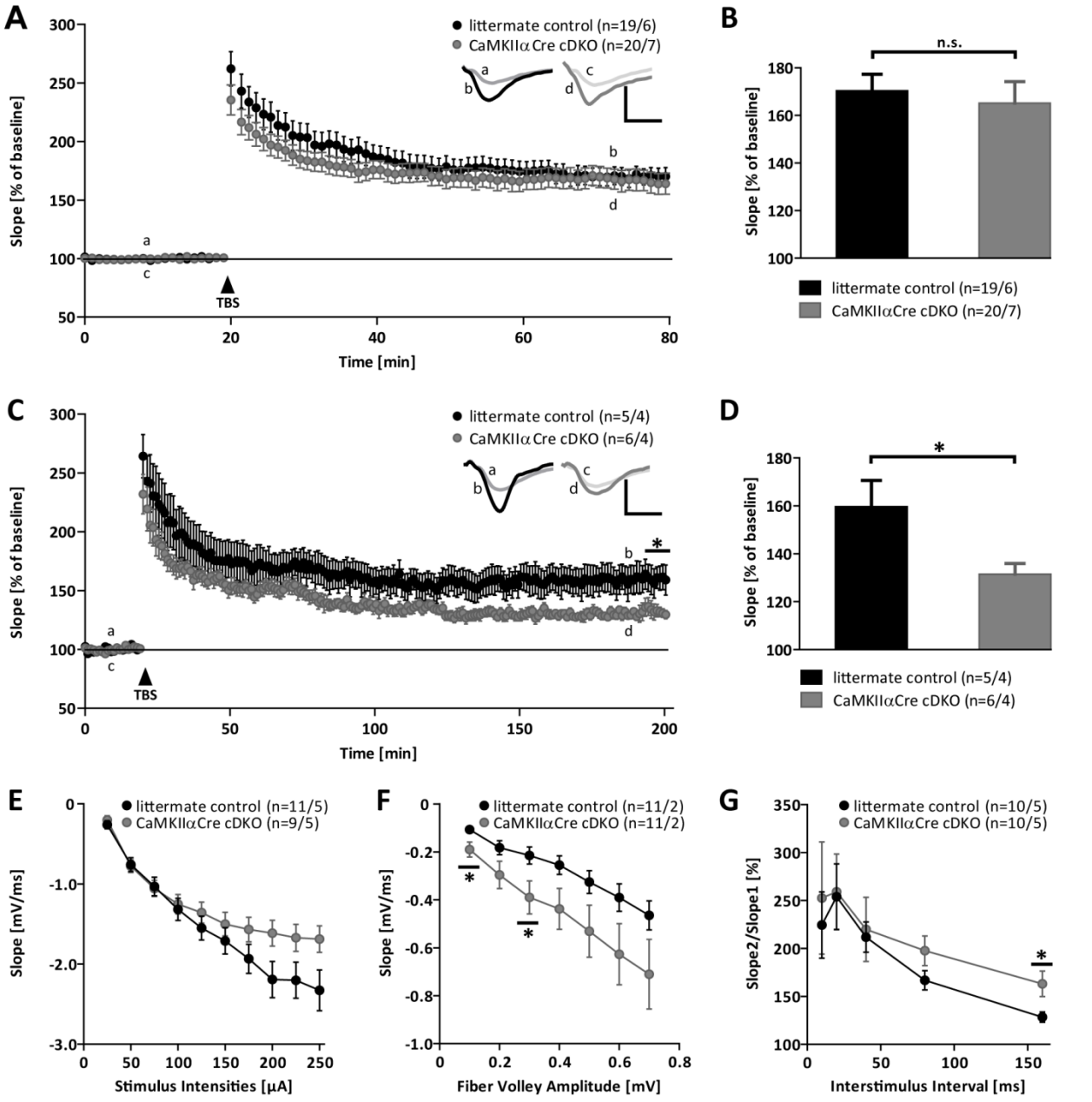

Figure 3.4 LTP experiments in adult 2x tamoxifen treated CaMKIIαCre cDKO mice.
(A+B) *TBS (arrow) application induced a strong and stable LTP in littermate controls of 170 ± 6.9 % (black circles) and in CaMKIIαCre cDKO of 165 ± 8.9 % (grey circles) for t75 – 80 min (p = 0.659, t-test), which resulted in overlapping curves.* ***(C+D)*** *Contrary results were obtained for L-LTP. Again a robust induction phase was observed in both genotypes which turned into a significant difference between littermate controls of 160 ± 11.0 % and CaMKIIαCre cDKO of 132 ± 4.5 % for t195 – 200 min in the plateau of L-LTP (p = 0.048, t-test).* ***(E)*** *Recording of fEPSP slope size at given stimulus intensities revealed no significant differences between genotypes.* ***(F)*** *Whereas, analysis of fEPSP slope at defined fiber volley amplitudes led to partially significant increase of postsynaptic function (0.1 mV: p = 0.033, 0.3 mV: p = 0.044, t-test).* ***(G)*** *Presynaptic functionality was affected as well as indicated by a significant deficit for an ISI of 160 ms (p = 0.034, t-test). Insets show original traces of representative individual experiments. Vertical scale bar = 1 mV, horizontal scale bar = 5 ms. Error bars indicate ± SEM. n.s. = not significant. n = number no of slices / number of mice used.*

To complement the investigations concerning the aspect of age, CaMKIIαCre cDKO mice and their littermate controls were treated twice with tamoxifen as described beforehand. In this experimental series aged individuals (12-13 months) have been analyzed. Figure 3.5 depicts results obtained from these recordings. The TBS application led to a strong LTP induction. Compared to adult individuals (Figure 3.4 A and C) the PTP was found not to be as pronounced in aged mice (Figure 3.5 A and B). Nevertheless, both genotypes revealed a stable plateau for LTP with 142 ± 6.0 % (n = 11 / 4) for littermate controls and 132 ± 4.3 % (n = 16 / 6) in CaMKIIαCre cDKO mice which was statistically indistinguishable (p = 0.177, t-test, Figure 3.5 A and B). These findings were supported by data obtained from L-LTP measurements (Figure 3.5 C and D) which uncovered no significant defect as curves almost overlapped the entire recording time (littermate control: 130 ± 2.3 %, n = 7 / 3; CaMKIIαCre cDKO: 135 ± 6.3 %, n = 8 / 5; p = 0.770, t-test). Postsynaptic functionality was unchanged irrespective of paradigm tested (Figure 3.5 E and F). In contrast to this, but in line with observations made in adult transgenic mice (Figure 3.4 G), short-term plasticity was highly significantly altered again at larger ISI of 160 ms (p = 0.003) and additionally at shorter ISI of 40 ms (p = 0.007, t-test, Figure 3.5 G).

All together the examination of $APP^{flox/flox}APLP2^{-/-}$ mice crossed to an inducible CaMKIIαCre line lead to a mild or not at all affected LTP as well as L-LTP. This suggests that a postnatal knock-out of APP on an APLP2 deficient background was not effective enough to cause a pronounced defect in potentiation. Aged mice receiving tamoxifen once revealed no significant deficit. This was sustained in adult and aged twice tamoxifen treated mice revealing only subtle effects as well. Possibly, the knock-out of APP during synaptogenesis might be already too late or too inefficient to cause a severe impairment in activity-dependent synaptic plasticity or neuronal network formation.

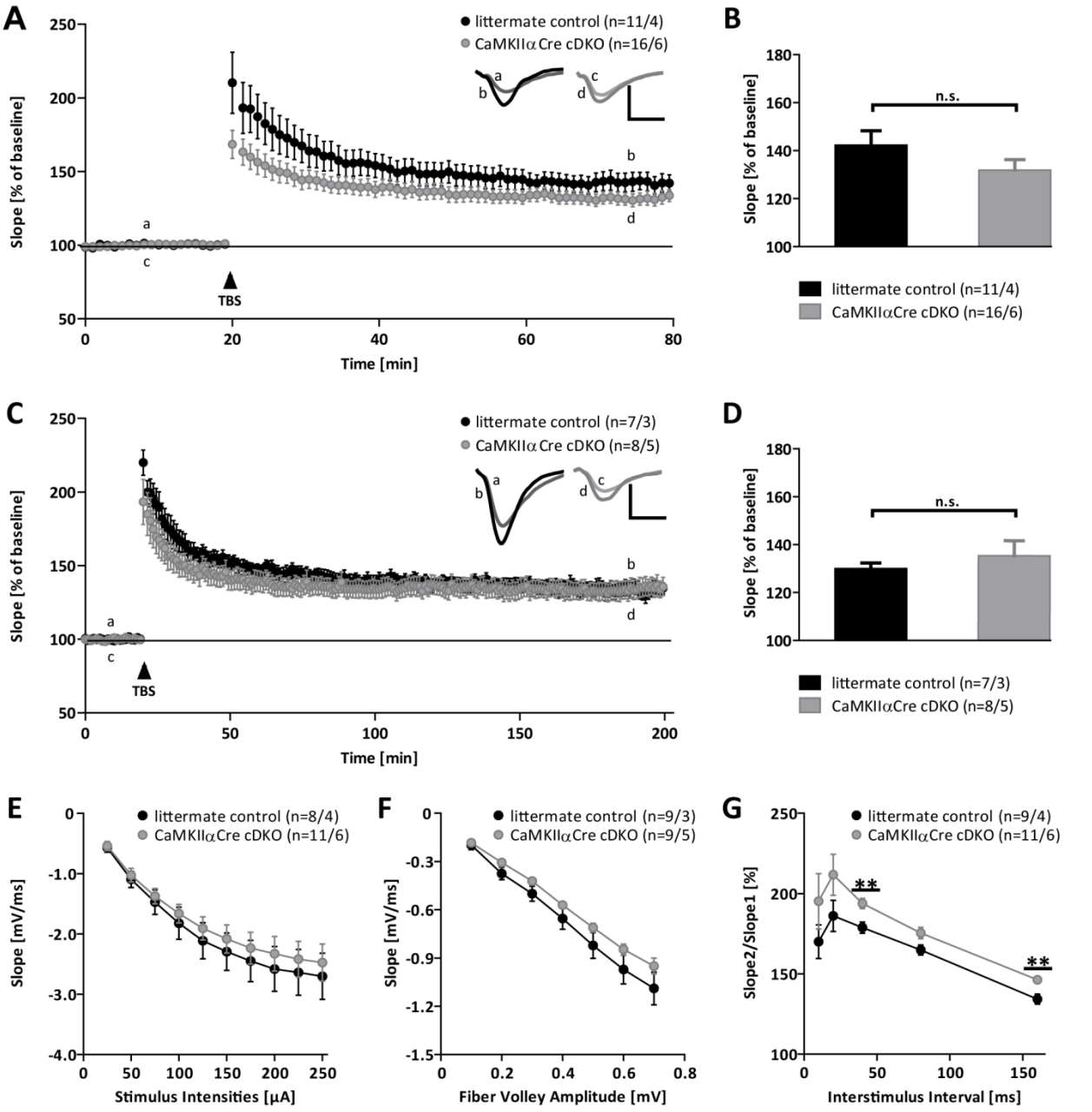

Figure 3.5 LTP experiments in aged 2x tamoxifen treated CaMKIIαCre cDKO mice.
(A+B) *Littermate controls (black circles) revealed an average potentiation of 142 ± 6.0 % for the final 5 min of LTP recording. These values were statistically indistinguishable to those obtained from CaMKIIαCre cDKO (132 ± 4.3 %, p = 0.177, t-test, light grey circles).* ***(C+D)*** *Comparable results were gained for protein synthesis dependent L-LTP. Here littermate control mice revealed average potentiation levels for t195-200 min of 130 ± 2.3 % and CaMKIIαCre cDKO 135 ± 6.3 % (p = 0.770, t-test).* ***(E+F)*** *Input-output strength was unaltered between genotypes.* ***(G)*** *Whereas a highly significant defect was observed for CaMKIIαCre cDKO in an ISI of 160 ms (p = 0.003) and 40 ms (p = 0.007, t-test) compared to littermate control individuals. Insets show original traces of representative individual experiments. Vertical scale bar = 1 mV, horizontal scale bar = 5 ms. Error bars indicate ± SEM. n.s. = not significant. n = number no of slices / number of mice used.*

3.1.3.2 NexCre Conditional Double Knock-out

Having established that once or twice tamoxifen treated CaMKIIαCre cDKO exhibited only mild or no defects at all in activity-dependent synaptic plasticity as well as hippocampus dependent learning tasks (Prof. Dr. David Wolfer, University of Zürich, unpublished data) I next assessed whether APP might be necessary during prenatal development (e.g. circuit formation or neuronal morphology). Therefore, $APP^{flox/flox}APLP2^{-/-}$ mice were bred with a NexCre-deleter strain (Goebbels et al., 2006). Again, this led to an APP ablation exclusively in excitatory forebrain neurons on an APLP2 deficient background. In contrast to CaMKIIαCre cDKO this occurred already prenatally from E11.5 onwards (for details see 2.1.2). Thus, I wanted to gain insight if an early deletion might result in neurodevelopmental defects that would affect synaptic plasticity in adult individuals (3-4 months of age).

Therefore, again the enlargement of fEPSP slope was recorded for either 60 min following TBS in order to cover the protein synthesis independent part of LTP (Figure 3.6 A and B) or in case of L-LTP for 180 min after TBS for analyzing protein synthesis dependent events (Figure 3.6 C and D). In both after induction a stable LTP was observed. Nevertheless, a pronounced defect of PTP as well as potentiation itself became obvious for NexCre cDKO mice (Figure 3.6 A). The average potentiation in slices from littermate controls was 161 ± 6.0 % (n = 31 / 8), whereas NexCre cDKOs revealed highly significant reduced levels of 127 ± 2.3 % (n = 26 / 8) for final the 5 min ($p = 0.00001$, t-test, Figure 3.6 B). Also in long-term recordings a decreased potentiation was observed, although it was not significant for t195 – 200 min (littermate control: 149 ± 10.6 %, n = 5 / 3; NexCre cDKO: 123 ± 8.3 %, n = 7 / 3, $p = 0.109$, t-test, Figure 3.6 C) but for t20 – 130 min ($p = 0.011$, t-test) probably due to the instable plateau of controls. To investigate if the detected LTP deficit was also reflected in disturbed basal synaptic properties, next pre- and postsynaptic functionality was explored. Figure 3.6 E and F illustrate that input-output strength was unaffected since fEPSP size did not differ significantly between genotypes neither at defined stimulus intensities nor at given fiber volley amplitudes. In order to explore if the LTP defect was accompanied by alterations in short-term plasticity PPF was analyzed. Indeed, NexCre cDKO mice exhibited a highly significant impairment at shorter ISIs of 10 ms ($p = 0.004$) and 20 ms ($p = 0.007$, t-test) compared to littermate control slices (Figure 3.6 G). Altogether these findings suggest an essential role of both APP and APLP2 during early development.

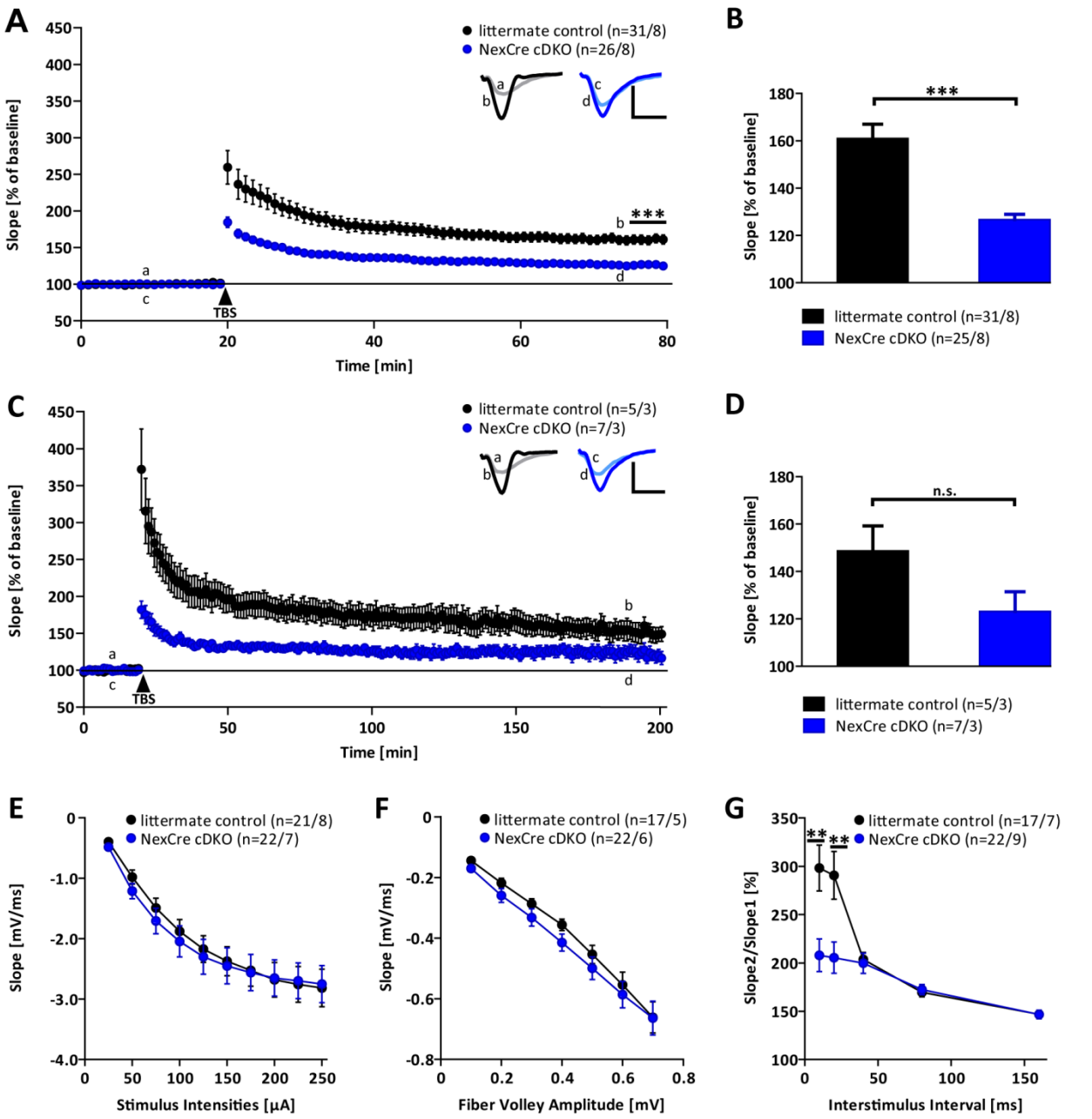

Figure 3.6 LTP experiments in adult NexCre cDKO mice.

(A) *After TBS (arrow) application littermate controls (black circles) revealed a robust and stable potentiation of 161 ± 6.0 % for the final 5 min of LTP recording* ***(B)****. In NexCre cDKO mice (blue circles) a highly significant defect in LTP induction as well as maintenance compared to controls was discovered (127 ± 2.3 %, p = 0.0001, t-test).* ***(C)*** *NexCre cDKO mice showed a deficit in L-LTP induction and maintenance, which was significant only from t20-130 min (p = 0.01) but not for t195-200 min (p = 0.109, t-test,* ***D****).* ***(E+F)*** *Input-output strength was unaltered.* ***(G)*** *PPF tested at defined ISIs revealed a pronounced and highly significant defect in short-term plasticity at lower ISIs in NexCre cDKO mice compared to the littermate controls (10 ms: p = 0.004, 20 ms: p = 0.007, t-test). Insets show original traces of representative individual experiments. Vertical scale bar = 1 mV, horizontal scale bar = 5 ms. Error bars indicate ± SEM. n.s. = not significant. n = number no of slices / number of mice used.*

3.1.3.3 Quantitative Ca^{2+} Imaging in Primary Hippocampal Dissociated NexCre cDKO Cultures

The previously investigated electrically evoked LTP is accompanied by a transient increase in postsynaptic calcium ions (Ca^{2+}). This process is crucial for the induction of activity-dependent synaptic plasticity (Zucker, 1999). When glutamate binds to AMPA receptors (AMPAR) they mediate the fast excitatory transmission (see 1.1.2). Together, back propagating action potentials and membrane depolarization of the dendritic spines open additionally voltage gated Ca^{2+} channels (VGCCs) which in part mediate the influx of Ca^{2+}. A wide variety of VGCCs are classified including high-voltage-activated L-, P/Q, N- and R-type channels and low-voltage-activated T-type channels. L-type channels were proven to be essential for synaptic plasticity since through Ca^{2+} entry they regulate gene transcription of immediate early genes and mediate the activation of CREB via stimulation of CaMKII pathway (Murphy et al., 1991; Wheeler et al., 2012). Since APP was shown to regulate the $Ca_v1.2$ L-type Ca^{2+} channel and its functionality in GABAergic short-term plasticity I asked whether inhibition of this channel might affect the Ca^{2+} dynamics in NexCre cDKOs (Yang et al., 2009). As a further effect of simultaneous glutamate binding and postsynaptic membrane depolarization NMDA receptors (NMDAR) open which mediate the main Ca^{2+} influx into the dendritic spine. Ca^{2+} influx through NMDAR is required for both LTP and LTD (see 1.1.2). In the following experimental series I investigated if a chemically induced LTP uncovers a comparable defect as observed in electrophysiological studies of NexCre cDKO. The NDMAR can be activated by glycine as this is a co-agonist for glutamate binding. To ensure that results obtained from these experiments exclusively based on NMDAR activation, additionally always Strychnine was applied to specifically block endogenous glycine receptors. When furthermore the NMDAR inhibitor APV was administered the opening of the NMDAR upon glycine binding should be abolished. After Ca^{2+} entered the neuron it triggers subsequent Ca^{2+} release from internal stores of the endoplasmatic reticulum (ER) through IP_3R and RyR. Reuptake of Ca^{2+} back into the ER by the sarco-/endoplasmic reticulum ATPase (SERCA) is mandatory for propagating future signals. Given that the frequent release of Ca^{2+} from internal stores is crucial to ensure the reaction upon neuronal stimulation and induction of synaptic plasticity I also inhibited the reload of Ca^{2+} into the ER by blocking the SERCA.

As recording Ca^{2+} signals is a feasible and widely used method to investigate action potential distribution *in vitro* I as well established this technique (see 2.6) to examine NexCre cDKO and

littermate control mice regarding Ca^{2+} dynamics. Figure 3.7 illustrates how Ca^{2+} signals for a randomly chosen experiment from littermate controls (A, black) and NexCre cDKO (B, blue) look like. First, the neurons with clearly apparent somata in the field of view are shown. Ca^{2+} transients were always measured in the soma. The adjacent graphs illustrate example traces from a single experiment over time and for each time-point imaged following the scheme described in Figure 2.5. Additionally, a heat map generated by a pseudo-line scan (pink bar) visualizes the Ca^{2+} alteration.

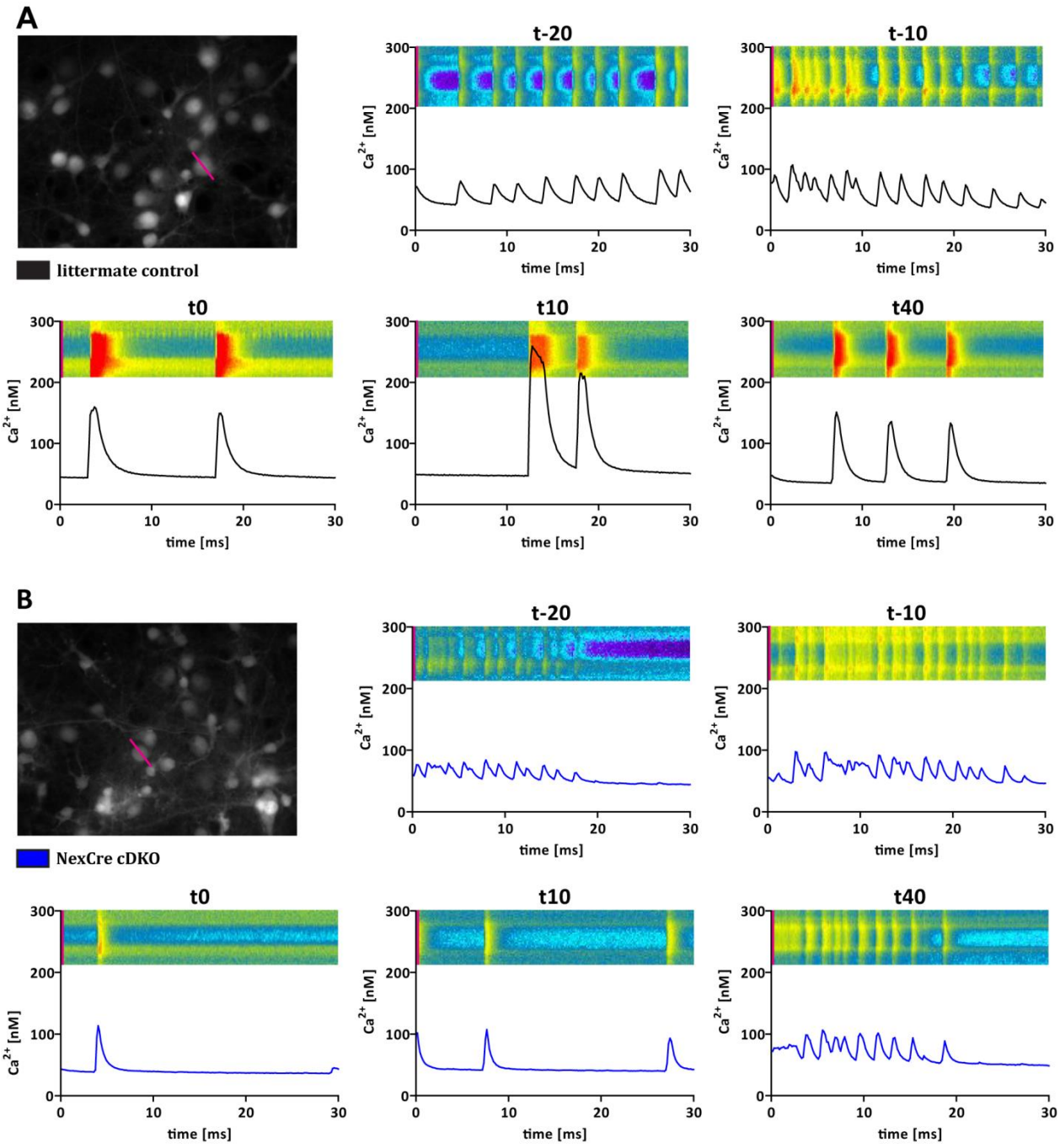

Figure 3.7 Example traces for cLTP induction by glycine in littermate controls and NexCre cDKO (previous page). *The scheme illustrates example traces obtained from one littermate control (**A**, black) and one NexCre cDKOs (**B**, blue) Ca^{2+} imaging experiment. The first image depicts the neurons in the field of view. Following graphs show one example trace of the Ca^{2+} signals recorded in the soma, separately for each time-point imaged (t-20, t-10, t0, t10, t40). In **A** and **B** above those graphs the pseudo-line scan (pink bar) additionally depicts these signals as a heat map over time.*

Figure 3.8, Figure 3.9 and Figure 3.10 illustrate data obtained from quantitative Ca^{2+} imaging. On the one hand, the amount of intracellular Ca^{2+} is depicted in nM and on the other hand the frequency of Ca^{2+} spikes / min. Following the experimental design illustrated in Figure 2.5, the amount of intracellular Ca^{2+} or the frequency of spontaneous activity were quantified. This includes the analysis of defined time points before (t-20, t-10) and upon (t0, t 10, t40) cLTP induction by glycine only, or additional drug application. For each treatment two ways of illustration were chosen to facilitate reviewing of the data. The first graph shows the results for littermate control (black) and NexCre cDKO (blue) separately. The second graph depicts every time-point imaged while comparing both genotypes.

When the amount of Ca^{2+} during spontaneous activity without stimulation was quantified, littermate controls revealed stable values of 32 ± 3.1 nM for t-20 being significantly different to NexCre cDKO with 17 ± 3.2 nM. However, with values of 34 ± 3.8 nM (littermate control) versus 23 ± 4.4 nM (NexCre cDKO) at t-10 (Figure 3.8 B) only a trend towards reduced Ca^{2+} responses was found. These results suggest that in NexCre cDKO already the Ca^{2+} signals before chemically induced LTP was lower than in controls. Upon glycine stimulation in both littermate controls as well as NexCre cDKO an increase of intracellular Ca^{2+} could be observed, although to a lesser and more instable extend in cDKOs. While in littermate controls t0 and t10 revealed comparable values of 80 ± 6.7 nM and 87 ± 10.0 nM, t40 showed a drop of intracellular Ca^{2+} amount to 53 ± 4.2 nM Ca^{2+} (Figure 3.8 A). When separately analyzing imaging time-points of t0 and t10 between genotypes for NexCre cDKO a significant defect was observed with values of 54 ± 6.7 nM (t0) and 39 ± 4.5 nM (t10). The same trend became visible for t40, although it was not significant (Figure 3.8 B). Nevertheless, when the normalized amplitude of both genotypes was analyzed in relation to the Ca^{2+} concentration of spontaneous activity before cLTP induction, it became clear that the relative change in intracellular Ca^{2+} was almost the same independent of genotype (Figure 3.9 A).

Inhibiting the NMDAR by APV prevented induction of LTP in both genotypes reflected by preserved resting Ca^{2+} levels (Figure 3.8 C). When those levels were compared at all time-points again the significantly less spontaneous activity at t-20 in NexCre cDKOs occured (littermate controls: 37 ± 4.1 nM vs. NexCre cDKO: 21 ± 3.9 nM). Additionally, a significant difference was found for t10 as well (littermate controls: 42 ± 3.9 nM vs. NexCre cDKO: 23 ± 4.7 nM, Figure 3.8 D). Still, when the amplitude was normalized to Ca^{2+} signals before cLTP induction no significant difference was found between genotypes (Figure 3.9 B). These observations indicate that the Ca^{2+} influx through the NMDAR is crucial for stimulating the rise of intracellular Ca^{2+} amongst others also the release from ER and thus triggering further synaptic plasticity related processes.

Following, I investigated if blocking the reuptake of Ca^{2+} via SERCA back into the ER by a co-application of CPA might influence the effect of glycine administration. Analysis revealed that in littermate controls the significant increase of Ca^{2+} upon stimulation seen in Figure 3.8 A was abolished although a tendency towards a rise was still obvious (Figure 3.8 E). Strikingly, the treatment of NexCre cDKO exhibited a highly significant increase in the cytoplasmatic Ca^{2+} amount of 80 ± 7.9 nM for t0 and 58 ± 8.2 nM for t10 following CPA application compared to the unstimulated state (Figure 3.8 E). The t0 value was surprisingly even higher than the one reached at the same time-point for solely glycine administration (Figure 3.8 A). Furthermore, CPA treated NexCre cDKO reached values of only glycine treated littermate controls at t0, indicating that the ER itself might be affected. These observations were even further supported when the values upon co-application of glycine and CPA were normalized to the unstimulated spontaneous activity of both genotypes exhibiting a significant defect (Figure 3.9 C). At later time-points in NexCre cDKOs the blockade of SERCA prevented the transport of Ca^{2+} back into the ER which is reflected by apparently decreasing values of 58 ± 8.2 nM for t10 and 35 ± 5.8 nM for t40. No stable increase of Ca^{2+} signals upon co-application of glycine and CPA was possible in NexCre cDKOs (Figure 3.8 E and D).

Next, both genotypes were investigated regarding the potential contribution of voltage gated L-type Ca^{2+} channels to the rise of intracellular Ca^{2+} concentration when, additionally to glycine, the selective L-type VGCC inhibitor Nifedipine was applied. It became clear that Nifedipine treatment prevented a significant increase of Ca^{2+} in littermate controls as well as in NexCre cDKOs upon cLTP induction (Figure 3.8 G and H). Still, a trend towards an increase upon glycine

and Nifedipine application was observable in the illustration of absolute (Figure 3.8 G and H) as well as relative (Figure 3.9 D) values for the Ca^{2+} amount which might be explained by the Ca^{2+} influx through the NMDAR. However, this was not strong enough to induce a significant elevation of intracellular Ca^{2+}. These results suggest a partial contribution of voltage gated L-type Ca^{2+} channels to the rise of intracellular Ca^{2+} upon cLTP induction in addition to the activation of NMDAR (Moosmang et al., 2005).

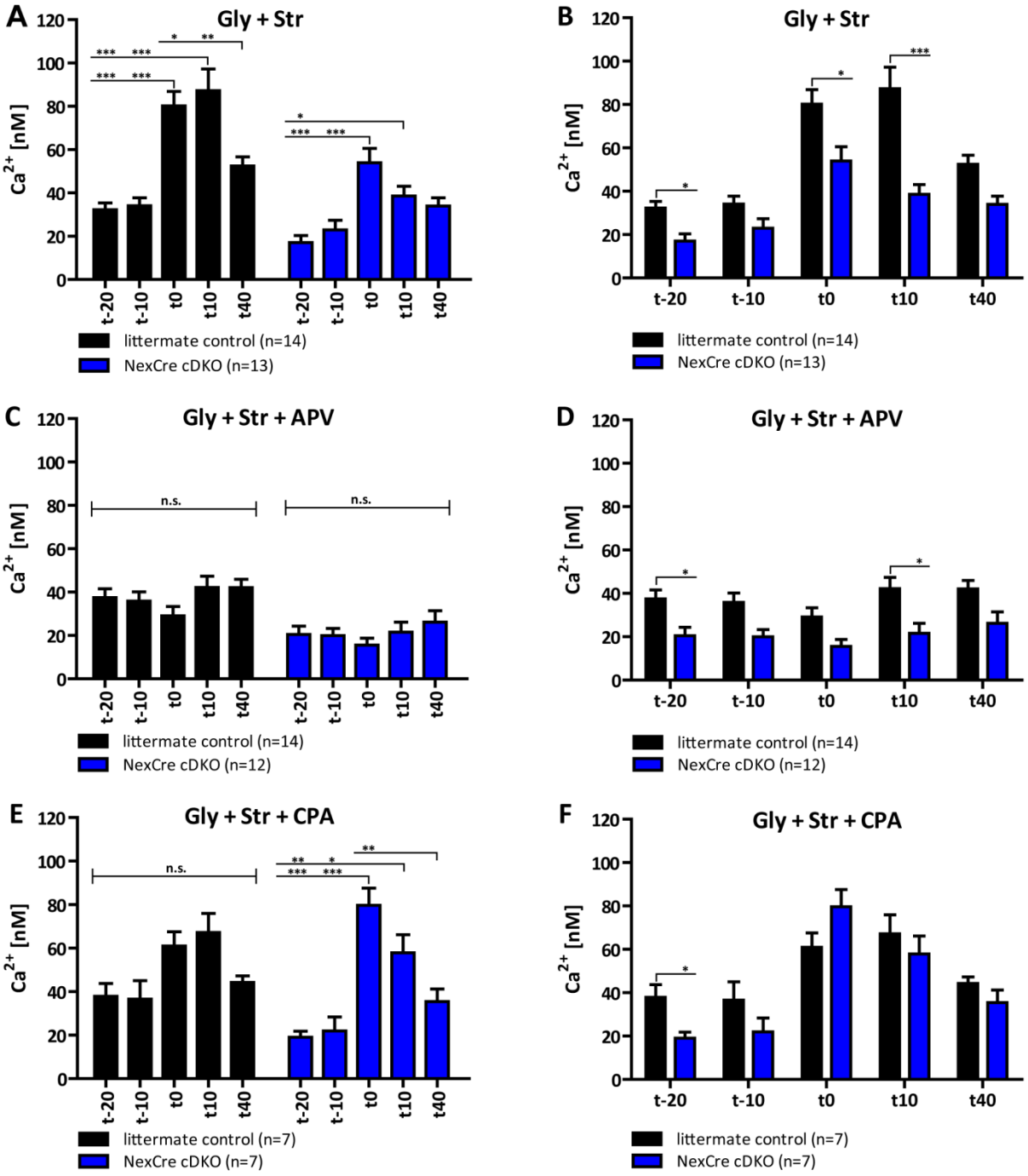

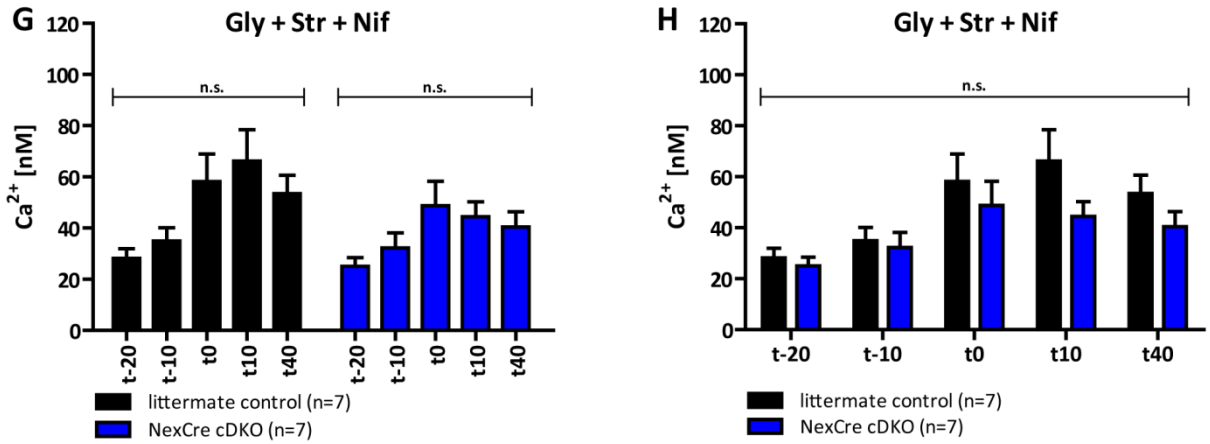

Figure 3.8 Quantitative Ca^{2+} imaging in NexCre cDKO revealed a severe defect in Ca^{2+} amount before and upon stimulation (continued from previous page).

Imaging time-points t-20 and t-10 reflect the resting Ca^{2+} concentration. Whereas t0, t10 and t40 depict the quantification the Ca^{2+} amount upon glycine stimulation only or additional drug application. At the x-axis all time-points imaged are plotted in minutes. ***(A)*** *Upon glycine (Gly) application a strong and partially highly significant increase of cytoplasmatic Ca^{2+} concentration was observed in both genotypes. However, NexCre cDKO cultures (blue) exhibited minor values compared to littermate controls (black).* ***(B)*** *These differences became even more obvious when both genotypes were plotted for each imaging time-point. Here, already at basal Ca^{2+} levels a significant defect in NexCre cDKOs was observed at t-20 which was not as pronounced for t-10 but still found by trend. Furthermore, this deficit was sustained upon glycine administration at t0 and t10. Again, only a tendency was found at t40.* ***(C)*** *A co-application of glycine and APV (NMDAR inhibitor) prevented Ca^{2+} increase in both genotypes.* ***(D)*** *Again, partially significant lower resting Ca^{2+} concentration was observed in NexCre cDKO.* ***(E)*** *An application of CPA (SERCA inhibitor, no reuptake of Ca^{2+} into the ER) together with glycine prevented a significant increase of Ca^{2+} in littermate controls while still a significant defect was observable in NexCre cDKOs. Strikingly, the values for t0 reached even higher Ca^{2+} levels upon stimulation with both glycine and CPA than solely glycine.* ***(F)*** *However, this high mount of Ca^{2+} concentration was not stable and decreased continuously when t10 and t40 were investigated.* ***(G+H)*** *A co-treatment with glycine and Nifedipine (voltage gated L-type Ca^{2+} channel blocker, Nif) prohibited a significant rise of cytoplasmatic Ca^{2+} amount compared to resting Ca^{2+} levels in both littermate control and NexCre cDKO cultures. Significances were plotted as $*p < 0.05$, $**p < 0.01$ and $***p < 0.001$. Error bars indicate ± SEM. n = number of experiments. Str = strychnine.*

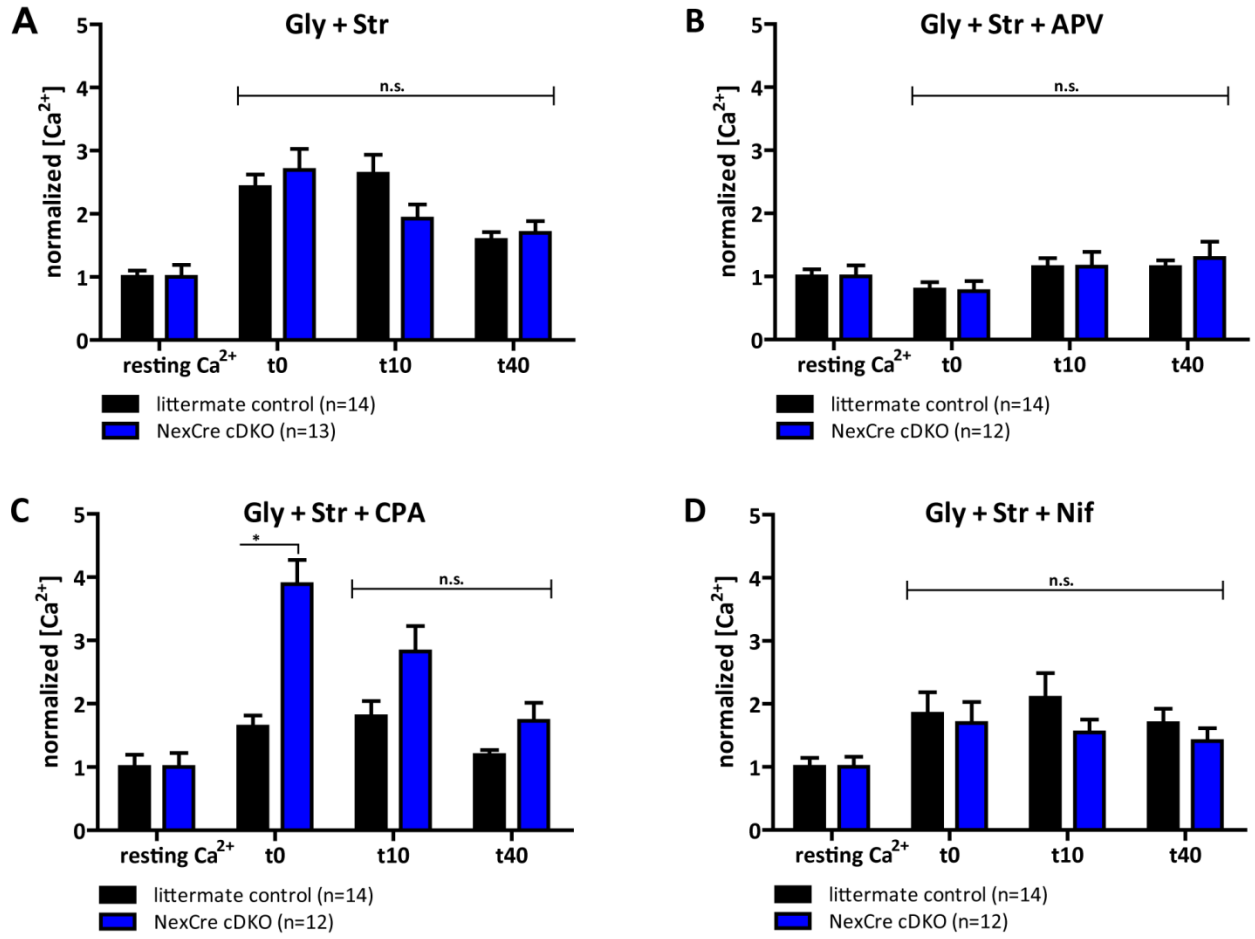

Figure 3.9 Relative Ca^{2+} concentration uncovered a significant increase in NexCre cDKO upon glycine and CPA co-administration.

Bar graphs depict Ca^{2+} amount normalized onto resting Ca^{2+} concentration (averaged t-20 and t-10) upon glycine solely or additional drug administration. ***(A)*** *Chemically induced LTP by glycine (Gly) application led to comparable values reached for the amount of Ca^{2+} and was thus statistically indistinguishable for NexCre cDKO (blue) and littermate control (black).* ***(B)*** *Co-treatment with APV prevented rise of Ca^{2+} concentration in both genotypes to the same extend.* ***(C)*** *Remarkably, the co-administration of glycine and CPA led to a pronounced and significant increase of Ca^{2+} in NexCre cDKO cultures compared to littermate controls at t0 ($p = 0.034$, t-test). The normalized visualization highlights this more clearly than absolute values in Figure 3.8 C. However, at t10 and t40 the values were not significant any longer.* ***(D)*** *Nifedipine (Nif) treatment resulted in similar Ca^{2+} concentrations for both genotypes. Significances were plotted as *$p < 0.05$, **$p < 0.01$ and ***$p < 0.001$. Error bars indicate ± SEM. n = number of experiments. Str = strychnine.*

In addition to the quantification of intracellular Ca^{2+} amounts onto stimulation and inhibitor application, this method also enables the experimenter to investigate the frequency of occurring Ca^{2+} events. These are highly variable since the imaging time window chosen might sometimes cover a very active phase whereas other neurons are less active. Nevertheless, still convincing conclusions can be drawn from these results.

Comparably to the depiction of Ca^{2+} amounts, again first all time-points for every single genotype were shown, whereas the second graph illustrates a direct comparison of each time-point between the genotypes. The application of glycine revealed a significant decrease of 5 ± 1.1 spikes / min at t-20 and 6 ± 1.1 spikes / min at t-10 to 3 ± 0.9 spikes / min at t0, 3 ± 0.6 spikes / min at t10 and 3 ± 0.7 spikes / min at t40 in littermate controls. This effect was not observed in NexCre cDKO (Figure 3.10 A) suggesting that a defect in network activity or a decreased number of synaptic contacts might lead to less network synchronization in the cultures. Nevertheless, the values obtained for each imaging time-point per genotype were comparable and thus statistically indistinguishable (Figure 3.10 B).

APV treatment prevented the decrease of spikes / min upon additional glycine application thus reflecting again that not only the amount of cytoplasmatic Ca^{2+} but also the frequency is partially regulated by the NMDAR. Surprisingly, in NexCre cDKOs the values for t-10 and t0 were significantly different. This might be reasoned in a relatively high value of 7 ± 1.1 spikes / min at t-10 under unstimulated conditions in APV and glycine treatment experiments which was lower with 6 ± 1.1 spikes / min at the t-10 in solely glycine treatment experiments (Figure 3.10 A and C). Nevertheless, this effect was only minor and all other parameters did not reveal a significant defect in NexCre cDKOs (Figure 3.10 C and D).

The application of CPA resulted in no significant decrease in the frequency upon co-treatment with glycine in both genotypes irrespective if separately littermate controls and NexCre cDKOs (Figure 3.10 E) or imaging time-points were analyzed (Figure 3.10 F). However, while in littermate control cultures the frequency was stable for t0, t10 and t40 upon chemically induced LTP the frequency of Ca^{2+} events in NexCre cDKOs cultures increased constantly for each of the three time points imaged.

Treating the dissociated hippocampal neurons of littermate controls and NexCre cDKOs with Nifedipine resulted in a significant decrease of 6 ± 1.4 spikes / min at t-20 compared to t40 with 2.5 ± 0.5 spikes / min in littermate controls while the cDKO was statistically indistinguishable (Figure 3.10 G). The results suggest that this difference based on a relatively high value of 6 ± 1.4 spikes / min a t-20 whilst t-10 displayed only values of 4 ± 1.2 spikes / min. Overall, these results revealed a pronounced variability, indicated by a high SEM which additionally led to no significance when analyzing the time-points (Figure 3.10 H).

Taken together, in line with observation made using electrophysiological techniques quantitative Ca^{2+} imaging uncovered a defect in spontaneous Ca^{2+} events under unstimulated conditions as well as a significantly decreased Ca^{2+} response when activity-dependent synaptic plasticity was induced by glycine application. Mechanistically, this could be due to a more efficient reuptake of Ca^{2+} into the ER or an alteration in Ca^{2+} buffer proteins like calbindin, calretinin, parvalbumin and calmodulin whereby the excess of unbound Ca^{2+} might be transported into the ER.

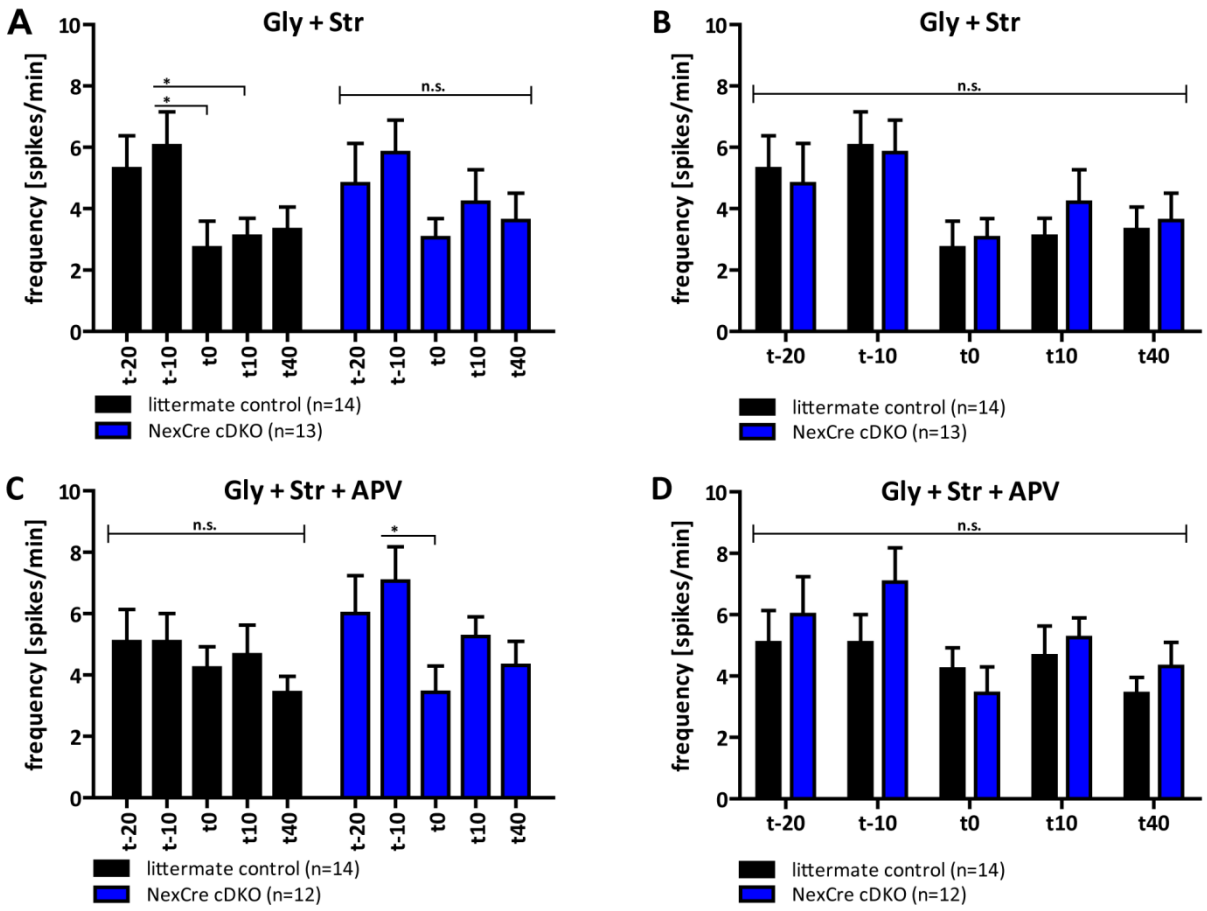

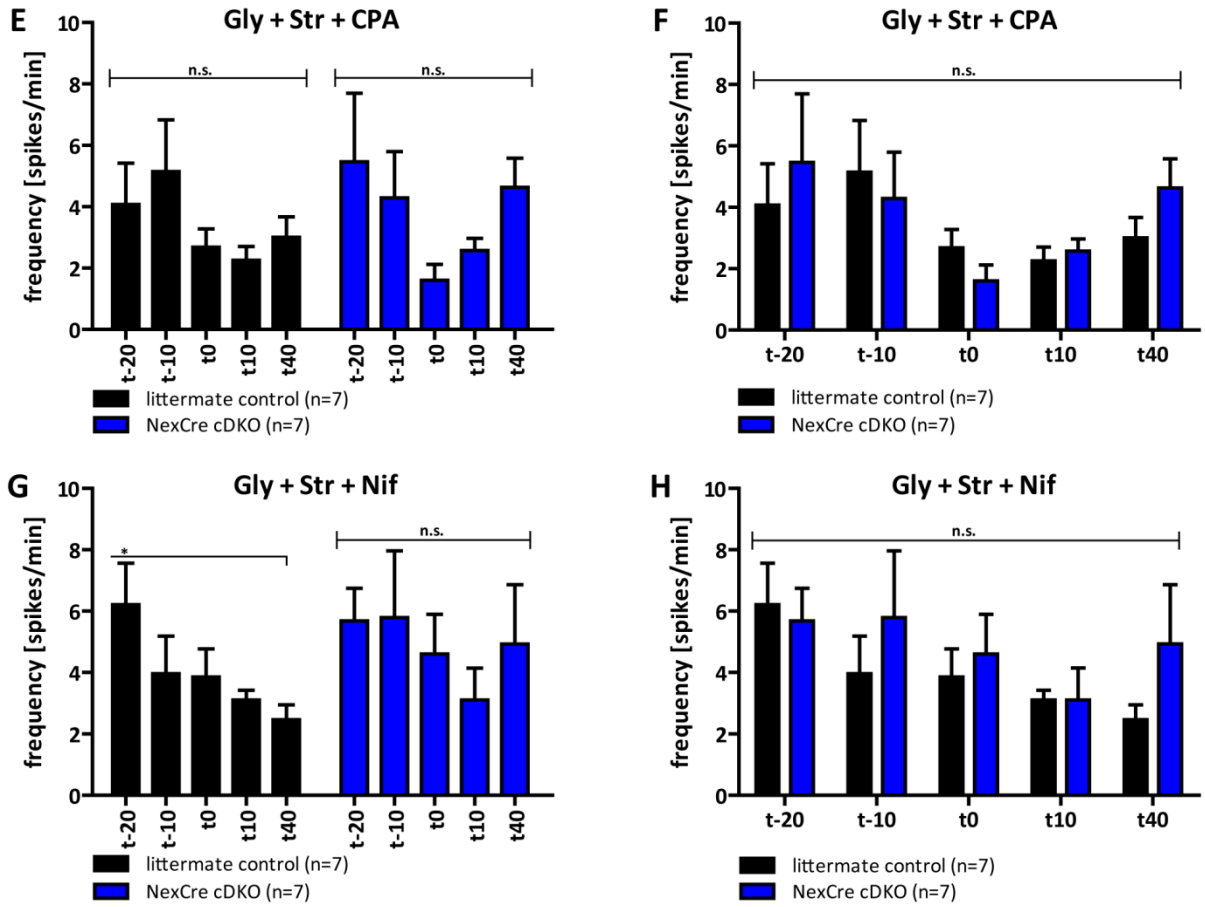

Figure 3.10 Quantitative Ca^{2+} imaging in NexCre cDKO revealed a defect in frequency of spikes upon stimulation (continued from previous page).

Imaging time-points t-20 and t-10 reflect the frequency in number of spikes / min at resting Ca^{2+} concentration. t0, t10 and t40 depict the quantification of spikes / min upon glycine stimulation only or additional drug administration. At the x-axis all time-points imaged are plotted in minutes. ***(A)*** *Onto glycine (Gly) stimulation in littermate control cultures (black) the frequency of Ca^{2+} events significantly decreased while NexCre cDKOs (blue) were statistically indistinguishable.* ***(B)*** *In contrast, the comparison of both genotypes at each single imaging time-point was unaltered.* ***(C)*** *Application of APV abolished the frequency reduction in littermate controls. However, here NexCre cDKO cultures revealed a significant decrease of spikes / min before and directly after glycine and APV treatment.* ***(D)*** *At defined time-points genotypes were statistically indistinguishable.* ***(E+F)*** *Although in both genotypes a trend towards a lower frequency upon glycine and CPA administration was observable this was neither significant for only genotypes plotted nor at defined imaging time-points.* ***(G)*** *Glycine and Nifedipine (Nif) treatment reduced the frequency to significant extend in littermate control when t-20 was compared to t40. All other values were not significant to each other. NexCre cDKO was unaltered as well.* ***(H)*** *Comparing single imaging time-points exhibited again no significant difference. Significances were plotted as *p < 0.05, **p < 0.01 and ***p < 0.001. Error bars indicate ± SEM. n = number of experiments. Str = strychnine.*

3.1.3.4 Gain of Function and Rescue Experiments in the NexCre cDKO: *ex vivo* Application of recAPPsα and recAPPsβ

Besides the role of APP and its homologue APLP2 in embryonic development I was also interested in the physiological and acute function of proteolytic fragments, deriving from full length APP processing, which may for instance modulate dynamic properties of synapses. I therefore focused on APPsα which is generated by α-secretase ADAM10 cleavage of full length APP and released into the extracellular space upon neuronal activity (Gakhar-Koppole et al., 2008; Hoey et al., 2009) see 1.3.1). Although the precise function of APPsα has not been clarified and its receptor is not identified to date, several studies showed beneficial properties for instance in processes related to learning and memory (Ishida et al., 1997; Meziane et al., 1998; Ring et al., 2007; Taylor et al., 2008; Weyer et al., 2011). This brought me to design an experimental setting in which it was possible to investigate the effects of an *ex vivo* application of recombinant APPsα or recAPPsβ on activity-dependent synaptic plasticity (see 2.4.5). I asked if low amounts of recAPPsα might be sufficient to restore the LTP defect observed in NexCre cDKOs (Figure 3.6 and Figure 3.11) or even increase the LTP in littermate controls in which still endogenous APPsα could be generated (Figure 3.17). Furthermore, I performed complementary experiments with recAPPsβ (Figure 3.16). In order to test these suggestions slices from NexCre cDKOs were pre-incubated 1 h and also during the entire recordings with the respective peptide or boiled control (for details see 2.4.5).

In line with my hypothesis the exogenous application of recAPPsα was sufficient to restore the deficits in PTP and LTP observed in naïve NexCre cDKO slices back to potentiation levels of naïve littermate controls (Figure 3.6 A and B compare to Figure 3.11 A and B). Thus an average potentiation of 143 ± 5.1 % (n = 12 / 8) for t75-80 min was reached, whereas NexCre cDKO treated with the boiled recAPPsα peptide revealed only 130 ± 2.3 % (n = 14 / 8, p = 0.029, t-test, Figure 3.11 B). These values were comparable to those obtained from untreated NexCre cDKO beforehand (Figure 3.6 A and B). The analysis of the input-output strength discovered that recAPPsα had not significant effect on fEPSP slope size when analyzed at defined stimulus intensities (Figure 3.11 C) being consistent with what was observed in naïve NexCre cDKO slices (Figure 3.6 E). However, the correlation of fEPSP slope size to given fiber volley amplitudes uncovered significant differences comparing the boiled-control to recAPPsα treated NexCre

cDKO for amplitudes of 0.2 mV (p = 0.001) and 0.3 mV (p = 0.019, t-test, Figure 3.11 D). These findings may suggest an additional effect of recAPPsα on postsynaptic compartment. Strikingly and in line with our hypothesis as well as results for rescued LTP upon recAPPsα treatment, the short-term plasticity was now not any longer significantly changed. The application of the intact peptide led to comparable values found in naïve littermate controls for the PPF paradigm. However, the boiled control should display a PPF comparable to naïve NexCre cDKO but that was not evident here (Figure 3.6 G). These observations support the idea that APPsα most likely functions as a mediator of activity dependent synaptic plasticity in the adult CNS.

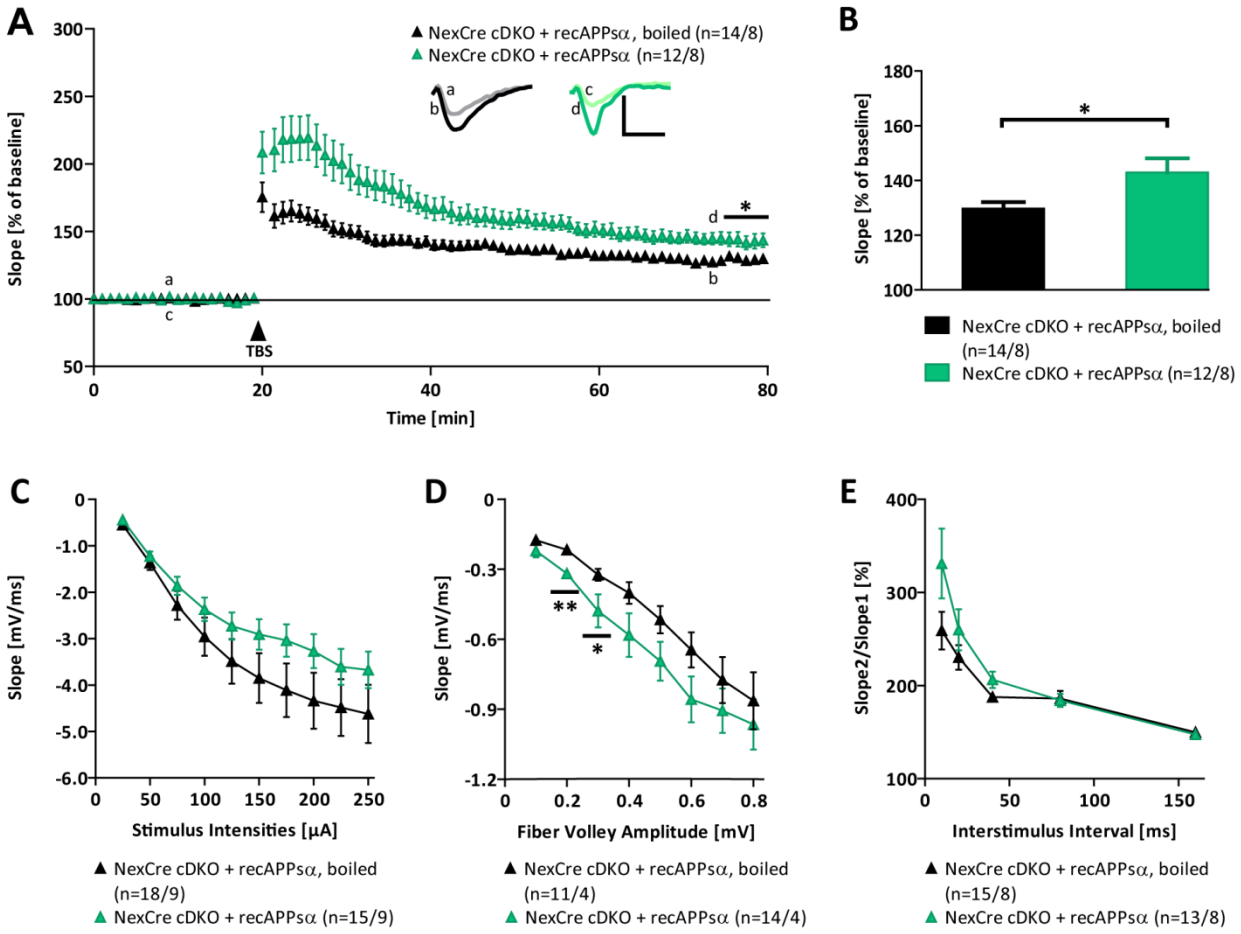

Figure 3.11 Acute application of recAPPsα rescues the LTP defect observed in NexCre cDKOs.
(A+B) *Exogenous recAPPsα application 1 h before and during entire recording resulted in a significant rescue (mean t75-80 min: 143 ± 5.1 %, green diamonds) of PTP as well as LTP defect observed in NexCre cDKO slices treated with boiled recAPPsα (mean t75-80 min: 130 ± 2.3 %, black diamonds, p = 0.029, t-test).* ***(C)*** *recAPPsα treated NexCre cDKO slices revealed a slightly, but not significantly decreased input-output strength.* ***(D)*** *Nevertheless, correlation fEPSP slope size to given fiber volley amplitudes showed a significant defect for 0.2 mV (p = 0.001) and 0.3 mV (p = 0.019, t-test).* ***(E)*** *Presynaptic functionality was found to be unaffected indicating a potential rescue for recAPPsα treated slices to naive littermate control levels (see Figure 3.6 G). Insets show original traces of representative individual experiments. Vertical scale bar = 1 mV, horizontal scale bar = 5 ms. Error bars indicate ± SEM. n.s. = not significant. n = number no of slices / number of mice used.*

3.1.3.5 Gain of Function and Rescue Experiments in the NexCre cDKO for Quantitative Ca^{2+} Imaging: Adeno-associated Virus Expression of APPsα

Based on these results which proved the beneficial function of APPsα for activity-dependent synaptic plasticity this raised the question whether the introduction of an APPsα containing vector by AAV might have comparable effects on the Ca^{2+} dynamics. Therefore, NexCre cDKO dissociated hippocampal cultures were incubated for 6 days with an AAV comprising a vector in which under the synapsin promoter either only the yellow fluorescent venus protein or additionally APPsα was encoded (for details see 2.6.3.2). Subsequent quantitative Ca^{2+} imaging was performed according to the protocol described and used before when solely glycine and strychnine were applied. Results for the amount of Ca^{2+} are depicted in Figure 3.12 and Figure 3.13 whereas Figure 3.14 and Figure 3.15 illustrate the frequency of Ca^{2+} events.

Consistent with my hypothesis again APPsα expression in cultures of NexCre cDKOs led to a robust and significant increase of cytoplasmatic Ca^{2+} when glycine was applied (Figure 3.12 A). Such a strong rise could not be observed in NexCre cDKO cultures expressing only venus thus reflecting the phenotype of NexCre observed in Figure 3.8 A and B. Analysis of the Ca^{2+} amount at defined time-points exhibited a slight increase already at resting Ca^{2+} concentration and a highly significant increase of Ca^{2+} amount upon glycine stimulation for t0 (48 ± 6.0 nM versus 73 ± 5.4 nM) and t40 (37 ±4.1 nM versus 55 ± 3.9 nM) while t10 (53 ± 6.0 nM versus 63 ± 5.2 nM) only showed a tendency (Figure 3.12 B).

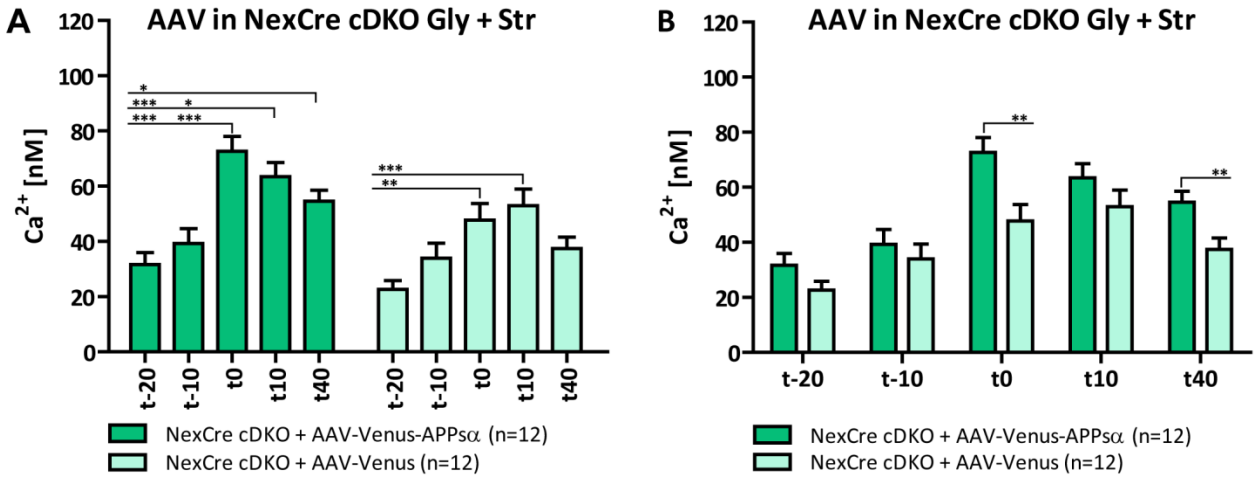

Figure 3.12 APPsα expression in NexCre cDKO cultures restored the defect in Ca^{2+} amount compared to those receiving the control vector (previous page).
Imaging time-points t-20 and t-10 reflect the resting Ca^{2+} concentration. Whereas t0, t10 and t40 depict the quantification the Ca^{2+} amount upon glycine stimulation. At the x-axis all time-points imaged are plotted in minutes. NexCre cDKO cultures were treated for 6 consecutive days with either AAV expressing venus only (light green, control) or additionally APPsα (dark green). ***(A)*** *Upon glycine (Gly) stimulation an in part highly significant increase of cytoplasmatic Ca^{2+} was observed for NexCre cDKOs expressing APPsα or control vector in relation to resting Ca^{2+} amount. Due to an increase of basal Ca^{2+} levels for t-10 in both this significance was lower or even abolished.* ***(B)*** *The rescue effect of APPsα became even clearer when the results for the Ca^{2+} levels were depicted for each time point separately. The obtained values uncovered a highly significant defect at t0 and t40 while t10 only showed a tendency towards that direction. Significances were plotted as *p < 0.05, **p < 0.01 and ***p < 0.001. Error bars indicate ± SEM. n = number of experiments. Str = strychnine.*

When plotting the data obtained from quantitative Ca^{2+} imaging of littermate controls (pooled with littermate controls expressing control construct as data was statistically indistinguishable), NexCre cDKO (pooled with NexCre cDKO expressing control construct as data was statistically indistinguishable) and NexCre cDKO expressing APPsα the previously described rescue effect became even more prominent (Figure 3.13). When analyzing the data regarding results of each genotype separately it turned out that the expression of APPsα was able to restore the Ca^{2+} amount before and upon stimulation by glycine to levels comparable to the littermate control (Figure 3.13 A). These findings became even more obvious when the illustration for each time-point imaged was chosen. At t-20 the NexCre cDKO revealed a resting Ca^{2+} concentration of 20 ± 2.3 nM whereas both littermate controls and NexCre cDKO expressing APPsα exhibited comparable values of 31 ± 2.8 nM and 32 ± 4.3 nM. This difference was significant and reflected the ability of solely APPsα to restore already the defect of lower basal Ca^{2+} amount observed before back to control levels (Figure 3.13 B). However, this pronounced effect could not be observed when the resting Ca^{2+} concentration was estimated 10 min later. But still a tendency towards this effect was found with 28 ± 3.6 nM for NexCre cDKO, 34 ± 3.3 nM for littermate controls and 39 ± 5.4 nM for NexCre cDKO expressing APPsα. Furthermore, when the cells were stimulated with glycine this resulted in a strong increase in the amplitude of the Ca^{2+} signal in littermate controls (76 ± 6.3 nM) and APPsα expressing NexCre cDKOs (73 ± 5.4 nM) while NexCre cDKO revealed significantly decreased levels of 51 ± 4.5 nM. These findings were supported as well by analyzing t10. There the NexCre cDKO exhibited a highly significant defect compared to littermate controls with values of 45 ± 3.8 nM versus 81 ± 9.0 nM. However, for this imaging time-point the expression of APPsα was not sufficient to restore the Ca^{2+} back to

control levels with reached 63 ± 5.2 nM. Nevertheless, for t40 again a full rescue of cytoplasmatic Ca^{2+} to values of littermate control (52 ± 4.1 nM) was achieved for NexCre cDKO expressing APPsα (55 ± 3.9 nM). This effect was highly significant compared to NexCre cDKO which reached values of only 36 ± 2.8 nM (Figure 3.13 B).

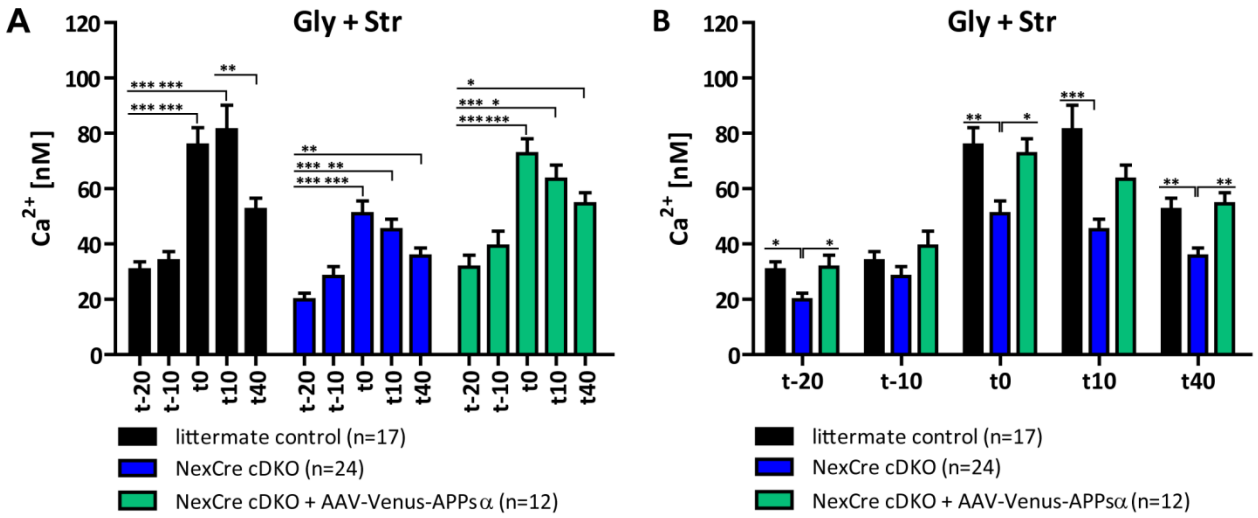

Figure 3.13 Comparative overview of results obtained for the Ca^{2+} amount from littermate controls, NexCre cDKO with and without APPsα expression.

Imaging time-points t-20 and t-10 reflect the resting Ca^{2+} concentration. Whereas t0, t10 and t40 depict the quantification the Ca^{2+} amount upon glycine stimulation. At the x-axis all time-points imaged are plotted in minutes. NexCre cDKO cultures were treated for 6 consecutive days with AAV expressing venus and APPsα. Since littermate controls treated with AAV expressing only venus were statistically indistinguishable to littermate controls without AAV application data were pooled. The same procedure was applied for NexCre cDKO expressing the control construct and naïve NexCre cDKOs. ***(A)*** *Glycine (Gly) application induced in all groups an increase of intracellular Ca^{2+} amounts. The comparison of littermate controls (black) and NexCre cDKO expressing APPsα (dark green) revealed comparable levels which were found to be lower in naïve NexCre cDKO (blue).* ***(B)*** *A direct evaluation at defined imaging time-points clearly indicated a rescue effect of resting Ca^{2+} amount, when APPsα was expressed, back to littermate control levels at t-20. However this was only observed by trend at t-10. Upon glycine application this pronounced and significant re-storage effect was found for t0 and t40 while t10 again exhibited only a tendency for a recue by APPsα expression. Significances were plotted as *p < 0.05, **p < 0.01 and ***p < 0.001. Error bars indicate ± SEM. n = number of experiments. Str = strychnine.*

Following the same approach, again the frequency was analyzed for NexCre cDKO expressing venus alone or additionally APPsα (Figure 3.14). Interestingly, cultures from NexCre cDKOs expressing APPsα revealed a stable frequency for resting Ca^{2+} events of 7 ± 1.5 spikes / min for both t-20 and t-10 which significantly decreased to 3 ± 0.6 spikes / min for t0, 4 ± 1.0 spikes / min for t10 and 4 ± 0.6 spikes / min for t40 upon glycine treatment. This observation was not made for NexCre cDKOs expressing solely the control construct. There only t-20 exhibited a high frequency of 8 ± 2.0 spikes / min while at t-10 only 4 ± 1.3 spikes / min occurred. These values

were significantly different. When glycine was applied the strong and significant decrease was not observed in NexCre cDKO cultures (Figure 3.14 A). This further supports the predicted defect in Ca^{2+} dynamics in NexCre cDKO. Anyhow, when the imaging time-points were compared separately, only t0 was highly significant impaired between both NexCre cDKO expressing APPsα or only venus (Figure 3.14 B) suggesting a pronounced impaired reaction upon stimulation.

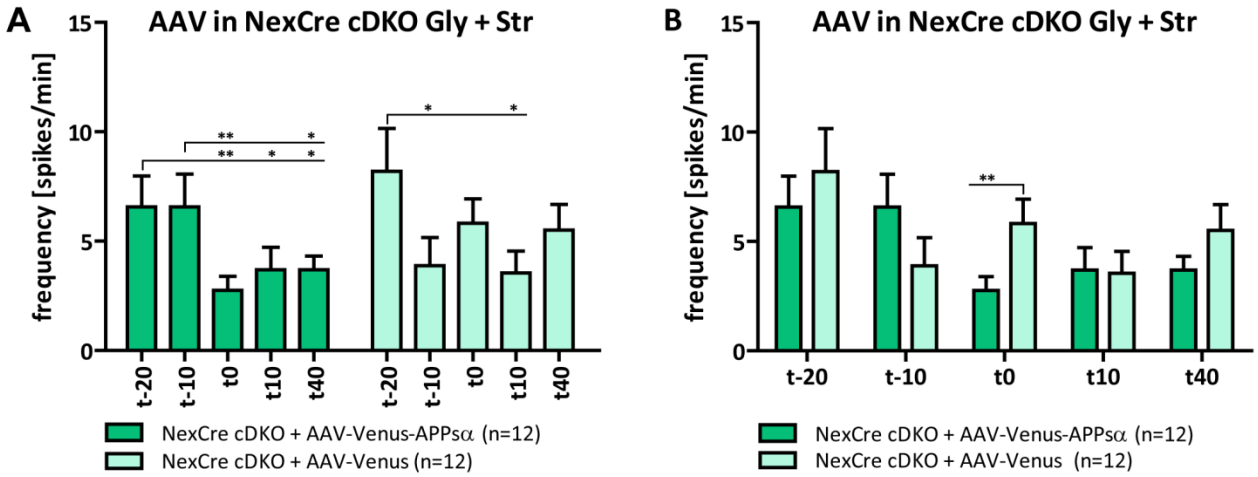

Figure 3.14 APPsα expression in NexCre cDKO cultures restored the defect in the frequency of Ca^{2+} spikes compared to those receiving the control vector.

Imaging time-points t-20 and t-10 reflect the frequency in number of spikes / min at resting Ca^{2+} concentration. t0, t10 and t40 depict the quantification of spikes / min upon glycine. At the x-axis all time-points imaged are plotted in minutes. NexCre cDKO cultures were treated for 6 consecutive days with AAV either expressing venus only (light green) or additionally APPsα (dark green). ***(A)*** *Upon glycine (Gly) stimulation NexCre cDKO expressing APPsα exhibited a significant decrease of Ca^{2+} spikes / min while this was not observed in such a strong extent in the controls.* ***(B)*** *Plotting the imaging time-points separately only t0 revealed a significant difference between groups. Significances were plotted as *p < 0.05, **p < 0.01 and ***p < 0.001. Error bars indicate ± SEM. n = number of experiments. Str = strychnine.*

Next, the data gained from quantitative Ca^{2+} imaging of littermate controls (pooled with littermate controls expressing control construct as data was statistically indistinguishable), NexCre cDKO (pooled with NexCre cDKO expressing control construct as data was statistically indistinguishable) and NexCre cDKO expressing APPsα the previously described effect became even more obvious (Figure 3.15). Comparably to observations made for the increase of cytoplasmatic Ca^{2+} concentration again an expression of APPsα in NexCre cDKO restored the frequency back to littermate control frequency when glycine was applied. This was indicated by a significant decrease of spikes / min while this was not observed in NexCre cDKOs (Figure 3.15

A). Still, values plotted for each imaging time-point were statistically indistinguishable (Figure 3.15 B). Results presented for the frequency are difficult to interpret due to high variability.

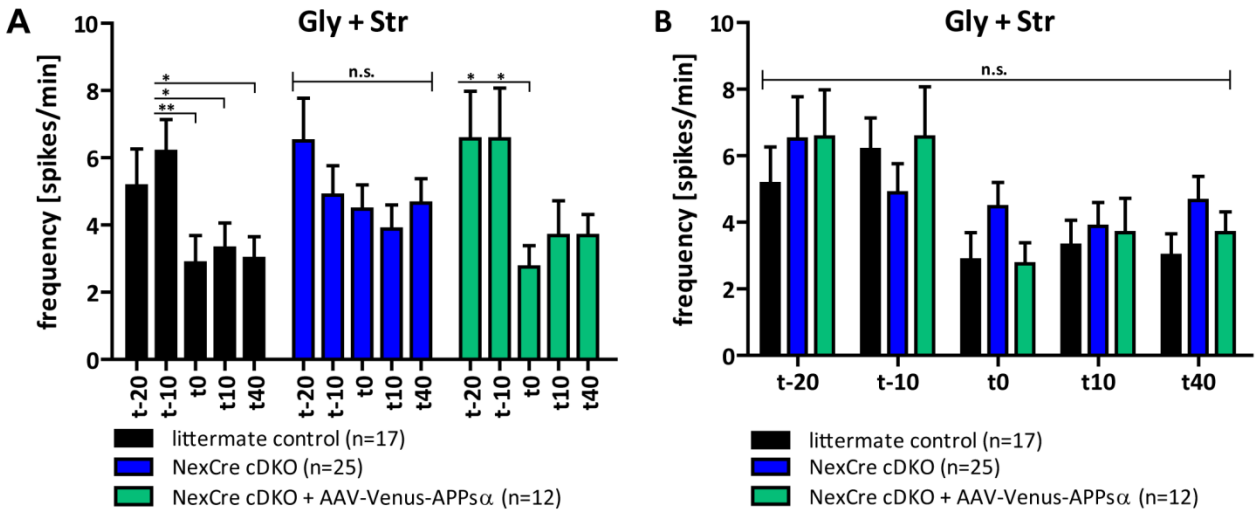

Figure 3.15 Comparative overview of results obtained for the frequency of Ca^{2+} events from littermate controls, NexCre cDKO with and without APPsα expression.

Imaging time-points t-20 and t-10 reflect the frequency in number of spikes / min at resting Ca^{2+} concentration. t0, t10 and t40 depict the quantification of spikes / min upon glycine stimulation. At the x-axis all time-points imaged are plotted in minutes. NexCre cDKO cultures were treated for 6 consecutive days with AAV expressing venus and APPsα. Since littermate controls treated with AAV expressing only venus were statistically indistinguishable to littermate controls without AAV application data were pooled. The same procedure was applied for NexCre cDKOs expressing the control construct and naïve NexCre cDKOs. ***(A)*** *In line with observations made for the Ca^{2+} amount again the expression of APPsα in NexCre cDKOs (dark green) rescued the frequency defect of naïve NexCre cDKOs (blue) back to littermate control levels (black). Upon glycine (Gly) stimulation a partially significant decrease of Ca^{2+} spikes / min was observed for littermate controls and NexCre cDKOs expressing APPsα but not for naïve NexCre cDKO cultures. Significances were plotted as *p < 0.05, **p < 0.01 and ***p < 0.001. Error bars indicate ± SEM. n = number of experiments. Str = strychnine.*

3.1.3.6 Gain of Function and Rescue Experiments in the NexCre cDKO: *ex vivo* Application of recAPPsβ

In the amyloidogenic way of APP processing endogenous APPsβ is formed upon β-secretase BACE1 activity and again, like APPsα, secreted extracellular (see 1.3.1). Since APPsβ is slightly shorter and was so far not implicated to be crucial for synaptic plasticity I additionally examined its ability to rescue the NexCre cDKO LTP defect. Therefore, again electrophysiological recordings were applied. Interestingly, LTP induction as well as maintenance was still affected upon recAPPsβ application (Figure 3.16 A). The average potentiation for the final 5 min of LTP recording was statistically indistinguishable irrespective of whether native (126 ± 4.5 %) or boiled recAPPsβ peptide (119 ± 3.9 %, p = 0.281, t-test) was applied to NexCre cDKO slices

(Figure 3.16 B). In contrast to recAPPsα treatment no postsynaptic alterations were found in boiled and native recAPPsβ treated NexCre cDKOs slices as indicated by overlapping curves (Figure 3.16 C and D). Comparable to recAPPsα also native recAPPsβ seemed to restore the PPF defect of naïve NexCre cDKO slices although the difference between application of boiled (which should reflect the naïve NexCre cDKO state) and native recAPPsβ was not significant at any ISI tested. These findings suggest that APPsβ, possibly due to the lack of 17 amino acids compared to APPsα, was no longer sufficient to promote activity-dependent synaptic plasticity even though it was applied at 5 times higher concentration as recAPPsα.

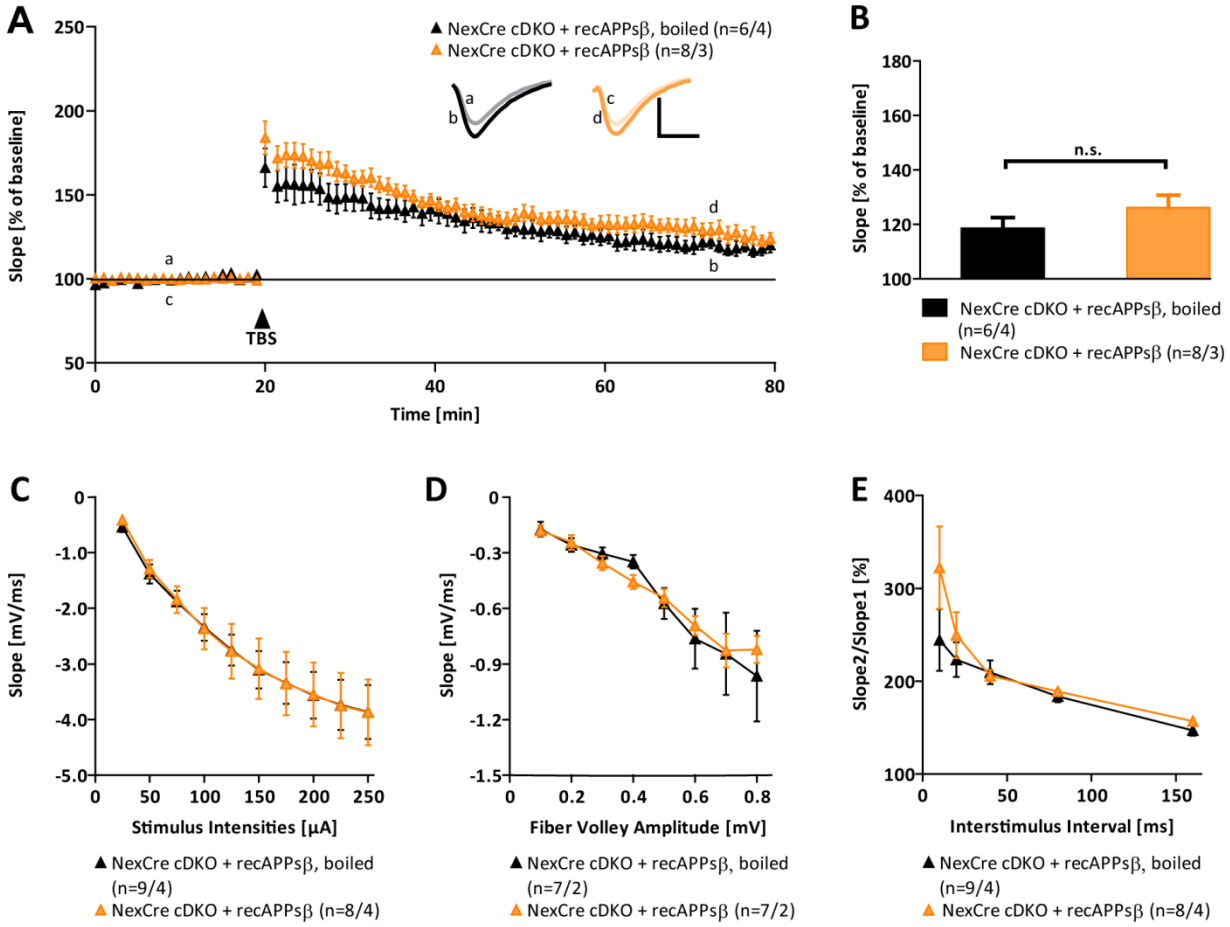

Figure 3.16 Acute application of recAPPsβ is not sufficient to rescue the LTP defect observed in NexCre cDKOs. ***(A+B)*** *After 20 min of stable baseline recording, while recAPPsβ was present, LTP was induced by TBS (arrow) revealing no significant difference between boiled (119 ± 3.9 %, black diamonds) and native (126 ± 4.5 %, orange diamonds, p = 0.281, t-test) peptide treated NexCre cDKO slices. These potentiation levels were comparable to those obtained from naïve NexCre cDKOs slices (see Figure 3.6 A and B). Neither input-output strength measured at defined stimulus intensities* ***(C)*** *nor given fiber volley amplitudes* ***(D)*** *nor presynaptic functions* ***(E)*** *were changed upon treatment with recAPPsβ or boiled control. Insets show original traces of representative individual experiments. Vertical scale bar = 1 mV, horizontal scale bar = 5 ms. Error bars indicate ± SEM. n.s. = not significant. n = number no of slices / number of mice used.*

3.1.3.7 Gain of Function Experiments in Littermate Controls: *ex vivo* Application of recAPPsα

Having established the beneficial effects of recAPPsα I next investigated if an exogenous application of recAPPsα additionally to endogenous upon TBS released APPsα, shown by Nitsch and colleagues might potentiate the LTP even further (Nitsch et al., 1992). Therefore, littermate control mice which still express APP on an APLP2 deficient background were analyzed. Indeed, slices treated with recAPPsα revealed a much stronger and significantly increased posttetanic potentiation following TBS (t20-43 min: $p = 0.023$, t-test) compared to the boiled peptide treated control group (Figure 3.17 A). Nevertheless, the final 5 min of LTP recording were not statistically different although the trend for an increased LTP was still preserved ($p = 0.441$, t-test, Figure 3.17 B). Remarkably, the slices treated with recAPPsα showed a prolonged induction phase since the formation of a stable plateau took longer than in slices receiving the boiled recAPPsα (Figure 3.17 A). These findings point towards its essential role during induction and early phase of LTP which was also shown by (Taylor et al., 2008). Results from basal synaptic transmission studies revealed an enlarged fEPSP slope size at set stimulus intensities (Figure 3.17 C). This trend became significant at defined fiber volley amplitudes (0.2 mV: $p = 0.026$, 0.5 mV: $p = 0.049$, t-test, Figure 3.17 D). Strikingly, short-term plasticity and thus presynaptic function were enhanced by recAPPsα application as well. This was indicated by a larger ratio of slope 2 / slope 1 at smaller ISIs even though this trend was not significant (Figure 3.17 E). All in all these findings encourage predicted beneficial characteristics of APPsα. Although this data indicate a potentiating effect of APPsα it was shown that high amounts of APPsα (3.3 µM) act contrariwise in decreasing synaptic efficacy suggesting dose-dependent relations (Taylor et al., 2008).

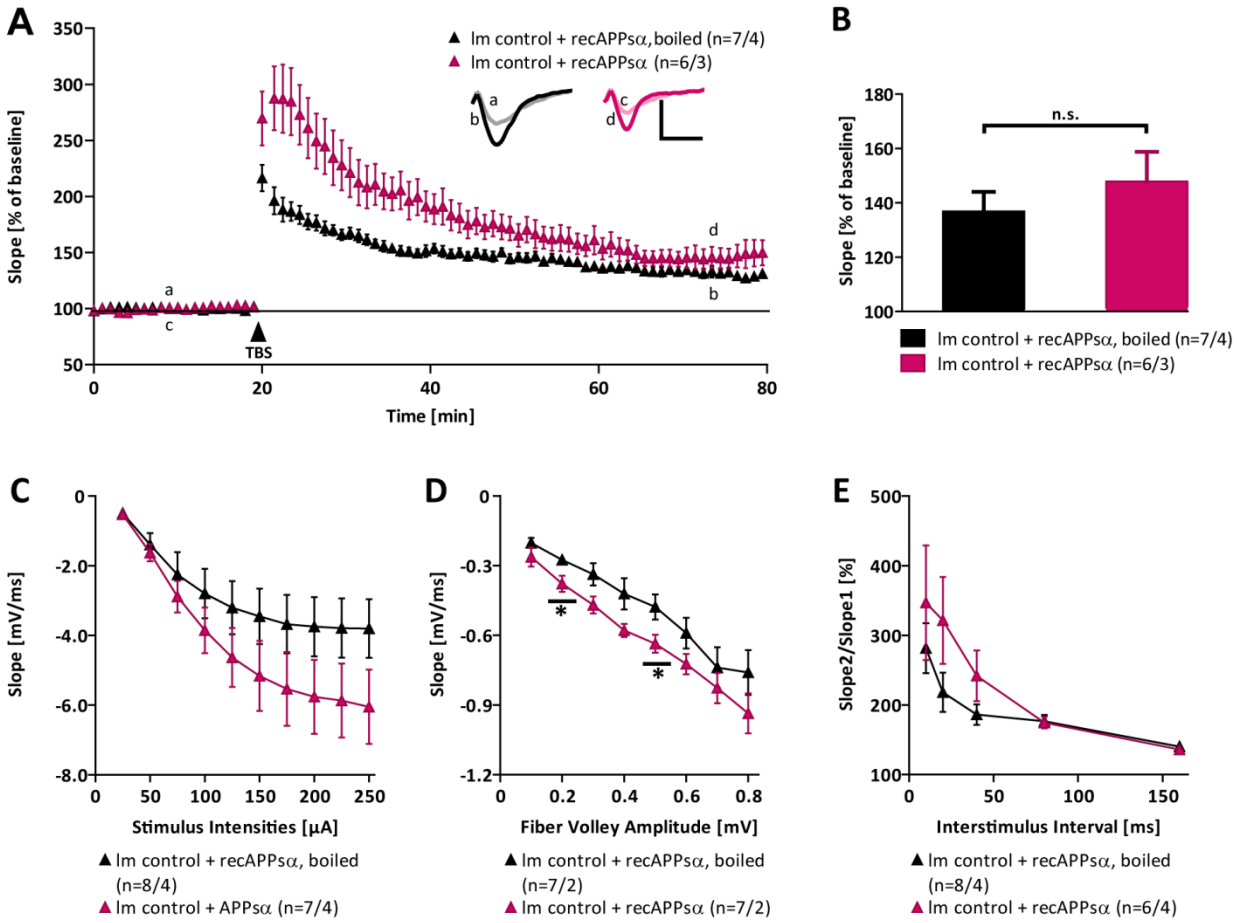

Figure 3.17 Acute application of recAPPsα enhanced LTP in littermate control slices.
(A) *LTP induction via TBS (arrow) induced a very robust and significantly stronger PTP in littermate controls upon recAPPsα treatment (t20-43 min: p = 0.023, t-test, pink diamonds). Remarkably, plateau formation needed much longer compared to littermate slices treated with boiled recAPPsα (black diamonds). Finally, the average potentiation of t75-80 min was still higher, although not significant, in native peptide treated NexCre cDKO slice (147 ± 10.9 %) than in the control condition (136 ± 7.2 %, p = 0.441, t-test,* ***B****).* ***(C)*** *Slices from littermate controls treated with recAPPsα exhibited a more pronounced and partially significant input-output strength (0.2 mV: p = 0.026, 0.5 mV: p = 0.049, t-test,* ***D****).* ***(E)*** *The presynaptic compartment was as well positively influenced since ratio values tended to be larger upon native peptide application. Insets show original traces of representative individual experiments. Vertical scale bar = 1 mV, horizontal scale bar = 5 ms. Error bars indicate ± SEM. n.s. = not significant. n = number no of slices / number of mice used.*

Figure 3.18 summarizes all genotypes, treatments, age relations and results obtained from all electrophysiological experiments in this study.

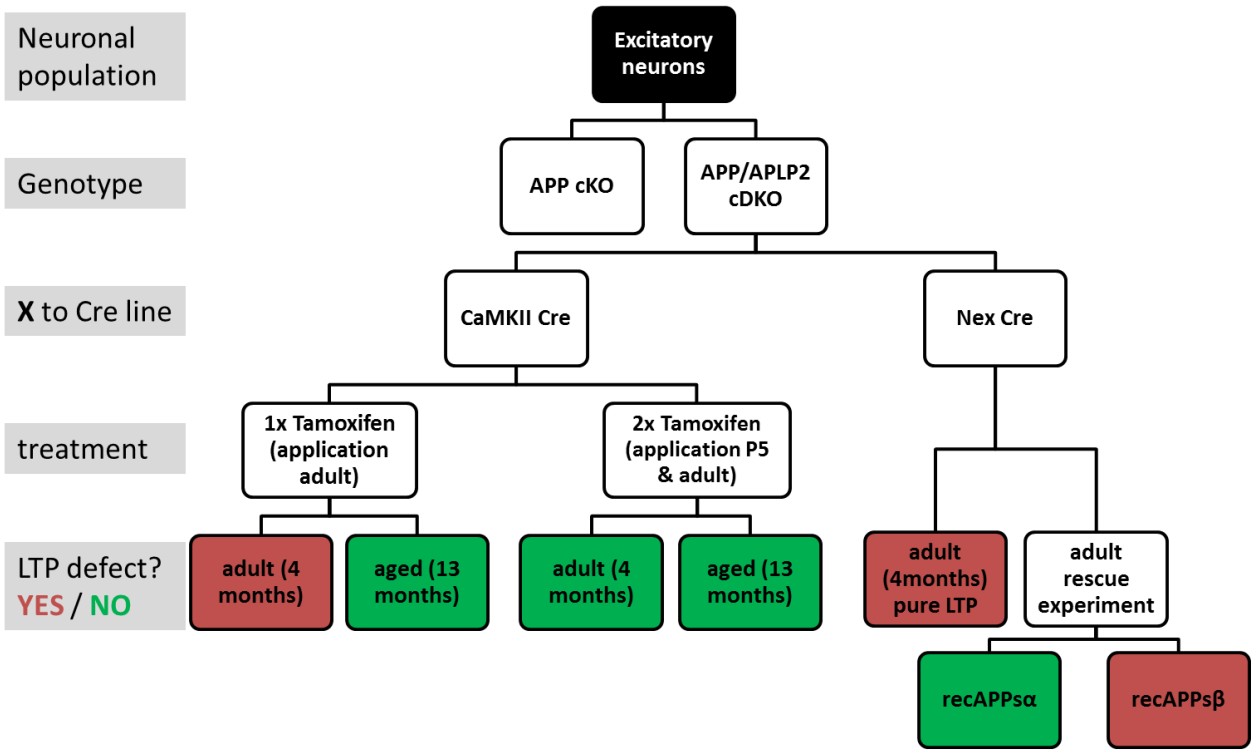

Figure 3.18 Overview about results obtained from $APP^{flox/flox}APLP2^{-/-}$ crossed to excitatory Cre-deleter lines.

3.2 The Role of the APP Protein Family for Synaptic Plasticity in Inhibitory Interneurons

The analysis of NexCre cDKO provided emerging evidence that APP and APLP2 are needed during processes of embryonic brain development and acutely at active synapses of excitatory neurons. Even though the hippocampus is built up of ~95 % excitatory neurons it is mandatory to take also the role of APP and APLP2 in inhibitory neurons into account. Previous investigations evidenced that inhibitory input contributes to the phenotype as well. In APPsα-DM mice an application of $GABA_A$ receptor inhibitor picrotoxin 10 min before TBS and during the entire recording restored the LTP defect, observed before, back to littermate control levels (Weyer et al., 2011). Moreover, the constitutive APP-KO revealed a paired pulse depression of GABA mediated inhibitory postsynaptic currents and a high susceptibility for kainate-induced seizures which was again rescued by Picrotoxin (Steinbach et al., 1998; Seabrook et al., 1999; Fitzjohn et al., 2000). It might be reasonable that the excitation-inhibition balance (E-I balance) is affected when both proteins are knocked out in one neuronal subtype. E-I balance is known to be a form of homeostatic plasticity necessary to maintain and regulate activity in a neuronal circuitry. Since this balance is usually established during brain development it might be conceivable that the cDKO of both proteins in either excitatory or inhibitory neurons disrupts this balance. This led me to investigate transgenic mice being deficient of both APP and APLP2 or lacking solely APP in inhibitory neurons.

3.2.1 Conditional APP Knock-out on an APLP2 Expressing Background

This experimental series was designed to uncover potential age-dependent effects. This idea based on findings that constitutive APP-KO mice showed no overt LTP defect at 3-4 months but surprisingly at 12-13 months of age (Dawson et al., 1999; Seabrook et al., 1999). This defect was rescued by the constitutive expression of the neurotrophic APPsα fragment (Ring et al., 2007). This fragment was additionally shown to have different effects on synaptic protein synthesis at different months of age. It was evidenced that 3-4 months old rats revealed a significantly stronger APPsα-stimulated up-regulation of synaptic protein synthesis compared to 20-22 months individuals. This age-related effect was not found in rats treated with APPsβ (Claasen et al., 2009). Nevertheless, it should be taken into account that in constitutive APP-KO and in

APPsα-KI mice still APLP2 was expressed. It has been shown that APLP2 is highly homological to APP and processed similarly although it lacks the Aβ domain (Walsh et al., 2007). Thus it might be feasible that APP and APLP2 share partially redundant functions for mechanisms of synaptic plasticity. This is supported by the observation that if APPsα is expressed solely on an APLP2 deficient background (APPsα-DM) the LTP defect is then already seen in adult mice (Weyer et al., 2011). Predicted compensatory function of APLP2 were strengthened by morphological alterations found in OHC cultures of constitutive APP / APLP2 DKO but not in APLP2-KO mice (Weyer et al., 2014).

3.2.1.1 DlxCre Conditional Knock-out

According to the hypothesis proposed before adult 3-4 months old DlxCre cKO mice exhibited no gross alterations in activity-dependent synaptic plasticity depicted in Figure 3.19. Both genotypes revealed an overall and statistically indistinguishable increase in synaptic strength for LTP (littermate control: 139 ± 4.8 %, n = 18 / 6, DlxCre cKO: 135 ± 4.2 %, n = 16 / 5, p = 0.568, t-test, Figure 3.19 A and B) and L-LTP (littermate control: 138 ± 5.8 %, n = 7 / 6, DlxCre cKO: 137 ± 11.3 %, n = 8 / 5, p = 0.953, t-test, Figure 3.19 C and D). Consistently, the input-output strength was unaffected likewise when the fEPSP slope size was correlated to defined stimulus intensities (Figure 3.19 E) or fiber volley amplitudes (Figure 3.19 F). Although the analysis of short-term plasticity by the PPF paradigm was not significantly compromised, adult DlxCre cKO mice displayed a trend towards decreased presynaptic activity compared to littermate control (Figure 3.19 G). Overall, these results provide further evidence that APLP2 may be able to compensate the loss of APP in adult DlxCre cKO mice. Nevertheless, it cannot be ruled out that the absence of a LTP defect was additionally based on diffusion processes of APP cleavage products as the majority of neighboring neurons were excitatory and thus still expressed APP.

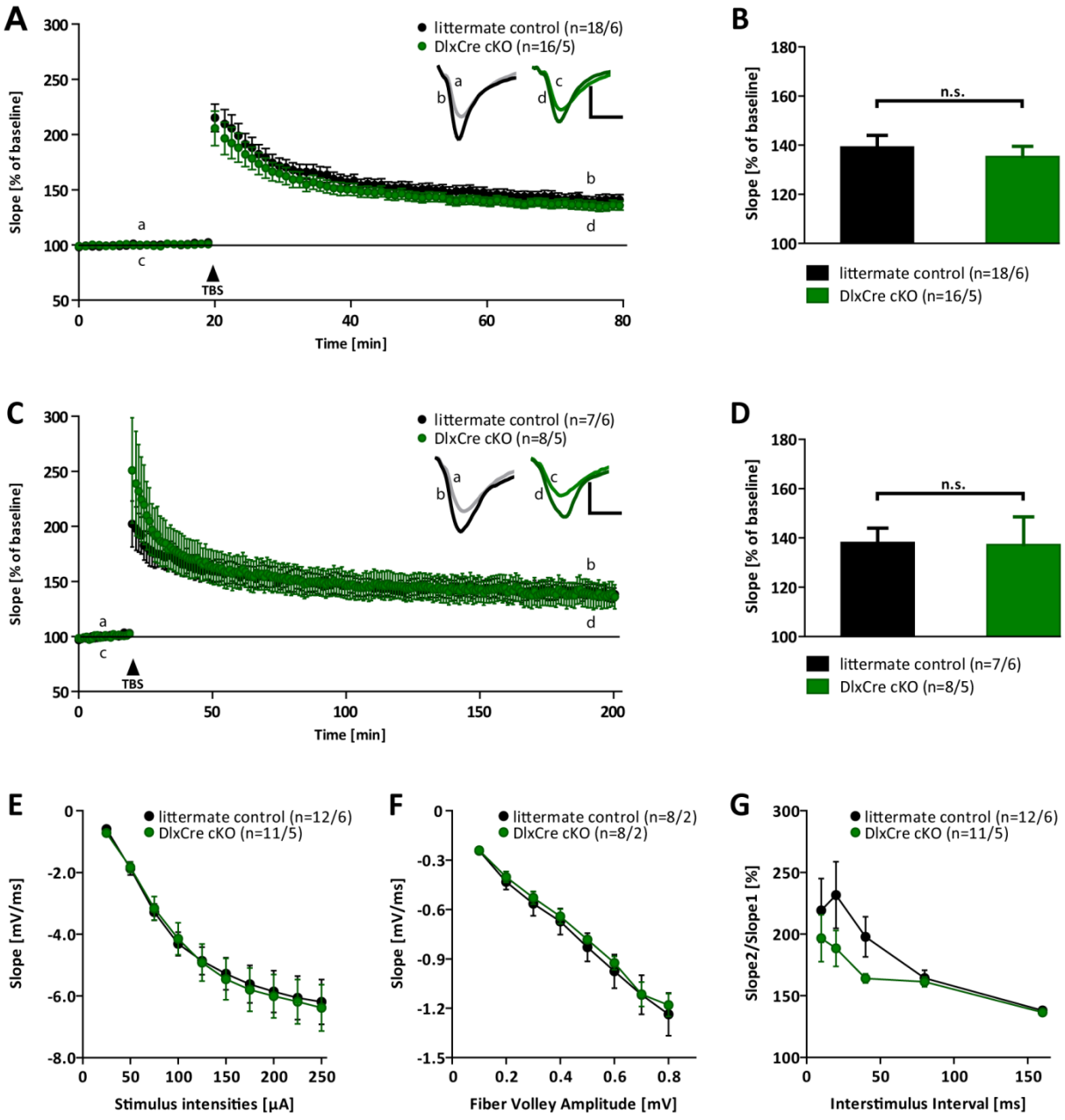

Figure 3.19 LTP experiments in adult DlxCre cKO mice.

(A+C) *Adult DlxCre cKO mice revealed no overt LTP or L-LTP defect indicated by almost overlapping curves with control group. In both genotypes the induction by TBS (arrow) resulted in a robust and stable potentiation over time. Littermate control slices (black circles) exhibited potentiation levels of 139 ± 4.8 % for t75-80 min in LTP* ***(B)*** *and 138 ± 5.8 % for t195-200 min in L-LTP recordings* ***(D)****. DlxCre cKO slices (dark green circles) showed average potentiation levels of 135 ± 4.2 % for the final 5 min of LTP* ***(B)*** *as well as 137 ± 11.3 % for L-LTP* ***(D)****. Statistical analysis by t-test led to p = 0.568 (LTP) and p = 0.953 (L-LTP). Input-output strength at given stimulus intensities* ***(E)*** *or defined fiber volley amplitudes* ***(F)*** *and PPF* ***(G)*** *were not significantly changed. Insets show original traces of representative individual experiments. Vertical scale bar = 1 mV, horizontal scale bar = 5 ms. Error bars indicate ± SEM. n.s. = not significant. n = number no of slices / number of mice used.*

To rule out whether the unaffected LTP and L-LTP of adult DlxCre cKO was due to cleavage products of APP from surrounding excitatory neurons or contributed by APLP2 accomplishment next aged DlxCre cKO mice (12-13 months) were analyzed (Figure 3.20). In both LTP and L-LTP recordings littermate controls revealed a higher LTP magnitude compared to DlxCre cKO. Strikingly, the PTP was heavily impaired between genotypes in LTP as well as L-LTP (Figure 3.20 A and C). This defect became less prominent with time. For LTP the average potentiation of t75-80 min was 142 ± 6.1 % for littermate control slices (n = 23 / 6) and 125 ± 3.2 % for DlxCre cKO slices (n = 26 / 5, p = 0.019, t-test, Figure 3.20 B). The significance was abolished when the final 5 min of L-LTP recordings were analyzed (littermate control: 132 ± 9.7 %, n = 9 / 5, DlxCre cKO: 114 ± 3.0 %, n = 10 / 5, p = 0.088, t-test, Figure 3.20 D). Comparably to adult DlxCre cKO mice again input-output strength and thus postsynaptic functionality was unaltered at any condition tested (Figure 3.20 E and F). Opposing to adult DlxCre cKO individuals aged ones had a severely impaired short-term plasticity including a defect of presynaptic function (Figure 3.20 G). Values for ratio of slope 2 / slope 1 revealed a strong and partially significant deficit of DlxCre cKO at lower ISIs (20 ms: p = 0.048, t-test). All in all, results obtained from adult and aged DlxCre cKO mice reflected abnormalities observed in constitutive global APP-KO mice beforehand.

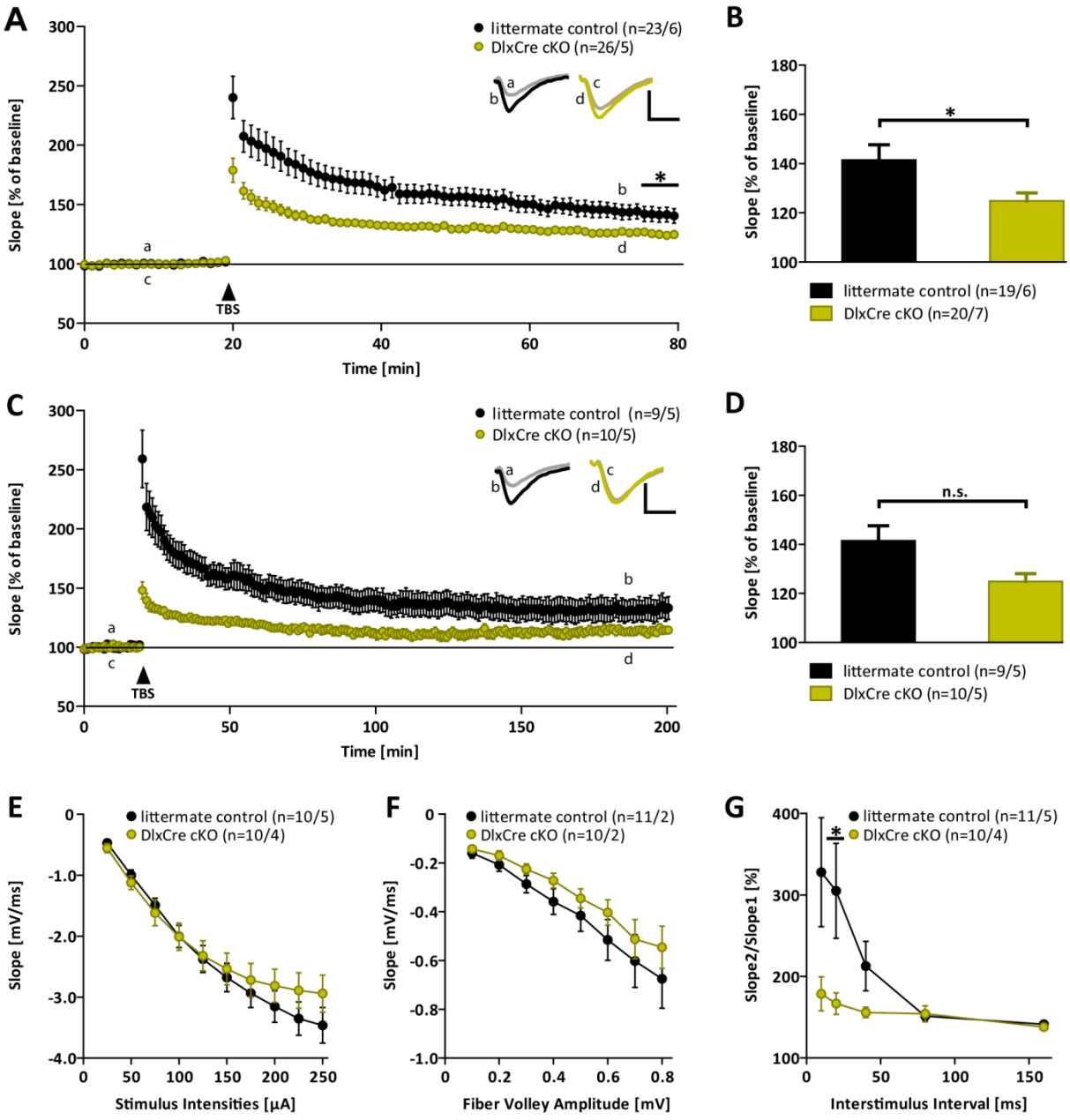

Figure 3.20 LTP experiments in aged DlxCre cKO mice.

(A+B) *After 20 min of stable baseline recording TBS (arrow) induced a robust PTP and maintained LTP in littermate controls (142 ± 6.1 %, black circles). However, DlxCre cKO slices (light green circles) revealed a strong and significant impairment for PTP as well as for the final 5 min of LTP recording (125 ± 3.2 %, p = 0.048, t-test).* ***(C+D)*** *Regarding L-LTP again a pronounced deficit in PTP and early LTP could be observed which was consistent during the entire recording time, but finally not significant any longer for t195-200 min (littermate control: 132 ± 9.7 % and DlxCre cKO: 114 ± 3.0 %, p = 0.088, t-test).* ***(E+F)*** *Input-output strength among genotypes was affected neither at given stimulus intensities nor at defined fiber volley amplitudes.* ***(G)*** *In contrast, PPF was significantly impaired at lower ISIs (20 ms: p = 0.048, t-test). Insets show original traces of representative individual experiments. Vertical scale bar = 1 mV, horizontal scale bar = 5 ms. Error bars indicate ± SEM. n.s. = not significant. n = number no of slices / number of mice used.*

3.2.2 Conditional APP Knock-out on APLP2 Deficient Background

Investigations of DlxCre cKOs revealed an age-related LTP defect. Compared to adult transgenic mice aged animals showed a significant deficit for LTP induction and maintenance (see 3.2.1.1.). I assumed that APLP2 was able to compensate the loss of APP in adult but not in aged mice. To test this hypothesis DlxCre cDKO were generated which additionally lacked APLP2. Therefore, I expected to observe the LTP impairment in adult individuals as well. As a second transgenic mouse line GADCre cDKO mice were investigated in which the APP knock-out again was restricted to only inhibitory neurons on an APLP2 deficient background (see 2.1.3). This provided the advantage to make use of another Cre-deleter line to verify the results.

3.2.2.1 DlxCre Conditional Double Knock-out

Following a stable baseline recording of 20 min, TBS induced LTP showed an overall robust and maintained increase in synaptic efficacy in both adult DlxCre cDKO mice and littermate controls (3-4 months, Figure 3.21 A). Nevertheless, a clear and highly significant defect of DlxCre cDKO with 129 ± 3.8 % (t 75-80 min, n = 25 / 6) compared to littermate controls with 147 ± 4.6 % (n = 29 / 6, p = 0.005, t-test, Figure 3.21 B) became obvious. Remarkably, this pronounced deficit was not reproducible in protein synthesis dependent L-LTP recordings (Figure 3.21 C). This was reflected in potentiation values of 132 ± 8.1 % (littermate control, n = 7 / 5) and 115 ± 5.2 % (DlxCre cDKO, n = 11 / 6, p = 0.096, t-test, Figure 3.21 D) for the final 5 min of recording. The significant LTP defect was partially accompanied by alterations in the post- and presynaptic compartment (Figure 3.21 E-G). While the correlation of the fEPSP slope size to various stimulus intensities was not impaired among genotypes (Figure 3.21 E) the correlation to defined fiber volley amplitudes was significantly altered (0.4 mV: p = 0.037, 0.5 mV: p = 0.042, t-test, Figure 3.21 F). This observation goes along with a defect of short-term plasticity. At short ISI the ratio of slope 2 / 1 was significantly larger in DlxCre cDKO compared to littermate controls (ISI 10 ms: p = 0.043, t-test). All together the data obtained from DlxCre cKO and cDKO established a compensatory function of APLP2 in adult transgenic mice and a reproduction of age-dependency already uncovered in constitutive global APP-KO.

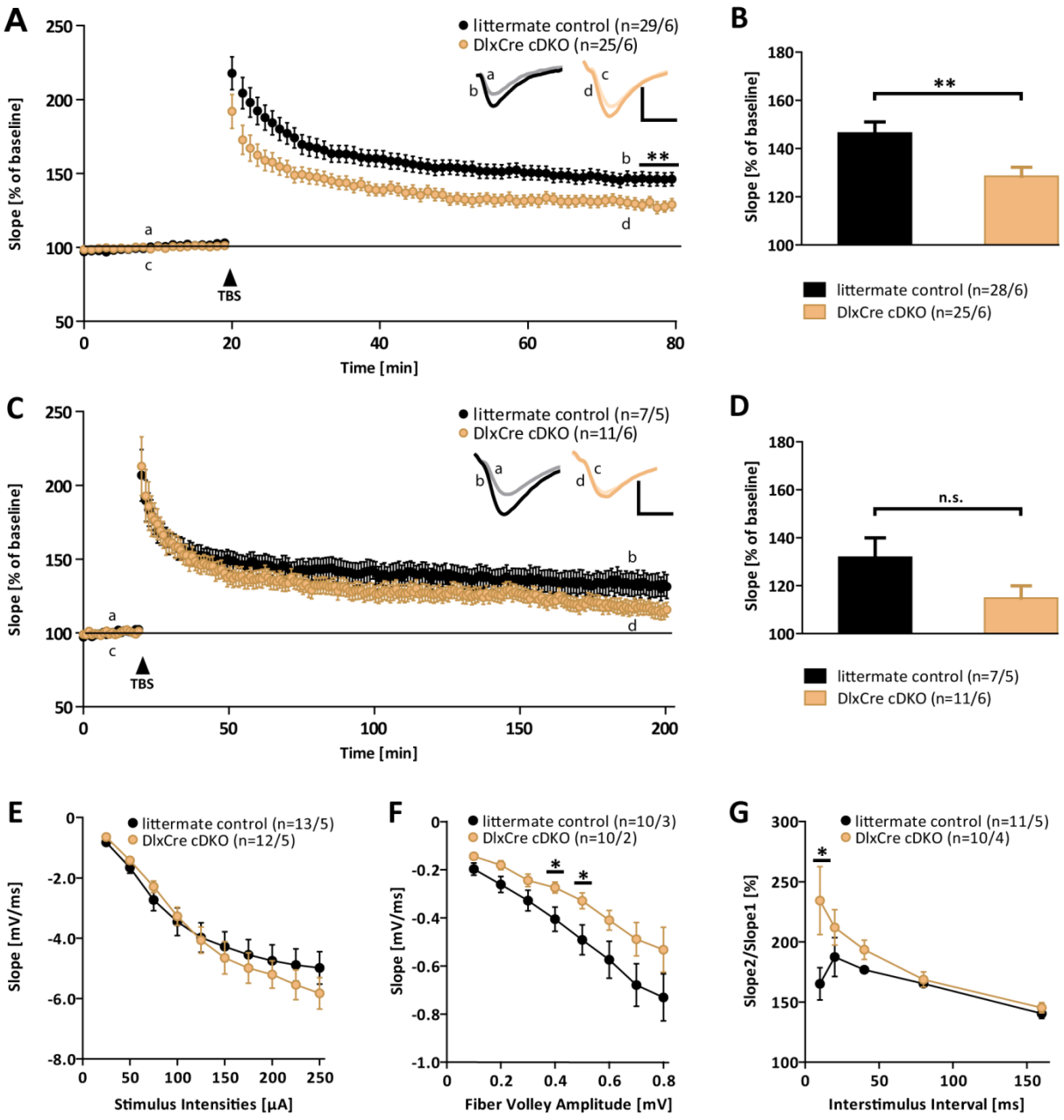

Figure 3.21 LTP experiments in adult DlxCre cDKO mice.

(A+B) *LTP induction by TBS (arrow) led to an overall increase of synaptic efficacy which was highly significant altered between genotypes (littermate controls: 147 ± 4.6 %, black circles, DlxCre cDKO: 129 ± 3.8 %, orange circles, p = 0.005, t-test).* ***(C+D)*** *Surprisingly, this defect was not observable in L-LTP recordings (t195-200 min, littermate controls: 132 ± 8.1 %, DlxCre cDKO: 115 ± 5.2 %, p = 0.096, t-test). Although a trend to this difference was visible towards the end of the recording.* ***(E+F)*** *While a correlation of given stimulus intensities showed no overt deficit, the correlation to defined fiber volley amplitudes pointed towards an alteration of input-output strength in DlxCre cDKOs (0.4 mV: p = 0.037, 0.5 mV: p = 0.042, t-test).* ***(G)*** *These findings were corroborated by a significant defect of short-term plasticity (ISI 10 ms: p = 0.043, t-test). Insets show original traces of representative individual experiments. Vertical scale bar = 1 mV, horizontal scale bar = 5 ms. Error bars indicate ± SEM. n.s. = not significant. n = number no of slices / number of mice used.*

3.2.2.2 GADCre Conditional Double Knock-out

TBS application led to a successful, robust induction and maintained LTP in both genotypes (Figure 3.22 A). While recordings were performed, a LTP defect became visible which was significant for the final 5 min when littermate control slices (154 ± 6.7 %, n = 12 / 4) were compared to GADCre cDKO mice (135 ± 4.2 %, n = 25 / 6, p = 0.022, t-test, Figure 3.22 B). This difference became even more pronounced during the entire recording when protein synthesis dependent L-LTP was investigated (Figure 3.22 C). Average potentiation of t195-200 min revealed a highly significant defect of p = 0.0004 (t-test) in littermate controls of 160 ± 6.3 % (n = 4 / 3) versus GADCre cDKO of 126 ± 2.7 % (n = 8 / 6, Figure 3.22 D). Nonetheless, this distinct phenotype was not accompanied by alterations of neither short-term plasticity (Figure 3.22 G) nor input-output strength when correlated to given stimulus intensities (Figure 3.22 E) or fiber volley amplitudes (Figure 3.22 F). Collectively, the results from mice with APP and APLP2 cDKOs restricted to inhibitory interneurons were comparable to results obtained from the cDKO in excitatory neurons in NexCre cDKO. An exception was the data from the PPF paradigm where a clear defect was found in NexCre cDKO but not in GADCre cDKO. However, it is necessary to mention that further analysis of GADCre cDKO mice uncovered spontaneous germ-line recombination activities in GADCre-deleter lines. This led to a global APP-KO in the entire organism and was thus no longer restricted to inhibitory neurons in the brain. Therefore, it is questionable whether data obtained for activity dependent synaptic plasticity reflected the physiological state or resulted from side effects of global KO.

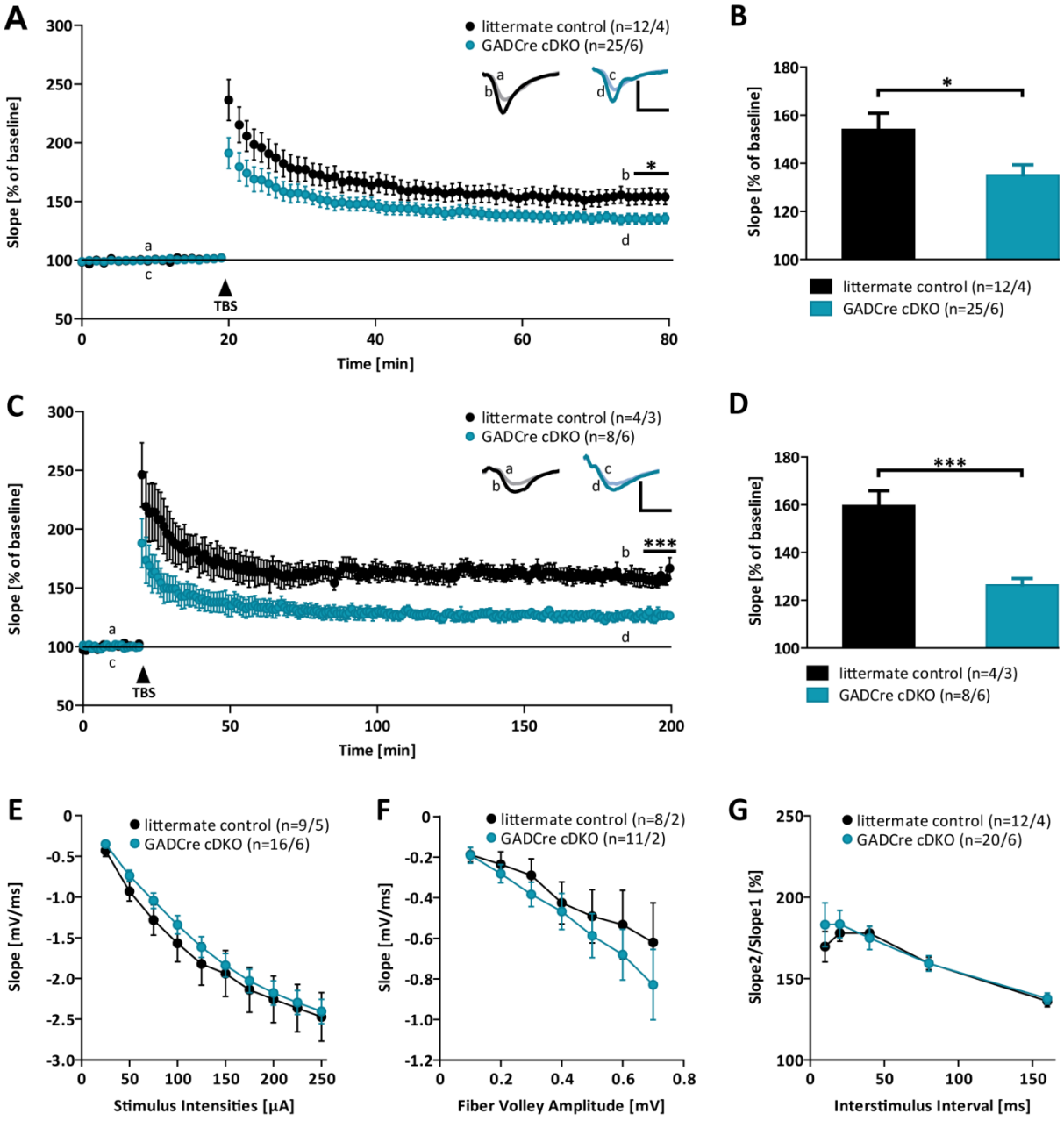

Figure 3.22 LTP experiments in aged GAD67Cre cDKO mice.
(A+B) *TBS (arrow) application induced a strong and stable LTP in littermate controls of 154 ± 6.7 % (black circles) and in GADCre cDKO of 135 ± 4.2 % (turquois circles) for t75-80 min, which resulted in a significant difference between genotypes (p = 0.022, t-test).* ***(C+D)*** *Strikingly, the defect was even stronger in results obtained for L-LTP. Again a robust induction phase was observed in both genotypes which turned into a highly significant difference between littermate controls of 160 ± 6.3 % and GADCre cDKO of 126 ± 2.7 % for t195-200 min in the L-LTP plateau (p = 0.0004, t-test).* ***(E+F)*** *Recording of fEPSP slope size at given stimulus intensities and fiber volley amplitudes revealed no significant differences among genotypes.* ***(G)*** *Presynaptic function and thus short-term plasticity was as well not affected. Insets show original traces of representative individual experiments. Vertical scale bar = 1 mV, horizontal scale bar = 5 ms. Error bars indicate ± SEM. n.s. = not significant. n = number no of slices / number of mice used.*

Figure 3.23 summarizes all results obtained from investigations of the role of APP and APLP2 in activity dependent synaptic transmission in inhibitory neurons.

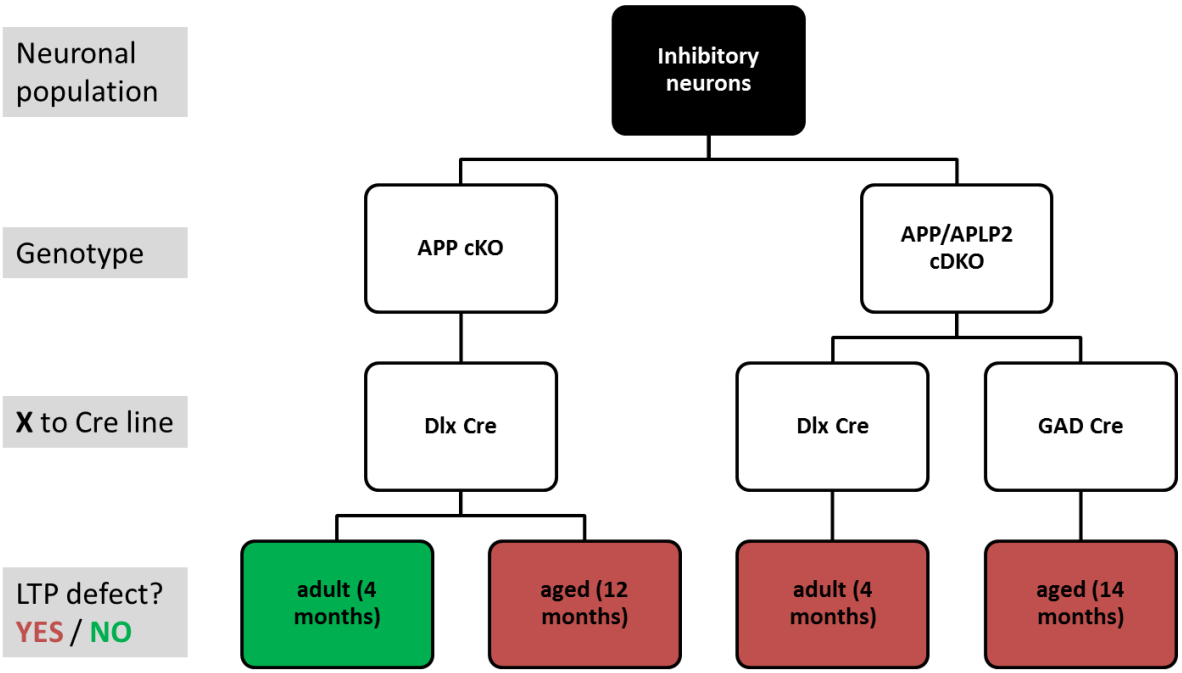

Figure 3.23 Overview about results obtained from $APP^{flox/flox}APLP2^{-/-}$ crossed to inhibitory Cre-deleter lines.

4 Discussion

4.1 Considerable Role of the APP Protein Family in Synaptic Plasticity

The synapse is the site for dynamic modulations such as strengthening and weakening in case of LTP and LTD, respectively. Those mechanisms promote functional and structural plasticity at the synapse. Thereby, Ca^{2+} represents a potent second messenger which activates various enzymes to trigger further downstream cascades modifying finally the gene expression of plasticity related proteins. The modulation of synaptic plasticity depends on the action of a variety of proteins. One of these is the Amyloid precursor protein (APP) which belongs to a family including the homologues proteins APLP1 and APLP2. In this thesis, I investigated the role of the APP protein family and its cleavage products for the modulation of activity-dependent synaptic plasticity in the hippocampal CA3-CA1 pathway. Thereby, I differentiated between the involvement of these proteins during brain development as well as the acute function at active synapses in the adult CNS.

Main findings from transgenic mice lacking APP and APLP2 in inhibitory or excitatory forebrain neurons uncovered an imbalanced excitation-inhibition ratio that might result from impaired network formation during brain development. The lethality of constitutive triple and almost all double KO mice, a distinct hint for the involvement of the APP protein family in brain development processes, so far precluded the analysis. Intriguingly, I confirmed that APP and APLP2 have redundant functions which enable APLP2 to compensate for the loss of APP. However, this was only observed in adult but not aged transgenic mice. The two approaches applied in this thesis, organotypic hippocampal cultures (OHCs) treated with a specific α-secretase inhibitor and the conditional deletion of APP on an APLP2 deficient background, convincingly showed that a deficiency of both proteins during the formation of neuronal networks consequently impairs synaptic plasticity in combination with an altered Ca^{2+} dynamic. The acute function of APP, more precisely the α-secretase processing product APPsα, for the modulation of activity-dependent synaptic plasticity became obvious when I showed that exogenously applied recAPPsα fully restored the impaired LTP of NexCre cDKO. Consistently, virally expressed APPsα on a NexCre cDKO background rescued the Ca^{2+} dynamic defect. Taken together, the results further underline the role of APPsα for potential therapeutic strategies on a long road towards a treatment of the devastating Alzheimer's disease.

4.1.1 APP Deficiency Leads to a Disturbed Excitation-Inhibition Balance

For a successful LTP induction a balanced and well-coordinated tonic excitatory and inhibitory input is mandatory. This notion is supported by the finding that the inhibition of $GABA_A$ receptors facilitates LTP and leads to hyperexcitability causing epileptic seizures (Wigstrom and Gustafsson, 1983, 1985; Casasola et al., 2004). The GABAergic system is involved during the induction and the early maintenance period of LTP for instance through presynaptic $GABA_B$ autoreceptors on GABAergic neurons providing a disinhibitory mechanism (Davies and Collingridge, 1993; Mott et al., 1993). By this means, alterations in the GABAergic system might contribute to the impaired synaptic plasticity of APP/APLP2 transgenic mice.

This is supported by previous reports which showed an increased susceptibility for kainate-induced seizures in constitutive APP-KO mice pointing towards a decreased inhibitory input (Steinbach et al., 1998). However, more evidence is provided for an increased inhibitory input in APP deficient mice. The beforehand mentioned $GABA_B$ receptor was recently identified to interact with APP (Norstrom et al., 2010). Still, the *in vivo* relevance of this interaction needs to be specified but it might be speculated that a lack of APP disturbs presynaptic inhibitory and regulatory $GABA_B$ dependent mechanisms leading to increased inhibitory currents. This hypothesis was further supported by studies showing that the inhibition of $GABA_A$ receptors by Picrotoxin in either APP-KO or APPsα- double mutant (APPsα-DM: *APPsα*$^{+/+}$ *APLP2*$^{-/-}$) rescued the LTP defect to control levels presumably because the postsynaptic depolarization is facilitated (Fitzjohn et al., 2000; Weyer et al., 2011). Moreover, APP was shown to be a regulator of GABAergic short term plasticity in dissociated hippocampal and striatal neurons. An study hippocampal and striatal APP-KO neurons showed increased L-type voltage gated Ca^{2+} channel (VGCC) levels and function accompanied by elevated GABAergic Ca^{2+} currents (Yang et al., 2009). These impairments were rescued if APP was again expressed. The increased inhibition might therefore be linked to the LTP defects observed in this study since the threshold for LTP induction and maintenance could have been higher. This explanation is supported by the finding that APP/APLP2 transgenic mice like the NexCre cDKO (see Figure 3.6) revealed already directly after LTP induction significant defects in the Posttetanic Potentiation. Since the inhibitory input mainly contributes to the induction and the early maintenance of LTP one might consider that the threshold for LTP was higher due to an increased inhibitory input (Davies and Collingridge,

1993; Mott et al., 1993). Additionally, the APP-KO might also affect L-type VGCCs in excitatory neurons. The importance of APP and L-type VGCCs interaction in excitatory neurons was shown by Santos and colleagues. They found that the acute inhibition of endogenous APP in cortical neurons affects the Ca^{2+} homeostasis by decreasing the amplitude but increasing the frequency of Ca^{2+} events (Santos et al., 2009). Thus, a crucial function of APP in regulating excitation-inhibition balance via this APP – L-type VGCCs interaction might be likely.

APP and APLP2 could act directly by being part of intracellular signaling cascades or indirectly trigger those cascades through a secondary homeostatic effect which are essential for a balanced inhibition. A recent study reported that PKC activators are capable to enhance GABAergic neurotransmission (Xu et al., 2014). On the other hand PKC mediated phosphorylation of APP was shown to increase α-secretase and decrease the β-secretase processing (Buxbaum et al., 1993). Thus, one might speculate that fragments of APP processing deriving from the non-amyloidogenic pathway are crucial for modulating the excitation-inhibition balance as a consequence of activity-dependent synaptic plasticity. These ideas are even further supported by the results from LTP studies presented here. The knock-out of both APP and APLP2 in either excitatory (NexCre cDKO: $NexCre^{+/T}$ $APP^{flox/flox}$ $APLP2^{-/-}$, see Figure 3.10) or inhibitory (DlxCre cDKO: $DlxCre^{+/T}$ $APP^{flox/flox}$ $APLP2^{-/-}$, see Figure 3.21) neurons resulted in a pronounced and significant LTP defect which was rescued by exogenous recAPPsα application at least in NexCre cDKO mice (see Figure 3.11) implicating an essential role for this α-secretase cleavage product (Hick et al., 2015). In future experiments a neuron specific, prenatal APP / APLP2 cDKO by using the CAGCre-deleter line could be applied to study an APP function in both inhibitory and excitatory neurons simultaneously.

4.1.2 Age-dependent Compensatory Function of APP and APLP2

Multiple lines of evidence indicate a LTP defect in aged but not adult conventional APP-KO mice (Dawson et al., 1999; Seabrook et al., 1999; Ring et al., 2007). Notably, these transgenic animals revealed severe gliosis which at least in part might contribute to the altered synaptic plasticity (Zheng et al., 1995; Dawson et al., 1999). Glia cells are known to be essential for a proper neuronal function as they are part of the tripartite synapse promoting the reuptake of presynaptically released glutamate and maintaining the ion homeostasis (Eroglu and Barres,

2010). Surprisingly, an alternative strain of APP-KO mice didn't show gliosis any longer but still revealed the previously observed LTP defect in aged individuals solely (Ring et al., 2007; Tyan et al., 2012). Tyan and colleagues, furthermore, found a pronounced reduction of CA1 pyramidal neuron complexity and spine density only for aged APP-KO mice whereas adults were indistinguishable to controls. Presumably, the decreased spine number in aged APP-KO mice might result from increased spine elimination (Tyan et al., 2012). Still, the question remains why this defect was not observed in adult APP-KO mice. Since the APLP2 protein displays a high degree of sequence homology to APP and both reveal overlapping processing and expression patterns a compensatory function during adulthood is likely which seems to diminish with age (Wasco et al., 1993; Nicolas and Hassan, 2014). A study investigating conventional APLP2-KO mice addressed this question and found no alterations on neuronal morphology and function independent of age suggesting that APP contains features that are either distinct from APLP2 or dominant to APLP2 (Weyer et al., 2011; Midthune et al., 2012).

To prevent the potential compensatory mechanism a double knock-out (DKO) of both APP and APLP2 is necessary. Unfortunately, these mice die shortly after birth due to neuro-muscular deficits (von Koch et al., 1997; Heber et al., 2000). Therefore, transgenic mouse-lines were generated in which the APP gene was replaced by either APPsα or APPΔCT15 on an APLP2 deficient background termed double mutant (APPsα-DM: *APPsα*$^{+/+}$ *APLP2*$^{-/-}$ or APPΔCT15-DM: *APPΔCT15*$^{+/+}$ *APLP2*$^{-/-}$). Interestingly, these two mouse-lines are viable and exhibit a significantly impaired LTP already in adult individuals (see Figure 3.2). This supports the idea of a compensatory function of APLP2 in adult mice (Weyer et al., 2011; Klevanski et al., in preparation). Nevertheless, APPsα or APPΔCT15 expression might mask further effects. The application of an alternative genetic technique, however, enabled us to generate a fully viable double knock-out via the conditional approach (cDKO). Besides investigating the role of APP and APLP2 in inhibitory neurons for the excitation-inhibition balance (see 4.1.1) I addressed the question whether in these mice the age dependency and the APLP2 compensatory function would be found as well. Therefore, in a first step adult and aged DlxCre cKO mice (*DlxCre*$^{+/T}$ *APP*$^{flox/flox}$) were analyzed in which APP is eliminated while APLP2 is still expressed. In line with the results from conventional APP-KO mice again no LTP defect and an unaltered basal synaptic transmission was found in adult DlxCre cKOs (see Figure 3.19). Solely aged DlxCre cKO mice

revealed a significantly lower LTP compared to controls (see Figure 3.20). It could be speculated that for example APPsα, released upon electrical stimulation from surrounding excitatory neurons, was not appropriate to prevent the LTP defect in aged individuals. Furthermore, it could be assumed that like in aged APP-KO mice APLP2 is not sufficient to compensate the defect any longer (Dawson et al., 1999; Seabrook et al., 1999; Ring et al., 2007). Thus, I next assessed adult DlxCre cDKO mice (*DlxCre*$^{+/T}$ *APP*$^{flox/flox}$ *APLP2*$^{-/-}$) lacking both APP and APLP2 were investigated and showed, indeed, an impaired LTP and basal synaptic transmission further underlining the compensatory age-dependent effect of APLP2 (see Figure 3.21). To verify these results another inhibitory neuron specific Cre-deleter mouse line was used. Aged GADCre cDKO (*GAD67Cre*$^{+/T}$ *APP*$^{flox/flox}$ *APLP2*$^{-/-}$) mice were analyzed and showed a significantly impaired activity-dependent synaptic plasticity for LTP which became even stronger when late-LTP was analyzed (see Figure 3.22). However, further analysis of this mouse-line revealed a spontaneous germ-line recombination activity in the GADCre-deleter line which led to a global APP-KO in the entire organism. Thus, the interpretation of results obtained from GADCre cDKO mice is difficult since one could not distinguish whether the defect reflects the physiological state or is caused by side effects of the global KO. Generally, both GADCre cDKO and DlxCre cDKOs revealed a comparably impaired activity-dependent synaptic plasticity induced by a DKO of both APP and APLP2 in solely inhibitory neurons.

In line with data obtained for the cDKO restricted to the inhibitory system, I could complementarily detect a LTP defect restricted to excitatory neurons of adult NexCre cDKO mice (*NexCre*$^{+/T}$ *APP*$^{flox/flox}$ *APLP2*$^{-/-}$, see Figure 3.6) as well confirming a functional complementation by APLP2 in adult APP-KO mice (Hick et al., 2015). Nevertheless, the question why the compensatory function of APLP2 in conditional or constitutive APP-KO becomes lost with age needs to be assessed further. It might be speculated that for instance normal aging processes in the brain significantly contribute or the APP or APLP2 protein expression itself is affected. The neuronal plasticity related to cognitive impairments in the aged compared to adult wildtype (wt) brain has been intensely investigated (Burke and Barnes, 2006). Beside studies on neuronal complexity, spine density and synapse numbers in aged compared to adult wt mice which revealed no gross overall alterations, in the CA3-CA1 pathway a disruption of Ca^{2+} homeostasis through higher levels of L-type VGCCs was shown (Foster and Norris, 1997; Burke and Barnes,

2006). Moreover, this was accompanied by lower cAMP levels in aged wt (Tombaugh et al., 2005). All together this increases the threshold for excitability compared to adult wt CA1 neurons. Notably, this could not be confirmed in *in vivo* recordings. Another theory states that hippocampal perforated synapses become silent or non-functional with normal aging contributing to the cognitive decline (Nicholson et al., 2004). A large body of evidence is given for a defect of activity dependent synaptic plasticity in aged rodents. These deficits are, however, of complex nature, region specific and depend for LTP on the induction protocol used. Aged wt CA1 pyramidal neurons exhibited a weaker temporal summation of multiple EPSPs induced by high frequency stimulation. Thus, these neurons are less depolarized which might explain the observed induction defect (Rosenzweig et al., 1997). Paralleled to an altered neuronal function age-related changes in gene expression, a process which is crucial for L-LTP maintenance, were indicated (Burke and Barnes, 2006). Interestingly, it was shown that 10 nM of APPsα, an APP processing product deriving from the non amyloidogenic pathway via α-secretase cleavage, had less effects on the enhancement of protein synthesis in aged compared to adult rats (Claasen et al., 2009). So it might well be that levels of APLP2, the α-secretase cleavage product APLP2sα levels or other proteins of downstream signaling cascades are decreased leading to the loss of compensation. As a future direction this idea could be assessed by protein quantification via western blot from hippocampal lysates of adult versus aged APP-KO mice.

Collectively, my results described above provide evidence that both APP and APLP2 are synergistically required for activity-dependent processes of learning and memory. A loss of APP can be compensated by APLP2, suggestively via APLP2sα secretion, exclusively in adult and not in aged mice whereas a loss of APLP2 is compensated by APP, via APPsα release, throughout lifetime (Eggert et al., 2004; Endres et al., 2005; Weyer et al., 2011).

4.1.3 APP is Required for Brain Developmental Processes and the Acute Modulation of Synaptic Properties

One aim of this study was to distinguish between developmental and acute functions of the APP protein family and its processing fragments in the adult CNS in modulating the synaptic strength. It is well feasible that some functional deficits in APP- and / or APLP-deficient mice

result from an altered development. Studies showed an increase in APP expression in the brain development during peak periods of neurite outgrowth and synaptogenesis implicating that this protein is important for a proper neuronal network formation (Kirazov et al., 2001). Additionally, APP was shown to be involved in processes of neuronal progenitor proliferation and neuronal migration (Young-Pearse et al., 2007; Young-Pearse et al., 2010; Hu et al., 2013). This role is furthermore supported by the fact that an APP / APLP2 / APLP1 triple KO is lethal due to cortical dysplasia and partial loss of Cajal-Retzius cells (Herms et al., 2004). Furthermore, combined double KO (DKO) mice of APP / APLP2 or APLP1 / APLP2 die shortly after birth due to severe defects at the neuromuscular junction probably because an interaction of APP and acetylcholine receptors is required (Akaaboune et al., 2000). In contrast mice lacking only one protein family member are fully viable suggesting redundant functions (von Koch et al., 1997; Heber et al., 2000).

In this thesis the results of two different mouse strains are presented in which APP is knocked out exclusively in excitatory neurons via the conditional strategy on an APLP2 deficient background. The first strain is the CaMKIIαCre cDKO (*CaMKIIαCreER*$^{T2\ +/T}$ *APP*$^{flox/flox}$ *APLP2*$^{-/-}$) in which the KO of APP is tamoxifen inducible. I analyzed 1x (adult) and 2x (P5 and adult) tamoxifen treated mice at 3 – 4 and 12 – 13 months of age. Since solely P5 tamoxifen treated mice exhibited only a weak Cre activity during postnatal stages consequently just a small subset of CA3 and DG neurons was APP negative. In CA1 no APP deletion at all was found (Meike Hick, IPMB Heidelberg). Therefore, to achieve a maximal Cre activation and thus APP ablation tamoxifen was applied twice at P5 and in the adulthood. The central aim was to investigate the acute effects of APP and its processing products at active synapses. However, the early ablation of APP at P5 covers also functions of this protein in early postnatal brain development. Surprisingly, I could only observe a mild LTP impairment when activity dependent synaptic plasticity was analyzed for aged 1x tamoxifen treated CaMKIIαCre cDKO (see Figure 3.3) as well as for adult and aged 2x tamoxifen treated CaMKIIαCre cDKOs (see Figure 3.4 and Figure 3.5). Beforehand, these mice performed hippocampus-dependent memory tasks (in the lab of Prof. Dr. David Wolfer, Zürich). Interestingly, they showed a defect in place navigation when performing the Morris Water Maze task while the spatial working memory tested by the Radial Arm Maze task was not affected. Although the 2x tamoxifen applications should lead to ablation

of APP in most of the excitatory forebrain neurons, it cannot be ruled out that not all cells were targeted. This suggestion was supported by immunohistochemical and western blot analysis from Meike Hick (IPMB, Heidelberg, AG Müller) showing that the hippocampi from CaMKIIαCre cDKO mice still revealed a relatively high amount of ~20 % APP. Additionally, it should be considered that in these mice inhibitory neurons which comprise 5 % of hippocampal neurons as well as astrocytes still express APP which might contribute to the mild effect observed (Rossner, 2004). Moreover, as it was shown that APP and APLP2 are also involved in earlier processes during embryonic brain development the DKO via the CaMKIIα promoter which was activated postnatally at P5 might be too late (Herms et al., 2004). When interpreting this data it should also be taken to account that the induction of APP excision via tamoxifen represents a strong hormonal stress event which might cause undesired side effects. Tamoxifen is a synthetic estrogen derivate which is characterized as a selective estrogen-receptor modulator. Beside neurotransmitters also neurohormones deriving from the endocrine system contribute to an intact neuronal function. Thus, tamoxifen treatment might also change the physiological state of the brain since endogenous estrogen is shown to modulate the activation of potassium channels in the CNS (Kelly et al., 2003). However, since the littermate control mice received the same tamoxifen doses like the CaMKIIαCre cDKO this serves as an internal control.

To investigate an even earlier role of APP and to circumvent potential side effects of tamoxifen in a second approach the NexCre-deleter line was used to generate NexCre cDKO mice (*NexCre*$^{+/T}$ *APP*$^{flox/flox}$ *APLP2*$^{-/-}$). In these mice the APP ablation in excitatory forebrain neurons on an APLP2 deficient background is initiated conditionally already at E11.5. Strikingly, the analysis of NexCre cDKO mice revealed a strong defect in hippocampus-dependent memory when, again, Morris Water Maze and Radial Arm Maze task were tested which was accompanied by a pronounced impairment in activity-dependent synaptic plasticity (see Figure 3.6) including an altered presynaptic function (Hick et al., 2015). Furthermore, this defect was also reflected at the neuronal level by a decreased dendritic complexity accompanied by a reduced hippocampal volume. A deficit in spine density was associated with a shift towards more immature stubby spines characterized by a smaller PSD (Hick et al., 2015).

As already introduced in 4.1.1 the APP protein family seems to be important for an intact excitation-inhibition balance. Therefore, the data obtained from DlxCre cDKO, revealing a

pronounced LTP defect (see Figure 3.21), is well in line with results from NexCre cDKO. Both genes Dlx and Nex are expressed around E11. Thus, a crucial role of APP and APLP2 for dendritic architecture and neuronal network formation already at early developmental stages can be suggested. These alterations on the cellular level match with our recent observations from *in vitro* studies in OHCs in which APLP2-KO OHCs were indistinguishable to wt cultures, but APP-KO OHCs exhibited a neuronal branching defect which became even more pronounced when additionally APLP2 was gene targeted. Moreover, a decreased spine number was observed which notably was not further reduced in APP / APLP2 DKO OHCs (Weyer et al., 2014). Collectively, these data provide convincing evidence that both APP and APLP2 are crucial for normal morphology and function of pyramidal neurons. Furthermore, data obtained from OHC analysis hint towards a potential role of the APP protein family during early postnatal phases for the establishment and maturation of synaptic contacts since this period comprises the peak of APP protein expression (Loffler and Huber, 1992; Wang et al., 2009).

Next, I studied the functional role of APP and APLP2 α-secretase cleavage products in synaptic plasticity during early developmental processes (see Figure 3.1). Since the long-term incubation of a specific α-secretase inhibitor did not affect the LTP in acute slices I switched to OHCs to prolong the incubation time. Previous studies as well as results obtained in this thesis confirmed that APLP2-KO cultures, only treated with DMSO, still reveal potentiation levels comparable to wt controls. Interestingly, the specific inhibition of α-secretase ADAM10 for five consecutive days starting at DIV 14-19 should include late phases of synaptogenesis. The reduced LTP induction and maintenance in inhibitor treated APLP2-KO OHCs underlines the importance for APPsα as the α-secretase APP cleavage product (Hoettecke et al., 2010; Weyer et al., 2011). Wt OHCs did not show any impairment neither under DMSO nor inhibitor application implicating that still a sufficient amount of APPsα and APLP2sα, both being products of α-secretase cleavage, is left to promote LTP. Since this inhibitor specifically blocks the α-secretase ADAM10 but not the other ADAM family members like ADAM9, ADAM17 or ADAM19 which also process APP it might be speculated that through the action of the intact α-secretases still enough APPsα and APLP2sα for promoting proper synaptic function is generated (Hoettecke et al., 2010). Weyer and colleagues showed that OHCs from double mutants which only express the APPsα fragment on an APLP2 deficient background (*APPsα*$^{+/+}$ *APLP2*$^{-/-}$) did not exhibit any LTP already

under DMSO conditions. Presumably, the amount of constitutively generated APPsα was too low to promote LTP or permanently expressed APPsα cannot be efficiently transported to the active synapses (Weyer et al., 2011). Indeed, numerous studies showed that the secretion of APPsα is tightly linked to increased neuronal activity by NMDA or muscarinic acetylcholine receptor activation (Nitsch et al., 1992; Fazeli et al., 1994; Gakhar-Koppole et al., 2008; Hoey et al., 2009). This is furthermore supported by my observation that the LTP from APPΔCT15-DM OHCs (*APPΔCT15*$^{+/+}$ *APLP2*$^{-/-}$), expressing an APP fragment which is in contrast to APPsα membrane bound, is normal under DMSO treatment but significantly impaired when ADAM10 is inhibited. In summary, these studies in OHCs revealed a combined role of APP and APLP2 for dendritic architecture already at early developmental stages and a unique function of APPsα for spine density and synaptic plasticity.

4.1.4 The C-terminal Domain of APP is Crucial to Modulate the Expression of Plasticity Related Proteins

The intracellular C-terminal sequences are most highly conserved among the APP family members (see 1.3). The AICD is an important interaction site for phosphorylation and de-phosphorylation events, binding of adapter proteins and was implicated as transcription factor modulating the gene expression directly or indirectly (Muller et al., 2008; Pardossi-Piquard and Checler, 2012). It furthermore contains the YENPTY motif which is an internalization signal for endocytosis of APP localized at the membrane and this motif stimulates Aβ generation *in vitro* (Trowbridge et al., 1993; Lai et al., 1995; Perez et al., 1999). Moreover, recent evidence implicates that TrkA as a receptor for the nerve growth factor (NGF) is involved in the APP signaling pathway. It was reported that TrkA phosphorylates APP on Tyr residues within the YENPTY motif and directly binds APP which triggers further downstream cascades of NGF / TrkA signaling (Matrone et al., 2011; Matrone, 2013). In addition, this sequence suggestively regulates APP processing itself since a mutation of this phosphorylation sites shifts the APP processing more to the non amyloidogenic pathway. Alternatively, it could be argued that in this case the APP internalization is not working properly. Thus, more APP is membrane bound which than as a consequence leads to more APPsα secretion (Barbagallo et al., 2010). The same group showed opposing functions for two phosphorylation sites within the AICD of *APP*$^{mut/mut}$*/APLP2*$^{-/-}$

mice: a mutation of Tyr682 led to lethality due to severe neuromuscular defects while the mutated Tyr668 had no impact (Barbagallo et al., 2011a, b). This is in clear contrast to the APPΔCT15 double mutants (DM, *APPΔCT15*$^{+/+}$ *APLP2*$^{-/-}$) analyzed in this study which are viable although they lack the last C-terminal 15 amino acids including Tyr682 and Tyr668 on an APLP2-deficient background (Klevanski et al., in preparation).

One important APP adapter protein is Fe65 which binds the de-phosphorylated YENPTY motif inducing the shuttling of a multimeric complex of AICD / Fe65 / Tip60 into the nucleus to regulate the gene transcription (Cao and Sudhof, 2001). Comparably to APP the Fe65 protein family includes the homologues Fe65L1 and Fe65L2 all of which bind the APP protein family members (Guenette et al., 1996). Consistent with the APP / APLP2 DKO the double KO of Fe65 / Fe65L1 revealed a significant defect in activity-dependent synaptic plasticity implicating that APP-Fe65 interaction is crucial for synaptic function (Strecker et al., in preparation). In order to disrupt this interaction we generated the beforehand mentioned APPΔCT15-DM (*APPΔCT15*$^{+/+}$ *APLP2*$^{-/-}$). Acute hippocampal slices revealed a strongly impaired activity-dependent synaptic plasticity including a defect in early-LTP and postsynaptic properties while late-LTP showed only a trend towards a deficit (see Figure 3.2). In parallel these mice were analyzed regarding hippocampus dependent behavior which was found to be severely altered when the T- and Radial Arm Maze were applied. Notably, no Morris Water Maze task has been performed since these mice exhibited neuromuscular deficits shown by motor tasks. This was reasoned by an altered morphology of endplates and postsynaptic terminals mechanistically elicited by an impaired neuromuscular transmission (Klevanski et al., in preparation). Similar results were found when the APPsα-DM (*APPsα*$^{+/+}$ *APLP2*$^{-/-}$), expressing only the APPsα fragment on an APLP2-deficient background, was analyzed. Surprisingly and comparable to the APPΔCT15-DM, these morphological defects were only restricted to the PNS at the neuromuscular junction while CNS morphology was unaffected. Nevertheless, again at the functional level central glutamatergic synapses were affected shown by an impaired LTP accompanied by a compromised Radial Arm and T-Maze performance (Weyer et al., 2011). Interestingly, both mouse lines, APPsα- or APPΔCT15-DM, are viable whereas APPsβ-DM mice (*APPsβ*$^{+/+}$ *APLP2*$^{-/-}$) die, resembling the phenotype of full APP / APLP2 DM (Wang et al., 2005; Wang et al., 2009). APPsβ is only 17 amino acids shorter compared to APPsα which seems to contain a motif crucial

for animal survival (see 4.2.1). Nevertheless, an impaired neuromuscular function and morphology was observed in both APPsα- or APPΔCT15 DM compared to APLP2-KO controls suggesting that interaction sites like the YENPTY motif within the missing C-terminal domain contribute to normal neuronal morphology (Weyer et al., 2011; Klevanski et al., in preparation). Collectively, this proofs an essential function of the 15 C-terminal amino acids including the YENPTY motif in terms of APP-protein interactions like with the Fe65 protein family. In this thesis this interaction site was shown to be crucial for an intact activity-dependent synaptic plasticity. Additionally, again the redundant function of APP and APLP2 proteins became clear since mice that express APPsα or APPΔCT15 with an intact APLP2 background (*APPsα*$^{+/+}$ *or* *APPΔCT15*$^{+/+}$) exhibit no motor and synaptic plasticity deficits (Ring et al., 2007).

4.2 The Secreted APPsα Ectodomain is Essential for Regulating Synaptic Strength

Upon α-secretase cleavage of full length APP and APLP2 the large APPsα and APLP2sα ectodomains are released into the extracellular space (Lammich et al., 1999; Endres et al., 2005). Numerous studies confirmed that APPsα has an exceeding role in neuroprotection, synaptic plasticity and neuronal network function (Ring et al., 2007; Weyer et al., 2011; Kogel et al., 2012; Korte et al., 2012; Zhang et al., 2013; Hick et al., 2015). The APP processing by the α-secretase is activity-dependent and can thus be potentiated by neuronal depolarization, high frequency stimulation and activity of mGluR as well as mAChR (Nitsch et al., 1992; Nitsch et al., 1993; Fazeli et al., 1994; Gakhar-Koppole et al., 2008). Intriguingly, it was shown that endogenously produced APPsα is crucial for LTP induction, maintenance and enhancement (Ishida et al., 1997). A regulated APP cleavage by the α-secretase under physiological conditions is necessary to form APPsα which seems to be essential during synaptic activity to enhance NMDAR signaling during LTP (Weyer et al., 2011). Another reason why constitutive APP / APLP2 DKO mice die after birth was given by studies of embryonic stem cells which, when they were differentiated into glutamatergic neurons, showed a decreased expression of the vesicular glutamate transporter 2 resulting in a reduced synaptic transmission (Schrenk-Siemens et al., 2008). Moreover, they exhibited a decreased glutamate release which might be reasonable for

the observed impaired activity-dependent synaptic plasticity (see Figure 3.6) of NexCre cDKO mice (Hick et al., 2015). Suggestively, APPsα is able to enhance memory and regulate neuronal excitability. A recruitment of NMDARs through APP is discussed while contrariwise toxic Aβ oligomers decrease the number of AMPARs and NMDARs (Snyder et al., 2005; Hsieh et al., 2006a; Hoe et al., 2009). Recent studies showed that APP is associated to the NMDAR in the ER but also found at the cell surface integrated in the PSD (Hoe et al., 2009; Hoey et al., 2009). GluN2B subunit containing NMDARs are associated with APP that enhanced their cell surface recruitment shown by APP overexpression leading to increased NMDAR surface levels (Cousins et al., 2009; Hoe et al., 2009). Consistently, the activation of NMDARs stimulates the APP processing and simultaneously inhibits the Aβ generation (Hoey et al., 2009). Another publication suggests that endogenous APPsα specifically regulates NMDARs currents during high frequency stimulation which also could explain why the inhibition of GABAergic neurons or the application of recombinant APPsα (see Figure 3.11) restores the impaired LTP to control levels (Taylor et al., 2008; Hick et al., 2015). Therefore, it was tested whether the LTP defect of NexCre cDKO, in which the potential interaction with NMDARs is abolished, is attributed to a disturbed NMDAR expression or composition. Surprisingly, the analysis of spontaneous mEPSCs by patch clamp recordings showed no defect in amplitudes, kinetics or NMDA component of mixed EPSCs (Hick et al., 2015). Thus, a functional relevance for an APP – NMDAR interaction remains unclear. Nevertheless, the group of Prof. Dr. W.C. Abraham (University of Otago, New Zealand) showed a significant concentration-dependent effect of recombinant APPsα treatment in acute wt rat hippocampal slices (data presented at the neuroscience 2014, K.D. Parfitt, poster ID 405.05/D52). Lower doses decreased GluN1 and GluA1 expression whereas intermediate doses increased both respectively suggesting that APPsα has a fundamental role in the regulation of NMDAR and AMPAR subunit composition and receptor localization (data presented at the neuroscience 2014, K.D. Parfitt, poster ID 405.05/D52). Still, the observed defect in activity-dependent synaptic plasticity might be reasonable by the missing APPsα acting pre- and / or postsynaptically. This suggestion is supported since the knock-out of the α-secretase ADAM10, precluding the processing of both APP and APLP2, leads to comparable impairments observed in NexCre cDKO mice. Notably, they did not comment on the remaining cleavage activity of other ADAM family member (Prox et al., 2013; Hick et al., 2015).

4.2.1 recAPPsα, but not recAPPsβ, Restores the Functional LTP Defect of NexCre cDKO

The beforehand described neurotrophic characteristic of APPsα is also reflected by its LTP enhancing properties. These were shown by the infusion of APPsα which further increased LTP in wt acute slices compared to PBS treated control. Consistently, in my experiments the application of recAPPsα on acute slices of littermate control mice led to a significantly enhanced posttetanic potentiation (PTP) and a trend of an increased LTP compared to slices treated with the boiled peptide (see Figure 3.17). This is in line with the observation that APPsα acts on early stages of LTP induction like PTP (Ishida et al., 1997). Moreover, Taylor and colleagues showed a reduced tetanically evoked NMDAR current when an antibody against APPsα or an α-secretase inhibitor were applied. In a rescue of function experiment the co-application of an α-secretase inhibitor and additional recAPPsα restored the reduced LTP back to control level (Taylor et al., 2008). To distinguish acute effects of APP / APLP2 double knock-out from developmental effects, I implemented a comparable rescue of function experiment. The exogenous application of recAPPsα would only restore the previously observed LTP defect in NexCre cDKO mice if changes in the expression of APP or APLP2 are acutely necessary for synaptic function and modulation. Contrary, if the DKO of both proteins exerts its effects by developmental deficits, no rescue should be possible. Indeed, an application of 10 nM recAPPsα 1 h prior and during the entire experiment fully restored the LTP and short-term plasticity impairment (see Figure 3.11). These findings establish an endogenous role of APPsα for the acute modulation of synaptic properties on a fast time scale. This is corroborated by a reduced PSD95 level and a decreased mushroom type spine number (Hick et al., 2015).

Intriguingly, I found that the application of recAPPsα sufficiently restored the LTP defect in NexCre cDKO while recAPPsβ did not (see Figure 3.16, (Hick et al., 2015). This strongly implicates that the motif which is crucial to promote LTP is localized within the 17 amino acids of difference between APPsα and APPβ or that these are responsible for a confirmation that makes APPsβ less effective. This is supported by the fact that APPsβ was shown to be 100 x less potent in protecting hippocampal neurons against excitotoxicity compared to APPsα (Furukawa et al., 1996). Within this sequence difference a heparin-binding domain is localized which was suggested to influence the effectiveness (Furukawa et al., 1996). The emerging role of these 17 amino acids was further supported by an APPsβ-DM mouse line (*APPsβ*$^{+/+}$ *APLP2*$^{-/-}$) which was

not viable still showing severe neuromuscular defects compared to an APPsα-DM (*APPsα*$^{+/+}$ *APLP2*$^{-/-}$) which was fully viable but still as well shows neuromuscular deficits (Li et al., 2010; Weyer et al., 2011).

Furthermore, auto-regulatory mechanisms have been discovered whereby APPsα was capable to reduce the β-secretase activity and therefore decrease the APPsβ generation but simultaneously stimulate the α-secretase processing of APP (Obregon et al., 2012). However, the precise mechanism how APPsα exerts its neurotrophic as well as protective function and regulates neuronal excitability is unknown. The literature for the identification of its receptor is diffuse and often contradictory. APP itself has been proposed to be the receptor for APPsα since it was shown to disrupt APP dimers (Gralle et al., 2009). This needs to be queried with regard to the recAPPsα rescue results of NexCre cDKO mice since no APP is available in these individuals (Hick et al., 2015). Processes of learning and memory might be modulated by activating an unknown cell surface receptor that modulates the activity of potassium channels and also activates the transcription factor NF-κB (Barger and Mattson, 1996; Guo et al., 1998; Ryan et al., 2013). Furthermore, p75 receptor and APPsα as well as APPsβ were co-immunoprecipitated but only APPsα revealed neurotrophic properties in promoting neurite outgrowth (Hasebe et al., 2013). A recent study proposed the existence of a high-affinity receptor which binds APPsα by an interaction with its E1 domain promoting the function as a heparin-binding growth factor (Reinhard et al., 2013). However, the molecular link between the observed rescue ability of APPsα in case of activity-dependent synaptic plasticity in the NexCre cDKOs still remains elusive and thus precludes a definitive mechanistic explanation how it promotes this effect. Nevertheless, although the receptor in that case is unidentified one might speculate that via this unknown receptor the intracellular Ca^{2+} dynamics and release from internal stores is controlled and triggered. This is supported by my finding that a viral expression of APPsα in NexCre cDKO dissociated hippocampal cultures restored the observed defect in Ca^{2+} dynamics before and upon chemically induced LTP by glycine administration (see Figure 3.8 and Figure 3.10).

Numerous studies, including my results, implicated that APP exerts its physiological functions rather by the secreted APPsα than the APPsβ fragment. Tyan and colleagues recently showed that APPsα but not APPsβ partially rescued defects in dendritic spine number and morphology of primary hippocampal neurons from APP-KO mice (Tyan et al., 2012). Additionally, this

peptide restored an *in vivo* LTP defect, induced by inhibiting the α-secretase, back to control values. Notably, Taylor and colleagues showed a dose-dependency for the function of APPsα. The concentration applied to the hippocampus for LTP facilitation was 11 nM, comparable to such I used for the NexCre cDKO LTP rescue, while a much higher dose of 3300 nM acted contrariwise in decreasing the LTP compared to controls (Taylor et al., 2008). However, these high concentrations might cause side effects by peptide aggregation or the amount of peptides is toxic due to unphysiological levels. A comparable concentration of 10 nM APPsα was shown to upregulate the *de novo* protein synthesis of synaptic proteins implicating that this might contribute to long-lasting effects in synaptic plasticity (Claasen et al., 2009). In line with my observations that contrary to APPsα the application of APPsβ failed to restore the LTP defect of NexCre cDKOs, no significant increase in synaptic protein expression was observed when 10 nM APPsβ were applied (Claasen et al., 2009). Whereas, APPsα was shown to modulate the gene expression via activation of plasticity related transcription factors CREB and NF-κB (Claasen et al., 2009; Ryan et al., 2013). Notably, I decided to use a concentration of 50 nM recAPPsβ to consider the fact that this peptide was shown to be less potent than recAPPsα (Furukawa et al., 1996). Another approach to, indirectly increase the APPsα level was carried out by an overexpression of its producing α-secretase which finally led to a LTP rescue of the defect in these AD mouse mutant as well (Postina et al., 2004). Interestingly, a recent publication reported that LTP decreases ADAM10 surface levels by clathrin mediated endocytosis leading to a reduced overall ADAM10 activity whereas contrariwise the opposite was observed during LTD (Musardo et al., 2013). This is in clear contrast to findings from Postina and colleagues. Nevertheless, an overexpression does not represent the physiological state by which opposing results might be explained.

The beforehand described setup for LTP rescue experiments require large amounts of recAPPsα and β whose generation is relatively time consuming. Therefore, currently NexCre cDKO mice are established which express APPsα that is virally applied into the hippocampus. This enables to directly establish stable levels of APPsα *in vivo*. Furthermore, this allows testing whether a potential rescue is also observed at morphological and functional level like learning behavior or synaptic plasticity. This is promising since APPsα has been shown to increases synaptic density and improve memory retention when recAPPsα was infused into the brain (Roch et al., 1994;

Meziane et al., 1998; Taylor et al., 2008). A further support is given by the finding that the expression of APPsα in APP-KO mice restores the defect in spine density as well as spine subtype distribution (Weyer et al., 2014).

4.2.2 The Application of recAPPsα Further Increases Synaptic Strength: a Therapeutic Benefit

The intriguing observation that recAPPsα but not recAPPsβ is capable to restore the impaired LTP in NexCre cDKO mice provides an emerging potential in consideration of therapeutic strategies in Alzheimer's disease (AD). Therefore, the secretases which are involved in full length APP processing are of particular interest. The formation of toxic Aβ oligomers and plaques has been established to highly contribute to the cognitive decline in AD (Schaeffer et al., 2011). Additionally, the reduction of α-secretase cleavage might foster AD pathogenesis, potentially by increasing Aβ levels and decreasing the neuroprotective APPsα.

Loss-of-function mutations in the pro-domain of the α-secretase ADAM10 were discovered in families with late onset forms of AD leading to an APPsα reduction and Aβ raise (Kim et al., 2009). Consistently, the mutation within the ADAM10 gene led to an attenuated ADAM10 activity and as a result less APPsα was secreted but more β-secretase cleavage occurred (Suh et al., 2013). Furthermore, an impaired ADAM10 delivery to cell membranes in AD patients was shown (Musardo et al., 2013). In line, some, but not all studies analyzing APPsα levels in cerebrospinal fluid reported a reduction in AD versus control patients (Sennvik et al., 2000; Olsson et al., 2003; Fellgiebel et al., 2009). Low APPsα levels were also correlated with poor spatial memory performance in rats and humans (Almkvist et al., 1997; Anderson et al., 1999). Strikingly, the overexpression of APPsα in the hippocampus of old AD model mice restored the beforehand established LTP defect. This implicates that an APPsα expression in mice which already reveal an Aβ deposition still has the potential to ameliorate neurotoxic effects (Postina et al., 2004), data presented at the neuroscience 2014, M. F. Yahaya, University of Otago, New Zealand, poster ID 405.06/D53).

With respect to AD, the alterations of plasticity in APP deficient and APPsα-DM mice suggest that increasing α-secretase activity or the infusion of APPsα could be a promising therapeutic strategy (Kojro et al., 2001; Fahrenholz and Postina, 2006; McConlogue et al., 2007; Lichtenthaler, 2012). Vice versa a reduction of β-secretase BACE1 activity would be a further

potential target for an effective therapy or even prevention of AD since this enzyme selectively cleaves APP in the initial step of the amyloidogenic pathway (McConlogue et al., 2007; De Strooper et al., 2010). However, the establishment of suitable drugs that can be applied in humans remains challenging because besides the processing of APP those secretases are shown to be involved in various other biological processes. Their inhibition might cause undesired toxic side effects. Furthermore, the full length APP is processed by different α-secretases whose exact role in that process is still debated. Therefore, a direct and specific activation might be difficult. However, the inhibitor applied in this study to selectively inhibit the ADAM10 α-secretase activity was shown to be highly specific (Andrews et al., 2000; Hoettecke et al., 2010; Weyer et al., 2011). Another issue is the application of the compound since it needs to cross the blood-brain-barrier. Moreover, it needs to be considered that in the healthy brain APP processing follows a tight balance in which also low amounts of Aβ are crucial for a proper neuronal functionality and memory formation (Puzzo et al., 2008; Abramov et al., 2009; Puzzo et al., 2011). Alternatively, downstream targets like PKC, MAPK, tyrosine kinases or Ca^{2+} mediated pathways could be modulated by selective drugs (De Strooper et al., 2010). Collectively, the development of specific compounds for the beforehand described targets provides a high potential as a promising therapeutic strategy for this devastating disease.

4.2.3 An APP and APLP2 Deficiency Leads to an Impaired Ca^{2+} Dynamic Before and Upon Chemically Induced LTP

The pathological shift from the non amyloidogenic to more amyloidogenic processing of the full length APP also affects the neuronal Ca^{2+} homeostasis which is a prerequisite for a regulated neuronal excitability and synaptic plasticity. Many publications report an elevated intracellular Ca^{2+} concentration when, in case of Alzheimer's disease, Aβ accumulates extracellularly (LaFerla, 2002; Bezprozvanny and Mattson, 2008; Kuchibhotla et al., 2008; Lopez et al., 2008). This elevation arises from pores within the cell membrane formed by Aβ and an increased conductance of specific Ca^{2+} channels. Additionally, Aβ oligomers stimulate the release of Ca^{2+} from the ER through mGluR activation or increased IP3 production (Arispe et al., 1993; Renner et al., 2010; Demuro and Parker, 2013). This unphysiological Ca^{2+} amount has several functional consequences such as the modification of the cytoskeleton, induction of apoptosis and

disruption of spine-dendritic Ca^{2+} compartmentalization (Mattson et al., 1991; Kuchibhotla et al., 2008). The latter was shown to be crucial for neuronal signaling and synaptic communication (Yuste et al., 2000; Araya et al., 2006). All of these observations open the possibility of an important role of APP for a physiological Ca^{2+} homeostasis.

The relationship between APP, its cleavage products and Ca^{2+} is multifaceted and can be analyzed in a bidirectional manner. First, the question is raised in which way APP is involved in Ca^{2+} signaling and vice versa how Ca^{2+} dependent pathways influence APP processing. The analysis of NexCre cDKO primary hippocampal cultures revealed an impaired Ca^{2+} dynamic before and upon chemically induced LTP by glycine which might at least in part contribute to the impaired synaptic plasticity assessed by electrophysiological techniques (see Figure 3.8 A and B). These results point towards an important function of the APP-protein family in terms of Ca^{2+} dynamics. Consistently, APP-KO fibroblasts revealed a decreased Ca^{2+} release from internal stores. Comparable results were obtained when wt fibroblasts were treated with γ-secretase inhibitor indicating a crucial function of the intracellular AICD fragment and γ-secretase activity for Ca^{2+} dynamics. This was corroborated by the finding that an expression of the AICD fragment in APP-KO fibroblasts restored this defect (Leissring et al., 2002). Since the AICD fragment acts as a direct or indirect transcription factor (see 4.1.4) it modulates the gene expression (Jacobsen et al., 2006; Pardossi-Piquard and Checler, 2012). The importance of the internal APP C-terminal region, more precisely the final 15 amino acids, was also shown in this thesis by the analysis of APPΔCT15 DM mice (see Figure 3.2) which revealed an impaired activity dependent synaptic plasticity (Klevanski et al., in preparation). Thus, a disturbed Ca^{2+} dynamic is conceivable leading to the observed defect (Hamid et al., 2007). Interestingly, studies on a mouse model of murine trisomy revealed higher intracellular Ca^{2+} concentrations (Cardenas et al., 2002). This mouse line carries the APP gene on chromosome 16. As three of them exist, a specific gene dosage effect is observed. In line with the finding that hippocampal cultures from NexCre cDKO mice exhibited a significantly decreased Ca^{2+} response already before cLTP induction (see Figure 3.8 A and B), cells from mice with trisomy in which the APP expression was knocked down to 40 % showed a comparable defect (Rojas et al., 2008).

The question how elevated Ca^{2+} levels itself affect the APP processing is far less intensely studied than the opposing situation described beforehand. It was suggested that a high cytosolic

Ca^{2+} level further enhances amyloidogenic APP cleavage resulting in more Aβ generation (Querfurth and Selkoe, 1994). Mechanistically, high cytosolic Ca^{2+} amounts lead to a transient phosphorylation of APP which shifts to more Aβ production (Pierrot et al., 2006). However, these findings are debated. Buxbaum and colleagues showed that the inhibition of the sarco / endoplasmic reticulum calcium-ATPase (SERCA) decreased Aβ generation (Buxbaum et al., 1994).

To chemically induce LTP glycine stimulation was used which is in many aspects comparable to TBS induced LTP (Shahi et al., 1993). High concentrations of glycine induced long-lasting changes in synaptic efficacy in rat hippocampal slices (Shahi et al., 1993). Since in the present study hippocampal dissociated neuronal cultures which display a different network were used, a stable Ca^{2+} increase especially for later time points analyzed was unlikely. Indeed, in every result presented, t40 always revealed much lower Ca^{2+} concentrations irrespective of the genotype (see Figure 3.8). An explanation might be that hippocampal cultures lack the modulatory dopaminergic and cholinergic input. Furthermore, not all synapses are innervated which might as well clarify why these cultures could not be potentiated as strong and stable as expected. Moreover, these cultures do not represent the neuronal network which is found *in vivo*. Alternatively, OHCs could overcome this issue.

Maybe, the cultures used could not react with an enlargement of PSD upon stimulation because the induction was not strong enough to stimulate the required processes. At resting conditions cytosolic Ca^{2+} concentrations usually range between 50-300 nM which increases to several mM when neurons are activated (LaFerla, 2002). For the unstimulated condition the littermate control cultures reached 50 nM (see Figure 3.8). Also the increase upon cLTP induction was not as strong as expected. Therefore, it might be necessary to apply an optimized protocol. A pre-conditioning of the cultures with APV was shown to activate more NMDAR and thus increase the synchronous network activity (Molnar, 2011). Maybe without APV exposure the induction was not sufficient enough to trigger changes in protein expression which are crucial for long-lasting changes.

In conclusion, the lower Ca^{2+} response in NexCre cDKO cultures may indicate a lower bursting activity which might originate from an immature network (see Figure 3.8). As already shown by Hick and colleagues NexCre cDKO neurons exhibited a decreased spine number including a shift

from mature mushroom towards more immature stubby spines which was accompanied by a reduced PSD95 level (Hick et al., 2015). Fewer spine numbers which are less mature are correlated to a decreased synaptic activity accompanied by a reduced Ca^{2+} response. Nevertheless, in relation to the resting activity also NexCre cDKO cultures respond equally in comparison to littermate control cultures (see Figure 3.9) showing that although they have fewer spines those which are activated can be comparably potentiated. However, in addition to these morphological defects the impaired Ca^{2+} dynamics might be caused by affected internal stores or Ca^{2+} channels.

4.2.4 The Defect in Ca^{2+} Dynamics of NexCre cDKO Mice is Partially Based on an Impaired ER Function

To gain a mechanistic insight into the defect of Ca^{2+} dynamics in NexCre cDKO I co-applied glycine and specific inhibitors for distinct Ca^{2+} resources (see Figure 3.8 and Figure 3.10). Endogenous glycine receptors were always blocked by strychnine. First, I inhibited ionotropic NMDA receptors by a 2-amino-5-phosphonopentanoic acid (APV) application (see (see Figure 3.8 C and D, Figure 3.10 C and D). This way a cLTP induction was completely abolished similarly in both littermate control and NexCre cDKO cultures suggesting that NMDARs are the crucial and main component for Ca^{2+} increase permitting the potentiation via glycine stimulation.

Second, I co-applied glycine and cyclopiazoic acid (CPA) which selectively blocked the sarco / endoplasmic reticulum calcium-ATPase (SERCA) which promotes the reuptake of Ca^{2+} back into the ER (see Figure 3.8 E and F, Figure 3.10 E and F). The cLTP induction led to no significant increase in littermate control cultures showing that the reuptake is essential for Ca^{2+} oscillations in the intact CNS. Interestingly, the lack of APP in NexCre cDKO cultures seems to influence this process since a highly significant Ca^{2+} increase was found upon glycine application although the SERCA was inhibited by CPA. The values obtained for NexCre cDKO cultures directly after cLTP induction were much higher under glycine and CPA compared to only glycine treatment (see Figure 3.8 A,B,E,F). Furthermore, the analysis of the relative Ca^{2+} amount was exclusively significantly increased under glycine and CPA conditions (see Figure 3.9 C). The application of CPA resulted in no significant decrease in the frequency upon co-treatment with glycine in both genotypes irrespective if separately littermate controls and NexCre cDKOs (see Figure 3.10 E) or

imaging time-points were analyzed (see Figure 3.10 F). However, it is conspicuous that the comparison of data obtained from NexCre cDKO by measuring the Ca^{2+} concentration (see Figure 3.8 E) and the frequency (see Figure 3.10 E) uncovered an inverse correlation. Upon co-application of glycine and CPA, the amount of cytoplasmatic Ca^{2+} increased for t0, but then decreased continuously at t10 and t40 (seeFigure 3.8 E). The opposite was observed in terms of the frequency. Here upon glycine and CPA treatment an initial decrease of spikes / min was detected which then constantly increased during imaging 10 and 30 min later (see Figure 3.10 E). Reasons for this could be multifaceted: It may be speculated that in glycine treatment alone the SERCA might be very efficient in transporting the Ca^{2+} back to the ER, reflected by lower cytoplasmatic Ca^{2+}. Another suggestion might be that Ca^{2+} buffer proteins are affected e.g. by less functional or lower amounts. Since less Ca^{2+} may be bound to buffer proteins, more is taken up into the ER. If this hypothesis holds true specific buffer proteins could be tested regarding their expression levels by western blot analysis in future experiments. These ideas were further supported by the results for later time-points in NexCre cDKO cultures as due to the blockade of SERCA no longer Ca^{2+} could be transported back into the ER. Reflected by apparently decreasing values no stable increase of Ca^{2+} upon co-application of glycine and CPA was possible in NexCre cDKOs (see Figure 3.8 E).

Third, I inhibited L-type voltage gated calcium channels (VGCCs) via Nifedipine application (see Figure 3.8 G and H, Figure 3.10 G and H). The blockade prevented a significant cLTP induction in both littermate controls and NexCre cDKO, respectively. However, although no difference was observed when Nifedipine and glycine were co-applied the cLTP impairment in NexCre cDKO cultures under only glycine conditions could be explained by a relation of APP and L-type VGCCs in excitatory and inhibitory neurons. The acute expression of human APP in cortical neurons was reported to increase the L-type VGCC mediated Ca^{2+} currents which is consistent with my observation that a lack of APP and APLP2 decreased the Ca^{2+} response upon glycine application (Santos et al., 2009). Cortical neurons form networks in which oscillation processes are required for long-term consolidation of memory (Buzsaki and Draguhn, 2004). Primary cortical cultures also form such networks in which glutamatergic input leads to spontaneous synchronous Ca^{2+} oscillations. Interestingly, an overexpression of APP prevented these oscillations. Mechanistically, it is proposed that APP overexpression enhanced the L-type VGCC activity. The

following Ca^{2+} influx stimulates K^{+} channels which are responsible for the medium afterhyperpolarization which in turn decreases the excitability of APP overexpressing cells and finally leads to the inhibition of Ca^{2+} oscillations. Vice versa the knock-down of endogenous APP increased the frequency but simultaneously decreased the amplitude of these oscillations which was in line with my findings because NexCre cDKO cultures exhibited decreased Ca^{2+} amplitudes before and upon cLTP induction (Santos et al., 2009; Octave et al., 2013). Consistently, an upregulation of presynaptic L-type VGCC in GABAeric neurons was found which was accompanied by an impaired short-term plasticity in APP-KO striatal neurons (Yang et al., 2009). Collectively and in line with observation from Santos and colleagues a crucial function of APP for maintenance of neuronal Ca^{2+} dynamics can be stated. Furthermore, a loss of APP and APLP2 affects the ER function. Consequently, this might also be an explanation for the observed defects in activity-dependent synaptic plasticity since such Ca^{2+} homeostasis is important for synaptic transmission (Zucker, 1999; Rochefort and Konnerth, 2012; Octave et al., 2013; Brini et al., 2014). Nevertheless, to clarify the exact mechanisms how a loss of APP and APLP2 is connected to disturbed Ca^{2+} dynamics needs to be applied.

4.2.5 APPsα is Capable to Restore the Impaired Ca^{2+} Dynamics of NexCre cDKO Mice

Another APP processing product, APPsα, exhibits its neuroprotective properties in case of excitotoxicity by attenuating the Ca^{2+} response (Mattson et al., 1992; Mattson et al., 1993). In line with this APPsα was shown to stabilize the Ca^{2+} homeostasis via a mechanism which includes NF-κB activation in PC12 cells with a mutated Presenilin-1 gene thereby preventing apoptosis (Guo et al., 1998; Ryan et al., 2013). Interestingly, a modulation of NF-κB through TNF signaling was shown to regulate neuronal excitability and hippocampal synaptic plasticity (Albensi and Mattson, 2000). These observations might at least in part contribute to the rescue I showed for dissociated hippocampal cultures from NexCre cDKO embryos in which a viral expression of APPsα restored the observed defect in Ca^{2+} amounts before as well as upon cLTP induction by glycine application (see Figure 3.12 and Figure 3.14). The action of APPsα on the amount of intracellular Ca^{2+} is discussed controversially. On the one hand it was shown to lower the resting Ca^{2+} concentration and inhibit the Ca^{2+} increase induced by glutamate application in hippocampal cultures (Mattson, 1994; Furukawa et al., 1996). However, it was also reported

that besides this inhibitory function APPsα also was found to increase the intracellular Ca^{2+} amount via IP3-dependent mechanisms. Notably, this effect was only observed in 1-2 days cultured neurons. It successively disappeared with days *in vitro* indicating a functional role of APPsα during development (Koizumi et al., 1998). It might be speculated that the impaired LTP in NexCre cDKO and DlxCre cDKO (see Figure 3.6 and Figure 3.21) as well as the impaired Ca^{2+} dynamics in NexCre cDKO hippocampal cultures (see Figure 3.8 A and B) might arise from the lack of APPsα during synaptogenesis. This is consistent with the finding that a viral expression of APPsα restores the defect in the Ca^{2+} dynamics. However, the observation that an application of recAPPsα is sufficient to restore the LTP points towards two separate functions one during development the other as an acute mediator for activity-dependent synaptic plasticity.

4.3 Conclusions and Outlook

In this thesis, I could show an emerging physiological role of APP and APLP2. This role was further specified for brain development presumably during synapse and neuronal network formation as well as acutely at active synapses during LTP in the mature brain. For an intact neuronal function an excitation-inhibition balance is required. Since I could show a defect in activity-dependent synaptic plasticity when APP and APLP2 are knocked out in either excitatory or inhibitory neurons this balance likely is impaired. In these mice APP and APLP2 were still expressed in astrocytes and the respective neuronal subtype which was not targeted. In future experiments a ubiquitous postnatal ablation of both proteins throughout all neurons would be feasible by using the CAG-deleter line. This provides the possibility to investigate a full DKO situation which might increase the defect observed before.

I could again successfully reproduce the previously described age-related loss of compensatory functions of APLP2 in aged APP-KO mice while APP was still capable to restore the loss in aged APLP2-KO individuals. A possible explanation for this might be a reduction of APLP2 expression in aged individuals. This should be tested by Western Blot.

One important finding during my investigations was that recombinant APPsα fully restored the previously observed impaired activity-dependent synaptic plasticity in NexCre cDKO acute slices back to control levels. This emphasizes its necessity for a proper neuronal function and memory formation. However, to obtain stable levels a viral delivery of APPsα *in vivo* via hippocampal stereotactic injection could be performed. This ensures a re-introduction of APPsα into the NexCre cDKO mice and thus enables the experimenter to perform gain of function and rescue experiments. This would then be not only restricted to electrophysiological recording but these mice could also be analyzed regarding neuronal morphology and learning behavior which was shown to be significantly impaired in NexCre cDKO mice. Furthermore, this viral approach could be a useful tool to accomplish acute loss of function studies in adult mice by a delivery of the Cre-recombinase in floxed individuals.

The LTP defect observed in NexCre cDKO mice is tightly linked to a perturbed Ca^{2+} dynamic as implicated by my observations. One of the beforehand mentioned hypothesis stated that the Ca^{2+} buffer protein expression is lower compared to controls and the surplus of unbound Ca^{2+} is

transported into the endoplasmatic reticulum. This could be proven by Western Blot analysis for concentrations of candidate proteins like calbindin, calretinin, parvalbumin and calmodulin.

I could furthermore demonstrate that in contrast to recAPPsα the application of recAPPsβ was not capable to restore the LTP defect of NexCre cDKOs emphasizing the importance of the 17 amino acids of difference. To investigate whether comparable to this electrophysiology study also APPsβ is ineffective to restore the Ca^{2+} concentration before and upon cLTP induction APPsβ could be applied by AAV.

Since a viral delivery of APPsα was sufficient to restore the impaired Ca^{2+} dynamics it might be interesting to see whether this also restores the impaired spine morphology. Therefore, mApple or mCherry transfected cultures enable to perform Ca^{2+} imaging at the spine level paralleled by analyzing morphological changes.

As already noted in the discussion the imaging time point t40 always revealed decreased Ca^{2+} amount irrespective of genotype. One explanation is that the missing modulatory input might be responsible but also an insufficient NMDAR activation might be accountable for that. Therefore, the modification of the protocol for instance by preconditioning of cultures with APV might be an option. Alternatively to hippocampal dissociated cultures the quantitative Ca^{2+} imaging might be established in organotypic hippocampal cultures which have the advantage of an intact neuronal network comparable to the *in vivo* situation.

List of Abbreviations

AAV	Adeno-associated virus
AC	Adenylyl cyclase
ACFS	Artificial cerebrospinal fluid
AD	Alzheimer's disease
ADAM	A disintegrin and metalloproteinase
AICD	APP intracellular domain
AM	Acetoxymethyl
AMPAR	α-amino-3-hydroxy-5-methyl-4-isoxazole-propionic receptor
aPKC	Atypical protein kinase C
APLP	Amyloid precursor protein-like protein
APP	Amyloid precursor protein
APPsα or **sAPPα**	secreted Amyloid precursor protein ectodomain after α-secretase cleavage
APPsβ or **sAPPβ**	secreted Amyloid precursor protein ectodomain after β-secretase cleavage
APV	2-amino-5-phosphonopentanoic acid
BACE	β-site APP cleaving enzyme
BDNF	Brain-derived nerve neurotrophic
CA	Cornu ammonis (hippocampal subfields)
CaMKII	Calcium / calmodulin-dependent kinase II
cDKO	Conditional double knock-out
cKO	Conditional knock-out
cLTP	chemically induced long-term potentiation
CNS	Central nervous system
CPA	Cyclo piazoic acid
CREB	cAMP response element-binding protein
DG	Dentate gyrus
DIV	Days *in vitro*
DKO	Double knock-out
DM	Double mutant
DMSO	Dimethyl sulfoxide
EC	Entorhinal cortex
(f)EPSP	(Field) excitatory postsynaptic potential
ER	endoplasmatic reticulum
FV	Fiber volley
GABA	γ-aminobutyric acid
GAD	glutamate decarboxylase

IO	Input-output
IP3R	Inositol-1, 4, 5-tris-phosphate receptor
ISI	Inter-stimulus interval
KI	Knock-in
KO	Knock-out
LFS	Low-frequency stimulation
L-LTP	Late-long-term potentiation
LTD	Long-term depression
LTP	Long-term potentiation
mEPSC	miniature excitatory postsynaptic potential
Nex	neuronal helix-loop-helix protein 1
NFT	Neurofibrillary tangles
NF-κB	nuclear factor kappa-light-chain-enhancer of activated B cells
NGF	Nerve growth factor
NMDAR	N-methyl-D-aspartate receptor
NO	Nitric oxide
n.s.	Not significant
OHC	Organotypic hippocampal culture
p75NTR	Pan neurotrophin receptor 75
P	postnatal day
PPD	Paired pulse depression
PPF	Paired pulse facilitation
PSD	Postsynaptic density
PSEN	Presenilin
PTP	Post-tetanic potentiation
PKA	Protein kinase A
rec	recombinant
ROI	Region of interest
RRP	Readily releasable pool
RT	Room temperature
RyR	Ryanodine receptor
SEM	Standard error of the mean
SERCA	sarco / endoplasmic reticulum calcium-ATPase
TBS	Theta-burst stimulation
TNF	Tumor necrosis factor
TrkA	Tropomyosin receptor kinase A
Tyr	Tyrosin
VGCC	Voltage gated calcium channel
wt	Wildtype

List of Figures

List of Tables

References

Ables JL, Breunig JJ, Eisch AJ, Rakic P (2011) Not(ch) just development: Notch signalling in the adult brain. Nat Rev Neurosci 12:269-283.

Abraham WC, Williams JM (2008) LTP maintenance and its protein synthesis-dependence. Neurobiol Learn Mem 89:260-268.

Abramov E, Dolev I, Fogel H, Ciccotosto GD, Ruff E, Slutsky I (2009) Amyloid-beta as a positive endogenous regulator of release probability at hippocampal synapses. Nat Neurosci 12:1567-1576.

Akaaboune M, Allinquant B, Farza H, Roy K, Magoul R, Fiszman M, Festoff BW, Hantai D (2000) Developmental regulation of amyloid precursor protein at the neuromuscular junction in mouse skeletal muscle. Mol Cell Neurosci 15:355-367.

Albensi BC, Mattson MP (2000) Evidence for the involvement of TNF and NF-kappaB in hippocampal synaptic plasticity. Synapse 35:151-159.

Albensi BC, Oliver DR, Toupin J, Odero G (2007) Electrical stimulation protocols for hippocampal synaptic plasticity and neuronal hyper-excitability: are they effective or relevant? Exp Neurol 204:1-13.

Allinson TM, Parkin ET, Turner AJ, Hooper NM (2003) ADAMs family members as amyloid precursor protein alpha-secretases. JNeurosciRes 74:342-352.

Almeida CG, Tampellini D, Takahashi RH, Greengard P, Lin MT, Snyder EM, Gouras GK (2005) Beta-amyloid accumulation in APP mutant neurons reduces PSD-95 and GluR1 in synapses. NeurobiolDis 20:187-198.

Almkvist O, Basun H, Wagner SL, Rowe BA, Wahlund LO, Lannfelt L (1997) Cerebrospinal fluid levels of alpha-secretase-cleaved soluble amyloid precursor protein mirror cognition in a Swedish family with Alzheimer disease and a gene mutation. ArchNeurol 54:641-644.

Alzheimer A (1907) Über eine eigenartige Erkrankung der Hirnrinde. Vortrag in der Versammlung Südwestdeutscher Irrenärzte in Tübingen am 3. November 1906. Allgemeine Zeitschrift für Psychiatrie und psychisch-gerichtliche Medizin 64:146-148.

Anderson JJ, Holtz G, Baskin PP, Wang R, Mazzarelli L, Wagner SL, Menzaghi F (1999) Reduced cerebrospinal fluid levels of alpha-secretase-cleaved amyloid precursor protein in aged rats: correlation with spatial memory deficits. Neuroscience 93:1409-1420.

Andrews RC, Andersen MW, Cowan DJ, Deaton DN, Dickerson SH, Drewry DH, Gaul MD, Lussio MJ, Marron BE, Rabinowitz MH (2000) Preparation of peptidyl formamide compounds as therapeutic agents. In.

Araya R, Eisenthal KB, Yuste R (2006) Dendritic spines linearize the summation of excitatory potentials. Proc Natl Acad Sci U S A 103:18799-18804.

Arispe N, Rojas E, Pollard HB (1993) Alzheimer disease amyloid beta protein forms calcium channels in bilayer membranes: blockade by tromethamine and aluminum. Proc Natl Acad Sci U S A 90:567-571.

Aydin D, Weyer SW, Muller UC (2012) Functions of the APP gene family in the nervous system: insights from mouse models. ExpBrain Res 217:423-434.

Bai Y, Markham K, Chen F, Weerasekera R, Watts J, Horne P, Wakutani Y, Bagshaw R, Mathews PM, Fraser PE, Westaway D, St George-Hyslop P, Schmitt-Ulms G (2008) The in vivo brain interactome of the amyloid precursor protein. MolCell Proteomics 7:15-34.

Baratchi S, Evans J, Tate WP, Abraham WC, Connor B (2012) Secreted amyloid precursor proteins promote proliferation and glial differentiation of adult hippocampal neural progenitor cells. Hippocampus 22:1517-1527.

Barbagallo AP, Wang Z, Zheng H, D'Adamio L (2011a) The intracellular threonine of amyloid precursor protein that is essential for docking of Pin1 is dispensable for developmental function. PLoS One 6:e18006.

Barbagallo AP, Wang Z, Zheng H, D'Adamio L (2011b) A single tyrosine residue in the amyloid precursor protein intracellular domain is essential for developmental function. J Biol Chem 286:8717-8721.

Barbagallo AP, Weldon R, Tamayev R, Zhou D, Giliberto L, Foreman O, D'Adamio L (2010) Tyr(682) in the intracellular domain of APP regulates amyloidogenic APP processing in vivo. PLoS One 5:e15503.

Barger SW, Mattson MP (1996) Induction of neuroprotective kappa B-dependent transcription by secreted forms of the Alzheimer's beta-amyloid precursor. Brain Res Mol Brain Res 40:116-126.

Beattie EC, Carroll RC, Yu X, Morishita W, Yasuda H, von Zastrow M, Malenka RC (2000) Regulation of AMPA receptor endocytosis by a signaling mechanism shared with LTD. Nat Neurosci 3:1291-1300.

Beher D, Hesse L, Masters CL, Multhaup G (1996) Regulation of amyloid protein precursor (APP) binding to collagen and mapping of the binding sites on APP and collagen type I. J Biol Chem 271:1613-1620.

Bellot A, Guivernau B, Tajes M, Bosch-Morato M, Valls-Comamala V, Munoz FJ (2014) The structure and function of actin cytoskeleton in mature glutamatergic dendritic spines. Brain Res 1573:1-16.

Bendotti C, Forloni GL, Morgan RA, O'Hara BF, Oster-Granite ML, Reeves RH, Gearhart JD, Coyle JT (1988) Neuroanatomical localization and quantification of amyloid precursor protein mRNA by in situ hybridization in the brains of normal, aneuploid, and lesioned mice. Proc Natl Acad Sci U S A 85:3628-3632.

Beyreuther K, Masters CL (1991) Amyloid precursor protein (APP) and beta A4 amyloid in the etiology of Alzheimer's disease: precursor-product relationships in the derangement of neuronal function. Brain Pathol 1:241-251.

Bezprozvanny I, Mattson MP (2008) Neuronal calcium mishandling and the pathogenesis of Alzheimer's disease. Trends Neurosci 31:454-463.

Bland BH (1986) The physiology and pharmacology of hippocampal formation theta rhythms. ProgNeurobiol 26:1-54.

Bliss TV, Gardner-Medwin AR (1973) Long-lasting potentiation of synaptic transmission in the dentate area of the unanaestetized rabbit following stimulation of the perforant path. J Physiol 232:357-374.

Bliss TV, Lomo T (1973) Long-lasting potentiation of synaptic transmission in the dentate area of the anaesthetized rabbit following stimulation of the perforant path. JPhysiol 232:331-356.

Bliss TV, Collingridge GL (1993) A synaptic model of memory: long-term potentiation in the hippocampus. Nature 361:31-39.

Bosch M, Hayashi Y (2012) Structural plasticity of dendritic spines. Curr Opin Neurobiol 22:383-388.

Braak H, Braak E (1991) Neuropathological stageing of Alzheimer-related changes. Acta Neuropathol 82:239-259.

Brini M, Cali T, Ottolini D, Carafoli E (2014) Neuronal calcium signaling: function and dysfunction. Cell Mol Life Sci 71:2787-2814.

Burke SN, Barnes CA (2006) Neural plasticity in the ageing brain. Nat Rev Neurosci 7:30-40.

Buxbaum JD, Koo EH, Greengard P (1993) Protein phosphorylation inhibits production of Alzheimer amyloid beta/A4 peptide. ProcNatlAcadSciUSA 90:9195-9198.

Buxbaum JD, Ruefli AA, Parker CA, Cypess AM, Greengard P (1994) Calcium regulates processing of the Alzheimer amyloid protein precursor in a protein kinase C-independent manner. Proc Natl Acad Sci U S A 91:4489-4493.

Buxbaum JD, Liu KN, Luo Y, Slack JL, Stocking KL, Peschon JJ, Johnson RS, Castner BJ, Cerretti DP, Black RA (1998) Evidence that tumor necrosis factor alpha converting enzyme is involved

in regulated alpha-secretase cleavage of the Alzheimer amyloid protein precursor. JBiolChem 273:27765-27767.

Buzsaki G (2002) Theta oscillations in the hippocampus. Neuron 33:325-340.

Buzsaki G, Draguhn A (2004) Neuronal oscillations in cortical networks. Science 304:1926-1929.

Cai H, Wang Y, McCarthy D, Wen H, Borchelt DR, Price DL, Wong PC (2001) BACE1 is the major beta-secretase for generation of Abeta peptides by neurons. Nat Neurosci 4:233-234.

Cajal RSy (1907) Die histogenetischen Beweise der Neuronentheorie von His und Forel. Anatomischer Anzeiger 30:113-144.

Cao X, Sudhof TC (2001) A transcriptionally [correction of transcriptively] active complex of APP with Fe65 and histone acetyltransferase Tip60. Science 293:115-120.

Cardenas AM, Allen DD, Arriagada C, Olivares A, Bennett LB, Caviedes R, Dagnino-Subiabre A, Mendoza IE, Segura-Aguilar J, Rapoport SI, Caviedes P (2002) Establishment and characterization of immortalized neuronal cell lines derived from the spinal cord of normal and trisomy 16 fetal mice, an animal model of Down syndrome. J Neurosci Res 68:46-58.

Casasola C, Montiel T, Calixto E, Brailowsky S (2004) Hyperexcitability induced by GABA withdrawal facilitates hippocampal long-term potentiation. Neuroscience 126:163-171.

Catterall WA, Few AP (2008) Calcium channel regulation and presynaptic plasticity. Neuron 59:882-901.

Claasen AM, Guevremont D, Mason-Parker SE, Bourne K, Tate WP, Abraham WC, Williams JM (2009) Secreted amyloid precursor protein-alpha upregulates synaptic protein synthesis by a protein kinase G-dependent mechanism. NeurosciLett 460:92-96.

Clarris HJ, Cappai R, Heffernan D, Beyreuther K, Masters CL, Small DH (1997) Identification of heparin-binding domains in the amyloid precursor protein of Alzheimer's disease by deletion mutagenesis and peptide mapping. J Neurochem 68:1164-1172.

Colgin LL, Moser EI (2010) Gamma oscillations in the hippocampus. Physiology (Bethesda) 25:319-329.

Collingridge GL, Kehl SJ, McLennan H (1983) Excitatory amino acids in synaptic transmission in the Schaffer collateral-commissural pathway of the rat hippocampus. JPhysiol 334:33-46.

Collingridge GL, Herron CE, Lester RA (1988) Synaptic activation of N-methyl-D-aspartate receptors in the Schaffer collateral-commissural pathway of rat hippocampus. JPhysiol 399:283-300.

Cousins SL, Hoey SE, Anne Stephenson F, Perkinton MS (2009) Amyloid precursor protein 695 associates with assembled NR2A- and NR2B-containing NMDA receptors to result in the enhancement of their cell surface delivery. J Neurochem 111:1501-1513.

Cummings JA, Mulkey RM, Nicoll RA, Malenka RC (1996a) Ca2+ signaling requirements for long-term depression in the hippocampus. Neuron 16:825-833.

Cummings JA, Mulkey RM, Nicoll RA, Malenka RC (1996b) Ca2+ signaling requirements for long-term depression in the hippocampus. Neuron 16:825-833.

Davies CH, Collingridge GL (1993) The physiological regulation of synaptic inhibition by GABAB autoreceptors in rat hippocampus. JPhysiol 472:245-265.

Dawson GR, Seabrook GR, Zheng H, Smith DW, Graham S, O'Dowd G, Bowery BJ, Boyce S, Trumbauer ME, Chen HY, Van der Ploeg LH, Sirinathsinghji DJ (1999) Age-related cognitive deficits, impaired long-term potentiation and reduction in synaptic marker density in mice lacking the beta-amyloid precursor protein. Neuroscience 90:1-13.

de Calignon A, Polydoro M, Suarez-Calvet M, William C, Adamowicz DH, Kopeikina KJ, Pitstick R, Sahara N, Ashe KH, Carlson GA, Spires-Jones TL, Hyman BT (2012) Propagation of tau pathology in a model of early Alzheimer's disease. Neuron 73:685-697.

De Strooper B, Vassar R, Golde T (2010) The secretases: enzymes with therapeutic potential in Alzheimer disease. Nat Rev Neurol 6:99-107.

Demars MP, Bartholomew A, Strakova Z, Lazarov O (2011) Soluble amyloid precursor protein: a novel proliferation factor of adult progenitor cells of ectodermal and mesodermal origin. Stem Cell Res Ther 2:36.

Demuro A, Parker I (2013) Cytotoxicity of intracellular abeta42 amyloid oligomers involves Ca2+ release from the endoplasmic reticulum by stimulated production of inositol trisphosphate. J Neurosci 33:3824-3833.

Deng W, Aimone JB, Gage FH (2010) New neurons and new memories: how does adult hippocampal neurogenesis affect learning and memory? Nat Rev Neurosci 11:339-350.

Derkach V, Barria A, Soderling TR (1999) Ca2+/calmodulin-kinase II enhances channel conductance of alpha-amino-3-hydroxy-5-methyl-4-isoxazolepropionate type glutamate receptors. Proc Natl Acad Sci U S A 96:3269-3274.

Drever BD, Riedel G, Platt B (2011) The cholinergic system and hippocampal plasticity. Behav Brain Res 221:505-514.

Dudek SM, Bear MF (1992) Homosynaptic long-term depression in area CA1 of hippocampus and effects of N-methyl-D-aspartate receptor blockade. ProcNatlAcadSciUSA 89:4363-4367.

Dudek SM, Bear MF (1993) Bidirectional long-term modification of synaptic effectiveness in the adult and immature hippocampus. JNeurosci 13:2910-2918.

Duff K, Eckman C, Zehr C, Yu X, Prada CM, Perez-tur J, Hutton M, Buee L, Harigaya Y, Yager D, Morgan D, Gordon MN, Holcomb L, Refolo L, Zenk B, Hardy J, Younkin S (1996) Increased amyloid-beta42(43) in brains of mice expressing mutant presenilin 1. Nature 383:710-713.

Dyrks T, Weidemann A, Multhaup G, Salbaum JM, Lemaire HG, Kang J, Muller-Hill B, Masters CL, Beyreuther K (1988) Identification, transmembrane orientation and biogenesis of the amyloid A4 precursor of Alzheimer's disease. EMBO J 7:949-957.

Edwards DR, Handsley MM, Pennington CJ (2008) The ADAM metalloproteinases. Mol Aspects Med 29:258-289.

Eggert S, Paliga K, Soba P, Evin G, Masters CL, Weidemann A, Beyreuther K (2004) The proteolytic processing of the amyloid precursor protein gene family members APLP-1 and APLP-2 involves alpha-, beta-, gamma-, and epsilon-like cleavages: modulation of APLP-1 processing by n-glycosylation. JBiolChem 279:18146-18156.

Endres K, Postina R, Schroeder A, Mueller U, Fahrenholz F (2005) Shedding of the amyloid precursor protein-like protein APLP2 by disintegrin-metalloproteinases. FEBS J 272:5808-5820.

Erdmann G, Schutz G, Berger S (2007) Inducible gene inactivation in neurons of the adult mouse forebrain. BMC Neurosci 8:63.

Eroglu C, Barres BA (2010) Regulation of synaptic connectivity by glia. Nature 468:223-231.

Fahrenholz F, Postina R (2006) Alpha-secretase activation--an approach to Alzheimer's disease therapy. NeurodegenerDis 3:255-261.

Fazeli MS, Breen K, Errington ML, Bliss TV (1994) Increase in extracellular NCAM and amyloid precursor protein following induction of long-term potentiation in the dentate gyrus of anaesthetized rats. NeurosciLett 169:77-80.

Fellgiebel A, Kojro E, Muller MJ, Scheurich A, Schmidt LG, Fahrenholz F (2009) CSF APPs alpha and phosphorylated tau protein levels in mild cognitive impairment and dementia of Alzheimer's type. J Geriatr Psychiatry Neurol 22:3-9.

Fioravante D, Regehr WG (2011) Short-term forms of presynaptic plasticity. Curr Opin Neurobiol 21:269-274.

Fitzjohn SM, Morton RA, Kuenzi F, Davies CH, Seabrook GR, Collingridge GL (2000) Similar levels of long-term potentiation in amyloid precursor protein -null and wild-type mice in the CA1 region of picrotoxin treated slices. NeurosciLett 288:9-12.

Foster TC, Norris CM (1997) Age-associated changes in Ca(2+)-dependent processes: relation to hippocampal synaptic plasticity. Hippocampus 7:602-612.

Freude KK, Penjwini M, Davis JL, Laferla FM, Blurton-Jones M (2011) Soluble amyloid precursor protein induces rapid neural differentiation of human embryonic stem cells. JBiolChem 286:24264-24274.

Freund TF, Buzsaki G (1996) Interneurons of the hippocampus. Hippocampus 6:347-470.

Frey U, Krug M, Reymann KG, Matthies H (1988) Anisomycin, an inhibitor of protein synthesis, blocks late phases of LTP phenomena in the hippocampal CA1 region in vitro. Brain Res 452:57-65.

Furukawa K, Sopher BL, Rydel RE, Begley JG, Pham DG, Martin GM, Fox M, Mattson MP (1996) Increased activity-regulating and neuroprotective efficacy of alpha-secretase-derived secreted amyloid precursor protein conferred by a C-terminal heparin-binding domain. J Neurochem 67:1882-1896.

Gähwiler B, Capogna M, Debanne D, McKinney R, Thompson S (1997) Organotypic slice cultures: a technique has come of age. Trends in neurosciences 20:471-477.

Gakhar-Koppole N, Hundeshagen P, Mandl C, Weyer SW, Allinquant B, Muller U, Ciccolini F (2008) Activity requires soluble amyloid precursor protein alpha to promote neurite outgrowth in neural stem cell-derived neurons via activation of the MAPK pathway. EurJNeurosci 28:871-882.

Galizia CG, Lledo P-M (2013) Neurosciences--from Molecule to Behavior: A University Textbook: Springer Spektrum.

Gao Y, Pimplikar SW (2001) The gamma -secretase-cleaved C-terminal fragment of amyloid precursor protein mediates signaling to the nucleus. Proc Natl Acad Sci U S A 98:14979-14984.

Goebbels S, Bormuth I, Bode U, Hermanson O, Schwab MH, Nave KA (2006) Genetic targeting of principal neurons in neocortex and hippocampus of NEX-Cre mice. Genesis 44:611-621.

Goedert M, Spillantini MG (2006) A century of Alzheimer's disease. Science 314:777-781.

Goedert M, Wischik CM, Crowther RA, Walker JE, Klug A (1988) Cloning and sequencing of the cDNA encoding a core protein of the paired helical filament of Alzheimer disease: identification as the microtubule-associated protein tau. ProcNatlAcadSciUSA 85:4051-4055.

Golgi C, Bentivoglio M, Swanson L (2001) On the fine structure of the pes Hippocampi major (with plates XIII-XXIII). 1886. Brain ResBull 54:461-483.

Gomez-Isla T, Hollister R, West H, Mui S, Growdon JH, Petersen RC, Parisi JE, Hyman BT (1997) Neuronal loss correlates with but exceeds neurofibrillary tangles in Alzheimer's disease. Ann Neurol 41:17-24.

Gralle M, Botelho MG, Wouters FS (2009) Neuroprotective secreted amyloid precursor protein acts by disrupting amyloid precursor protein dimers. J Biol Chem 284:15016-15025.

Grynkiewicz G, Poenie M, Tsien RY (1985) A new generation of Ca2+ indicators with greatly improved fluorescence properties. JBiolChem 260:3440-3450.

Guenette SY, Chen J, Jondro PD, Tanzi RE (1996) Association of a novel human FE65-like protein with the cytoplasmic domain of the beta-amyloid precursor protein. Proc Natl Acad Sci U S A 93:10832-10837.

Guo Q, Robinson N, Mattson MP (1998) Secreted beta-amyloid precursor protein counteracts the proapoptotic action of mutant presenilin-1 by activation of NF-kappaB and stabilization of calcium homeostasis. J Biol Chem 273:12341-12351.

Haass C, Schlossmacher MG, Hung AY, Vigo-Pelfrey C, Mellon A, Ostaszewski BL, Lieberburg I, Koo EH, Schenk D, Teplow DB, et al. (1992) Amyloid beta-peptide is produced by cultured cells during normal metabolism. Nature 359:322-325.

Hamid R, Kilger E, Willem M, Vassallo N, Kostka M, Bornhovd C, Reichert AS, Kretzschmar HA, Haass C, Herms J (2007) Amyloid precursor protein intracellular domain modulates cellular calcium homeostasis and ATP content. JNeurochem 102:1264-1275.

Hasebe N, Fujita Y, Ueno M, Yoshimura K, Fujino Y, Yamashita T (2013) Soluble beta-amyloid Precursor Protein Alpha binds to p75 neurotrophin receptor to promote neurite outgrowth. PLoS One 8:e82321.

He L, Xue L, Xu J, McNeil BD, Bai L, Melicoff E, Adachi R, Wu LG (2009) Compound vesicle fusion increases quantal size and potentiates synaptic transmission. Nature 459:93-97.

Hebb DO (1949) The Organization of Behavior. A Neuropsychological Theory: Lawrence Erkbaum Associates, Inc., Publishers, Mahwah, New Jersey.

Heber S, Herms J, Gajic V, Hainfellner J, Aguzzi A, Rulicke T, von Kretzschmar H, von Koch C, Sisodia S, Tremml P, Lipp HP, Wolfer DP, Muller U (2000) Mice with combined gene knock-outs reveal essential and partially redundant functions of amyloid precursor protein family members. JNeurosci 20:7951-7963.

Heneka MT, O'Banion MK (2007) Inflammatory processes in Alzheimer's disease. J Neuroimmunol 184:69-91.

Heneka MT, Kummer MP, Latz E (2014) Innate immune activation in neurodegenerative disease. Nat Rev Immunol 14:463-477.

Henneberger C, Bard L, King C, Jennings A, Rusakov DA (2013) NMDA receptor activation: two targets for two co-agonists. Neurochem Res 38:1156-1162.

Herms J, Anliker B, Heber S, Ring S, Fuhrmann M, Kretzschmar H, Sisodia S, Muller U (2004) Cortical dysplasia resembling human type 2 lissencephaly in mice lacking all three APP family members. EMBO J 23:4106-4115.

Heynen AJ, Abraham WC, Bear MF (1996) Bidirectional modification of CA1 synapses in the adult hippocampus in vivo. Nature 381:163-166.

Hick M, Herrmann U, Weyer SW, Mallm J, Tschape J, Borgers M, Mercken M, Roth FC, Draguhn A, Slomianka L, Wolfer DP, Korte M, Muller UC (2015) Acute function of secreted amyloid precursor protein fragment APPsalpha in synaptic plasticity. Acta Neuropathol 129:21-37.

Hoe HS, Fu Z, Makarova A, Lee JY, Lu C, Feng L, Pajoohesh-Ganji A, Matsuoka Y, Hyman BT, Ehlers MD, Vicini S, Pak DT, Rebeck GW (2009) The effects of amyloid precursor protein on postsynaptic composition and activity. J Biol Chem 284:8495-8506.

Hoettecke N, Ludwig A, Foro S, Schmidt B (2010) Improved synthesis of ADAM10 inhibitor GI254023X. NeurodegenerDis 7:232-238.

Hoey SE, Williams RJ, Perkinton MS (2009) Synaptic NMDA receptor activation stimulates alpha-secretase amyloid precursor protein processing and inhibits amyloid-beta production. J Neurosci 29:4442-4460.

Holtzman DM, Morris JC, Goate AM (2011) Alzheimer's disease: the challenge of the second century. SciTranslMed 3:77sr71.

Honkura N, Matsuzaki M, Noguchi J, Ellis-Davies GC, Kasai H (2008) The subspine organization of actin fibers regulates the structure and plasticity of dendritic spines. Neuron 57:719-729.

Hornsten A, Lieberthal J, Fadia S, Malins R, Ha L, Xu X, Daigle I, Markowitz M, O'Connor G, Plasterk R, Li C (2007) APL-1, a Caenorhabditis elegans protein related to the human beta-amyloid precursor protein, is essential for viability. Proc Natl Acad Sci U S A 104:1971-1976.

Howard L, Lu X, Mitchell S, Griffiths S, Glynn P (1996) Molecular cloning of MADM: a catalytically active mammalian disintegrin-metalloprotease expressed in various cell types. Biochem J 317 (Pt 1):45-50.

Hsieh H, Boehm J, Sato C, Iwatsubo T, Tomita T, Sisodia S, Malinow R (2006a) AMPAR removal underlies Abeta-induced synaptic depression and dendritic spine loss. Neuron 52:831-843.

Hsieh H, Boehm J, Sato C, Iwatsubo T, Tomita T, Sisodia S, Malinow R (2006b) AMPAR removal underlies Abeta-induced synaptic depression and dendritic spine loss. Neuron 52:831-843.

Hu Y, Hung AC, Cui H, Dawkins E, Bolos M, Foa L, Young KM, Small DH (2013) Role of cystatin C in amyloid precursor protein-induced proliferation of neural stem/progenitor cells. J Biol Chem 288:18853-18862.

Huganir RL, Nicoll RA (2013) AMPARs and synaptic plasticity: the last 25 years. Neuron 80:704-717.

Hyman BT, Kromer LJ, Van Hoesen GW (1987) Reinnervation of the hippocampal perforant pathway zone in Alzheimer's disease. Ann Neurol 21:259-267.

Isbert S, Wagner K, Eggert S, Schweitzer A, Multhaup G, Weggen S, Kins S, Pietrzik CU (2012) APP dimer formation is initiated in the endoplasmic reticulum and differs between APP isoforms. Cell Mol Life Sci 69:1353-1375.

Ishida A, Furukawa K, Keller JN, Mattson MP (1997) Secreted form of beta-amyloid precursor protein shifts the frequency dependency for induction of LTD, and enhances LTP in hippocampal slices. Neuroreport 8:2133-2137.

Jacobsen JS, Wu CC, Redwine JM, Comery TA, Arias R, Bowlby M, Martone R, Morrison JH, Pangalos MN, Reinhart PH, Bloom FE (2006) Early-onset behavioral and synaptic deficits in a mouse model of Alzheimer's disease. ProcNatlAcadSciUSA 103:5161-5166.

Jacobsen KT, Iverfeldt K (2009) Amyloid precursor protein and its homologues: a family of proteolysis-dependent receptors. Cell MolLife Sci 66:2299-2318.

Jorissen E, Prox J, Bernreuther C, Weber S, Schwanbeck R, Serneels L, Snellinx A, Craessaerts K, Thathiah A, Tesseur I, Bartsch U, Weskamp G, Blobel CP, Glatzel M, De SB, Saftig P (2010) The disintegrin/metalloproteinase ADAM10 is essential for the establishment of the brain cortex. JNeurosci 30:4833-4844.

Jurado S, Biou V, Malenka RC (2010) A calcineurin/AKAP complex is required for NMDA receptor-dependent long-term depression. Nat Neurosci 13:1053-1055.

Katz B, Miledi R (1968) The role of calcium in neuromuscular facilitation. JPhysiol 195:481-492.

Kelly MJ, Qiu J, Ronnekleiv OK (2003) Estrogen modulation of G-protein-coupled receptor activation of potassium channels in the central nervous system. Ann N Y Acad Sci 1007:6-16.

Kenney J, Manahan-Vaughan D (2013) Learning-facilitated synaptic plasticity occurs in the intermediate hippocampus in association with spatial learning. Front Synaptic Neurosci 5:10.

Kibbey MC, Jucker M, Weeks BS, Neve RL, Van Nostrand WE, Kleinman HK (1993) beta-Amyloid precursor protein binds to the neurite-promoting IKVAV site of laminin. Proc Natl Acad Sci U S A 90:10150-10153.

Kim M, Suh J, Romano D, Truong MH, Mullin K, Hooli B, Norton D, Tesco G, Elliott K, Wagner SL, Moir RD, Becker KD, Tanzi RE (2009) Potential late-onset Alzheimer's disease-associated mutations in the ADAM10 gene attenuate {alpha}-secretase activity. Hum Mol Genet 18:3987-3996.

Kimberly WT, Zheng JB, Guenette SY, Selkoe DJ (2001) The intracellular domain of the beta-amyloid precursor protein is stabilized by Fe65 and translocates to the nucleus in a notch-like manner. J Biol Chem 276:40288-40292.

Kirazov E, Kirazov L, Bigl V, Schliebs R (2001) Ontogenetic changes in protein level of amyloid precursor protein (APP) in growth cones and synaptosomes from rat brain and prenatal expression pattern of APP mRNA isoforms in developing rat embryo. Int J Dev Neurosci 19:287-296.

Klevanski M, Herrmann U, Weyer SW, Voikar V, Wolfer DP, Caldwell JH, Korte M, Müller UC (in preparation) The APP intracellular domain is required for normal synaptic morphology, synaptic plasticity and hippocampus dependent behavior. .

Kogel D, Deller T, Behl C (2012) Roles of amyloid precursor protein family members in neuroprotection, stress signaling and aging. Exp Brain Res 217:471-479.

Koike H, Tomioka S, Sorimachi H, Saido TC, Maruyama K, Okuyama A, Fujisawa-Sehara A, Ohno S, Suzuki K, Ishiura S (1999) Membrane-anchored metalloprotease MDC9 has an alpha-secretase activity responsible for processing the amyloid precursor protein. Biochem J 343 Pt 2:371-375.

Koizumi S, Ishiguro M, Ohsawa I, Morimoto T, Takamura C, Inoue K, Kohsaka S (1998) The effect of a secreted form of beta-amyloid-precursor protein on intracellular Ca2+ increase in rat cultured hippocampal neurones. BrJPharmacol 123:1483-1489.

Kojro E, Gimpl G, Lammich S, Marz W, Fahrenholz F (2001) Low cholesterol stimulates the nonamyloidogenic pathway by its effect on the alpha -secretase ADAM 10. Proc Natl Acad Sci U S A 98:5815-5820.

Koo EH, Squazzo SL (1994) Evidence that production and release of amyloid beta-protein involves the endocytic pathway. JBiolChem 269:17386-17389.

Koo EH, Squazzo SL, Selkoe DJ, Koo CH (1996) Trafficking of cell-surface amyloid beta-protein precursor. I. Secretion, endocytosis and recycling as detected by labeled monoclonal antibody. J Cell Sci 109 (Pt 5):991-998.

Korogod N, Lou X, Schneggenburger R (2007) Posttetanic potentiation critically depends on an enhanced Ca(2+) sensitivity of vesicle fusion mediated by presynaptic PKC. Proc Natl Acad Sci U S A 104:15923-15928.

Korte M, Herrmann U, Zhang X, Draguhn A (2012) The role of APP and APLP for synaptic transmission, plasticity, and network function: lessons from genetic mouse models. Exp Brain Res 217:435-440.

Korte M, Carroll P, Wolf E, Brem G, Thoenen H, Bonhoeffer T (1995) Hippocampal long-term potentiation is impaired in mice lacking brain-derived neurotrophic factor. ProcNatlAcadSciUSA 92:8856-8860.

Kristensen AS, Jenkins MA, Banke TG, Schousboe A, Makino Y, Johnson RC, Huganir R, Traynelis SF (2011) Mechanism of Ca2+/calmodulin-dependent kinase II regulation of AMPA receptor gating. Nat Neurosci 14:727-735.

Krug M, Lossner B, Ott T (1984) Anisomycin blocks the late phase of long-term potentiation in the dentate gyrus of freely moving rats. Brain ResBull 13:39-42.

Kuchibhotla KV, Goldman ST, Lattarulo CR, Wu HY, Hyman BT, Bacskai BJ (2008) Abeta plaques lead to aberrant regulation of calcium homeostasis in vivo resulting in structural and functional disruption of neuronal networks. Neuron 59:214-225.

Kuhn PH, Wang H, Dislich B, Colombo A, Zeitschel U, Ellwart JW, Kremmer E, Rossner S, Lichtenthaler SF (2010) ADAM10 is the physiologically relevant, constitutive alpha-secretase of the amyloid precursor protein in primary neurons. EMBO J 29:3020-3032.

Kumar A (2011) Long-Term Potentiation at CA3-CA1 Hippocampal Synapses with Special Emphasis on Aging, Disease, and Stress. Front Aging Neurosci 3:7.

LaFerla FM (2002) Calcium dyshomeostasis and intracellular signalling in Alzheimer's disease. Nat Rev Neurosci 3:862-872.

Lai A, Sisodia SS, Trowbridge IS (1995) Characterization of sorting signals in the beta-amyloid precursor protein cytoplasmic domain. J Biol Chem 270:3565-3573.

Lammich S, Kojro E, Postina R, Gilbert S, Pfeiffer R, Jasionowski M, Haass C, Fahrenholz F (1999) Constitutive and regulated alpha-secretase cleavage of Alzheimer's amyloid precursor protein by a disintegrin metalloprotease. Proc Natl Acad Sci U S A 96:3922-3927.

Larson J, Lynch G (1986) Induction of synaptic potentiation in hippocampus by patterned stimulation involves two events. Science 232:985-988.

LeBlanc AC, Koutroumanis M, Goodyer CG (1998) Protein kinase C activation increases release of secreted amyloid precursor protein without decreasing Abeta production in human primary neuron cultures. JNeurosci 18:2907-2913.

Lee AM, Kanter BR, Wang D, Lim JP, Zou ME, Qiu C, McMahon T, Dadgar J, Fischbach-Weiss SC, Messing RO (2013) Prkcz null mice show normal learning and memory. Nature 493:416-419.

Lee HK, Kameyama K, Huganir RL, Bear MF (1998) NMDA induces long-term synaptic depression and dephosphorylation of the GluR1 subunit of AMPA receptors in hippocampus. Neuron 21:1151-1162.

Lee HK, Takamiya K, Han JS, Man H, Kim CH, Rumbaugh G, Yu S, Ding L, He C, Petralia RS, Wenthold RJ, Gallagher M, Huganir RL (2003) Phosphorylation of the AMPA receptor GluR1 subunit is required for synaptic plasticity and retention of spatial memory. Cell 112:631-643.

Lee KJ, Moussa CE, Lee Y, Sung Y, Howell BW, Turner RS, Pak DT, Hoe HS (2010) Beta amyloid-independent role of amyloid precursor protein in generation and maintenance of dendritic spines. Neuroscience 169:344-356.

Lee SF, Shah S, Li H, Yu C, Han W, Yu G (2002) Mammalian APH-1 interacts with presenilin and nicastrin and is required for intramembrane proteolysis of amyloid-beta precursor protein and Notch. J Biol Chem 277:45013-45019.

Leissring MA, Murphy MP, Mead TR, Akbari Y, Sugarman MC, Jannatipour M, Anliker B, Muller U, Saftig P, De SB, Wolfe MS, Golde TE, Laferla FM (2002) A physiologic signaling role for the gamma -secretase-derived intracellular fragment of APP. ProcNatlAcadSciUSA 99:4697-4702.

Li H, Wang B, Wang Z, Guo Q, Tabuchi K, Hammer RE, Sudhof TC, Zheng H (2010) Soluble amyloid precursor protein (APP) regulates transthyretin and Klotho gene expression without rescuing the essential function of APP. Proc Natl Acad Sci U S A 107:17362-17367.

Lichtenthaler SF (2012) Alpha-secretase cleavage of the amyloid precursor protein: proteolysis regulated by signaling pathways and protein trafficking. Curr Alzheimer Res 9:165-177.

Lichtenthaler SF, Haass C, Steiner H (2011) Regulated intramembrane proteolysis--lessons from amyloid precursor protein processing. J Neurochem 117:779-796.

Ling DS, Benardo LS, Serrano PA, Blace N, Kelly MT, Crary JF, Sacktor TC (2002) Protein kinase Mzeta is necessary and sufficient for LTP maintenance. NatNeurosci 5:295-296.

Lisman J (1989) A mechanism for the Hebb and the anti-Hebb processes underlying learning and memory. ProcNatlAcadSciUSA 86:9574-9578.

Loffler J, Huber G (1992) Beta-amyloid precursor protein isoforms in various rat brain regions and during brain development. J Neurochem 59:1316-1324.

Lopez-Garcia JC (1998) Two different forms of long-term potentiation in the hippocampus. Neurobiology (Bp) 6:75-98.

Lopez JR, Lyckman A, Oddo S, Laferla FM, Querfurth HW, Shtifman A (2008) Increased intraneuronal resting [Ca2+] in adult Alzheimer's disease mice. J Neurochem 105:262-271.

Lorent K, Overbergh L, Moechars D, De SB, Van LF, Van den Berghe H (1995) Expression in mouse embryos and in adult mouse brain of three members of the amyloid precursor protein family, of the alpha-2-macroglobulin receptor/low density lipoprotein receptor-related protein and of its ligands apolipoprotein E, lipoprotein lipase, alpha-2-macroglobulin and the 40,000 molecular weight receptor-associated protein. Neuroscience 65:1009-1025.

Lou X, Korogod N, Brose N, Schneggenburger R (2008) Phorbol esters modulate spontaneous and Ca2+-evoked transmitter release via acting on both Munc13 and protein kinase C. J Neurosci 28:8257-8267.

Ludwig A, Hundhausen C, Lambert MH, Broadway N, Andrews RC, Bickett DM, Leesnitzer MA, Becherer JD (2005) Metalloproteinase inhibitors for the disintegrin-like metalloproteinases ADAM10 and ADAM17 that differentially block constitutive and phorbol ester-inducible shedding of cell surface molecules. CombChemHigh ThroughputScreen 8:161-171.

Lynch G, Larson J, Kelso S, Barrionuevo G, Schottler F (1983) Intracellular injections of EGTA block induction of hippocampal long-term potentiation. Nature 305:719-721.

Magara F, Muller U, Li ZW, Lipp HP, Weissmann C, Stagljar M, Wolfer DP (1999) Genetic background changes the pattern of forebrain commissure defects in transgenic mice underexpressing the beta-amyloid-precursor protein. Proc Natl Acad Sci U S A 96:4656-4661.

Maggio N, Vlachos A (2014) Synaptic plasticity at the interface of health and disease: New insights on the role of endoplasmic reticulum intracellular calcium stores. Neuroscience 281C:135-146.

Magno L, Kretz O, Bert B, Ersozlu S, Vogt J, Fink H, Kimura S, Vogt A, Monyer H, Nitsch R, Naumann T (2011) The integrity of cholinergic basal forebrain neurons depends on expression of Nkx2-1. Eur J Neurosci 34:1767-1782.

Malenka RC, Bear MF (2004) LTP and LTD: an embarrassment of riches. Neuron 44:5-21.

Malenka RC, Kauer JA, Perkel DJ, Mauk MD, Kelly PT, Nicoll RA, Waxham MN (1989) An essential role for postsynaptic calmodulin and protein kinase activity in long-term potentiation. Nature 340:554-557.

Malinow R, Schulman H, Tsien RW (1989) Inhibition of postsynaptic PKC or CaMKII blocks induction but not expression of LTP. Science 245:862-866.

Malinverno M, Carta M, Epis R, Marcello E, Verpelli C, Cattabeni F, Sala C, Mulle C, Di LM, Gardoni F (2010) Synaptic Localization and Activity of ADAM10 Regulate Excitatory Synapses through N-Cadherin Cleavage. JNeurosci 30:16343-16355.

Mallm JP, Tschape JA, Hick M, Filippov MA, Muller UC (2010) Generation of conditional null alleles for APP and APLP2. Genesis 48:200-206.

Manabe T (1997) Two forms of hippocampal long-term depression, the counterpart of long-term potentiation. Rev Neurosci 8:179-193.

Manahan-Vaughan D, Kulla A, Frey JU (2000) Requirement of translation but not transcription for the maintenance of long-term depression in the CA1 region of freely moving rats. JNeurosci 20:8572-8576.

Masters CL, Selkoe DJ (2012) Biochemistry of amyloid beta-protein and amyloid deposits in Alzheimer disease. Cold Spring Harb Perspect Med 2:a006262.

Matrone C (2013) A new molecular explanation for age-related neurodegeneration: the Tyr682 residue of amyloid precursor protein. Bioessays 35:847-852.

Matrone C, Barbagallo AP, La Rosa LR, Florenzano F, Ciotti MT, Mercanti D, Chao MV, Calissano P, D'Adamio L (2011) APP is Phosphorylated by TrkA and Regulates NGF/TrkA Signaling. JNeurosci 31:11756-11761.

Matsuzaki M, Honkura N, Ellis-Davies GC, Kasai H (2004) Structural basis of long-term potentiation in single dendritic spines. Nature 429:761-766.

Mattson MP (1994) Secreted forms of beta-amyloid precursor protein modulate dendrite outgrowth and calcium responses to glutamate in cultured embryonic hippocampal neurons. J Neurobiol 25:439-450.

Mattson MP, Engle MG, Rychlik B (1991) Effects of elevated intracellular calcium levels on the cytoskeleton and tau in cultured human cortical neurons. Mol Chem Neuropathol 15:117-142.

Mattson MP, Cheng B, Davis D, Bryant K, Lieberburg I, Rydel RE (1992) beta-Amyloid peptides destabilize calcium homeostasis and render human cortical neurons vulnerable to excitotoxicity. J Neurosci 12:376-389.

Mattson MP, Cheng B, Culwell AR, Esch FS, Lieberburg I, Rydel RE (1993) Evidence for excitoprotective and intraneuronal calcium-regulating roles for secreted forms of the beta-amyloid precursor protein. Neuron 10:243-254.

Matveev V, Zucker RS, Sherman A (2004) Facilitation through buffer saturation: constraints on endogenous buffering properties. Biophys J 86:2691-2709.

Mayer ML, Westbrook GL, Guthrie PB (1984) Voltage-dependent block by Mg2+ of NMDA responses in spinal cord neurones. Nature 309:261-263.

McConlogue L, Buttini M, Anderson JP, Brigham EF, Chen KS, Freedman SB, Games D, Johnson-Wood K, Lee M, Zeller M, Liu W, Motter R, Sinha S (2007) Partial Reduction of BACE1 Has Dramatic Effects on Alzheimer Plaque and Synaptic Pathology in APP Transgenic Mice. JBiolChem 282:26326-26334.

Meziane H, Dodart JC, Mathis C, Little S, Clemens J, Paul SM, Ungerer A (1998) Memory-enhancing effects of secreted forms of the beta-amyloid precursor protein in normal and amnestic mice. Proc Natl Acad Sci U S A 95:12683-12688.

Midthune B, Tyan SH, Walsh JJ, Sarsoza F, Eggert S, Hof PR, Dickstein DL, Koo EH (2012) Deletion of the amyloid precursor-like protein 2 (APLP2) does not affect hippocampal neuron morphology or function. MolCell Neurosci 49:448-455.

Mochida S, Few AP, Scheuer T, Catterall WA (2008) Regulation of presynaptic Ca(V)2.1 channels by Ca2+ sensor proteins mediates short-term synaptic plasticity. Neuron 57:210-216.

Molnar E (2011) Long-term potentiation in cultured hippocampal neurons. Semin Cell Dev Biol 22:506-513.

Moosmang S, Haider N, Klugbauer N, Adelsberger H, Langwieser N, Muller J, Stiess M, Marais E, Schulla V, Lacinova L, Goebbels S, Nave KA, Storm DR, Hofmann F, Kleppisch T (2005) Role of hippocampal Cav1.2 Ca2+ channels in NMDA receptor-independent synaptic plasticity and spatial memory. J Neurosci 25:9883-9892.

Morgan SL, Teyler TJ (1999) VDCCs and NMDARs underlie two forms of LTP in CA1 hippocampus in vivo. J Neurophysiol 82:736-740.

Morris RG (1989) Synaptic plasticity and learning: selective impairment of learning rats and blockade of long-term potentiation in vivo by the N-methyl-D-aspartate receptor antagonist AP5. JNeurosci 9:3040-3057.

Mott DD, Xie CW, Wilson WA, Swartzwelder HS, Lewis DV (1993) GABAB autoreceptors mediate activity-dependent disinhibition and enhance signal transmission in the dentate gyrus. J Neurophysiol 69:674-691.

Mukherjee S, Manahan-Vaughan D (2013) Role of metabotropic glutamate receptors in persistent forms of hippocampal plasticity and learning. Neuropharmacology 66:65-81.

Mulkey RM, Herron CE, Malenka RC (1993) An essential role for protein phosphatases in hippocampal long-term depression. Science 261:1051-1055.

Muller T, Meyer HE, Egensperger R, Marcus K (2008) The amyloid precursor protein intracellular domain (AICD) as modulator of gene expression, apoptosis, and cytoskeletal dynamics-relevance for Alzheimer's disease. Prog Neurobiol 85:393-406.

Muller U, Cristina N, Li ZW, Wolfer DP, Lipp HP, Rulicke T, Brandner S, Aguzzi A, Weissmann C (1994) Behavioral and anatomical deficits in mice homozygous for a modified beta-amyloid precursor protein gene. Cell 79:755-765.

Muller UC, Zheng H (2012) Physiological Functions of APP Family Proteins. Cold Spring HarbPerspectMed 2:a006288.

Mumby DG, Astur RS, Weisend MP, Sutherland RJ (1999) Retrograde amnesia and selective damage to the hippocampal formation: memory for places and object discriminations. Behav Brain Res 106:97-107.

Murphy TH, Worley PF, Baraban JM (1991) L-type voltage-sensitive calcium channels mediate synaptic activation of immediate early genes. Neuron 7:625-635.

Musardo S, Marcello E, Gardoni F, Di LM (2013) ADAM10 in Synaptic Physiology and Pathology. NeurodegenerDis.

Nhan HS, Chiang K, Koo EH (2014) The multifaceted nature of amyloid precursor protein and its proteolytic fragments: friends and foes. Acta Neuropathol.

Nicholson DA, Yoshida R, Berry RW, Gallagher M, Geinisman Y (2004) Reduction in size of perforated postsynaptic densities in hippocampal axospinous synapses and age-related spatial learning impairments. J Neurosci 24:7648-7653.

Nicolas M, Hassan BA (2014) Amyloid precursor protein and neural development. Development 141:2543-2548.

Nicoll RA, Kauer JA, Malenka RC (1988) The current excitement in long-term potentiation. Neuron 1:97-103.

Nishiyama M, Hong K, Mikoshiba K, Poo MM, Kato K (2000) Calcium stores regulate the polarity and input specificity of synaptic modification. Nature 408:584-588.

Nitsch RM, Slack BE, Wurtman RJ, Growdon JH (1992) Release of Alzheimer amyloid precursor derivatives stimulated by activation of muscarinic acetylcholine receptors. Science 258:304-307.

Nitsch RM, Farber SA, Growdon JH, Wurtman RJ (1993) Release of amyloid beta-protein precursor derivatives by electrical depolarization of rat hippocampal slices. Proc Natl Acad Sci U S A 90:5191-5193.

Norstrom EM, Zhang C, Tanzi R, Sisodia SS (2010) Identification of NEEP21 as a ss-amyloid precursor protein-interacting protein in vivo that modulates amyloidogenic processing in vitro. JNeurosci 30:15677-15685.

Nowak L, Bregestovski P, Ascher P, Herbet A, Prochiantz A (1984) Magnesium gates glutamate-activated channels in mouse central neurones. Nature 307:462-465.

Obregon D, Hou H, Deng J, Giunta B, Tian J, Darlington D, Shahaduzzaman M, Zhu Y, Mori T, Mattson MP, Tan J (2012) Soluble amyloid precursor protein-alpha modulates beta-secretase activity and amyloid-beta generation. NatCommun 3:777.

Octave JN, Pierrot N, Ferao SS, Nalivaeva NN, Turner AJ (2013) From synaptic spines to nuclear signaling: nuclear and synaptic actions of the amyloid precursor protein. JNeurochem 126:183-190.

Okamoto K, Nagai T, Miyawaki A, Hayashi Y (2004) Rapid and persistent modulation of actin dynamics regulates postsynaptic reorganization underlying bidirectional plasticity. Nat Neurosci 7:1104-1112.

Olsson A, Hoglund K, Sjogren M, Andreasen N, Minthon L, Lannfelt L, Buerger K, Moller HJ, Hampel H, Davidsson P, Blennow K (2003) Measurement of alpha- and beta-secretase cleaved amyloid precursor protein in cerebrospinal fluid from Alzheimer patients. Exp Neurol 183:74-80.

Opazo P, Choquet D (2011) A three-step model for the synaptic recruitment of AMPA receptors. Mol Cell Neurosci 46:1-8.

Opazo P, Labrecque S, Tigaret CM, Frouin A, Wiseman PW, De Koninck P, Choquet D (2010) CaMKII triggers the diffusional trapping of surface AMPARs through phosphorylation of stargazin. Neuron 67:239-252.

Otani S, Abraham WC (1989) Inhibition of protein synthesis in the dentate gyrus, but not the entorhinal cortex, blocks maintenance of long-term potentiation in rats. NeurosciLett 106:175-180.

Pardossi-Piquard R, Checler F (2012) The physiology of the beta-amyloid precursor protein intracellular domain AICD. J Neurochem 120 Suppl 1:109-124.

Park H, Poo MM (2013) Neurotrophin regulation of neural circuit development and function. Nat Rev Neurosci 14:7-23.

Pastalkova E, Serrano P, Pinkhasova D, Wallace E, Fenton AA, Sacktor TC (2006) Storage of spatial information by the maintenance mechanism of LTP. Science 313:1141-1144.

Patterson MA, Szatmari EM, Yasuda R (2010) AMPA receptors are exocytosed in stimulated spines and adjacent dendrites in a Ras-ERK-dependent manner during long-term potentiation. Proc Natl Acad Sci U S A 107:15951-15956.

Perez RG, Soriano S, Hayes JD, Ostaszewski B, Xia W, Selkoe DJ, Chen X, Stokin GB, Koo EH (1999) Mutagenesis identifies new signals for beta-amyloid precursor protein endocytosis, turnover, and the generation of secreted fragments, including Abeta42. JBiolChem 274:18851-18856.

Perrin RJ, Fagan AM, Holtzman DM (2009) Multimodal techniques for diagnosis and prognosis of Alzheimer's disease. Nature 461:916-922.

Phinney AL, Calhoun ME, Wolfer DP, Lipp HP, Zheng H, Jucker M (1999) No hippocampal neuron or synaptic bouton loss in learning-impaired aged beta-amyloid precursor protein-null mice. Neuroscience 90:1207-1216.

Pierrot N, Santos SF, Feyt C, Morel M, Brion JP, Octave JN (2006) Calcium-mediated transient phosphorylation of tau and amyloid precursor protein followed by intraneuronal amyloid-beta accumulation. J Biol Chem 281:39907-39914.

Pietrzik CU, Hoffmann J, Stober K, Chen CY, Bauer C, Otero DA, Roch JM, Herzog V (1998) From differentiation to proliferation: the secretory amyloid precursor protein as a local mediator of growth in thyroid epithelial cells. Proc Natl Acad Sci U S A 95:1770-1775.

Popugaeva E, Bezprozvanny I (2013) Role of endoplasmic reticulum Ca2+ signaling in the pathogenesis of Alzheimer disease. Front Mol Neurosci 6:29.

Postina R, Schroeder A, Dewachter I, Bohl J, Schmitt U, Kojro E, Prinzen C, Endres K, Hiemke C, Blessing M, Flamez P, Dequenne A, Godaux E, van Leuven F, Fahrenholz F (2004) A disintegrin-metalloproteinase prevents amyloid plaque formation and hippocampal defects in an Alzheimer disease mouse model. J Clin Invest 113:1456-1464.

Povova J, Ambroz P, Bar M, Pavukova V, Sery O, Tomaskova H, Janout V (2012) Epidemiological of and risk factors for Alzheimer's disease: a review. Biomed Pap Med Fac Univ Palacky Olomouc Czech Repub 156:108-114.

Prox J, Bernreuther C, Altmeppen H, Grendel J, Glatzel M, D'Hooge R, Stroobants S, Ahmed T, Balschun D, Willem M, Lammich S, Isbrandt D, Schweizer M, Horre K, De SB, Saftig P (2013) Postnatal Disruption of the Disintegrin/Metalloproteinase ADAM10 in Brain Causes Epileptic Seizures, Learning Deficits, Altered Spine Morphology, and Defective Synaptic Functions. JNeurosci 33:12915-12928.

Puzzo D, Privitera L, Leznik E, Fa M, Staniszewski A, Palmeri A, Arancio O (2008) Picomolar amyloid-beta positively modulates synaptic plasticity and memory in hippocampus. J Neurosci 28:14537-14545.

Puzzo D, Privitera L, Fa' M, Staniszewski A, Hashimoto G, Aziz F, Sakurai M, Ribe EM, Troy CM, Mercken M, Jung SS, Palmeri A, Arancio O (2011) Endogenous amyloid-beta is necessary for hippocampal synaptic plasticity and memory. AnnNeurol 69:819-830.

Querfurth HW, Selkoe DJ (1994) Calcium ionophore increases amyloid beta peptide production by cultured cells. Biochemistry 33:4550-4561.

Regehr WG (2012) Short-term presynaptic plasticity. Cold Spring Harb Perspect Biol 4:a005702.

Reinhard C, Borgers M, David G, De SB (2013) Soluble amyloid-beta precursor protein binds its cell surface receptor in a cooperative fashion with glypican and syndecan proteoglycans. JCell Sci.

Renner M, Lacor PN, Velasco PT, Xu J, Contractor A, Klein WL, Triller A (2010) Deleterious effects of amyloid beta oligomers acting as an extracellular scaffold for mGluR5. Neuron 66:739-754.

Ring S, Weyer SW, Kilian SB, Waldron E, Pietrzik CU, Filippov MA, Herms J, Buchholz C, Eckman CB, Korte M, Wolfer DP, Muller UC (2007) The secreted beta-amyloid precursor protein ectodomain APPs alpha is sufficient to rescue the anatomical, behavioral, and electrophysiological abnormalities of APP-deficient mice. JNeurosci 27:7817-7826.

Robakis NK, Ramakrishna N, Wolfe G, Wisniewski HM (1987) Molecular cloning and characterization of a cDNA encoding the cerebrovascular and the neuritic plaque amyloid peptides. Proc Natl Acad Sci U S A 84:4190-4194.

Roch JM, Masliah E, Roch-Levecq AC, Sundsmo MP, Otero DA, Veinbergs I, Saitoh T (1994) Increase of synaptic density and memory retention by a peptide representing the trophic domain of the amyloid beta/A4 protein precursor. Proc Natl Acad Sci U S A 91:7450-7454.

Rochefort NL, Konnerth A (2012) Dendritic spines: from structure to in vivo function. EMBO Rep 13:699-708.

Rojas G, Cardenas AM, Fernandez-Olivares P, Shimahara T, Segura-Aguilar J, Caviedes R, Caviedes P (2008) Effect of the knockdown of amyloid precursor protein on intracellular calcium increases in a neuronal cell line derived from the cerebral cortex of a trisomy 16 mouse. ExpNeurol 209:234-242.

Rosenberg T, Gal-Ben-Ari S, Dieterich DC, Kreutz MR, Ziv NE, Gundelfinger ED, Rosenblum K (2014) The roles of protein expression in synaptic plasticity and memory consolidation. Front Mol Neurosci 7:86.

Rosenzweig ES, Rao G, McNaughton BL, Barnes CA (1997) Role of temporal summation in age-related long-term potentiation-induction deficits. Hippocampus 7:549-558.

Rossner S (2004) New players in old amyloid precursor protein-processing pathways. IntJDevNeurosci 22:467-474.

Ryan MM, Morris GP, Mockett BG, Bourne K, Abraham WC, Tate WP, Williams JM (2013) Time-dependent changes in gene expression induced by secreted amyloid precursor protein-alpha in the rat hippocampus. BMC Genomics 14:376.

Sainsbury RS, Heynen A, Montoya CP (1987) Behavioral correlates of hippocampal type 2 theta in the rat. Physiol Behav 39:513-519.

Sajikumar S, Frey JU (2003) Anisomycin inhibits the late maintenance of long-term depression in rat hippocampal slices in vitro. NeurosciLett 338:147-150.

Sajikumar S, Navakkode S, Sacktor TC, Frey JU (2005) Synaptic tagging and cross-tagging: the role of protein kinase Mzeta in maintaining long-term potentiation but not long-term depression. JNeurosci 25:5750-5756.

Santos SF, Pierrot N, Morel N, Gailly P, Sindic C, Octave JN (2009) Expression of human amyloid precursor protein in rat cortical neurons inhibits calcium oscillations. JNeurosci 29:4708-4718.

Schaeffer EL, Figueiro M, Gattaz WF (2011) Insights into Alzheimer disease pathogenesis from studies in transgenic animal models. Clinics(Sao Paulo) 66 Suppl 1:45-54.

Schrenk-Siemens K, Perez-Alcala S, Richter J, Lacroix E, Rahuel J, Korte M, Muller U, Barde YA, Bibel M (2008) Embryonic stem cell-derived neurons as a cellular system to study gene function: lack of amyloid precursor proteins APP and APLP2 leads to defective synaptic transmission. Stem Cells 26:2153-2163.

Scoville WB, Milner B (1957) Loss of recent memory after bilateral hippocampal lesions. J Neurol Neurosurg Psychiatry 20:11-21.

Seabrook GR, Smith DW, Bowery BJ, Easter A, Reynolds T, Fitzjohn SM, Morton RA, Zheng H, Dawson GR, Sirinathsinghji DJ, Davies CH, Collingridge GL, Hill RG (1999) Mechanisms contributing to the deficits in hippocampal synaptic plasticity in mice lacking amyloid precursor protein. Neuropharmacology 38:349-359.

Segal M, Korkotian E (2014) Endoplasmic reticulum calcium stores in dendritic spines. Front Neuroanat 8:64.

Selkoe D, Kopan R (2003) Notch and Presenilin: regulated intramembrane proteolysis links development and degeneration. AnnuRevNeurosci 26:565-597.

Selkoe DJ (2008) Soluble oligomers of the amyloid beta-protein impair synaptic plasticity and behavior. Behav Brain Res 192:106-113.

Sennvik K, Fastbom J, Blomberg M, Wahlund LO, Winblad B, Benedikz E (2000) Levels of alpha- and beta-secretase cleaved amyloid precursor protein in the cerebrospinal fluid of Alzheimer's disease patients. Neurosci Lett 278:169-172.

Serrano P, Yao Y, Sacktor TC (2005) Persistent phosphorylation by protein kinase Mzeta maintains late-phase long-term potentiation. JNeurosci 25:1979-1984.

Shahi K, Marvizon JC, Baudry M (1993) High concentrations of glycine induce long-lasting changes in synaptic efficacy in rat hippocampal slices. Neurosci Lett 149:185-188.

Shankar GM, Li S, Mehta TH, Garcia-Munoz A, Shepardson NE, Smith I, Brett FM, Farrell MA, Rowan MJ, Lemere CA, Regan CM, Walsh DM, Sabatini BL, Selkoe DJ (2008) Amyloid-beta protein dimers isolated directly from Alzheimer's brains impair synaptic plasticity and memory. NatMed 14:837-842.

Shepherd JD, Huganir RL (2007) The cell biology of synaptic plasticity: AMPA receptor trafficking. Annu Rev Cell Dev Biol 23:613-643.

Silva AJ, Paylor R, Wehner JM, Tonegawa S (1992) Impaired spatial learning in alpha-calcium-calmodulin kinase II mutant mice. Science 257:206-211.

Snyder EM, Nong Y, Almeida CG, Paul S, Moran T, Choi EY, Nairn AC, Salter MW, Lombroso PJ, Gouras GK, Greengard P (2005) Regulation of NMDA receptor trafficking by amyloid-beta. NatNeurosci 8:1051-1058.

Soba P, Eggert S, Wagner K, Zentgraf H, Siehl K, Kreger S, Lower A, Langer A, Merdes G, Paro R, Masters CL, Muller U, Kins S, Beyreuther K (2005) Homo- and heterodimerization of APP family members promotes intercellular adhesion. EMBO J 24:3624-3634.

Spillantini MG, Goedert M (2013) Tau pathology and neurodegeneration. Lancet Neurol 12:609-622.

Spires-Jones TL, Hyman BT (2014) The intersection of amyloid beta and tau at synapses in Alzheimer's disease. Neuron 82:756-771.

Steinbach JP, Muller U, Leist M, Li ZW, Nicotera P, Aguzzi A (1998) Hypersensitivity to seizures in beta-amyloid precursor protein deficient mice. Cell DeathDiffer 5:858-866.

Stoppini L, Buchs PA, Muller D (1991) A simple method for organotypic cultures of nervous tissue. JNeurosciMethods 37:173-182.

Strecker P, Ludewig S, Krächan E, Mehrfeld C, Mundinger T, Korte M, Herz J, Rust M, Guénette S, Kins S (in preparation) The APP adaptor proteins Fe65 and Fe65L1 have distinct and overlapping functions in the PNS and CNS synapses for formation, learning and LTP.

Strekalova T, Zorner B, Zacher C, Sadovska G, Herdegen T, Gass P (2003) Memory retrieval after contextual fear conditioning induces c-Fos and JunB expression in CA1 hippocampus. Genes Brain Behav 2:3-10.

Stuhmer T, Puelles L, Ekker M, Rubenstein JL (2002) Expression from a Dlx gene enhancer marks adult mouse cortical GABAergic neurons. CerebCortex 12:75-85.

Suh J, Choi SH, Romano DM, Gannon MA, Lesinski AN, Kim DY, Tanzi RE (2013) ADAM10 missense mutations potentiate beta-amyloid accumulation by impairing prodomain chaperone function. Neuron 80:385-401.

Takahashi T, Svoboda K, Malinow R (2003) Experience strengthening transmission by driving AMPA receptors into synapses. Science 299:1585-1588.

Tan J, Evin G (2012) Beta-site APP-cleaving enzyme 1 trafficking and Alzheimer's disease pathogenesis. J Neurochem 120:869-880.

Tao X, Finkbeiner S, Arnold DB, Shaywitz AJ, Greenberg ME (1998) Ca2+ influx regulates BDNF transcription by a CREB family transcription factor-dependent mechanism. Neuron 20:709-726.

Taylor CJ, Ireland DR, Ballagh I, Bourne K, Marechal NM, Turner PR, Bilkey DK, Tate WP, Abraham WC (2008) Endogenous secreted amyloid precursor protein-alpha regulates hippocampal NMDA receptor function, long-term potentiation and spatial memory. NeurobiolDis 31:250-260.

Thinakaran G, Koo EH (2008) Amyloid precursor protein trafficking, processing, and function. JBiolChem 283:29615-29619.

Thornton E, Vink R, Blumbergs PC, Van Den Heuvel C (2006) Soluble amyloid precursor protein alpha reduces neuronal injury and improves functional outcome following diffuse traumatic brain injury in rats. Brain Res 1094:38-46.

Tombaugh GC, Rowe WB, Rose GM (2005) The slow afterhyperpolarization in hippocampal CA1 neurons covaries with spatial learning ability in aged Fisher 344 rats. J Neurosci 25:2609-2616.

Trowbridge IS, Collawn JF, Hopkins CR (1993) Signal-dependent membrane protein trafficking in the endocytic pathway. Annu Rev Cell Biol 9:129-161.

Tsien R, Pozzan T (1989) Measurement of cytosolic free Ca2+ with quin2. Methods Enzymol 172:230-262.

Tyan SH, Shih AY, Walsh JJ, Maruyama H, Sarsoza F, Ku L, Eggert S, Hof PR, Koo EH, Dickstein DL (2012) Amyloid precursor protein (APP) regulates synaptic structure and function. Mol Cell Neurosci 51:43-52.

Uemura K, Farner KC, Nasser-Ghodsi N, Jones P, Berezovska O (2011) Reciprocal relationship between APP positioning relative to the membrane and PS1 conformation. Mol Neurodegener 6:15.

Ultanir SK, Kim JE, Hall BJ, Deerinck T, Ellisman M, Ghosh A (2007) Regulation of spine morphology and spine density by NMDA receptor signaling in vivo. Proc Natl Acad Sci U S A 104:19553-19558.

Vassar R (2004) BACE1: the beta-secretase enzyme in Alzheimer's disease. J Mol Neurosci 23:105-114.

Vassar R, Bennett BD, Babu-Khan S, Kahn S, Mendiaz EA, Denis P, Teplow DB, Ross S, Amarante P, Loeloff R, Luo Y, Fisher S, Fuller J, Edenson S, Lile J, Jarosinski MA, Biere AL, Curran E, Burgess T, Louis JC, Collins F, Treanor J, Rogers G, Citron M (1999) Beta-secretase cleavage of Alzheimer's amyloid precursor protein by the transmembrane aspartic protease BACE. Science 286:735-741.

Vetrivel KS, Zhang YW, Xu H, Thinakaran G (2006) Pathological and physiological functions of presenilins. Mol Neurodegener 1:4.

Volk LJ, Bachman JL, Johnson R, Yu Y, Huganir RL (2013) PKM-zeta is not required for hippocampal synaptic plasticity, learning and memory. Nature 493:420-423.

von Koch CS, Zheng H, Chen H, Trumbauer M, Thinakaran G, Van der Ploeg LH, Price DL, Sisodia SS (1997) Generation of APLP2 KO mice and early postnatal lethality in APLP2/APP double KO mice. NeurobiolAging 18:661-669.

Walsh DM, Minogue AM, Sala FC, Fadeeva JV, Wasco W, Selkoe DJ (2007) The APP family of proteins: similarities and differences. BiochemSocTrans 35:416-420.

Walsh DM, Fadeeva JV, LaVoie MJ, Paliga K, Eggert S, Kimberly WT, Wasco W, Selkoe DJ (2003) gamma-Secretase cleavage and binding to FE65 regulate the nuclear translocation of the intracellular C-terminal domain (ICD) of the APP family of proteins. Biochemistry 42:6664-6673.

Wang P, Yang G, Mosier DR, Chang P, Zaidi T, Gong YD, Zhao NM, Dominguez B, Lee KF, Gan WB, Zheng H (2005) Defective neuromuscular synapses in mice lacking amyloid precursor protein (APP) and APP-Like protein 2. JNeurosci 25:1219-1225.

Wang Z, Wang B, Yang L, Guo Q, Aithmitti N, Songyang Z, Zheng H (2009) Presynaptic and postsynaptic interaction of the amyloid precursor protein promotes peripheral and central synaptogenesis. J Neurosci 29:10788-10801.

Wasco W, Gurubhagavatula S, Paradis MD, Romano DM, Sisodia SS, Hyman BT, Neve RL, Tanzi RE (1993) Isolation and characterization of APLP2 encoding a homologue of the Alzheimer's associated amyloid beta protein precursor. NatGenet 5:95-100.

Weskamp G, Cai H, Brodie TA, Higashyama S, Manova K, Ludwig T, Blobel CP (2002) Mice lacking the metalloprotease-disintegrin MDC9 (ADAM9) have no evident major abnormalities during development or adult life. Mol Cell Biol 22:1537-1544.

Weyer SW, Zagrebelsky M, Herrmann U, Hick M, Ganss L, Gobbert J, Gruber M, Altmann C, Korte M, Deller T, Muller UC (2014) Comparative analysis of single and combined APP/APLP knockouts reveals reduced spine density in APP-KO mice that is prevented by APPsalpha expression. Acta Neuropathol Commun 2:36.

Weyer SW, Klevanski M, Delekate A, Voikar V, Aydin D, Hick M, Filippov M, Drost N, Schaller KL, Saar M, Vogt MA, Gass P, Samanta A, Jaschke A, Korte M, Wolfer DP, Caldwell JH, Muller UC (2011) APP and APLP2 are essential at PNS and CNS synapses for transmission, spatial learning and LTP. EMBO J.

Wheeler DG, Groth RD, Ma H, Barrett CF, Owen SF, Safa P, Tsien RW (2012) Ca(V)1 and Ca(V)2 channels engage distinct modes of Ca(2+) signaling to control CREB-dependent gene expression. Cell 149:1112-1124.

Whitlock JR, Heynen AJ, Shuler MG, Bear MF (2006) Learning induces long-term potentiation in the hippocampus. Science 313:1093-1097.

Wigstrom H, Gustafsson B (1983) Facilitated induction of hippocampal long-lasting potentiation during blockade of inhibition. Nature 301:603-604.

Wigstrom H, Gustafsson B (1985) Facilitation of hippocampal long-lasting potentiation by GABA antagonists. Acta Physiol Scand 125:159-172.

Wigstrom H, Gustafsson B, Huang YY, Abraham WC (1986) Hippocampal long-term potentiation is induced by pairing single afferent volleys with intracellularly injected depolarizing current pulses. Acta Physiol Scand 126:317-319.

Wimo A, Jonsson L, Bond J, Prince M, Winblad B, Alzheimer Disease I (2013) The worldwide economic impact of dementia 2010. Alzheimers Dement 9:1-11 e13.

Winson J (1978) Loss of hippocampal theta rhythm results in spatial memory deficit in the rat. Science 201:160-163.

Wolfe MS, Guenette SY (2007) APP at a glance. J Cell Sci 120:3157-3161.

Xu C, Liu QY, Alkon DL (2014) PKC activators enhance GABAergic neurotransmission and paired-pulse facilitation in hippocampal CA1 pyramidal neurons. Neuroscience 268:75-86.

Yang L, Wang Z, Wang B, Justice NJ, Zheng H (2009) Amyloid precursor protein regulates Cav1.2 L-type calcium channel levels and function to influence GABAergic short-term plasticity. JNeurosci 29:15660-15668.

Yang Y, Calakos N (2013) Presynaptic long-term plasticity. Front Synaptic Neurosci 5:8.

Yoshikai S, Sasaki H, Doh-ura K, Furuya H, Sakaki Y (1990) Genomic organization of the human amyloid beta-protein precursor gene. Gene 87:257-263.

Young-Pearse TL, Chen AC, Chang R, Marquez C, Selkoe DJ (2008) Secreted APP regulates the function of full-length APP in neurite outgrowth through interaction with integrin beta1. Neural Dev 3:15.

Young-Pearse TL, Suth S, Luth ES, Sawa A, Selkoe DJ (2010) Biochemical and functional interaction of disrupted-in-schizophrenia 1 and amyloid precursor protein regulates neuronal migration during mammalian cortical development. J Neurosci 30:10431-10440.

Young-Pearse TL, Bai J, Chang R, Zheng JB, LoTurco JJ, Selkoe DJ (2007) A critical function for beta-amyloid precursor protein in neuronal migration revealed by in utero RNA interference. J Neurosci 27:14459-14469.

Yuste R, Majewska A, Holthoff K (2000) From form to function: calcium compartmentalization in dendritic spines. Nat Neurosci 3:653-659.

Zhang X, Herrmann U, Weyer SW, Both M, Muller UC, Korte M, Draguhn A (2013) Hippocampal Network Oscillations in APP/APLP2-Deficient Mice. PLoSOne 8:e61198.

Zheng H, Jiang M, Trumbauer ME, Sirinathsinghji DJ, Hopkins R, Smith DW, Heavens RP, Dawson GR, Boyce S, Conner MW, Stevens KA, Slunt HH, Sisoda SS, Chen HY, Van der Ploeg LH (1995) beta-Amyloid precursor protein-deficient mice show reactive gliosis and decreased locomotor activity. Cell 81:525-531.

Zucker RS (1999) Calcium- and activity-dependent synaptic plasticity. CurrOpinNeurobiol 9:305-313.

Zucker RS, Regehr WG (2002) Short-term synaptic plasticity. AnnuRevPhysiol 64:355-405.

Danksagung

An dieser Stelle möchte ich die Möglichkeit nutzen, um mich bei allen Menschen zu bedanken, die direkt oder indirekt zum Gelingen dieser Dissertation beigetragen haben:

Zunächst danke ich meinem Doktorvater Prof. Dr. Martin Korte für die vertrauensvolle und erfolgreiche Zusammenarbeit, mit der er es mir ermöglichte, die Promotion in seiner Arbeitsgruppe anzufertigen.

Prof. Dr. Reinhard Köster danke ich für die Übernahme des Koreferates, sowie PD Dr. Florian Bittner für die Leitung der Prüfungskommission.

Ich danke Prof. Dr. Ulrike Müller für die gute wissenschaftliche Zusammenarbeit in diesem Projekt.

Ein großer Dank gilt Dr. Kristin Michaelsen-Preusse für ihre wunderbare Unterstützung bei der Etablierung des quantitativen Calcium imagings und beim Verfassen der Dissertation.

Ebenso möchte ich mich bei Dr. Martin Rothkegel, Dr. Marta Zagrebelsky und Dr. Gayane Grigoryan für wertvolle Ratschläge und sachkundige Diskussionen bedanken.

Ein riesiges Dankeschön geht an Diane Mundil für die unendlich wertvolle Unterstützung bei der Anfertigung der Kulturen und an Reinhard Huwe für die vielen technischen Hilfen und Raffinessen in der Elektrophysiologie.

Tania Messerschmidt, Eva Saxinger, Heike Kessler danke ich für die Übernahme aller Bestellungen und Genotypisierungen.

Besonders möchte ich meinen liebgewonnen Bürokolleginnen Dr. Andrea Delekate und Susann Ludewig für eine ganz tolle und freundschaftliche gemeinsame Zeit danken.

Für den fachlichen Austausch und die schöne Zeit miteinander danke ich zum einen den ehemaligen Doktoranden Dr. Anita Remus, Dr. Stefanie Schweinhuber, Dr. Sabine Zessin, Melissa O'Brien, Dr. Yves Kellner, Dr. Andrea Delekate, Dr. Martin Polack und natürlich allen derzeitigen Doktoranden Nina Gödecke, Marinna Weller, Susann Ludewig, Franziska Scharkowski, Jan Kleveman, Qin Li, Cristina Iobbi, Shirin Hosseini. Ich wünsche euch noch eine erfolgreiche Zeit hier und alles Gute für eure Zukunft!

Meike Hick möchte ich für die intensive und sehr freundschaftliche Zusammenarbeit in diesem Projekt danken. Jedes Zusammentreffen war die reinste Freude. Viel Erfolg weiterhin!

Einen ganz besonderen und herzlichen Dank haben Siegfried, Barbara und Andrea für das geduldige und intensive Korrekturlesen dieser Arbeit verdient! Dadurch habt ihr die Dissertation ein ganzes Stück voran gebracht!

Marco hat mich in all der Zeit begleitet, bestärkt und es geschafft, dass der Arbeitsstress vor der Tür blieb. Danke! Ich liebe dich!

Zu guter Letzt danke ich meiner wunderbaren Familie, Mama, Papa, Oma und Opa, dass ihr immer für mich da wart und seid. Auf euch ist jederzeit Verlass! Ihr seid die Besten!